Isolation of microalgae from Kuching, Sarawak, and assessment of their potential for biofuel production and bioremediation of nutrient-rich media

By

Samson Lee Tze Hung

THESIS

Submitted in partial fulfillment of the requirements for the degree of Master of Science in Faculty of Engineering, Computing and Science in the Swinburne University of Technology Sarawak

2017

Supervisor:

Dr. Moritz Müller

Co-supervisors:

Dr. Aazani Mujahid

A/P Po-Teen Lim

Dr. Chui-Pin Leaw

Abstract

Current technologies of nutrient waste treatment are largely dependent on environmentally hazardous and expensive chemical treatments to treat nutrient waste in wastewater. While modern treatment technologies which uses bioreactors are slowly being adopted, microalgae can be utilized to bioremediate nutrient as well as generate biomass which can be processed into fuel and fertilizer and thus reduce cost of waste treatment significantly. In this research study, local microalgae were isolated freshwater and marine water sources, identified through genetic and morphological analysis, tested in growth experiments with different concentrations of nutrients and assessed by their of Fatty Acid Methyl Esters (FAME) profiles extracted from biomass grown from the nutrient experiment. 13 freshwater and 3 marine microalgae strains were isolated of which 11 of the freshwater microalgae were identified. In the growth experiment, the freshwater *Nephrochlamys subsolitaria* (FSE), *Scenedesmus acutus* (FTA1) and *Acutodesmus obliquus* (FDP) displayed positive growth in from 0 to 10 times the nutrient concentration while *Nitzchia sp./Pseudo-nitzschia sp*. (FSB), FSA and *Nitzchia sp./Pseudo-nitzschia sp.* (FBP3) show the same positive growth for up to 5 times the nutrient concentration. Exceptional freshwater bioremediators were *Nitzchia sp./Pseudo-nitzschia sp.* (FBP3) which had the highest culture growth of nearly 50 times its initial cell count in a week and *Scenedesmus acutus* (FTA1) which showed the highest nutrient tolerance, growing healthily in the highest nutrient concentration (10x) and had potential in growing better in more nutrient concentrated environments. Marine bioremediators include MTAR and MTA1 with MTAR showing a similar trend to *Scenedesmus acutus* (FTA1). FAME profiles extracted from the generated biomass indicated poor amounts of lipids save for *Nitzchia sp./Pseudo-nitzschia sp.* (FBP3) starved in 0x which gave the highest level of FAME of 25% of the biomass weight. MTA1 gave the highest energy per kilogram at -36.36 MJ/kg in 5x while the highest energy observed was -0.00075 kJ by FTAR3 in 5x. All of the microalgae samples surpassed ethanol, methanol and coal in energy potential but were lower than standard biofuels and fossil fuels. Viable applications of the selected microalgae include nutrient waste bioremediation and its biomass used as burning fuel or agricultural fertilizer.

Acknowledgements

First and foremost, I would like to express my humblest gratitude to my primary coordinating supervisor, Dr. Moritz Müller for his unending support and guidance throughout the period of this research. His guidance help overcome difficulties encountered during the research and also introduced me to various connections that aided in the completion of this research.

I am grateful to Dr. Aazani Mujahid for her insightful comments and support given, when I present my research updates during meetings. Dr. Aazani also allowed access to laboratories in University Malaysia Sarawak (UNIMAS) that gave the crucial help in my research.

I would also like to extend my deepest appreciation to Dr. Lim Po Teen and his student Tan Toh Hii, who passed on important techniques of microalgae isolation and culture which laid the foundation of my research. I would also thank Dr. Phang Siew Moi and Vejeysri Vello from University Malaya (UM) for allowing me access to their laboratories and their gas chromatography equipment.

I also convey heartfelt thanks to the Biotechnology laboratory officers and technicians Chua Jia Ni, Dyg. Rafika Atiqah, and Nurul Arina for allowing me access to Swinburne's laboratories and facilities as well as apparatus and chemicals that were used in my research.

I am grateful to all of my lab colleagues who had become my friends and collaborated with each other to complete everyone's research: Ang, Changi Wong, Edwin Sia, Angelica, Yao Long Lew, Felicity, Fay, Tasha, Ing, Jessica Song, Shirley Bong, and Julianna Ho. I am happy to work in the lab with you I'm and thankful for your support and encouragement.

I would like to thank my family; my parents and sister for their support in my research. Their encouragement and attention allowed me to strive against the complications that appeared during my research.

Lastly, I am grateful to the Swinburne University for allowing me to start my research and granting me a student scholarship and access to their labs and facilities.

Declaration

I hereby declare that this research thesis titled “Isolation of microalgae from Kuching, Sarawak, and assessment of their potential for biofuel production and bioremediation of nutrient-rich wastewater” is an original work done of my own effort and contains no material which has been accepted for the award to the candidate of any other degree or diploma, except where due reference is made in the text of the examinable outcome; to the best of my knowledge contains no material previously published or written by another person except where due reference is made in the text of the examinable outcome; and where work is based on joint research or publications, discloses the relative contributions of the respective workers or authors.

(SAMSON LEE TZE HUNG)

Table of Contents

Abstract 2
Acknowledgements 3
Declaration 4
List of Figures 7
List of Tables 11
Introduction 13
Environmental Pollution 13
Nutrient Loss 13
Eutrophication 14
Algae 15
Microalgae 15
Bioremediation 18
Bioremediation in Malaysia 22
Microalgae's potential in bioremediation 23
Microalgae's Potential in Biofuel Production 29
Lipids 29
Biofuel 31
Identifying the problem 35
Hypothesis 35
Aims and Objectives 35
Methodology 36
Field Sampling 37
Sarawak River 37
Bau - Kampung Apar 38
Kampung Telaga Air 39
Tunku Abdul Rahman National Park 39
Microalgae Culture 40
ESDK Microalgae Culture Stock Preparation 40
Isolation of Microalgae cells 41
DNA Extraction and Processing 42
Freeze and Thaw Method 42
CTAB Method 43
DNA – DTAB CTAB Method 44
Mobio PowerWater DNA Isolation Kit 45
Gel Electrophoresis 47
Polymerase Chain Reaction (PCR) 48

Culture Growth under Nutrient Stress 49
Estimating Cell Number and Measuring Culture Optical Density 50
Culturing the Algae under Nutrient Stress 51
Growth Culture Analysis 52
Microalgae Biomass Analysis 52
Lipid Analysis 53
Bligh and Dyer Lipid Extraction 53
Transesterification 54
Energy Calculation 57
Results 61
Microalgae Isolation 61
Electrophoresis Gel 63
Identification of Microalgae 64
Sequenced Microalgae Strains 64
Unsequenced Microalgae Strains 81
FAME Analysis 84
Microalgae Profiles 84
Energy Calculation of Microalgae 104
Discussion 112
Culture Growth under Nutrient Stress 112
Total FAME 113
Total FAME Percentage 114
Further Analysis of Microalgae Culture in Different Nutrient Conditions 115
FAME Composition 116
Microalgae as a Bioremediator 117
Microalgae as a Biofuel Producer 118
Application 121
Bioremediation of nutrient waste. 121
Biomass energy 122
Fertilizer 123
Conclusion and Further Research 124
References 126
In-text References 126
Figure and Table References 142
Appendix 147

List of Figures

FIGURE 1: EUTROPHICATION PROCESS. OBTAINED FROM BBC. <HTTP://WWW.BBC.CO.UK/>..... 14
FIGURE 2: EXAMPLES OF MICROALGAE AND THEIR UNIQUE MORPHOLOGY. OBTAINED FROM PROFESSOR SCHMID'S BIOLOGY WEBSITE. <HTTP://CLASSROOM.SDMESA.EDU/ESCHMID/> 17
FIGURE 3: A DIAGRAM OF THE AEROBIC FLUIDIZED-BED BIOREMEDIATION SYSTEM FOR GROUNDWATER CONTAMINATED WITH CHLOROPHENOL. OBTAINED FROM ENVIRONMENTAL SCIENCE AND TECHNOLOGY. JARVINEN ET AL. (1994). 19
FIGURE 4: THE SCHEMATIC DIAGRAM OF BIOREACTOR UTILIZING FILAMENTOUS BAMBOO. OBTAINED FROM ECOLOGICAL ENGINEERING, WENPING ET AL. (2012). 20
FIGURE 5: THE MOLECULAR STRUCTURE FOR CYPERMETHRIN. OBTAINED FROM PESTICIDE ACTION NETWORK (PAN) PESTICIDE DATABASE. <HTTP://WWW.PESTICIDEINFO.ORG/> 21
FIGURE 6: MICROGRAPHS OF HETEROCOCCOLITHOPHORIDS EMILIANIA HUXLEYI (A, B, C) AND PLEUROCHRYSIS CARTERAE (D, E, F). (A) AND (D) OBTAINED BY LIGHT MICROGRAPH, (B) AND (E) OBTAINED BY SCANNING ELECTRON MICROSCOPE, AND IMAGES (C) AND (F) OBTAINED FROM NATURAL HISTORY MUSEUM SEM DATABASE. OBTAINED FROM DOCTOR OF PHILOSOPHY THESIS 'THE CULTURE OF COCCOLITHOPHORID MICROALGAE FOR CARBON DIOXIDE BIOREMEDIATION'. MOHEIMANI (2005) 24
FIGURE 7: BAR CHARTS SHOWING (A) THE PERCENTAGE OF REDUCTION IN TOTAL DISSOLVED SOLIDS (TDS), AMMONIUM, BIOLOGICAL OXYGEN DEMAND (BOD), AND NITRATE OF SEWAGE WASTEWATER BY DIFFERENT MICROALGAE; CHLORELLA, SCENDESMUS, NOSTOC, AND A CONSORTIA, RESPECTIVELY, AND (B) THE N:P:K RATIO OF BIOMASS GENERATED BY THE SAME MICROALGAE DURING THE PROCESS. TAKEN FROM SHARMA AND KHAN (2013). 26
FIGURE 8:TRANSESTERIFICATION PROCESS OF TRIGLYCERIDE AND METHANOL PRODUCING METHYL ESTERS (FAME) AND GLYCEROL, OBTAINED FROM GLOBAL CCS INSTITUTE, <HTTP://WWW.GLOBALCCSINSTITUTE.COM/> 29
FIGURE 9: (A) THE ESTERIFICATION MIXTURE CONTAINING BIODIESEL AND RESIDUE, (B) THE ALGAE BIOMASS TO BE PROCESSED INTO BIOFUEL, AND (C) THE RESULTING BIODIESEL AFTER REFINING. HOSSAIN ET AL. (2008) 34
FIGURE 10: FLOW CHART SUMMARIZING THE METHODOLOGY USED IN THIS RESEARCH PROJECT. 36
FIGURE 11: SAMPLING LOCATIONS IN THE SARAWAK RIVER FOR WATER SAMPLES AND THEIR RESPECTIVE GPS COORDINATES. OBTAINED FROM GOOGLE MAPS <HTTPS://MAPS.GOOGLE.COM/>..... 37
FIGURE 12: SAMPLING LOCATION IN KAMPUNG APAR FOR THE WATER SAMPLES (INDICATED BY THE BLUE STAR) AND THE KAMPUNG APAR'S GPS COORDINATES. OBTAINED FROM GOOGLE EARTH. 38
FIGURE 13: SAMPLING LOCATIONS IN TELAGA AIR FOR THE MARINE WATER AND THE LOCATION'S GPS COORDINATES. OBTAINED FROM GOOGLE EARTH. 39
FIGURE 14: SAMPLING LOCATION IN TUNKU ADBUL RAHMAN NATIONAL PARK IN SABAH FOR THE MARINE WATER AND THE LOCATION'S GPS COORDINATES. OBTAINED FROM GOOGLE MAPS <HTTPS://MAPS.GOOGLE.COM/>. 39
FIGURE 15: MOBIO POWERWATER DNA ISOLATION KIT. OBTAINED FROM MO BIO LABORATORIES. <HTTPS://MOBIO.COM> 45
FIGURE 16: DIAGRAM FOR AN AGAROSE GEL SETUP FOR GEL ELECTROPHORESIS. OBTAINED FROM MIT OPEN COURSE WARE.<HTTP://OCW.MIT.EDU/> 47
FIGURE 17: GRAPH OF ABSORBANCE AGAINST CELL CONCENTRATION FOR SAMPLE FSA. 50
FIGURE 18: DIAGRAM OF EXPERIMENTAL SET UP FOR CULTURING MICROALGAE. 51
FIGURE 19: THE BLIGH AND DYER LIPID EXTRACTION FROM THE DRY BIOMASS. 53
FIGURE 20: THE TRANSESTERIFICATION OF THE FATTY ACID SAMPLE. 54
FIGURE 21: RETENTION TIMES OF THE FAMES IN THE STANDARD AS WELL AS THEIR RESPECTIVE IDENTITIES. 56
FIGURE 22: LABELING SYSTEM OF THE MICROALGAE STRAINS. 61
FIGURE 23: THE ELECTROPHORESIS GEL VIEWED UNDER UV LIGHT WITH THE 50BP LADDER REFERENCE OBTAINED FROM NEW ENGLAND BIOLABS. <HTTPS://WWW.NEB.COM/> THE BANDS IN THE WELLS THAT RANGED BETWEEN 500 BP TP 800 BP WERE SUCCESSFUL PCR ATTEMPTS AT REPLICATING MICROALGAE DNA. EMPTY WELLS IN THE GEL WERE UNSUCCESSFUL ATTEMPTS. 63
FIGURE 24: MICROALGAE FSA WHICH HAS A VERY SMALL CELL SIZE 64
FIGURE 25: PHYLOGENETIC TREE DETAILING THE GENETIC RELATIONSHIP OF FSA WITH OTHER MICROALGAE SPECIES. THE OUTLIER SPECIES USED WAS SCENEDESMUS COSTATUS. 65
FIGURE 26: FSB AND *NITZSCHIA NAVICULA*; OBTAINED FROM UNIVERSITY OF WISCONSIN PLANT TEACHING COLLECTION <HTTP://BOTIT.BOTANY.WISC.EDU/>. 65
FIGURE 27: PHYLOGENETIC TREE DETAILING THE GENETIC RELATIONSHIP OF FSB WITH OTHER MICROALGAE SPECIES. THE OUTLIER SPECIES USED WAS SCENEDESMUS COSTATUS. 66
FIGURE 28: FSD AND (I) *SCENEDESMUS PECTINATUS*, (II) *PECTINODESDUS PECTINATUS*, (III) *PECTINODESMUS HOLTMANNII*; (I) OBTAINED FROM PLINGFACTORY: LIFE IN WATER <HTTP://WWW.PLINGFACTORY.DE/PLING.HTML> ;(II) AND (III) (HEGEWALD 2013) OBTAINED FROM FOTTEA. 67
FIGURE 29: PHYLOGENETIC TREE DETAILING THE GENETIC RELATIONSHIP OF FSD WITH OTHER MICROALGAE SPECIES. THE OUTLIER SPECIES USED WAS *PSEUDO-NITZSCHIA DELICATISSIMA*. 67

Figure 30: FSE and Nephrochlamys subsolitaria; obtained from Protist Information Server <http://protist.i.hosei.ac.jp/index.html>. 68
Figure 31: Phylogenetic tree detailing the genetic relationship of FSE with other microalgae species. The outlier species used was *Scenedesmus costatus*. 69
Figure 32: FBP1 and Ankistrodesmus sp.; obtained from Protist Information Server < http://protist.i.hosei.ac.jp/index.html>. 69
Figure 33: Phylogenetic tree detailing the genetic relationship of FBP1 with other microalgae species. The Outlier species used was Scenedesmus costatus. 70
Figure 34: FBP2 and *Chlamydomonas moewusii*; obtained from Protist Information Server < http://protist.i.hosei.ac.jp/index.html>. 70
Figure 35: Phylogenetic tree detailing the genetic relationship of FBP2 with other microalgae species. The outlier species used was *Pseudo-nitzschia delicatissima*. 71
Figure 36: FDP and *Scenedesmus Obliquus*, another identity of *Acutodesmus obliquus*; obtained from Labroots.com, <http://legacy.labroots.com/default/index/index> 72
Figure 37: Phylogenetic tree detailing the genetic relationship of FDP with other microalgae species. The outlier species used was *Pseudo-nitzschia delicatissima*. 72
Figure 38: FTA1 and (i) *Scenedesmus acutus* and (ii) *Scenedesmus dimorphus*; (i) (Tsukii 1977) obtained from Protist Information Server <http://protist.i.hosei.ac.jp/index.html>, (ii) obtained from America Pink < http://america.pink/>. 73
Figure 39: Phylogenetic tree detailing the genetic relationship of FTA1 with other microalgae species. The outlier species used are *Scenedesmus costatus* and *Scenedesmus ellipticus* respectively. 74
Figure 40: FTA2 and *Ourococcus multisporus*. Obtained from Center for Freshwater Biology. <http://cfb.unh.edu/>. 75
Figure 41: Phylogenetic tree detailing the genetic relationship of FTA2 with other microalgae species. The outlier species used was *Pseudo-nitzschia delicatissima*. 75
Figure 42: FTAR and (i) *Desmodesmus serratus* and (ii) *Scenedesmus incrassatulus*; (i) (Hansen n.d.) obtained from Nordic Microalgae and Aquatic protozoa <http://nordicmicroalgae.org/>, (ii) (Tsukii 1977) obtained from Protist Information Server <http://protist.i.hosei.ac.jp/index.html>. 76
Figure 43: Phylogenetic tree detailing the genetic relationship of FTAR with other microalgae species. 77
Figure 44: FTAR2 and (i) *Desmodesmus pirkollei* and (ii) *Desmodesmus communis*; (i) and (ii) (Hegewald n.d.) obtained from Barcoding P.A.T.H.S. 78
Figure 45: Phylogenetic tree detailing the genetic relationship of FTAR2 with other microalgae species. The outlier species used are *Scenedesmus costatus* and *Scenedesmus ellipticus* respectively. 78
Figure 46: FBP3 and Nitzschia sp. Obtained from Kaikorai tributary, Otago Regional Council and Landcare Research. <https://www.landcareresearch.co.nz> 81
Figure 47: FTAR3 isolated from the Tunku Abdul Rahman Marine Park. 81
Figure 48: MAT1 isolated from the Telaga Air pier. 82
Figure 49: MTA2 microalgae isolated from the Telaga Air pier. 82
Figure 50: MTAR microalgae isolated from the Telaga Air pier. 83
Figure 51: The growth of the culture of micro algae FSA under different nutrient conditions. 85
Figure 52: The growth of the culture of microalgae *Nitzchia sp./Pseudo-nitzschia sp*. (FSB) under different nutrient conditions. 86
Figure 53: The growth of the culture of microalgae *Pectinodesmus pectinatus* (FSD) under different nutrient conditions. 87
Figure 54: The growth of the culture of microalgae *Nephrochlamys subsolitaria* (FSE) under different nutrient conditions. 88
Figure 55 The growth of the culture of microalgae *Ankistrodesmus gracilis* (FBP1) under different nutrient conditions. 90
Figure 56: The growth of the culture of microalgae *Chlamydomonas moewusii* (FBP2) under different nutrient conditions. 91
Figure 57: The growth of the culture of microalgae *Nitzchia sp./Pseudo-nitzschia sp*. (FBP3) under different nutrient conditions. 92
Figure 58: The growth of the culture of microalgae *Scenedesmus acutus* (FTA1) under different nutrient conditions. 93
Figure 59: The growth of the culture of microalgae *Ourococcus multisporus* (FTA2) under different nutrient conditions. 94

FIGURE 60: THE GROWTH OF THE CULTURE OF MICROALGAE *SCENEDESMUS INCRASSATULUS* (FTAR) UNDER DIFFERENT NUTRIENT CONDITIONS. 96
FIGURE 61: THE GROWTH OF THE CULTURE OF MICROALGAE *DESMODESMUS PIRKOLLEI* (FTAR2) UNDER DIFFERENT NUTRIENT CONDITIONS. 98
FIGURE 62: THE GROWTH OF THE CULTURE OF MICROALGAE (FTAR3) UNDER DIFFERENT NUTRIENT CONDITIONS. 99
FIGURE 63: THE GROWTH OF THE CULTURE OF MICROALGAE *ACUTODESMUS OBLIQUUS* (FDP) UNDER DIFFERENT NUTRIENT CONDITIONS. 100
FIGURE 64: THE GROWTH OF THE CULTURE OF MICROALGAE MTA1 UNDER DIFFERENT NUTRIENT CONDITIONS. 101
FIGURE 65: THE GROWTH OF THE CULTURE OF MICROALGAE MTA2 UNDER DIFFERENT NUTRIENT CONDITIONS. 102
FIGURE 66: THE GROWTH OF THE CULTURE OF MICROALGAE MTAR UNDER DIFFERENT NUTRIENT CONDITIONS. 103
FIGURE 67: PIE CHART OF TOTAL MOLE TO FAME 116
FIGURE 68 SHOWS THE ALGAE SLURRY, THE RESULTING CRUDE OIL AFTER THE HYDROTHERMAL LIQUEFACTION PROCESS AND THE OIL AFTER REFINING. OBTAINED FROM PACIFIC NORTHWEST NATIONAL LABORATORY. <HTTP://WWW.PNNL.GOV/> 125
FIGURE 69: FSA FAME SAMPLE (0X) CHROMATOGRAPH 150
FIGURE 70: FSA FAME SAMPLE (1X) CHROMATOGRAPH 150
FIGURE 71: FSA FAME SAMPLE (5X) CHROMATOGRAPH 151
FIGURE 72: FSA FAME SAMPLE (10X) CHROMATOGRAPH 151
FIGURE 73: FSB FAME SAMPLE (0X) CHROMATOGRAPH 152
FIGURE 74: FSB FAME SAMPLE (1X) CHROMATOGRAPH 152
FIGURE 75: FSB FAME SAMPLE (5X) CHROMATOGRAPH 153
FIGURE 76: FSB FAME SAMPLE (10X) CHROMATOGRAPH 153
FIGURE 77: FSD FAME SAMPLE (0X) CHROMATOGRAPH 154
FIGURE 78: FSD FAME SAMPLE (1X) CHROMATOGRAPH 154
FIGURE 79: FSD FAME SAMPLE (5X) CHROMATOGRAPH 155
FIGURE 80: FSD FAME SAMPLE (10X) CHROMATOGRAPH 155
FIGURE 81: FSE FAME SAMPLE (0X) CHROMATOGRAPH 156
FIGURE 82: FSE FAME SAMPLE (1X) CHROMATOGRAPH 156
FIGURE 83: FSE FAME SAMPLE (5X) CHROMATOGRAPH 157
FIGURE 84: FSE FAME SAMPLE (10X) CHROMATOGRAPH 157
FIGURE 85: FBP1 FAME SAMPLE (0X) CHROMATOGRAPH 158
FIGURE 86: FBP1 FAME SAMPLE (1X) CHROMATOGRAPH 158
FIGURE 87: FBP1 FAME SAMPLE (5X) CHROMATOGRAPH 159
FIGURE 88: FBP1 FAME SAMPLE (10X) CHROMATOGRAPH 159
FIGURE 89: FBP2 FAME SAMPLE (0X) CHROMATOGRAPH 160
FIGURE 90: FBP2 FAME SAMPLE (1X) CHROMATOGRAPH 160
FIGURE 91: FBP2 FAME SAMPLE (5X) CHROMATOGRAPH 161
FIGURE 92: FBP2 FAME SAMPLE (10X) CHROMATOGRAPH 161
FIGURE 93: FBP3 FAME SAMPLE (0X) CHROMATOGRAPH 162
FIGURE 94: FBP3 FAME SAMPLE (1X) CHROMATOGRAPH 162
FIGURE 95: FBP3 FAME SAMPLE (5X) CHROMATOGRAPH 163
FIGURE 96: FBP3 FAME SAMPLE (10X) CHROMATOGRAPH 163
FIGURE 97: FTA1 FAME SAMPLE (0X) CHROMATOGRAPH 164
FIGURE 98: FTA1 FAME SAMPLE (1X) CHROMATOGRAPH 164
FIGURE 99: FTA1 FAME SAMPLE (5X) CHROMATOGRAPH 165
FIGURE 100: FTA1 FAME SAMPLE (10X) CHROMATOGRAPH 165
FIGURE 101: FTA2 FAME SAMPLE (0X) CHROMATOGRAPH 166
FIGURE 102: FTA2 FAME SAMPLE (1X) CHROMATOGRAPH 166
FIGURE 103: FTA2 FAME SAMPLE (5X) CHROMATOGRAPH 167
FIGURE 104: FTA2 FAME SAMPLE (10X) CHROMATOGRAPH 167
FIGURE 105: MTA1 FAME SAMPLE (0X) CHROMATOGRAPH 168
FIGURE 106: MTA1 FAME SAMPLE (1X) CHROMATOGRAPH 168
FIGURE 107: MTA1 FAME SAMPLE (5X) CHROMATOGRAPH 169
FIGURE 108: MTA1 FAME SAMPLE (10X) CHROMATOGRAPH 169
FIGURE 109: MTA2 FAME SAMPLE (0X) CHROMATOGRAPH 170
FIGURE 110: MTA2 FAME SAMPLE (1X) CHROMATOGRAPH 170
FIGURE 111: MTA2 FAME SAMPLE (5X) CHROMATOGRAPH 171
FIGURE 112: MTA2 FAME SAMPLE (10X) CHROMATOGRAPH 171

FIGURE 113: FTAR FAME SAMPLE (0X) CHROMATOGRAPH 172
FIGURE 114: FTAR FAME SAMPLE (1X) CHROMATOGRAPH 172
FIGURE 115: FTAR FAME SAMPLE (5X) CHROMATOGRAPH 173
FIGURE 116: FTAR FAME SAMPLE (10X) CHROMATOGRAPH 173
FIGURE 117: FTAR2 FAME SAMPLE (0X) CHROMATOGRAPH 174
FIGURE 118: FTAR2 FAME SAMPLE (1X) CHROMATOGRAPH 174
FIGURE 119: FTAR2 FAME SAMPLE (5X) CHROMATOGRAPH 175
FIGURE 120: FTAR2 FAME SAMPLE (10X) CHROMATOGRAPH 175
FIGURE 121: FTAR3 FAME SAMPLE (0X) CHROMATOGRAPH 176
FIGURE 122: FTAR3 FAME SAMPLE (1X) CHROMATOGRAPH 176
FIGURE 123: FTAR3 FAME SAMPLE (5X) CHROMATOGRAPH 177
FIGURE 124: FTAR3 FAME SAMPLE (10X) CHROMATOGRAPH 177
FIGURE 125: MTAR FAME SAMPLE (0X) CHROMATOGRAPH 178
FIGURE 126: MTAR FAME SAMPLE (1X) CHROMATOGRAPH 178
FIGURE 127: MTAR FAME SAMPLE (5X) CHROMATOGRAPH 179
FIGURE 128: MTAR FAME SAMPLE (10X) CHROMATOGRAPH 179
FIGURE 129: FDP FAME SAMPLE (0X) CHROMATOGRAPH 180
FIGURE 130: FDP FAME SAMPLE (1X) CHROMATOGRAPH 180
FIGURE 131: FDP FAME SAMPLE (5X) CHROMATOGRAPH 181
FIGURE 132: FDP FAME SAMPLE (10X) CHROMATOGRAPH 181

List of Tables

TABLE 1: OVERVIEW OF MAIN MICROALGAE GROUPS AND THEIR CHARACTERISTICS. 16
TABLE 2: LIST OF MATERIALS TO PREPARE THE FE STOCK OF THE ESDK STOCK. THE SOLUTION IS BROUGHT TO A FINAL VOLUME OF 500 ML USING MILLIPORE H2O. 40
TABLE 3: LIST OF MATERIALS TO PREPARE THE P2 STOCK OF THE ESDK STOCK. THE SOLUTION IS BROUGHT TO A FINAL VOLUME OF 400 ML USING MILLIPORE H2O. 41
TABLE 4: LIST OF MATERIALS TO PREPARE THE ESDK STOCK. THE SOLUTION IS BROUGHT TO A FINAL VOLUME OF 400 ML USING MILLIPORE H2O. 41
TABLE 5: LIST OF MATERIALS THAT MAKE UP THE CTAB BUFFER 43
TABLE 6: THE STANDARD PROTOCOL OF MYTAQ RED PIX PCR KIT. OBTAINED FROM MYTAQ RED MIX PRODUCT MANUAL. (BIOLINE N.D.) 48
TABLE 7: THE PHOSPHATE (PO4) AND NITRATE (NO3) CONCENTRATION OF 1X, 5X AND 10X USED IN THE CULTURE GROWTH EXPERIMENT 49
TABLE 8: IDENTITIES, MOLECULAR CHARACTERISTICS AND ENERGY POTENTIAL OF THE FATTY ACID METHYL ESTERS DETECTABLE BY THE GCMS 59
TABLE 9: MICROALGAE STRAINS ISOLATED FROM THE WATER SAMPLES LISTED WITH THEIR LABEL, ORIGIN AND CHARACTERISTICS 62
TABLE 10: IDENTITY STATISTICS OF FSA 65
TABLE 11: IDENTITY STATISTICS OF FSB. 66
TABLE 12: IDENTITY STATISTICS OF FSD. 68
TABLE 13: IDENTITY STATISTICS OF FSE 69
TABLE 14: IDENTITY STATISTICS OF FBP1 70
TABLE 15: IDENTITY STATISTICS OF FBP2 71
TABLE 16: IDENTITY STATISTICS OF FDP. 73
TABLE 17: IDENTITY STATISTICS OF FTA1 74
TABLE 18: IDENTITY STATISTICS OF FTA2 76
TABLE 19: IDENTITY STATISTICS OF FTAR. 77
TABLE 20: IDENTITY STATISTICS OF FTAR2 79
TABLE 21: SUMMARY OF THE IDENTITIES OF THE SEQUENCED MICROALGAE SAMPLES 80
TABLE 22: THE AMOUNT OF FAME PRODUCED AND FATS (%) OF MICROALGAE FSA UNDER DIFFERENT NUTRIENT CONDITIONS. 85
TABLE 23: THE AMOUNT OF FAME PRODUCED AND FATS (%) OF MICROALGAE *NITZCHIA SP./PSEUDO-NITZSCHIA SP.* (FSB) UNDER DIFFERENT NUTRIENT CONDITIONS. 86
TABLE 24: THE AMOUNT OF FAME PRODUCED AND FATS (%) OF MICROALGAE *PECTINODESMUS PECTINATUS* (FSD) UNDER DIFFERENT NUTRIENT CONDITIONS. 87
TABLE 25: THE AMOUNT OF FAME PRODUCED AND FATS (%) OF MICROALGAE *NEPHROCHLAMYS SUBSOLITARIA* (FSE) UNDER DIFFERENT NUTRIENT CONDITIONS. 88
TABLE 26: THE AMOUNT OF FAME PRODUCED AND FATS (%) OF MICROALGAE *ANKISTRODESMUS GRACILIS* (FBP1) UNDER DIFFERENT NUTRIENT CONDITIONS. 90
TABLE 27: THE AMOUNT OF FAME PRODUCED AND FATS (%) OF MICROALGAE *CHLAMYDOMONAS MOEWUSII* (FBP2) UNDER DIFFERENT NUTRIENT CONDITIONS. 91
TABLE 28: THE AMOUNT OF FAME PRODUCED AND FATS (%) OF MICROALGAE *NITZCHIA SP./PSEUDO-NITZSCHIA SP.* (FBP3) UNDER DIFFERENT NUTRIENT CONDITIONS. 92
TABLE 29: THE AMOUNT OF FAME PRODUCED AND FATS (%) OF MICROALGAE *SCENEDESMUS ACUTUS* (FTA1) UNDER DIFFERENT NUTRIENT CONDITIONS. 93
TABLE 30: THE AMOUNT OF FAME PRODUCED AND FATS (%) OF MICROALGAE *OUROCOCCUS MULTISPORUS* (FTA2) UNDER DIFFERENT NUTRIENT CONDITIONS. 94
TABLE 31: THE AMOUNT OF FAME PRODUCED AND FATS (%) OF MICROALGAE *SCENEDESMUS INCRASSATULUS* (FTAR) UNDER DIFFERENT NUTRIENT CONDITIONS. 96
TABLE 32: THE AMOUNT OF FAME PRODUCED AND FATS (%) OF MICROALGAE *DESMODESMUS PIRKOLLEI* (FTAR2) UNDER DIFFERENT NUTRIENT CONDITIONS. 97
TABLE 33: THE AMOUNT OF FAME PRODUCED AND FATS (%) OF MICROALGAE (FTAR3) UNDER DIFFERENT NUTRIENT CONDITIONS. 99
TABLE 34: THE AMOUNT OF FAME PRODUCED AND FATS (%) OF MICROALGAE *ACUTODESMUS OBLIQUUS* (FDP) UNDER DIFFERENT NUTRIENT CONDITIONS. 100
TABLE 35: THE AMOUNT OF FAME PRODUCED AND FATS (%) OF MICROALGAE MTA1 UNDER DIFFERENT NUTRIENT CONDITIONS. 101
TABLE 36: THE AMOUNT OF FAME PRODUCED AND FATS (%) OF MICROALGAE MTA2 UNDER DIFFERENT NUTRIENT CONDITIONS. 102

TABLE 37: THE AMOUNT OF FAME PRODUCED AND TOTAL FATS (%) OF MICROALGAE MTAR UNDER DIFFERENT NUTRIENT CONDITIONS. 103
TABLE 38: ENERGY VALUES OF THE FAME PRODUCED BY FSA 104
TABLE 39: ENERGY VALUES OF THE FAME PRODUCED BY *NITZCHIA SP./PSEUDO-NITZSCHIA SP.* (FSB). 104
TABLE 40: ENERGY VALUES OF THE FAME PRODUCED BY *PECTINODESMUS PECTINATUS* (FSD). 105
TABLE 41: ENERGY VALUES OF THE FAME PRODUCED BY *NEPHROCHLAMYS SUBSOLITARIA* (FSE). 105
TABLE 42: ENERGY VALUES OF THE FAME PRODUCED BY *ANKISTRODESMUS GRACILIS* (FBP1). 106
TABLE 43: ENERGY VALUES OF THE FAME PRODUCED BY *CHLAMYDOMONAS MOEWUSII* (FBP2). 106
TABLE 44: ENERGY VALUES OF THE FAME PRODUCED BY *NITZCHIA SP./PSEUDO-NITZSCHIA SP*. (FBP3). 107
TABLE 45: ENERGY VALUES OF THE FAME PRODUCED BY *SCENEDESMUS ACUTUS* (FTA1). 107
TABLE 46: ENERGY VALUES OF THE FAME PRODUCED BY *OUROCOCCUS MULTISPORUS* (FTA2) 108
TABLE 47: ENERGY VALUES OF THE FAME PRODUCED BY *SCENEDESMUS INCRASSATULUS* (FTAR). 108
TABLE 48: ENERGY VALUES OF THE FAME PRODUCED BY *DESMODESMUS PIRKOLLEI* (FTAR2). 109
TABLE 49: ENERGY VALUES OF THE FAME PRODUCED BY FTAR3. 109
TABLE 50: ENERGY VALUES OF THE FAME PRODUCED BY *ACUTODESMUS OBLIQUUS* (FDP). 110
TABLE 51: ENERGY VALUES OF THE FAME PRODUCED BY MTA1. 110
TABLE 52: ENERGY VALUES OF THE FAME PRODUCED BY MTA2. 111
TABLE 53: ENERGY VALUES OF THE FAME PRODUCED BY MTAR. 111
TABLE 54: COMPARISON OF MTA1 (5X), ACUTODESMUS OBLIQUUS (FDP) (5X), NITZCHIA SP./PSEUDO-NITZSCHIA SP. (FSB) (10X), FTAR3 (5X), NITZCHIA SP./PSEUDO-NITZSCHIA SP. (FBP3) (1X) AND (5X) WITH OTHER BIOFUELS AND FOSSIL FUELS 120
TABLE 55: DRY MASS OF FSA 147
TABLE 56: DRY MASS OF FSB 147
TABLE 57: DRY MASS OF FSD 147
TABLE 58: DRY MASS OF FSE 147
TABLE 59: DRY MASS OF FBP1 147
TABLE 60: DRY MASS OF FBP2 148
TABLE 61: DRY MASS OF FBP3 148
TABLE 62: DRY MASS OF FTA1 148
TABLE 63: DRY MASS OF FTA2 148
TABLE 64: DRY MASS OF MTA1 148
TABLE 65: DRY MASS OF MTA2 148
TABLE 66: DRY MASS OF FTAR 149
TABLE 67: DRY MASS OF FTAR2 149
TABLE 68: DRY MASS OF FTAR3 149
TABLE 69: DRY MASS OF MTAR 149
TABLE 70: DRY MASS OF FDP 149

Introduction

Environmental Pollution

Environmental pollution comes from a variety of anthropological sources and activities (Schell & Denham 2003). When a human population releases more waste than the environment can handle, the delicate balance is upset and the ecosystem is endangered, usually by the waste itself or problematic organisms that arrive due to the waste (Rao 2007). One example of an environmental pollution is nutrient pollution in which excess nutrients is introduced to the environment causing damage to the ecosystem and biology (*NOAA's National Ocean Service: Nonpoint Source Pollution* 2007).

Nutrient Loss

Nutrient loss is a phenomenon where a system loses its nutrients to a nutrient sink. The highest nutrient loss could be observed in agricultural lands where the nutrients are leeched off the land through the crops as they grow and the crop is harvested to be fed to humans and animals, leaving the land stripped of nutrients (*Nutrient management on your dairy farm* 2013). This will result in a net loss of nutrients for the agricultural land, making it incapable of restoring its nutrients, rendering it infertile. The nutrients are routinely replenished with fertilizers but the chemicals in the fertilizers are easily dissolved in water (Ma et al. 2012), generating nutrient rich runoff which causes havoc to the natural ecosystem. As a result, pockets of high nutrient loads are created (Bianchi et al. 2006), killing of biodiversity and encouraging less desirable species like pathogenic microbes and pests to thrive. This problem is further discussed in the following paragraph. Furthermore, the agricultural industry is dependent on chemical fertilizers (Ghosh 2004) which ultimately accelerate the problem.

Eutrophication

Eutrophication is the enrichment of an ecosystem with nutrients, typically compounds containing nitrogen and phosphorus, and promotes excessive growth and decay of simple algae and plankton (Nixon 1995), causing a severe reduction in water quality (Wang et al. 1999).

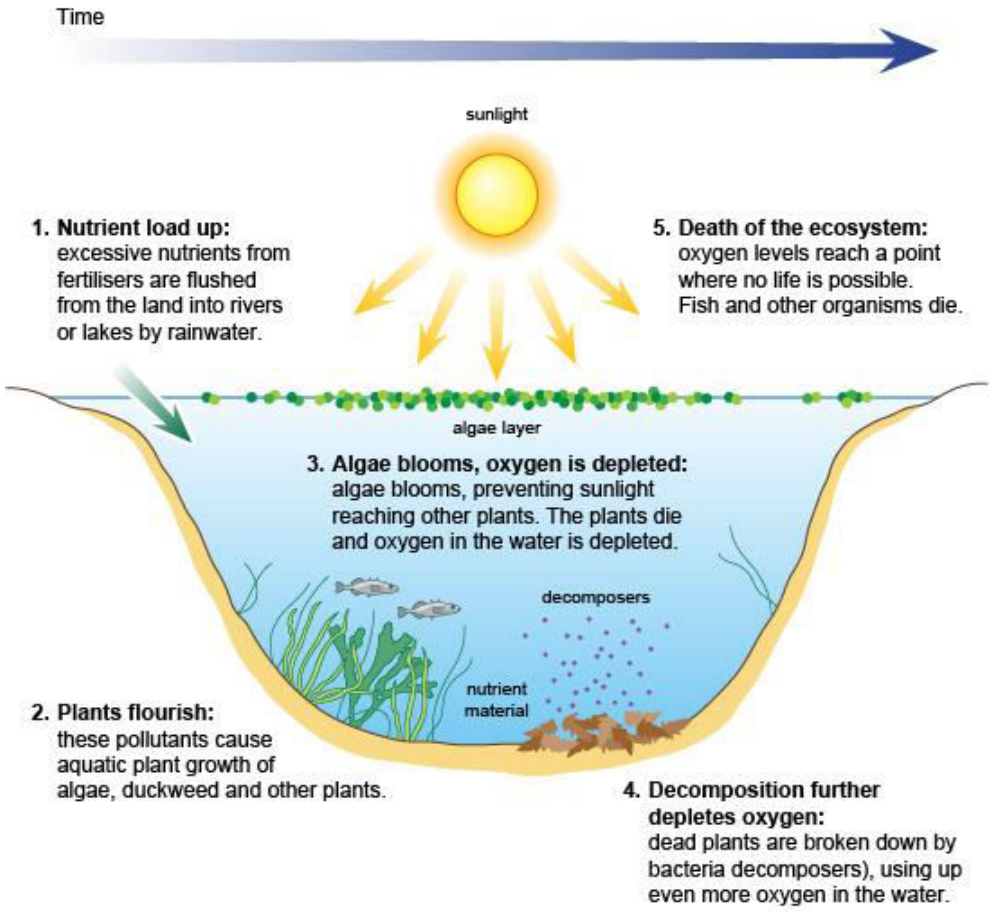

Figure 1: Eutrophication process. Obtained from BBC. <http://www.bbc.co.uk/>

When an algal bloom dies off, the dead biomass promotes the growth of decomposing bacteria which accelerates the decomposition of the biomass. This process will use up all the oxygen dissolved in the water, creating a state of hypoxia or oxygen depleted zone, suffocating and killing most of the biodiversity in the water body (Figure 1). Furthermore, some algal blooms are harmful as they consist of a microalgae species that produce toxins that can accumulate up the food chain increasing species mortality (Anderson 1994). Neurotoxins and hepatotoxins can also accumulate in animals which are eaten by humans (Lawton and Codd 1991), causing illness that may result in death.

Algae

Natural water bodies ranging from rivers and lakes to seas and oceans often boast elaborate food webs (*The Food Web* 2004). Algae are producers at the bottom of the food chain and consist of a large, diverse eukaryotic group of autotrophs (Rosemond et al. 1993). Algae have recently garnered scientific interest stemmed from the interest of mapping biodiversity (Kerswell 2006), aquaculture (Borowitzka 1997), or finding a solution to looming energy demands (Demirbas 2010). Algae only need sunlight and nutrients to grow (Rosemond et al. 1993), making it easy to cultivate them with little effort. Their biodiversity is enormous and encompass as many as 72,500 species (Guiry 2012). Furthermore, microalgae (see next paragraph for a more detailed description) produce a wide variety of compounds (Cardozo et al. 2007) such as antioxidants, carotenoids, enzymes, fatty acids, peptides, polymers, sterols, and toxins.

Microalgae

Microphytes, or more familiarly, microalgae, are microscopic algae that exist individually in nature in freshwater and marine systems (Thurman 1997). They are unicellular and range in sizes from a few micrometers to a few hundred micrometers (Thrush et al. 2006). Microalgae lack roots, stems, or leaves that make up the basic anatomy of multicellular plants but they are capable of photosynthesis (Thrush et al. 2006). Very much as bigger plants, they are important to life on earth as they contribute a large portion of the Earth's atmospheric oxygen and absorb a great amount of greenhouse gas CO_2 (Biello 2009). Owning the characteristics of a microorganism, the microalgae outpaces the growth rates of common plants as the cells can double their numbers within a day. Microalgae can be divided into two types; phytoplankton which commonly inhabit the water surface and benthic algae which attaches itself to surfaces like rocks and bottoms (Gully and Kennedy 1987). Table 1 provides an overview of the various genus that sport different cell shapes and colors.

Table 1: Overview of main microalgae groups and their characteristics.

Group	Description	Reference
Cyanobacteria	Blue-green microalgae and a class of prokaryotic aquatic bacteria	Allaby 1992
Prochlorophyta	Oligotrophic organisms abundant in nutrient poor tropical waters. Use a unique photosynthetic pigment, divinyl-chlorophyll, to absorb light and acquire energy	Lewin 2002
Glaucophyta	Freshwater microalgae consisting of red and green algae	Nozaki et al. 2009
Rhodophyta	Red algae which are one of the oldest and largest groups of eukaryotic algae	Lee 2008 Thomas 2002
Chrysophyta	Commonly golden colored algae	Margulis et.al. 1990
Phaeophyta	Brown marine algae	Earle 1968
Chlorophyta	Most common aquatic algae	Hoek 1995
Diatoms	Unicellular organism enclosed within a silica cell wall	Waggoner n.d.
Euglenophyta	Group of flagellates which have mitochondria and chloroplasts	Keeling 2008
Dinoflagellata	Flagellate protists commonly in fresh water	Stoecker 1999

The diversity and impressive range of shapes and colors is illustrated in Figure 2 below which provides an overview of various microalgae.

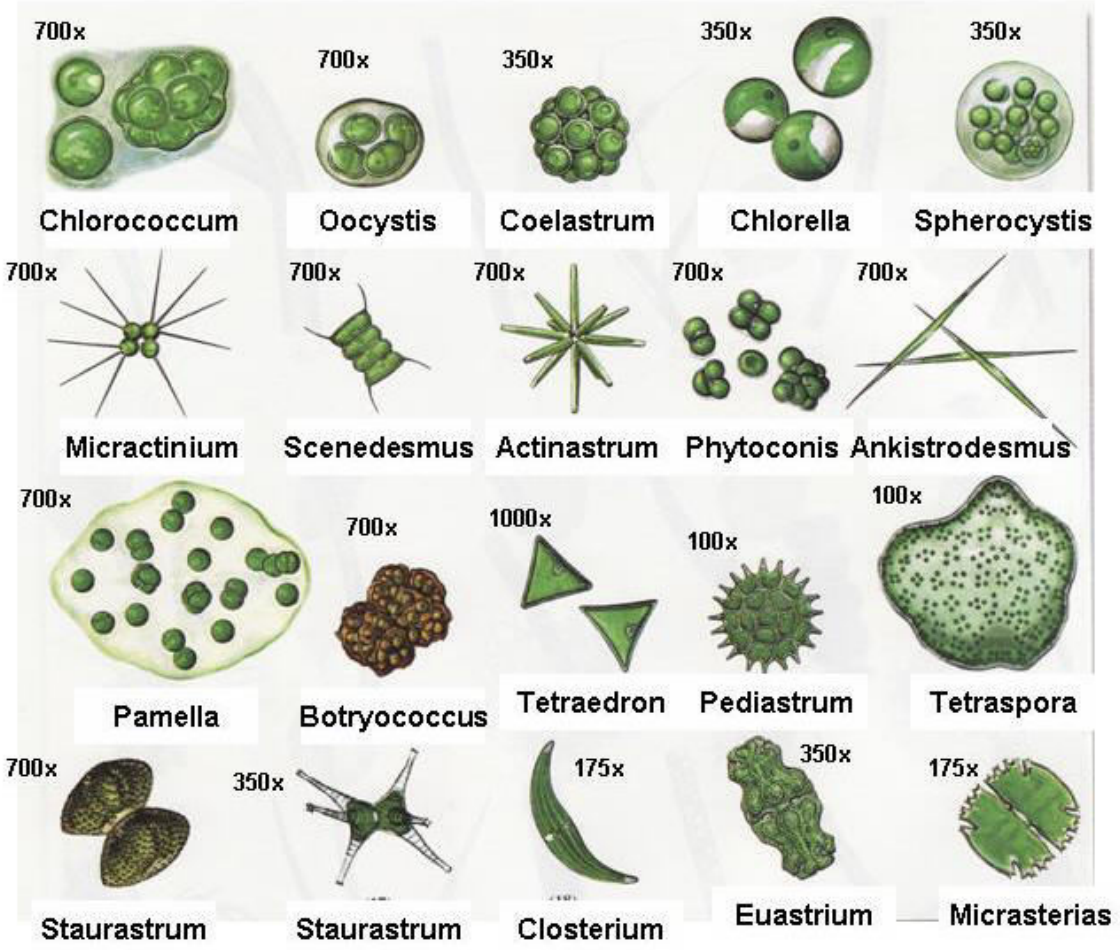

Figure 2: Examples of microalgae and their unique morphology. Obtained from Professor Schmid's Biology Website. <http://classroom.sdmesa.edu/eschmid/>

Microalgae have found application in many areas, as mentioned above, however, the one that is of particular concern to this thesis, is their use as bioremediation agents, which will be introduced in the following.

Bioremediation

Bioremediation is a waste management technique which utilizes biological organisms to treat contaminated sites (Baker and Herson 1994). Bioremediation has been touted as a better option of waste treatment compared to chemical treatment (Philp 2015) as it does not produce other harmful by-products and allows treatment to be carried out on site. Bioremediation usually consists of two different approaches:

1. Introduction of required nutrients to stimulate growth of the indigenous bioremediators so natural bioremediation can be sped up (Baker and Herson 1994).
2. Introduction of bioremediators to a polluted site to bioremediate pollutants that are toxic to most indigenous microorganisms (Baker and Herson 1994).

A commercial example of bioremediation is the system employed by Biogenie Inc. which combines bioremediation and volatilization. Polluted soil is dug up and collected into a biopile at the treatment site. The biopile system consists of a solid platform for the biopile, a suspended spray irrigation system for moisture and nutrient introduction, a drainage system for leachate, an air pump for aeration, and waterproof sheeting for moisture and aeration control. Hydrocarbon pollutants like diesel fuel, gasoline and other petroleum products present in the soil are targeted by desired heterotrophic aerobic microorganisms. The bioremediation method which boasts an efficiency of 80% for mineral oils and grease and 95% for monocyclic aromatic hydrocarbons has the advantages of minimal space requirement, low cost and generates no liquid waste or risks of contamination of targeted site (Lei et al. 1994).

Another example of bioremediation includes the use of microbes to biodegrade chlorophenol contaminated groundwater. Pentachlorophenol, a wood preservative, persists in the groundwater due to the absences of chlorophenol-degrading organisms or relatively limited conditions necessary for bioremediation (Jarvinen et al. 1994). Jarvinen et al. (1994) demonstrated that *flavobacterium* and *rhodococcus* bacteria in an aerobic fluidized-bed system (Figure 3) could biodegrade the chlorophenol to concentrations comparable to drinking water quality.

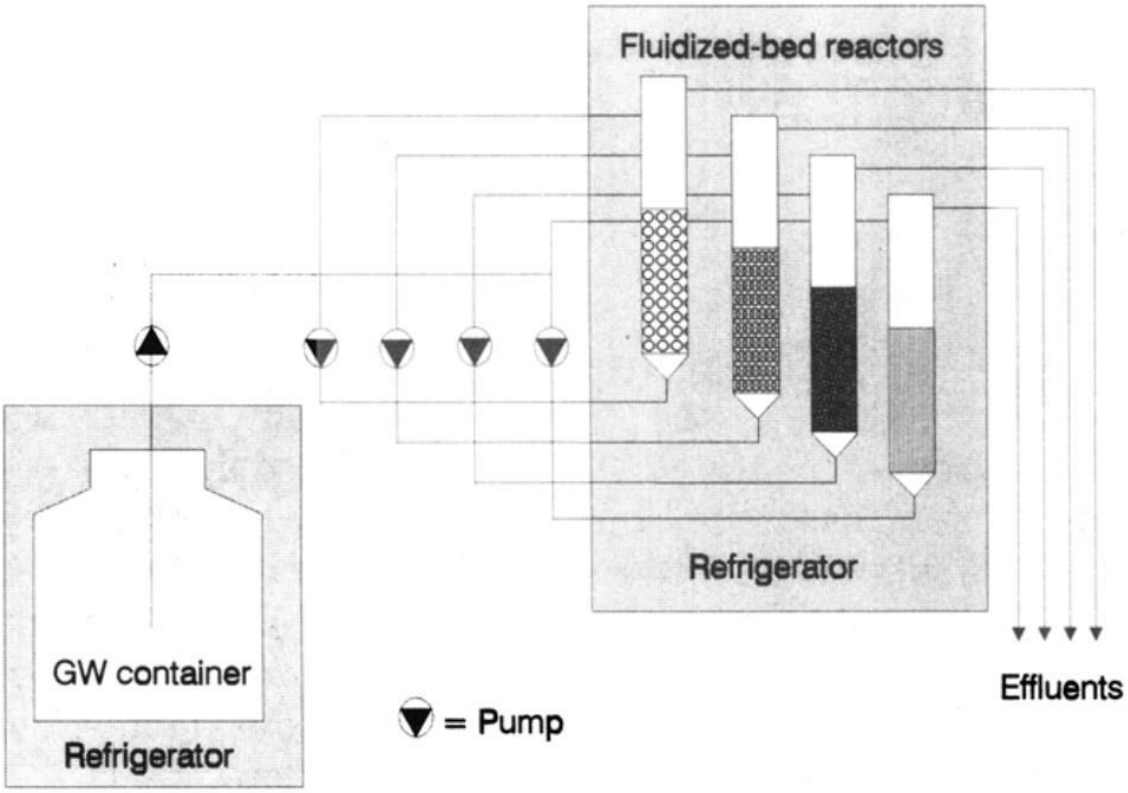

Figure 3: A diagram of the aerobic fluidized-bed bioremediation system for groundwater contaminated with chlorophenol. Obtained from Environmental Science and Technology. Jarvinen et al. (1994).

In China, bioremediation was used to treat pollution in water bodies affected by domestic wastewater effluent and agricultural runoff which triggered algal blooms resulting in odorous, blackened water, void of aquatic life (Qian et al. 2007). A bioreactor system (Figure 4) was chosen above ecological floating bed and constructed wetlands due to the aforementioned methods producing secondary pollution, being time-consuming, having poor efficiency during low temperature periods during winter (Li et al. 2010). The batch reactor removed 66.1% of the CODcr (Chemical Oxygen Demand; K2Cr2O7 as oxidizer) and the continuous flow reactor yielded 11.2–74.3% removal rate of CODMn (permanganate index), 2.2–56.1% removal for ammonia nitrogen, 20–100% turbidity, and a 88.6% bacterial community with a 3.5 hour retention time (Wenping et al. 2012). Wenping et al. (2012) concluded that the bioremediation procedure is practical and efficient, proposing that polluted surface water can be remediated with biofilms on filamentous bamboo due to the rich microbial community formed on the bamboo.

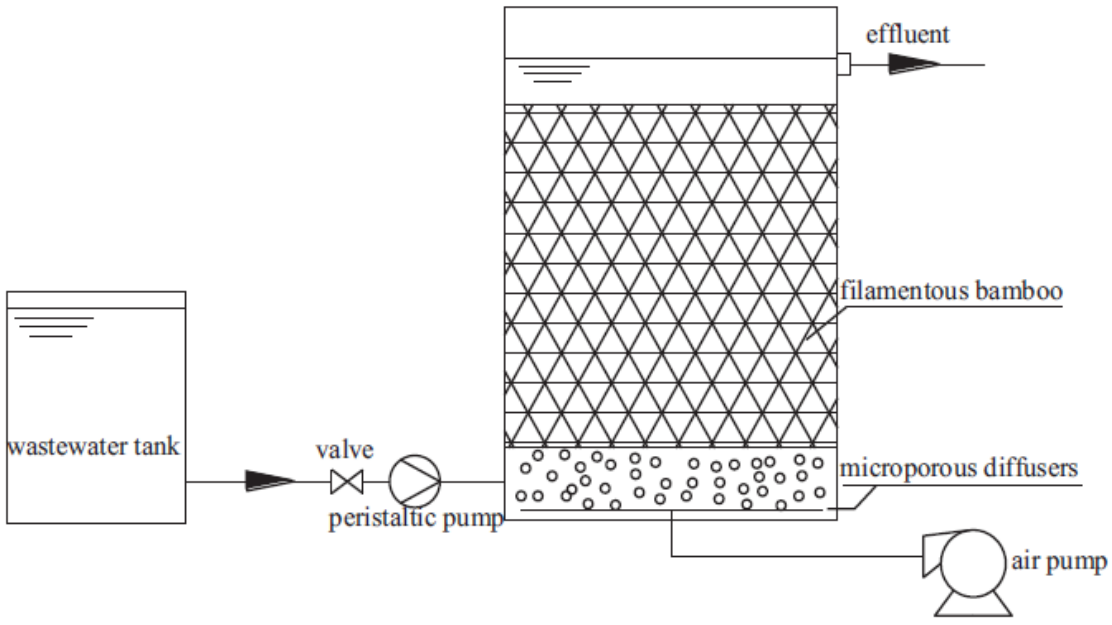

Figure 4: The schematic diagram of bioreactor utilizing filamentous bamboo. Obtained from Ecological Engineering, Wenping et al. (2012).

India, the largest producer of pesticides in Asia with an annual production of 90000 tons, exposes 56.7% of its population who works in the agricultural industry to pesticides used in agriculture (Boricha and Fulekar 2009). A research in 2009 assesses and utilizes the potential of microorganisms isolated from animal waste, specifically from cows to remove the pesticide cypermethrin from agricultural runoff (Boricha and Fulekar 2009). *Actinomycetes sp*., *Alcaligens sp*., *Bacillus sp*., *Cellulomonas sp*., *Escherichia coli*, *Flavobacterium sp*., *Nocardia sp*., *Pseudomonas sp*., *Salmonella sp*., *Sarcina sp*., *Serratia sp*., *Staphylococcus aureus*, and fungi *Aspergillu sp*., *Mucor sp*., *Penicillium sp*., and *Rhizopus sp*. were isolated from the cow waste and were tested on their ability to bioremediate cypermethrin (Figure 5), a pesticide used as a neurotoxin to pest insects. Utilizing a scale-up technique by increasing concentrations of cypermethrin of 10 mg/L, 25 mg/L, 50 mg/L and 100 mg/L (Boricha and Fulekar 2009), the strain that survived the higher concentrations of cypermethrin was *Pseudomonas plecoglossicida*, a novel organism for bioremediation of cypermethrin.

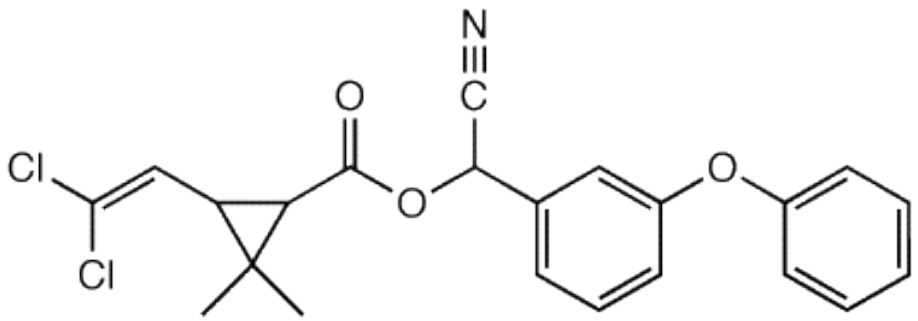

Figure 5: The molecular structure for cypermethrin. Obtained from Pesticide Action Network (PAN) Pesticide Database. <http://www.pesticideinfo.org/>

Another research from India focuses on the bioremediation of Phenols, a significant pollutant in industrial waste water (Kanekar et al. 1998). Alkaliphillic bacteria were isolated from an alkaline lake in Lonar, Maharashtra, to bioremediate phenol in the waste water. Bacteria were selectively isolated through phenol enrichment at pH 10 and phenol concentration of 500 mg/L. Alkaliphilic strains of *Arthrobacter sp*., *Bacillus cereus*, *Citrobacter freundii*, *Micrococcus agilis* and *Pseudomonas putida biovar. B* were described to completely remove phenol from the waste water within 48 hours of incubation in shake culture conditions at temperatures of 26 to 30 °C (Kanekar et al. 1998).

Bioremediation in Malaysia

In Malaysia, a majority of bioremediation efforts are centred towards treatment of pollution caused by petroleum products and industrial waste. Hamzah et al. (2013) isolated and identified *Pseudomonas aeruginosa* and *Rhodococcus sp*. from groundwater of a petroleum refinery plant. The bacterial isolates and consortia of the bacterial strains showed preferences for nitrogen for optimum growth as well as well as the ability to biodegrade Tapis Massa Oil at a rate of 97.6-99.9% (Hazmah et al. 2013).

Another bioremediation effort catered to the textile industry as the industry is considered a major producer of toxic wastewater laced with chemicals from wet processing (Rakmi 1993). A prototype treatment system, was constructed by Idris et al. (2007), consisting of four major components which involve pre-treatment, bio-treatment, polishing and bio-sludge treatment. The system yielded an average removal of 98% of Chemical Oxygen Demand (COD), 92% of colouring chemicals, 98.8% of ammonia nitrogen and 89% of Total Suspended Solids (TSS) (Idris et al. 2007).

Aside from the oil and textile industry, research efforts in utilizing bioremediation are also undertaken in the aquaculture industry. Devaraja (2002) isolated *Bacillus pumilus*, *Bacillus subtilis*, and *Bacillus lichenifonnis* were isolated from brackish water and sediment samples collected around the west coast of Peninsular Malaysia and analysed for their potential in bioremediation. The bacteria tolerated ammonia levels up to 20 mg/L and exhibited stunted growth at 25 mg/L. They secreted extracellular enzymes amylase, gelatinase, lipase and protease and were compatible with each other in mixed culture conditions. They were able to reduce ammonia levels as well as inhibit shrimp-pathogenic bacteria of the Vibrio genus (Devaraja 2002).

Microalgae's potential in bioremediation

Phycoremediation is a bioremediation process that uses macroalgae and microalgae to treat contaminated or polluted sites (Olguin 2003). Garnering significant attention and research on microalgae on heavy metal biosorption (Karthikeyan et al. 2007), microalgae is a viable bioremediation candidate as its potential in nutrient waste bioremediation could supplement nutrient waste treatment at a time where energy problems and the rising cost of maintenance and chemicals start to arise.

Utilizing algal cultures as a mean for carbon sequestration, bioremediation that involves carbon dioxide removal from the atmosphere (Sedjo and Sohngen 2012), Moheimani (2005) selected *Coccolithophorid* microalgae in this research because they sequestrate carbon in the form of calcium carbonate in addition to photosynthesis. The microalgae also produce large amounts of lipids which could be utilized in biofuel production. *Emiliania huxleyi*, *Gephyrocapsa oceanica*, *Pleurochrysis sp*., and *Pleurochrysis carterae* (Figure 6) were tested against different growth parameters including temperature, salinity, growth rate and pH. The species were found to tolerate high temperatures up to 28˚C. The highest productivity was observed in *Pleurochrysis carterae*, with 0.54 g/L per day for total dry weight, 0.12 g /L per day for lipid and 0.06 g/L per day for calcium carbonate. *P. carterae* and *E. huxleyi* were cultured in open raceway ponds and *E. huxleyi* was observed to be easily contaminated, resulting in the loss of the culture in three weeks while *P. carterae* showed positive growth with lipid and calcium carbonate content at 33% and 10%, respectively with little contamination interference from protozoa and bacteria. The medium pH was noted to peak at pH 11 during the day and was inferred as an important indicator of a healthy culture. Furthermore, medium of pH peak 8.5 during the day was indicative of the impending collapse of the culture. Seasonal environmental influences such as heavy rain and cold temperatures threatened the cultures while high summer temperatures favoured culture growth. The concentration of oxygen also affected the growth rate of the culture as high concentrations significantly impaired the photosynthesis of *P. carterae*. Moheimani (2005) concluded the research with the calculation of the cost of biomass generation in a 63-hectare raceway plant culturing *P. carterae* within the range of 7.35 Aus$/kg and 14.17 Aus$/kg with respect to the harvesting method used.

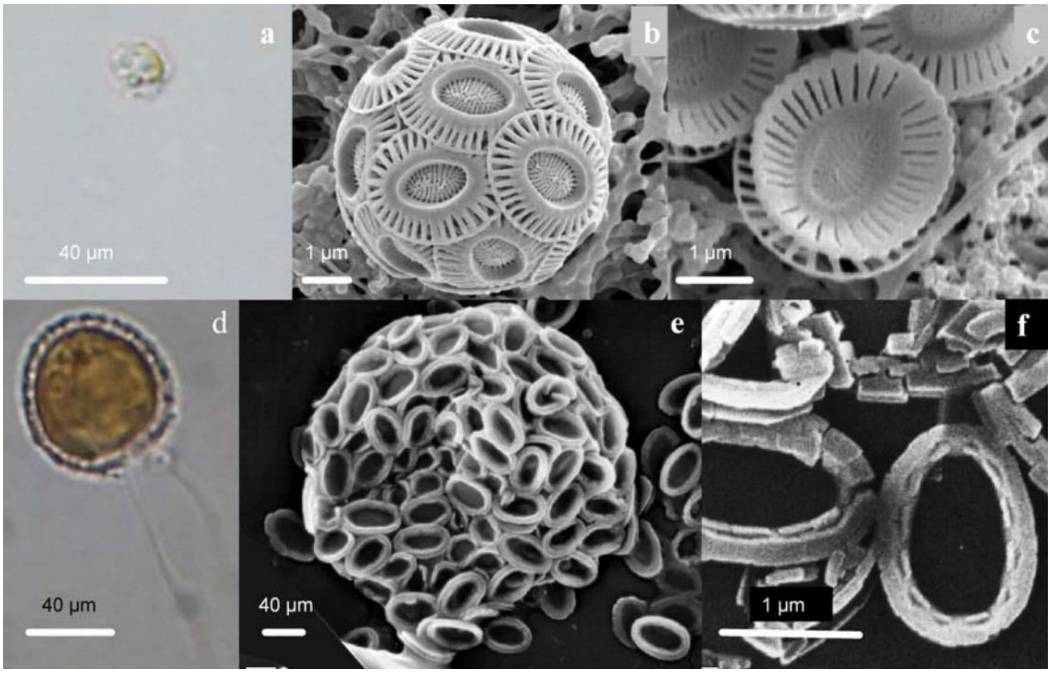

Figure 6: Micrographs of heterococcolithophorids Emiliania huxleyi (a, b, c) and Pleurochrysis carterae (d, e, f). (a) and (d) obtained by light micrograph, (b) and (e) obtained by scanning electron microscope, and images (c) and (f) obtained from Natural History Museum SEM database. Obtained from Doctor of Philosophy thesis 'The culture of coccolithophorid microalgae for carbon dioxide bioremediation'. Moheimani (2005)

Douskova et al. (2009) utilized the flue gas from municipal waste incineration as a source of carbon dioxide to grow the microalgae *Chlorella vulgaris* for biomass generation. The flue gas introduced to the agitated photobioreactor proved to be convenient. Flue gas with a gas composition of 10–13% carbon dioxide and 8–10% oxygen improved the growth rate of the algal culture compared to the control culture which used an air mixture with 11% pure carbon dioxide. Furthermore, the rate of carbon fixation is also higher for the flue gas fed culture at 4.4 g/L every 24 hours compared to 3.0 g/L every 24 hours for the control (Douskova et al. 2009). The drawback of the utilization of flue gas is the presence of mercury and other compounds in the biomass generated. Other heavy metals, polycyclic aromatic hydrocarbons, polychlorinated biphenyls, and polychlorinated dibenzodioxins and dibenzofurans were also detected in the biomass generated from the culture fed with flue gas albeit at levels below the limits set by the European Union (Douskova et al. 2009). The gaseous mercury was successfully removed by treating the flue gas in an activated carbon column prior to addition to the algal culture. The research concluded with a suggestion to repurpose the microalgae culture fed by flue gas for biofuel production due to the concern for customer rejection due to the flue gas originating from municipal waste (Douskova et al. 2009).

Khataee et al. (2010) investigated the bioremediation potential of microalgae against Malachite Green, a triphenylmethane dye that could endanger aquatic life by affecting the gills, gonads, liver, and kidneys, cause gastrointestinal irritation in humans, and skin rashes and permanent eye injury to humans and animals. Khataee et al. (2010) chose microalga from the *Chlorella*, *Cosmarium* and *Euglena* genus. An artificial neural network (ANN) model was devised to predict the decolourization rate of the microalgae against various parameters in tandem with the actual experiments. Its results demonstrated that the ANN generated reliable predictions, with correlation coefficients averaging at 0.98. The microalgae were found to be able to decolorize the water of the dye. Microalgae were capable of improving their decolorizing ability with increasing temperature within the range of 5˚C to 45˚C. A higher concentration of the dye improves the decolorizing rate of the microalgae indicating that the microalgae's absorption was done through osmosis. The decolourization rate was greatly influenced by pH, indicated by being significantly low in acidic pH and rapid rises as the pH increased from 4 to 8. Khataee et al. (2010) attributed this to the zero-point charge of the microalgae biomass as the microalgae cell surface is positively charged at low pH which repels the cationic Malachite Green dye and thus favors an alkaline medium for a higher decolorizing rate. The potential to reuse the microalgae indicated that they conducted biodegradation instead of biosorption to remove the dye.

The Indian Agricultural Research Institute attempted a research to bioremediate sewage wastewater with microalgae to generate biomass for manure production. Sharma and Khan (2013) chose the microalgae *Scenedesmus sp*., *Chlorella minutissima*, and blue-green microalgae *Nostoc muscorum* and tested the individual strains as well as variations of consortia on their nutrient removal ability from sewage waste water. The microalgae were shown to reduce the biochemical oxygen demand (BOD), chemical oxygen demand (COD), nitrate, ammonium nitrate, phosphate and total dissolved solids (TDS) of sewage wastewater (Figure 7a). Analysis of the harvest after 20 days indicated that the maximum biomass generated was observed in *C. minutissima* and *Scenedesmus sp*. while *C. minutissima* demonstrated the greatest potential as a bioremediators of sewage as it generate considerable biomass with the highest nitrogen and phosphorus content (Figure 7b). Sharma and Khan (2013) concluded *C. minutissima* as the best bioremediator candidate as it removed 95% BOD, 90 % COD, 97% TDS, 90% nitrogen and 70% phosphorus from the sewage wastewater (Figure 7a). The generated biomass was deemed suitable for use as manure in agriculture.

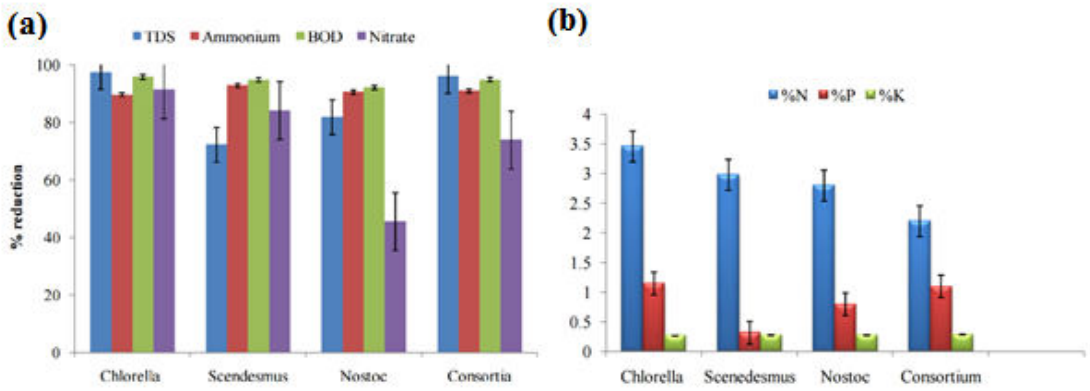

Figure 7: Bar charts showing (a) the percentage of reduction in Total Dissolved Solids (TDS), ammonium, Biological Oxygen Demand (BOD), and nitrate of sewage wastewater by different microalgae; Chlorella, Scendesmus, Nostoc, and a Consortia, respectively, and (b) the N:P:K ratio of biomass generated by the same microalgae during the process. Taken from Sharma and Khan (2013).

In China, fish farms have become a considerably large industry which results in rising concerns regarding the impact of organic matter and nutrient loading in coastal waters (Wu 1995). A significant portion of nitrogen and phosphorus is lost to the environment in the form of leftover feed and fish waste (Wu 1995) which could trigger the onset of eutrophication endangering aquatic life including the farmed fish. Thus, a sustainable system was developed by accommodating two or more ecologically compatible species in a system so they can mutually inhabit an environment without competition for space and food (Neori et al. 2000). As a result, the waste generated by the fish can become a source of nutrients to another organism in the system, providing bioremediation ability and nutrient balance in the system and economic product diversification (Chopin et al. 2001). However, during warm seasons, aquaculture farms have no macroalgae to cultivate with their livestock, so Zhou et al. (2006) investigated the red macroalgae *Gracilaria lemaneiformis*, adapted and cultured in the south of China for its potential to remove nutrients at high temperatures observed during the warm seasons. Despite being indigenous to the north of China, the algae was brought to the south of China to be cultivated during the longer warm seasons in the south compared to the north. Zhou et al. (2006) co-cultivated the algae with the fish *Sebastodes fuscescens*. Having adapted to the southern climate, the algae demonstrated itself to be an efficient nutrient pump, removing most of the nutrients from the system, and growing at a maximum rate of 11.03% per day. The average content of carbon, nitrogen and phosphorus of the dried thalli were 28.9%, 4.17% and 0.33%, indicating that an extrapolation of the results would show that a 1-hectare farm of the algae would generate 70 tons of *G. lemaneiformis* or 9 tons of dried thalli, sequestering 0.22 tons of nitrogen, 0.03 tons of phosphorus and 2.5 tons of carbon (Zhou et al. 2006).

In Malaysia, algal bioremediation has garnered some interest, particularly in industries which handle and produce environmentally hazardous materials. Lim et al. (2014) conducted a research investigating the potential application of microalgae in bioremediation of textile wastewater. Textile water tainted with Supranol Red 3BW EBNA was collected in a high rate algae pond (HRAP) systems and inoculated with a culture of *Chlorella vulgaris*. The decolorization rate ranged from 41.8% to 50.0% and nutrient contaminant removal ranged from 44.4% to 45.1% for ammonia nitrogen, 33.1% to 33.3% for phosphate and 38.3% to 62.3% for chemical oxygen demand (Lim et al. 2014). Introducing nutrients to the textile wastewater boosted biomass production but did not improve the decolorization or removal of pollutants, indicating that the mechanism of the pollutant removal was biosorption. The system of high rate algae pond using *C. vulgaris* offers a good solution of pollutant removal of textile wastewater before being discharged into the environment.

Lananan et al. (2014) investigated the symbiotic relationship of nitrogen and phosphorus during bioremediation. *Chlorella sp*. was paired with effective organisms to bioremediate wastewater and its bioremediation performance was compared with one performed solely by the microalgae. The symbiotic pair demonstrated a higher nutrient phosphorus removal of 99.15% compared with 49.73% performed by *Chlorella sp*. alone, respectively. However, the removal of ammonia nitrogen was not improved by the symbiotic pair (Lananan et al. 2014). The research proposed that optimization of symbiotic pairing could create a more efficient and economical wastewater treatment.

Ang (2008) explored the use of marine microalgae to bioremediate the nutrient pollutants in palm oil mill effluent (POME) and generated biomass to be used as feed for aquaculture. *Isochrysis sp*. was chosen as the best candidate as it displayed a high doubling rate of 0.84 days. Furthermore, 12 hours of light exposure period was determined as the best photo period with the microalgae generating an increase of total lipids by 49%, 40.2% increase of Docosahexaenoic Acid (DHA) and traces of Eicosapentaenoic Acid (EPA). The nutrient pollutants were successfully removed with an 87% reduction of orthophosphate, 38% reduction of nitrate , 39% of total nitrogen and 21.3% reduction of BOD (Ang 2008).

Microalgae's Potential in Biofuel Production

Lipids

Lipids are naturally occurring molecules which serve as energy storage, sensory signals, and cell membrane structures (Subramaniam et al. 2011). Lipid is produced by plants and animals to store energy in the form of triglyceride, a lipid formed from a glycerol molecule and three fatty acid molecules (Nelson and Cox 2000). Microalgae produce lipids from sugar molecules synthesized from photosynthesis (O'Leary 1988). The lipid component of interest is fatty acids which are long hydrocarbon chains with a carboxyl end (Ichihara and Fukubayashi 2010). These fatty acids are converted into fatty acid methyl esters (FAME), a main constituent of biofuel (Johnson and Wen 2009).

Fatty acid methyl ester

Fatty acid methyl esters (FAME) are hydrocarbon esters commonly derived from fatty acids via transesterification of triglycerides methanol (Ichihara and Fukubayashi 2010) (Figure 8). A practical use of FAMEs in research is the identification of organism samples using FAME profiles of the organism (Heyrman et al. 1999). Widely used in studying new species of bacteria, the FAMEs extracted from the bacterial culture are subjected through a gas chromatograph and the peak patterns unique to the strain are obtained from the readings. The FAME peaks are used as biomarkers that identify the organism and its FAME profile can be documented in a database for future identification purposes (Heyrman et al. 1999). This allows tying characteristics to newly discovered bacteria and also used in identifying pathogens. Aside from that, FAMEs are especially sought after due to their structure as a hydrocarbon chain which is also found in common fossil fuels and is easily combustible (Refaat 2009). This research focuses instead on the FAME mixture produced by the algae to estimate its energy yield and assess its potential as a biofuel.

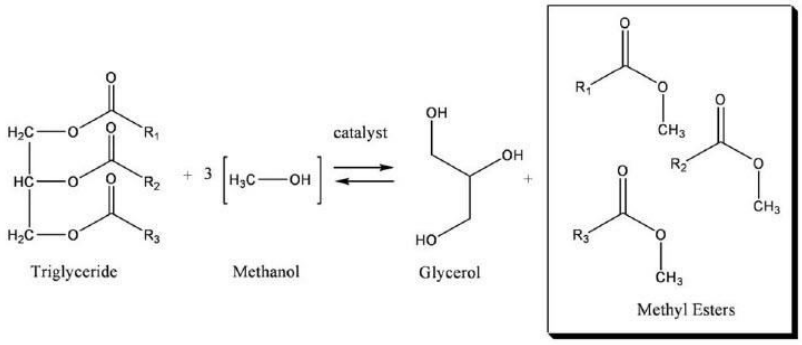

Figure 8:Transesterification process of triglyceride and methanol producing methyl esters (FAME) and glycerol, obtained from Global CCS Institute, <http://www.globalccsinstitute.com/>

Gas Chromatography (GC)

Gas chromatography (GC) is an analytical technique used to identify and quantify various thermally stable and volatile compounds in a sample (Pavial et. al. 2006). Its sensitivity allows detection of compounds in low concentrations and while its consistency allow direct comparison of its results with a standard fatty acid mixture (Conder & Young 1979). The sample was introduced into the GC machine via injection into a heated stationary phase which is specific to certain compounds like hydrocarbons. The sample is carried through the column with the aid of an inert gas like helium to a detector which detects the quantity of the compound (Harris 1999). The polarity of the column, the column's temperature, and carrier gas flow rate and column length determines the rate of interaction of the compound with column, allowing the compounds to migrate through the column at different speeds causing separation of the compounds (Higson 2004). This results with varying retentions times unique to each compound, allowing identification via comparison with a previously loaded standard (Erwin et al. 1961).

Biofuel

Biofuel is a fuel derived from natural biomass and biowaste (Demirbas et al. 2011). Biofuel is a renewable energy derived sustainably from existing resources, a sharp contrast to fossil fuel which is a limited resource gathered across millions of years (Mann et al. 2003). Biofuels today are classified into four generations. First generation biofuels use readily available food crops to produce fuel (Zinoviev et al. 2007) while the second generation of biofuels produces the same biofuel products from non-food crop sources which bypasses the food availability problem faced by the first generation biofuel (Zinoviev et al. 2007). Algae biofuel falls in the third generation of biofuel which involves the effort to directly cultivate fuel crop engineered specifically to maximize biofuel production (Zinoviev et al. 2007). The fourth generation of biofuels involves using genetically modified crops to absorb more carbon dioxide from the atmosphere while releasing less of it during combustion when the crop was processed into fuel, effectively sequestrating carbon from the atmosphere (Demirbas 2011). Despite biofuel's great potential, there is some debate as to whether resources and land dedicated to crops are economically viable to compete against fossil fuels (Demirbas 2011). Its impact on the land's food output would be significant as well and its demand will only increase over time; as with food demand (Demirbas 2011).

Many microalgae, spread across a diverse range of ecosystems with uniquely different environmental conditions, are capable of lipid production. Despite averaging with low lipid content, some algae species are capable of reaching levels as high as 90% of its dry weight in certain controlled conditions (Mata et al. 2010). A variety of fatty acid profiles could also be obtained from different combinations of nutrient levels (Xin et al. 2010), cultivation methods (Amaro et al. 2011) and growth phases (Amaro et al. 2011). This is due to the algae's response to external stimuli, namely its environment which stimulates modification of its lipid metabolism from biological pathways ingrained in its genetic material (Sharma et al. 2012).

History of algae biofuel

The idea of using microalgae as a precursor for biofuel is not considered as a new technology and was first proposed by Harder and Von Witsch in 1942. The research field was still in the early stages of development as interest was shifted after World War 2 and demand for an alternative to transportation fuel had dwindled. Interest rekindled in the 1970s when the oil embargo was introduced and the US Department of Energy established the Aquatic Species Program in 1978 (Sheehan et al. 1998). The effort was short lived as the costs of production could not compete with the prices of fossil fuel and the program was abandoned in 1996 (Ferrell and Sarisky-Reed 2010). However, recent hikes in oil prices sparked a revival of research on algae biofuel production with increased US federal funding (Ferrell and Sarisky-Reed 2010) and similar efforts had sprung up in various countries around the world (Pienkos and Darzins 2009).

Most research efforts centred on algae biofuel were conducted in the United States. Coerced by increasing energy demands and pressure to be independent of imported oil, algae biofuel offer an alternative solution to the energy industry (Pienkos and Darzins 2009).

Tang et al. (2011) investigated the microalgae *Dunaliella tertiolecta* to determine its characteristics and parameters for its optimum growth for maximum biomass for biofuel production. *D. tertiolecta* boasts a high salt tolerance making it able to use inorganic nutrients found in wastewater, brackish water and salt water. It also has a high growth rate and a tolerance for temperature and light, making it relatively easy to cultivate. Red and white LEDs and fluorescent light improves its growth rate and extending the photoperiod further boosts its productivity. However, different intensities of light did not improve the FAME composition which mainly consisted of methyl linolenate and methyl palmitate. High growth rates were also observed in high concentrations of carbon dioxide of 2%, 4%, and 6%. In conclusion, Tang et al. (2011) proposed *D. tertiolecta* as a suitable feedstock for biofuel production.

Hasan et al. (2014) assessed the potential of *Chlamydomonas reinhardtii*, *Chlamydomonas debaryana*, *Chlorella vulgaris*, *Neochloris oleoabundans* and *Scenedesmus dimorphus* to bioremediate swine wastewater. *N. oleoabundans* and *S. dimorphus* were observed to be unable to grow in the swine wastewater while the highest growth rate could be seen in *C. reinhardtii* and *C. vulgaris* with growth rates of 1.286 and 1.336 per day respectively. Furthermore they produced lipid contents of 15.2% and 21.7% respectively in comparison with *C. debaryana* with 19.7% lipid content. The lipids extracted comprised of various fatty acids well suited for biofuel production such as C16 Hexadecanoic Acid and three C18 fatty acids; C18:2n6c Linoleic, C18:3n3 Linolenic, and Octadecanoic acid (Hasan et al. 2014).

Recent commercial examples of success are companies Solazyme and Propel Fuels supplying algae biofuel to the public of California in 2012 (Voegele 2012) and Sapphire Energy's commercial deal with Tesoro corp in 2013 (Herndon 2013).

Hossain et al. (2008) used indigenous filamentous algae *Oedogonium sp*. and *Spirogyra sp*. to gauge their potential in biodiesel production. Petri dish samples collected from the university's phycology laboratory (Figure 9b) were grounded and lipids were extracted and transesterified (Figure 9a) before undergoing further refining and purification for analysis (Figure 9c). Analysis of the oil showed that *Oedogonium sp*. produced more lipids than *Spirogyra sp*. which also had a higher content of sediment (Hossain et al. 2008). The research ended with a conclusion stating that even macro algae are able to be processed into biofuel albeit that they have a lower lipid content than microalgae.

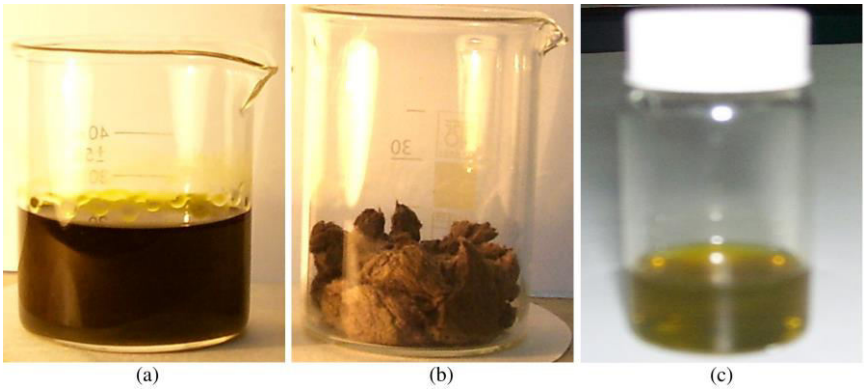

Figure 9: (a) the esterification mixture containing biodiesel and residue, (b) the algae biomass to be processed into biofuel, and (c) the resulting biodiesel after refining. Hossain et al. (2008)

One particularly promising research approach grew microalgae in sewage wastewater with the main aim of removing the nutrients from the water while producing feedstock for biofuel (Arias-Peñaranda et al. 2013). This approach forms the basis of this research project.

Identifying the problem

Malaysia's venture into oil palm agriculture to be the second largest exporter of palm oil has ravaged much of the nation's land and resources with deforestation and agriculture with 40% of its production assigned to biofuel production (Mekhillef et al 2011). Further increase in demand of biofuel production would put significant strain on vegetable oil production. This would result in industrial expansion to increase production and results in more destruction of Malaysia's forests (Koh and Wilcove 2008).

Hypothesis

Microalgae which have shown potential to produce more oil than most crops, preceding palm oil and other fuel crops by many magnitudes (Greenwell et al. 2009), could pose as a better alternative that mitigates the need to claim more land and resources. Some local strains can be used in bioremediating nutrient waste and generating biomass for biofuel that is comparable to other biofuels.

Aims and Objectives

Current research explores the potential use of algae in protein-based products and manufacture of valuable chemicals and substrates (Cardozo et al. 2007). Other directions of research ventured into the potential of algae in biofuel where oleaginous algae like the *Dunaliella tertiolecta* (Tang et al. 2011) and *Chlamydomonas debaryana* (Hasan et al. 2014) had been proposed as a promising biodiesel producers. Algal culture research in Malaysia has further targeted bioremediation of agricultural and industrial wastes such as bioremediating contaminated textile water (Lim et al. 2014), wastewater (Lananan et al. 2014), and palm oil mill effluent (Ang 2008) The overarching aims of this research are to (a) isolate and identify local microalgae and (b) gauge their potential use as bioremediation agents and biodiesel producers with a focus on their potential use under nutrient stress.

The objectives of this study are:

1. Isolation of local microalgae from freshwater and marine water sources.
2. Identification of local microalgae through molecular and morphological methods.
3. Assessment of growth of local microalgae under varying nutrient stress (nitrate and phosphate).
4. Assessment of Fatty Acid Methyl Esters (FAME) profiles of local microalgae under varying nutrient stress (nitrate and phosphate).

Methodology

An overview of the methodological approach of this research project is shown in the flow chart below (Figure 10). The research began with the collection of water samples from which single species were isolated through manual isolation and subsequent purification of the colonies. When pure microalgae cultures were established, they were identified based on (a) their morphology and (b) their DNA. The microalgae were then cultured in media with varying (low to high) nutrient concentrations and growth of the cultures monitored and biomass measured. The fatty acids from the biomass were extracted and transesterified into Fatty Acid Methyl Esters (FAME) which were then analyzed by gas chromatography and their energy content was analyzed and compared among the samples and to literature references.

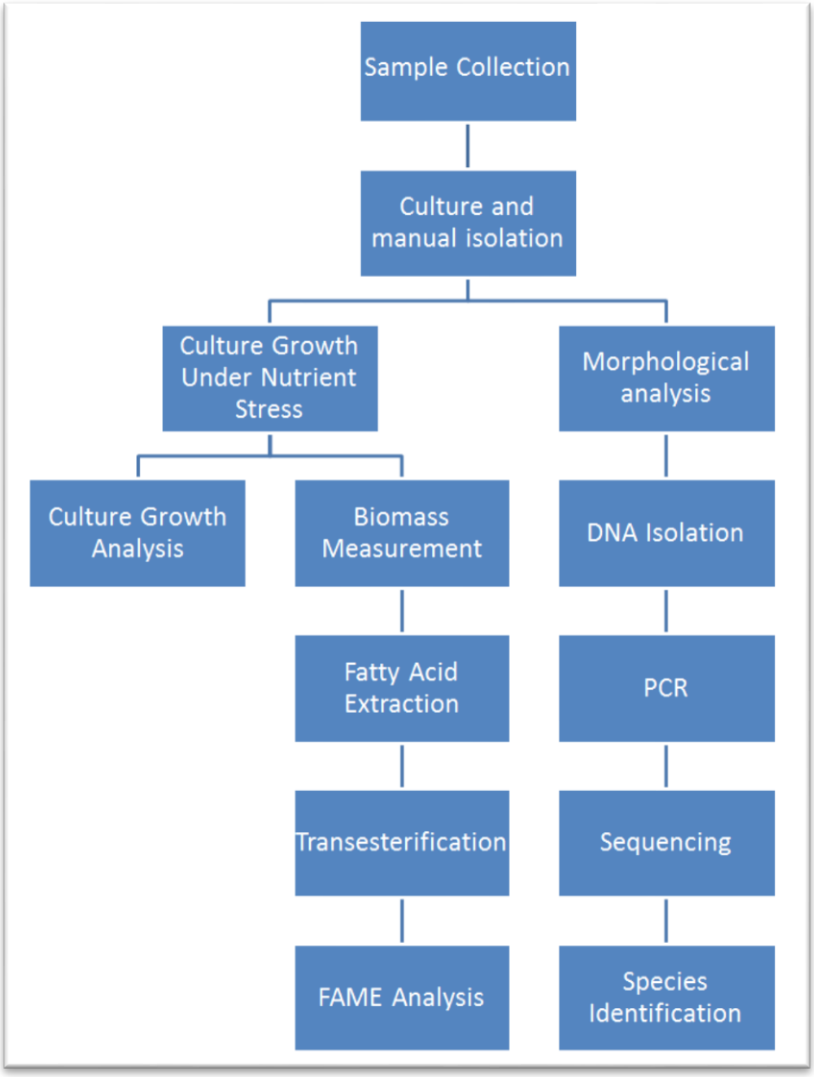

Figure 10: Flow chart summarizing the methodology used in this research project.

Field Sampling

All bottles and glassware used for sampling were autoclaved prior to the sampling trips to avoid contamination. Samples were collected from a variety of water bodies to obtain representatives from most microalgae genus. The sampling locations are introduced in the following.

Sarawak River

The microalgae were isolated from water samples obtained from five (5) stations along the Sarawak River near Batu Kawa road (Figure 11) shows the sampling locations and their GPS coordinates). Microalgae isolated from these water samples would likely contain microalgae with adaptations to higher nutrient waters contributed by the human settlements distributed near the river. 2 liters of water from the river was collected in sterile bottles at 30 cm depth, kept on ice until further processing in the laboratory.

Figure 11: Sampling locations in the Sarawak River for water samples and their respective GPS coordinates. Obtained from Google Maps <https://maps.google.com/>.

Bau - Kampung Apar

Water samples were obtained from Bau near Kampung Apar (Figure 12). The water sample was collected there to obtain microalgae that were not significantly influenced by human activities. The water sample was collected in a pond far from the village and at a higher elevation than the village. The algal community would be more diverse because the pond is far from the influence of human activities of the village (Liu et al. 2003), generating more algae strains for manual isolation. 30 mL water samples were collected from the water surface in small sterile glass vials.

Figure 12: Sampling location in Kampung Apar for the water samples (indicated by the blue star) and the Kampung Apar's GPS coordinates. Obtained from Google Earth.

Kampung Telaga Air

Marine microalgae were also sought after in this research to cover more diversity among the microalgae. Marine and freshwater microalgae were isolated from two marine water sample obtained at two piers in Kampung Telaga Air (Figure 13). 50 ml bottles were filled with surface water and kept on ice until taken back to the lab for isolation.

Figure 13: Sampling locations in Telaga Air for the marine water and the location's GPS coordinates. Obtained from Google Earth.

Tunku Abdul Rahman National Park

Another marine water samples were obtained from the Tunku Abdul Rahman National Park in Sabah (Figure 14). The water sample was collected from the water surface above the reefs situated around Pulau Manukan. The sampling bottles were opened underwater near the surface and the marine water collected and sent back to Sarawak for microalgae isolation.

Figure 14: Sampling location in Tunku Adbul Rahman National Park in Sabah for the marine water and the location's GPS coordinates. Obtained from Google Maps <https://maps.google.com/>.

Microalgae Culture

The water samples were assessed for microalgal diversity using manual isolation to isolate single algae cells for culture. Water samples with a low presence of algae were enriched with "Enriched Seawater by Donald & Kokinos" (ESDK) stock (Tables 2, 3, and 4) to encourage algae growth (Kokinos and Anderson 1995). The ESDK stock was used as the source of nutrients in the media prepared for the culture of the microalgae. In this research, the marine algae were grown in autoclaved seawater enriched with ESDK stock while the media for growing freshwater algae used autoclaved tap water instead of seawater. The prepared cultures were placed under 12:12 hour light cycles at laboratory temperature.

ESDK Microalgae Culture Stock Preparation

The ESDK stock was developed by Kokinos and Anderson (1995) to be added to sterile and filtered seawater to culture marine algae. The ESDK stock is prepared with two different solution stocks, the Fe stock and P2 stock (refer to Tables 2 and 3 below for list of materials used for preparation), along with a controlled amount of nitrate and phosphate, NaNO3 and Na-glycerophosphate respectively (Table 4). The solutions were autoclaved prior to use in algae culture.

Table 2: List of materials to prepare the Fe Stock of the ESDK stock. The solution is brought to a final volume of 500 mL using Millipore H2O.

Fe Stock	**(g)**
Fe(NH4)2(SO4).6H2O)	0.351
Na2-EDTA	0.3765
Make up to 500mL with Millipore H2O	

Table 3: List of materials to prepare the P2 Stock of the ESDK stock. The solution is brought to a final volume of 400 mL using Millipore H2O.

P2 Stock	(g)
Na2-EDTA	0.4
FeCl3.6H2O	0.126
H3BO3	0.456
MnSO4.7H2O	0.055
ZnSO4.7H2O	0.0088
CoSO4.7H2O	0.00192
Make up to 400mL with distilled H2O	

Table 4: List of materials to prepare the ESDK stock. The solution is brought to a final volume of 400 mL using Millipore H2O.

ESDK Working Stock	
NaNO3	1.4000g
Na-glycerophosphate	0.2000g
P2 Stock	100mL
Fe Stock	100mL

Isolation of Microalgae cells

Isolation of the algae cells was done using conventional agar plate methods using agar added with ESDK (Kokinos and Anderson 1995). Agar plates enriched with ESDK were prepared and the water samples spread across the plates. The microalgae cells grow out into tiny colonies that can be isolated into liquid ESDK enriched media. However, agar can be overgrown by bacterial colonies, contaminating the microalgae colonies. Furthermore, culturing the cells on a plate with antibiotics would result in no cell colonies forming. Thus, some microalgae require a more immediate approach to isolating the algae species.

Single cell isolation requires the use of a pipette with a microscopic sized tip. The tip of a glass pipette was heated and stretched using a flame of a bunsen burner. The tip was stretched until it was very fine and the melted sealed end was broken off. The end of the pipette resembles a microscopic tube. Single cells of the algae were manually isolated under a microscope and placed into wells of a culture plate. The wells were filled with ESDK enriched media.

DNA Extraction and Processing

The DNA of the microalgae strains were required for identification of the species. Thus, the microalgae cells had to be destroyed to release its DNA for further processing. Various methods were used in extracting DNA from the microalgae cells because of the cells' tough cell wall, making the cells resilient. Freeze and Thaw (Tsai and Olson 1991), modified versions of CTAB and DTAB-CTAB extraction (Fawley and Fawley 2004) and various DNA extraction kits were used to break down the cells and obtain the DNA. The different procedures are explained in the following.

Freeze and Thaw Method

The algae culture was inserted into a sterile microcentrifuge tube and centrifuged at 10,000 rpm for 1 minute. The supernatant was discarded and Proteinase K was added to the mixture and incubated for 30 minutes at 37 ºC. The proteinase K would break down proteins and inactivate nucleases like DNases and RNases (Hilz et al. 1975). The sample was placed in 3 freeze and thaw cycles; freezing phase of -80 ºC for 3 minutes and thawing phase of 85 ºC for 3 minutes. 100 µL Chloroform-Isoamylalcohol was added and gently mixed and centrifuged at 10,000 rpm for 10 minutes. The aqueous phase (upper phase) was transferred to a new sterile microcentrifuge tube. 120 µL of ice cold isopropanol was added to the aqueous phase and the sample was incubated at room temperature for 15 minutes, then -20 ºC for 15 minutes. The isopropanol would precipitate the DNA in the freezing temperature. The sample was centrifuged at 1,300 rpm at 4 ºC and the supernatant is discarded. The remaining pellet was dissolved in Millipore water and stored at -20 ºC (Tsai and Olson 1991).

CTAB Method

The CTAB buffer is prepared based on the final concentrations listed in Table 5 below.

Table 5: List of materials that make up the CTAB buffer

Final Concentration
2% or 2g/100mL CTAB (hexadecyltrimethylammonium bromide)
100 mM TrisHCl [pH=8]
20 mM EDTA,
1.4 M NaCl
0.2% β-mercaptoethanol [added just before use]
0.1 mg/mL proteinase K [added just before use])

The sample cells were resuspended in 800 µL of CTAB extraction buffer pre-warmed to 60 °C. The sample was incubated for an hour at 60 °C while gently missing the sample at 15 minute intervals. After incubation, 800 µL of chloroform/isoamylalcohol (24:1) mixture is added to the solution. The mixture was gently mixed and centrifuged at 13000 rpm. The upper aqueous layer was transferred into a new microcentrifuge tube. 600 µL of isopropanol was then added to the solution and gently mixed before left overnight at -20 °C to precipitate the DNA. The mixture was centrifuged at 13000 rpm for 15 minutes to form a DNA pellet. The supernatant mixture was discarded and the pellet is gently washed with ice cold 70% ethanol. The mixture was centrifuged at 13000 rpm for 15 minutes. The supernatant was discarded and the pellet was left to dry at room temperature. The DNA pellet was finally dissolved in sterile MilliQ water and stored at -20 °C (Fawley and Fawley 2004).

DNA – DTAB CTAB Method

The sample cells were spun down into a pellet and the supernatant was discarded. Tiny ceramic beads were added to the sample and 600 µL of dodecyltrimethyl ammonium bromide (DTAB) solution was added to the mixture. The sample was vortexed horizontally for 10 minutes at maximum speed. The sample was then incubated in a waterbath at 75 °C for 5 minutes and left to cool down to room temperature. The sample was vortexed again and centrifuged at 13000 rpm for 1 minute. 700 µL of chloroform was added and the mixture was vortexed thoroughly. The sample was centrifuged at 12000 rpm for 5 minutes and the aqueous upper layer was transferred to a new sterile microcentrifuge tube. 100 µL of hexadecyltrimethyl ammonium bromide (CTAB) solution and 900 µL of MilliQ water was added and mixed thoroughly. The sample was incubated at 75 °C for 5 minutes and left to cool down to room temperature. The sample was centrifuged at 12000 rpm for 5 minutes and the supernatant was discarded while the pellet form was dissolved in 150 µL of dissolving solution. The mixture was incubated at 75 °C for 5 minutes and left to cool down to room temperature before being centrifuged at 12000 rpm for 5 minutes. The supernatant was transferred into another sterile microcentrifuge tube with 300 µL of 95% ethanol and mixed thoroughly before being centrifuged at 12000 rpm for 5 minutes. The supernatant was discarded and the pellet is washed with 75% ethanol and centrifuged at 12000 rpm for 5 minutes again. The supernatant was discarded and the pellet was left to dry at room temperature before being dissolved in 20 µL of MilliQ water and stored at -20 °C (Fawley and Fawley 2004).

Mobio PowerWater DNA Isolation Kit

Figure 15: Mobio PowerWater DNA isolation kit. Obtained from MO BIO Laboratories. <https://mobio.com>

Procedures followed the supplier's instruction. The Mobio PowerWater DNA Isolation Kit (Figure 15) was used to extract DNA from the microalgae cells that were tougher against previous DNA extraction methods. Prior to the DNA extraction, Solution PW1 and Solution PW3 were warmed in a water bath at 55 °C for 5 to 10 minutes. The solutions had to be used while warm. The microalgae culture was transferred into a microcentrifuge tube and spun at 10000 rpm for 5 minutes. The supernatant media was removed without disturbing the cell collected in the pellet and on the wall of the microcentrifuge tube. More culture was added and the process was repeated until a considerable amount of biomass was collected. The pellet was resuspended with 500 µL of Solution PW1 and transferred to 5 mL PowerWater Bead Tube. Another 500 µL of Solution PW1 was transferred to the microcentrifuge tube to resuspend any residue and transferred into the PowerWater Bead Tube. The tube was fixed horizontally onto a vortex machine and vortexed at maximum speed for 5 minutes. The sample was centrifuged at 4000 rpm for 1 minute and the supernatant was transferred into a collection tube. All the supernatant was collected irrespective of any cell debris collected. The collection tube was centrigued at 13000 rpm for 1 minute and the supernatant was transferred to another clean collection tube without disturbing the pellet. 200 µL of Solution PW2 was added to the sample, vortexed briefly to mix and incubated at 4 °C for 5 minutes. The sample was centrifuged at 13000 rpm for 1 minute and the supernatant was collected in another collection tube. 650 µL of Solution PW3 was added to the sample and vortexed briefly. 650 µL of the mixture was transferred into a Spin Filter and centrifuged at 13000 rpm for 1 minute. The filtered flow through was discarded and the process was repeated with

another load of 650 µL of the mixture until the entire volume of the sample was filtered. The Spin Filter basket was removed and placed into a collection tube. Solution PW4 was shaken well before 650 µL of the solution was transferred into the Spin Filter basket and the sample was centrifuged at 13000 rpm for 1 minute. The flow through was discarded and 650 µL Solution PW5 was added before centrifuging at 13000 rpm for 1 minute. The flow through was discarded and the sample was centrifuged once more to remove any residual wash. The Spin Filter basket was placed into a sterile collection tube and 100 µL of Solution PW6 was added to the center of the white filter membrane. The sample was centrifuged for the last time at 13000 rpm for 5 minutes. The spin filter basket was discarded and the DNA sample was kept at a low temperature of -20 °C to 80 °C before any downstream application like gel electrophoresis and PCR.

Gel Electrophoresis

All DNA extracts were tested for presence and purity using gel electrophoresis. 1% agarose gel was prepared by mixing 1x TAE buffer with 1 g of agarose powder and heated to boiling point. The mixture was mixed thorough and 3 µL of Midori Green Dye was added to the mixture. While the mixture was hot, it was poured into the electrophoresis tank mold set up for the agarose gel to set. Gel combs which produce gel wells in the agarose gel were inserted onto the mold and the gel was left to set for 30 minutes. The gel combs was removed and the agarose gel was set in the correct orientation before setting up the electrophoresis experiment. 1x TAE buffer was poured into the electrophoresis tank until the agarose was immersed in the buffer. 1µL of the DNA ladder was added to the first well. 5 µL of the DNA sample were added to the consecutive wells and the electrophoresis was carried out at 100 V for 45 minutes (Figure 16).

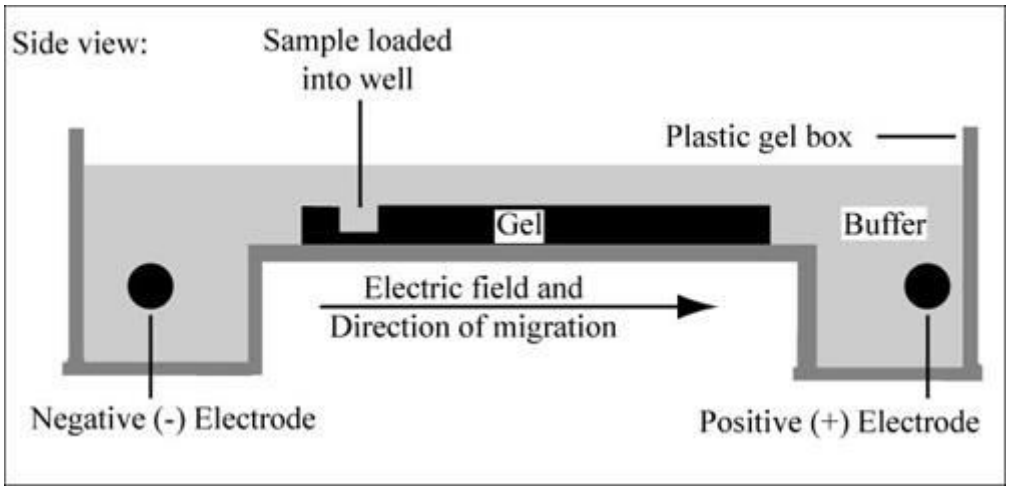

Figure 16: Diagram for an agarose gel setup for gel electrophoresis. Obtained from MIT Open Course Ware.<http://ocw.mit.edu/>

The resulting gel was taken out of the electrophoresis tank and placed in the observation platform of a UV emitter. The DNA in the gel will fluoresce in UV light forming bands or smears in the gel (Figure 23). The base pair size of the DNA was determines by comparing its position with the position of the bands of the DNA ladder which have known base pair lengths.

Polymerase Chain Reaction (PCR)

The DNA samples were amplified with PCR process using the MyTaq™ Red Mix from Bioline. The PCR mixture was prepared according to the manual provided by Bioline shown in Table 6 below. The primers used in the reactions were primer pairs ITS 1 (Sequence: TCCGTAGGTGAACCTGCGG) and ITS 4 (Sequence: TCCTCCGCTTATTGATATGC) (White et al. 1990) and 8F (Sequence: AGAGTTTGATCCTGGCTCAG) (Eden et al. 1991) and 519R (Sequence: GWATTACCGCGGCKGCTG) (Lane et al. 1985). Primer pair ITS 1 and 4 binds to the internal transcribed spacer in the ribosomal RNA (White et al. 1990) which are indicated to be conserved throughout the life history of plant species as demonstrated by Bast et. al. (2009) when the ITS sequence of between sexual and asexual strains of *Monostroma latissimum* were found to be identical. Primer pair 8f (Eden et al. 1991) and 519r (Lane et al. 1985) had a broader range which binds to the 16S ribosomal RNA commonly found in prokaryotes.

Table 6: The standard protocol of MyTaq Red Pix PCR kit. Obtained from mytaq red mix product manual. (Bioline n.d.)

Standard MyTaq Red Mix Protocol

The following protocol is for a standard 50µl reaction and can be used as a starting point for reaction optimization.

PCR reaction set-up:
All reactions must be set-up on ice.

Template	200ng
Primers (20µM each)	1µl
MyTaq Red Mix, 2x	25µl
Water (ddH_2O)	up to 50µl

PCR cycling conditions:
We suggest these conditions in the first instance:

Step	Temperature	Time	Cycles
Initial denaturation	95°C	1min	1
Denaturation	95°C	15s	25-35
Annealing*	User determined	15s	
Extension*	72°C	10s	

* These parameters may require optimization, please refer to the Important Considerations and PCR Optimization section if needed.

After PCR, the samples were checked again with another gel electrophoresis. Successful results would show clear bands of 500 to 800 base pairs and the samples that passed inspections were sent to Beijing Genomic Institute (BGI) for PCR purification and sequencing. The sequenced genes were analyzed using the Basic Local Alignment Search Tool (BLAST) program of the National Center for Biotechnology Information (NCBI - USA). Using the MEGA 6 program, the identity of the microalgae samples were deduced and a phylogenetic tree was constructed (Tamura et al. 2013).

Culture Growth under Nutrient Stress

Algae cultures were subjected to nutrient stress experiments. Since growth of the algae generates biomass which in turn uses up nutrients, the aim of the experiment was to measure the algae's potential to grow in high nutrient concentration which directly reflects the algae's potential in nutrient bioremediation. The nutrient concentrations were manipulated using the recommended nutrient concentration in the ESDK stock. 1x the ESDK stock nutrient load would be the recommended nutrient concentration (Kokinos and Anderson 1995) while 5 times the recommended nutrient load which mimics the nutrient concentration found in domestic wastewater set by the Environmental Protection Agency (EPA) and 10 times the nutrient load which covers the extreme nutrient concentration not listed by the Environmental Protection Agency (EPA) likely generated in rare circumstances in domestic waste and agricultural runoff or in industrial waste (Table 7).

Table 7: The Phosphate (PO4) and Nitrate (NO3) concentration of 1x, 5x and 10x used in the culture growth experiment.

	1x	5x	10x
Phosphate (PO4)	0.00002245	0.0001123	0.0002245
Nitrate (NO3)	0.0003994	0.001997	0.003994

Prior to the nutrient stress experiment, cell count and its respective optical density or absorbance was determined. A fully developed culture with a high cell count would result in a high absorbance. Thus, by performing cell counting and spectrophotometry on cell cultures diluted in series, a graph with the cell count and its respective absorbance was drawn. The graph was used as a standard reference for the results obtained in the nutrient stress experiment.

Estimating Cell Number and Measuring Culture Optical Density

An algae culture was cultured to its highest possible biomass prior to cell counting and absorbance reading. The algae culture was loaded onto the haemocytometer for cell counting. The pipette containing the algae culture was placed on the haemocytometer in front of the cover slip and the algae sample was loaded onto the haemocytometer under the coverslip via capillary action. The algae cells were counted in nine grids and an average cell count is calculated (Doyle and Griffiths 2000). The cell concentration was calculated with the following formula:

$$\text{Cell concentration (cells/mL)} = \text{average cell count} \times (1\ \text{mL/Volume of grid})$$

$$\text{Cell concentration (cells/mL)} = \text{average cell count} \times (1\ \text{mL}/0.004\mu\text{L})$$

The algae culture was then diluted with controlled media according to the dilution factors of 2, 4, 8, and 16. The cell counts of the diluted samples were calculated using the average cell count of the undiluted culture and the dilution factor.

The algae cultures along with their diluted samples were measured for its absorbance at 560 nm using a spectrophotometer. With the cell concentration and absorbance data, a linear graph of cell concentration against absorbance was plotted as shown in Figure 17. The equation of the graph would be used in calculating the cell concentration of the cultures at the end of the growth experiment.

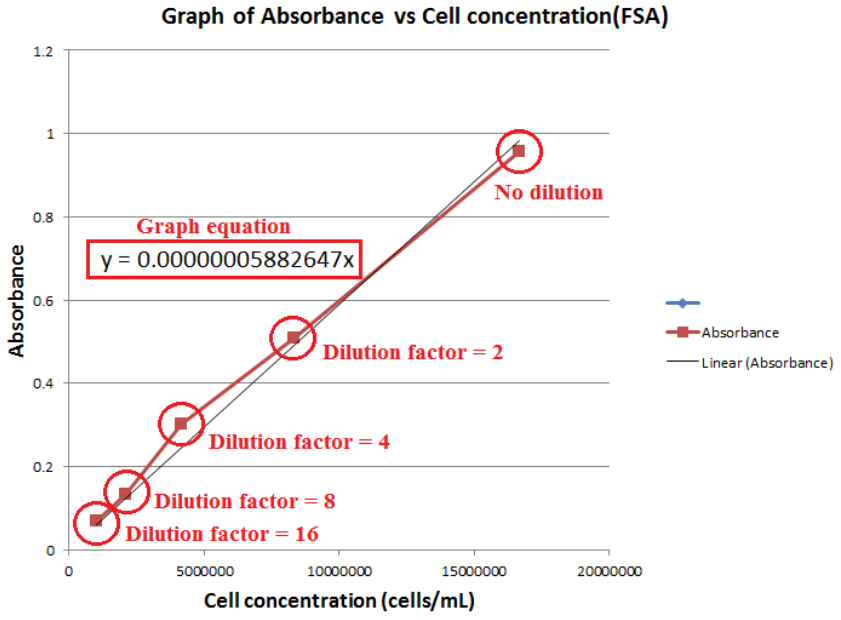

Figure 17: Graph of absorbance against cell concentration for sample FSA.

Culturing the Algae under Nutrient Stress

Sterile universal bottles were prepared and 9.5mL of ESDK enriched media with 1 times (1x), 5 times (5x), and 10 times (10x) the nutrient concentration of nitrate and phosphate. A set enriched with ESDK without nitrate and phosphate was prepared and set as the culture set without any nutrients present. 0.5 mL of the microalgae culture was transferred to all the universals bottles to a final volume of 10 mL and mixed thoroughly. The caps of the universal bottles were loosened slightly to allow the minimum amount of air circulation. Triplicate sets were made for each microalgae strain and a controlled set without any microalgae culture for 0x, 1x, 5x, and 10x the nutrient concentration was prepared as well. The universal bottles were left to incubate at laboratory temperature with a 12:12 hour light cycle under a 20 W white fluorescent lamp for one week in an experimental setup shown in Figure 18. On every day of the week, the universal bottles were resuspended and opened in a laminar flow to circulate air.

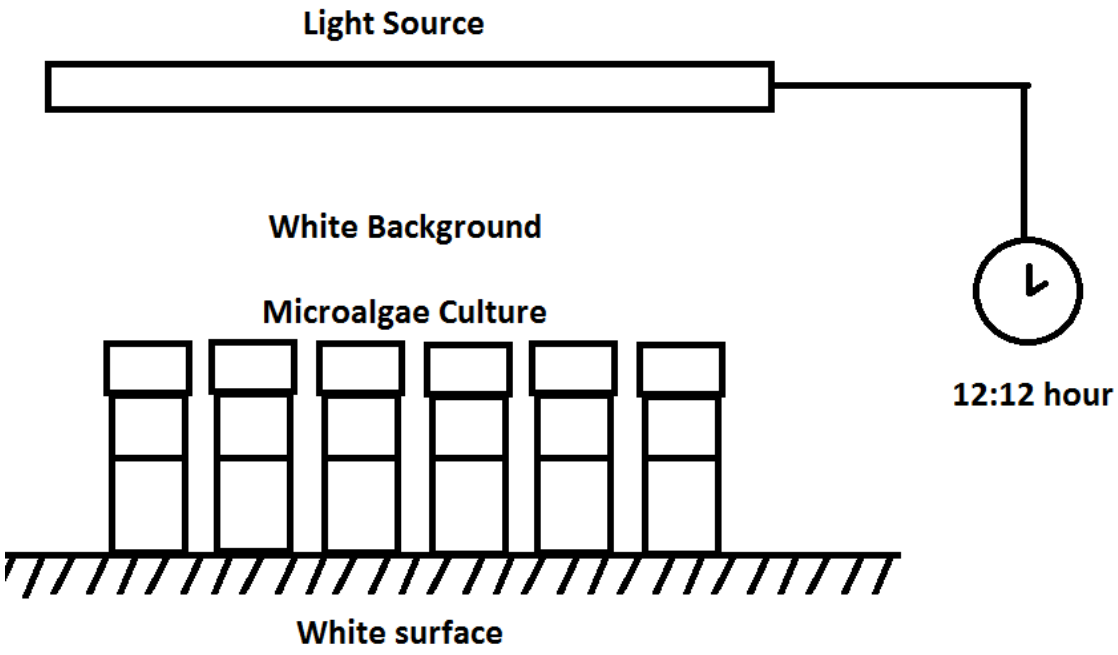

Figure 18: Diagram of experimental set up for culturing microalgae.

Growth Culture Analysis

After the incubation period, the absorbance readings for the contents of all the universal bottles were measured. The cell count was obtained by using the equation of the graph of 'Cell concentration against absorbance' as a reference. Thus, with the cell count of the culture microalgae strains, their growth was determined when compared with their initial cell number.

Microalgae Biomass Analysis

Beakers were prepared and wiped clean of any residue and dust particles. The mass of beakers were measured and recorded. The microalgae cultures were placed in a centrifuge and spun at 2000 rpm for 3 minutes. The supernatant media was carefully transferred out without disturbing the biomass collected at the bottom. The biomass was resuspended in the remaining media and transferred to the measured beaker. Universal bottle was rinsed with a small amount of distilled water and poured into the beaker. This was repeated with all the microalgae cultures in the nutrient stress experiment. The beakers were placed in a fume hood and left to dry overnight at room temperature of 25 ℃. After that, the beakers with the biomass were measured again and the masses of the dry biomass were obtained.

Lipid Analysis

The lipid was extracted from the microalgae biomass using Bligh and Dyer's method (1959) which involves removing the lipids through the use of solvents. The resulting lipid extract was subjected to a transesterification process devised by Ichihara and Fukubayashi (2010). The FAMEs were analyzed with a gas chromatography and their composition and energy content were calculated.

Bligh and Dyer Lipid Extraction

The Bligh and Dyer lipid extraction's process is detailed in Figure 19. Prior to the extraction, a 1:2 (v/v) mixture of chloroform: methanol was prepared. 1.9 mL of the mixture was added to the biomass and mixed thoroughly. 625 µL of chloroform and 625 µL of distilled water were add and mixed thoroughly between additions. The contents were transferred to a 15 mL Falcon tube and centrifuged at 1000 rpm for 5 minutes. This will result in a two phase mixture with an aqueous top and an organic bottom. The bottom phase was transferred to a sterile 15 mL falcon tube and left to dry an environment filled nitrogen gas. The process was repeated in all the samples and kept in -20 ˚C prior to transesterification (Bligh and Dyer 1959).

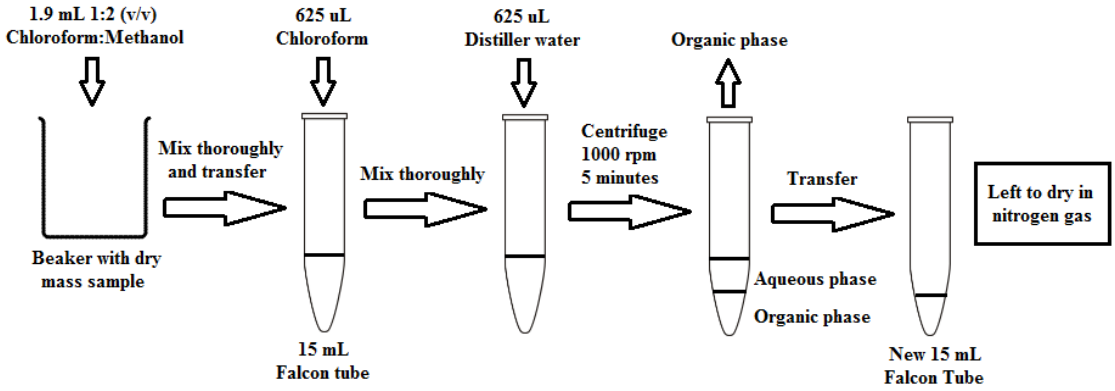

Figure 19: **The Bligh and Dyer lipid extraction from the dry biomass.**

Transesterification

The process of the transesterification of the fatty acid samples is shown in Figure 20. A 8% (w/v) HCl mixture must be prepared shortly before the transesterification procedure. 9.7 mL of concentrated HCl was diluted with 41.5 mL of methanol and mixing thoroughly before storing at -20 ˚C while preparing the fatty acid extracts for transesterification to prevent the HCl from reacting with the methanol. 200 µL of toluene was added to the fatty acid extract and mixed thoroughly to resuspend the fatty acids. After that, 1.5 mL of ice cold methanol was added to the mixture and mixed thoroughly. Finally, 300 µL of 8% HCl mixture was added to the mixture and shaken thoroughly. The final mixture was sealed tight with parafilm and incubated in a water bath at 45 ˚C overnight for 16 hours. The FAME produced was removed from the mixture by adding n-hexane before mixing thorough and removing the upper hexane layer and transferring it into a microcentrifuge tube (Ichihara and Fukubayashi 2010). After transesterification, analysis was conducted on the FAME extracts. The FAMEs were identified and quantified in order to properly calculate the energy potential of the FAMEs in terms of biofuel sourced from microalgae.

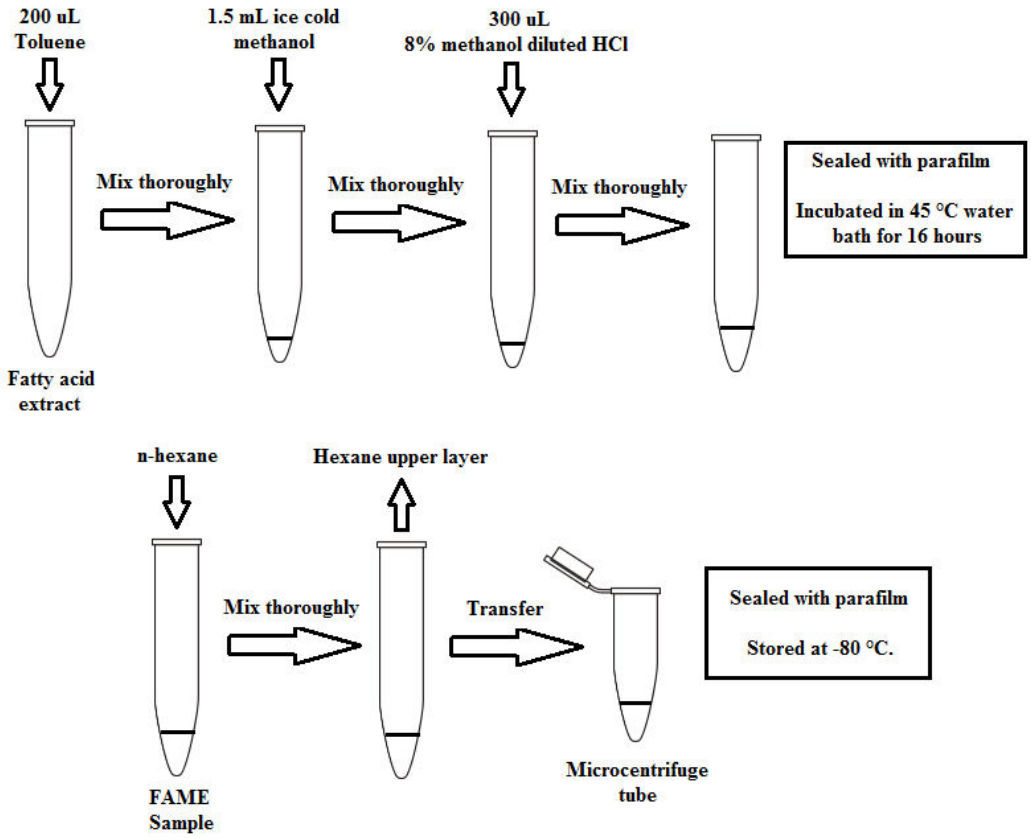

Figure 20: The transesterification of the fatty acid sample.

GC Analysis of FAMEs

Prior to the GC analysis, the FAME were dried in the presence of nitrogen gas and resuspended again with 100 µL of n-hexane. This enables the fatty acid concentration to be detectable by the GC. 1 µL of internal standard C7.0 (Sigma®, USA) was added to the FAME extracts. This internal standard would serve as a reference in determining the sample FAMEs' retention time. The FAME extracts were analyzed using the Agilent 7820A Gas Chromatograph equipped with the SLB-IL100 capillary column with dimensions of 30 m x 0.25 mm x 0.20 µm (Supelco, USA) and a flame ionization detector. The temperatures of the injector and detector were set at 250 °C and 260 °C respectively. The thermal cycles were set at140 °C for 5 min, followed by increments of 8 °C per minute up to 180 °C, then increments of 5 °C per minute up to 260 °C. Helium was used as a carrier gas at a flow rate of 4.41 mL per minute and the hydrogen gas and purified air were supplied at a flow rate of 30 mL per minute and 450 mL per minute respectively. Prior to the injection of the FAME samples, 1 µL of the FAME standard (Sigma-Aldrich®,USA) was injected into the GC and a graph showing the peaks of FAMEs in the standard was plotted (Figure 21).

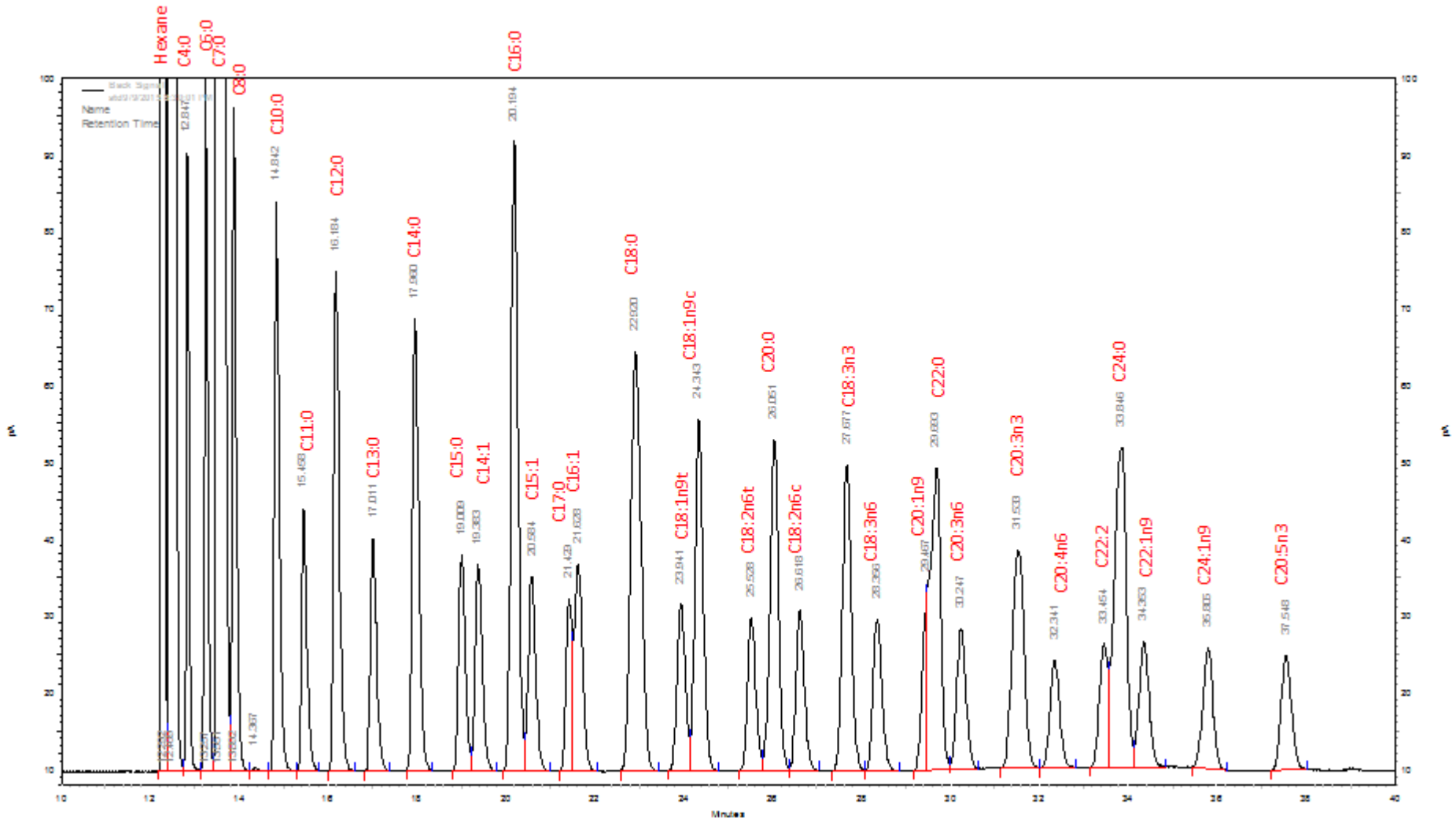

Figure 21: Retention times of the FAMEs in the standard as well as their respective identities.

Energy Calculation

The retention times of the FAMEs were recorded and the FAMEs were identified and quantified from the GC results (Table 8). Using the peak areas of the FAME in the standard FAME solution, the response factor of the FAME was calculated using the formula :

$$R_i \quad \frac{Ps_i}{Ps_{C\ 7:0}} \times \frac{W_{C\ 7:0}}{W_i}$$

R_i = response factor

Ps_i = Peak area of individual FAME in the standard FAME solution

$Ps_{C\ 7:0}$ = Peak area of C 7:0 internal standard in the standard FAME solution

$W_{C\ 7:0}$ = Weight of C 7:0 internal standard in the standard FAME solution

W_i = Weight of individual FAME in the standard FAME solution

Using the response time of the respective FAME and the peak area of the specific FAME in the sample, the weight of the specific FAME in the sample was calculated using the formula :

$$W_{FAMEi} = \frac{Pt_i \times Wt_{C\ 7:0} \times 1.0067}{Pt_{C\ 7:0} \times R_i}$$

W_{FAMEi} = Weight of the specific FAME in the sample

Pt_i = Peak area of the FAME in the sample

$Wt_{C\ 7:0}$ = Weight of internal standard added to the sample

g; 1.0067 = Conversion of internal standard from triglyceride to FAME

$Pt_{C\ 7:0}$ = Peak area of internal standard added to the sample

R_i = response factor

Using the weight of the specific FAME, the number of moles and the total fat percentage by mass of the sample was calculated.

No. of Moles = Weight of FAME/ Molecular weight of FAME

Total Fat (%) = Weight of all FAME/ Weight of dry biomass x 100%

With the number of moles for each FAME, the energy can be calculated based on the formula of the combustion reaction:

$$C_{(n)}H_{(2n-2s)}O_2+(n-1+(n-s)/2)O_2 \rightarrow (n)CO_2+(n-s)H_2O$$

n = the number of carbon atoms of the FAME

s = the number of unsaturations present

Based on the molecular formula, the energy for every bond of each molecule was calculated based on the energy value listed (Table []). The total energy released from the reaction was calculated using the formula:

$$\Delta H_{r(\mathrm{ME})} = (2n_\Delta H_{C=O(II)} + 2(n - s)_\Delta H_{O\text{-}H(I)}) - ((2n - 2s)_\Delta H_{C\text{-}H} + (n - s - 2)_\Delta H_{C\text{-}C} + \Delta H_{C=O(I)} + 2_\Delta H_{C\text{-}O} + s_\Delta H_{C=C} + (n - 1 + (n - s)/2)_\Delta H_{O=O})$$

n = the number of carbon atoms of the FAME

s = the number of unsaturations present

Table 8: Identities, molecular characteristics and energy potential of the fatty acid methyl esters detectable by the GCMS.

							Energy (kJ/mole)								
							-423	-367	-766	-350	-599	-803	-497	-498	
FAME	Name	Carbon	Hydrogen	Oxygen	C=C bonds	molecular weight	C-H	C-C	C=O(1)	C-O	C=C	C=O(2)	O-H(1)	O=O	Energy (kJ/mole)
C4:0	Butyric acid methyl ester	5	10	2	0	102	10	3	1	2	0	10	10	4.5	-2966
C6:0	Hexanoic acid methyl ester	7	14	2	0	130	14	5	1	2	0	14	14	6.5	-4246
C8:0	Caprylic acid methyl ester	9	18	2	0	158	18	7	1	2	0	18	18	8.5	-5526
C10:0	Decanoic acid methyl ester/Capric acid methyl ester	10	20	2	0	172	22	9	1	2	0	20	20	9.5	-6166
C11:0	Undecanoic acid methl ester	11	22	2	0	186	24	10	1	2	0	22	22	10.5	-6806
C12:0	Dodecanoic acid methyl ester/Lauric acid methl ester	13	26	2	0	214	26	11	1	2	0	26	26	12.5	-8086
C13:0	Tridecanoic acid methyl ester	14	28	2	0	228	28	12	1	2	0	28	28	13.5	-8726
C14:0	Myristic acid methyl ester	15	30	2	0	242	30	13	1	2	0	30	30	14.5	-9366
C15:0	Pentadecanoic acid methyl ester	16	32	2	0	256	32	14	1	2	0	32	32	15.5	-10006
C14:1	Myristoleic acid methyl ester	15	28	2	1	240	28	12	1	2	1	30	28	14	-9235
C16:0	Palmitic acid methyl ester	17	34	2	0	270	34	15	1	2	0	34	34	16.5	-10646
C15:1	10-pentadecenoic acid methyl ester	16	30	2	1	254	30	13	1	2	1	32	30	15	-9875
C17:0	Heptadecanoic acid methyl ester /Margaric acid methyl ester	18	36	2	0	284	36	16	1	2	0	36	36	17.5	-11286
C16:1	Palmitoleic acid methyl ester	17	32	2	1	268	32	14	1	2	1	34	32	16	-10515
C18:0	Stearic acid methyl ester	19	38	2	0	298	38	17	1	2	0	38	38	18.5	-11926
C18:1n9t	(E)-9-octadecenoic acid methyl ester/Elaidic acid methyl ester	19	36	2	1	296	36	16	1	2	1	38	36	18	-11795
C18:1n9c	Oleic acid methyl ester	19	36	2	1	296	36	16	1	2	1	38	36	18	-11795
C18:2n6t	Linolelaidic acid methyl ester	19	34	2	2	294	34	15	1	2	2	38	34	17.5	-11664
C20:0	Eicosanoic acid methyl ester	21	42	2	0	326	42	19	1	2	0	42	42	20.5	-13206
C18:2n6c	Linoleic acid methyl ester	19	34	2	2	294	34	15	1	2	2	38	34	17.5	-11664
C18:3n3	Linolenic acid methyl ester	19	32	2	3	292	32	14	1	2	3	38	32	17	-11533
C18:3n6	γ-Linolenic acid methyl ester	19	32	2	3	292	32	14	1	2	3	38	32	17	-11533
C20:1n9	cis-11-Eicosenoic acid methyl ester/Arachidic acid methyl ester	21	40	2	1	324	40	18	1	2	1	42	40	20	-13075
C22:0	Behenic acid methyl ester	23	46	2	0	354	46	21	1	2	0	46	46	22.5	-14486
C20:3n6	cis-8,11,14-Eicosatrienoic acid methyl ester	21	36	2	3	320	36	16	1	2	3	42	36	19	-12813
C20:3n3	cis-11,14,17-Eicosatrienoic acid methyl ester	21	36	2	3	320	36	16	1	2	3	42	36	19	-12813
C20:4n6	Arachidonic acid methyl ester	21	34	2	4	318	34	15	1	2	4	42	34	18.5	-12682
C22:2	cis-13,16-Docosadienoic acid methyl ester	23	42	2	2	350	42	19	1	2	2	46	42	21.5	-14224
C24:0	Tetracosanoic acid methyl ester	25	50	2	0	382	50	23	1	2	0	50	50	24.5	-15766
C22:1n9	Erucic acid methyl ester	23	44	2	1	352	44	20	1	2	1	46	44	22	-14355
C24:1n9	nervonic acid	25	48	2	1	380	48	22	1	2	1	50	48	24	-15635
C20:5n3	cis-5,8,11,14,17-Eicosapentaenoic acid methyl ester	21	32	2	5	316	32	14	1	2	5	42	32	18	-12551

Cryopreservation of Algae

Cryopreservation was essential to enable the preservation of microbes for future use without wasting materials and equipment on subculturing. The algae waspreserved in 10% glycerol stocks, which use glycerol as a cryoprotectant, similar to the standard cryopreservation of bacteria. The algae biomass is collected and resuspended in 500 µL of culture media. 150 µL or 10% volume of 100% autoclaved glycerol was transferred into a sterile microcentrifuge tube. 500 µL of the algae suspension and 850 µL of media were added to the microcentrifuge tube. The microcentrifuge tube was sealed with parafilm and the mixture is mixed thoroughly. The glycerol stock is placed in an ice bath for 45 minutes. This allows the algae cells to enter its hibernation phase. The cooled glycerol stocks were immediately stored in a cryogenic box at -80 ˚C. The glycerol stocks of the algae will remain viable for approximately 6 months to a year (Beaty and Parker 1992).

Results

Microalgae Isolation

The water samples collected from the site locations yielded various strains of microalgae from both freshwater and marine. Most of the microalgae culture sports a green color while a select few are brown cultures (Table 9).

All microalgae were assigned their own label (Figure 22) based on:

1. Whether they are freshwater or marine
2. Their sampling location
3. Assigned Number

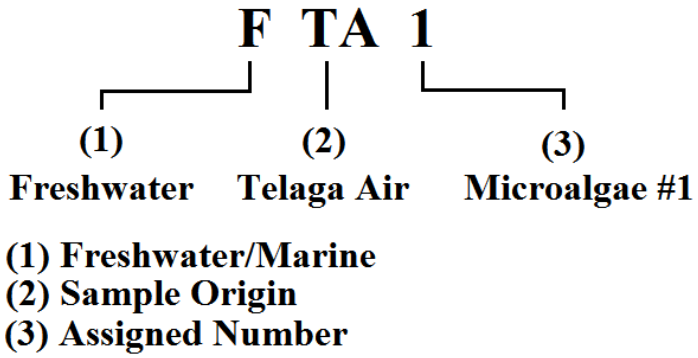

Figure 22: Labeling system of the microalgae strains.

Initially 33 isolates were obtained. 1 of them were discarded as they represented duplicates. In total, 16 different microalgae isolates were kept for subsequent experiments (Table 9).

Table 9: Microalgae strains isolated from the water samples listed with their label, origin and characteristics.

Label	Sample location	FreshWater/ Marine	Morphology
FSA	Sarawak river; Site A	Freshwater	Green small spherical cell
FSB	Sarawak river; Site B	Freshwater	Brown spindle cell
FSD	Sarawak river; Site D	Freshwater	Green spindle cell; chain groups
FSE	Sarawak river; Site E	Freshwater	Green crescent cell
FBP1	Kampung Apar Pond	Freshwater	Green long spindle cell
FBP2	Kampung Apar Pond	Freshwater	Green irregular cell
FBP3	Kampung Apar Pond	Freshwater	Brown spindle cell
FTA1	Telaga Air	Freshwater	Green spindle cell; chain groups
FTA2	Telaga Air	Freshwater	Green oval cell
MTA1	Telaga Air	Marine	Brown irregular cell
MTA2	Telaga Air	Marine	Green oval cell
FTAR	Tunku Abdul Rahman	Freshwater	Green oval cell; 4 cell group
FTAR2	Tunku Abdul Rahman	Freshwater	Green oval cell; 4 cell group
FTAR3	Tunku Abdul Rahman	Freshwater	Brown spindle cell
MTAR	Tunku Abdul Rahman	Marine	Green small spherical cell
FDP	Domestic Pond	Freshwater	Green oval cell; 8 cell group

The samples from Telaga Air and Tunku Abdul Rahman Marine Park yielded several freshwater species despite originating from a marine water sample. This was due to the weather event prior to the sampling as heavy rains occurred and may have caused freshwater microalgae to be washed away from freshwater bodies like small ponds upstream of Telaga Air or nearby land masses like Pulau Manukan in Tunku Abdul Rahman Marine Park into the marine water. The rain also produced a layer of freshwater above the marine water to allow the freshwater algae to survive extended periods of time in marine areas (Meffe and Snelson 1989).

Electrophoresis Gel

The 50 bp ladder from New England Biolabs was used as the band size reference in the gel analysis. The gel bands were produced by the DNA replicated by the PCR. Expected band size ranged from approximately 500bp to 800bp (Figure 23). It was noted that the wells that showed no band were unsuccesful PCR samples. The unccessful samples failed due to insufficient DNA template or incompatibility of the DNA with the primers used in the PCR.

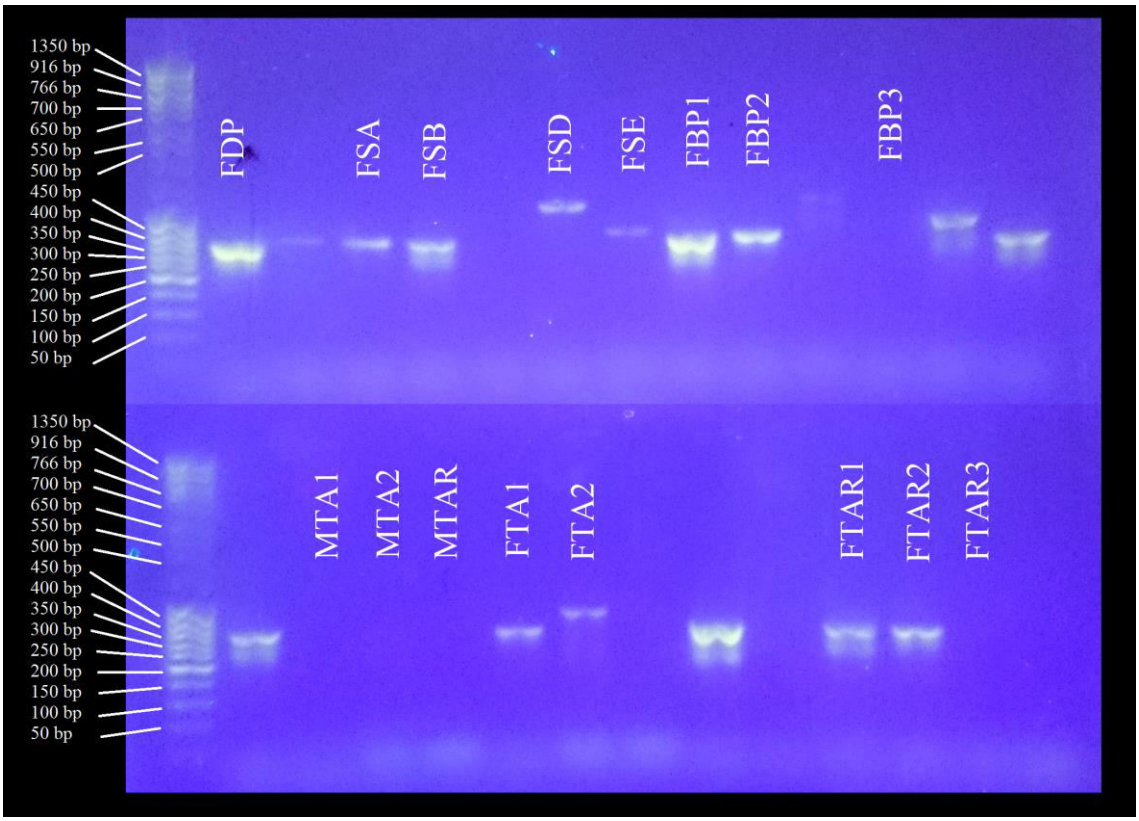

Figure 23: The electrophoresis gel viewed under UV light with the 50bp ladder reference obtained from New England Biolabs. <https://www.neb.com/> The bands in the wells that ranged between 500 bp tp 800 bp were successful PCR attempts at replicating microalgae DNA. Empty wells in the gel were unsuccessful attempts.

Identification of Microalgae

The DNA extraction of the microalgae strains yielded varying degrees of success due to the resilience of the cells against the DNA extraction methods employed. Using various methods and kits, however, all DNA were successfully extracted. The PCR carried out on the DNA extracts also yielded results with varying success. A significant number of freshwater samples were successfully sequenced by BGI while the marine samples showed no success and could not be identified. Strains without molecular data were identified purely on their morphological features. Strains with both sets of data were identified on both.

Sequenced Microalgae Strains

FSA

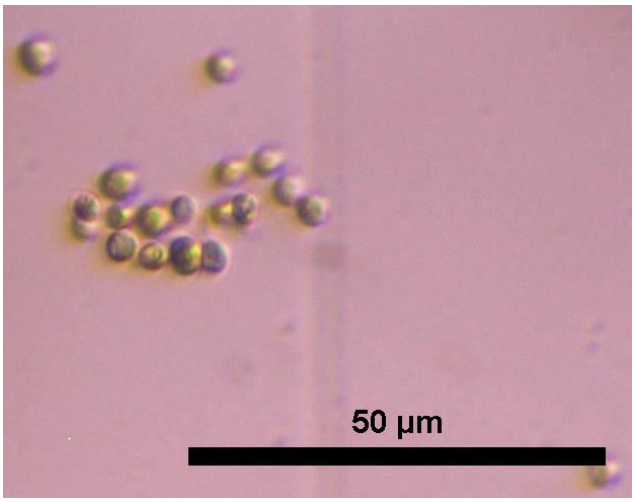

Figure 24: Microalgae FSA which has a very small cell size.

FSA was observed to have a very small cell size, measuring approximately 5µm (Figure 24). PCR using the ITS 1 and ITS 4 primer pair did not yield any results while PCR using primer pairs 8F (Eden et al. 1991) and 519R (Lane et al. 1985) yielded clean PCR products. Comparison of the DNA sequence with the NCBI database yielded little results. All of the matches were uncultured microalgae and bacteria which were unidentified. The microalgae best matches were with uncultured cyanobacterium and uncultured eukaryote at a high identity percentage of 100% and 95% respectively (Table 10). Phylogenetic analyses grouped it with them as well (Figure 25). Thus, concluding with the lack of results from the GenBank, FSA could very likely be a microalgae that has not been named or identified.

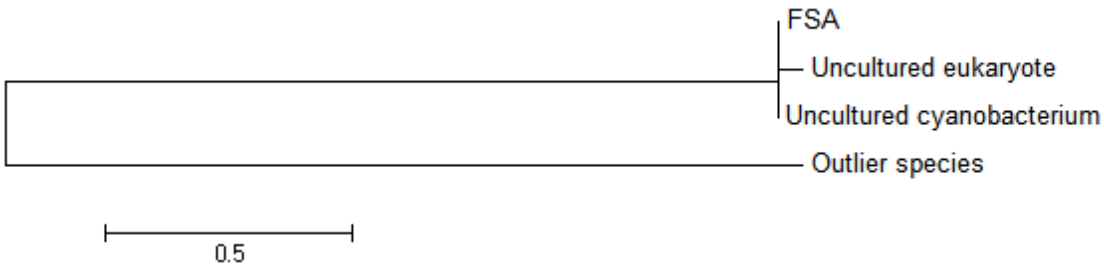

Figure 25: Phylogenetic tree detailing the genetic relationship of FSA with other microalgae species. The outlier species used was Scenedesmus costatus.

Table 10: Identity statistics of FSA

Identity matches	Query Cover	Base pair length (bp)	E Value	Identity (%)	Gene Bank Reference
Uncultured cyanobacterium	391/391	436	0	100	KF951520.1
Uncultured eukaryote	398/420	947	0	95	JN546842.1

FSB

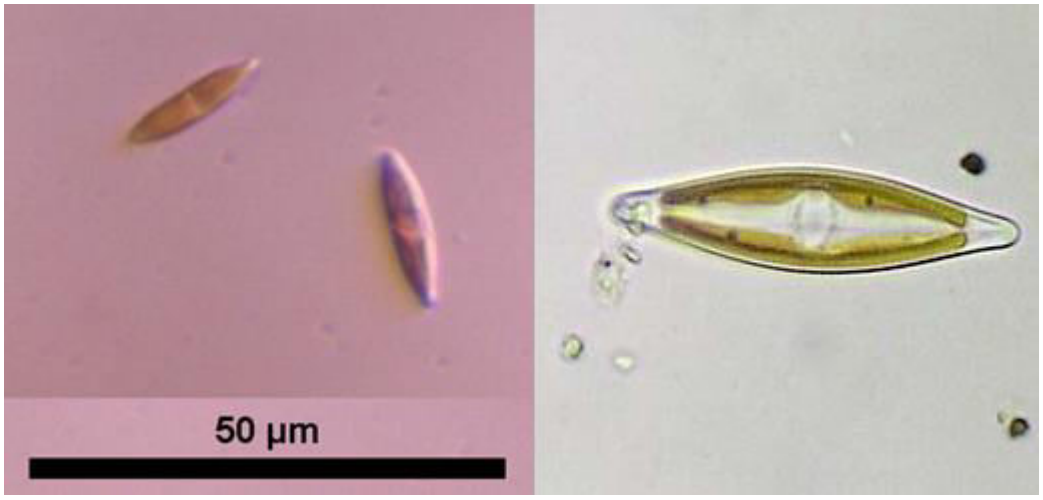

Figure 26: FSB and *Nitzschia Navicula*; obtained from University of Wisconsin Plant teaching Collection <http://botit.botany.wisc.edu/>.

FSB had a low identity match with many of the BLAST results (Table 11) (Figure 27). FSB matches included with *Nitzschia bizertensis*, *Nitzschia pusilla*, *Nitzschia ovalis*, *Nitzschia microcephala*, *Pseudo-nitzschia pungens*, and *Pseudo-nitzschia fukuyoi*. *Cylindrotheca fusiformis* and *Cylindrotheca closterium* had a notable identity similarity due to distinct similarities between their morphology. However, due to FSB'S DNA likeliness to the *Nitzchia* and *Pseudo-nitzschia* (Figure 26), FSB was suspected to be a species of either genus that had adapted to freshwater. Thus, FSB would likely be an uncultured species of *Nitzchia* or *Pseudo-nitzschia*.

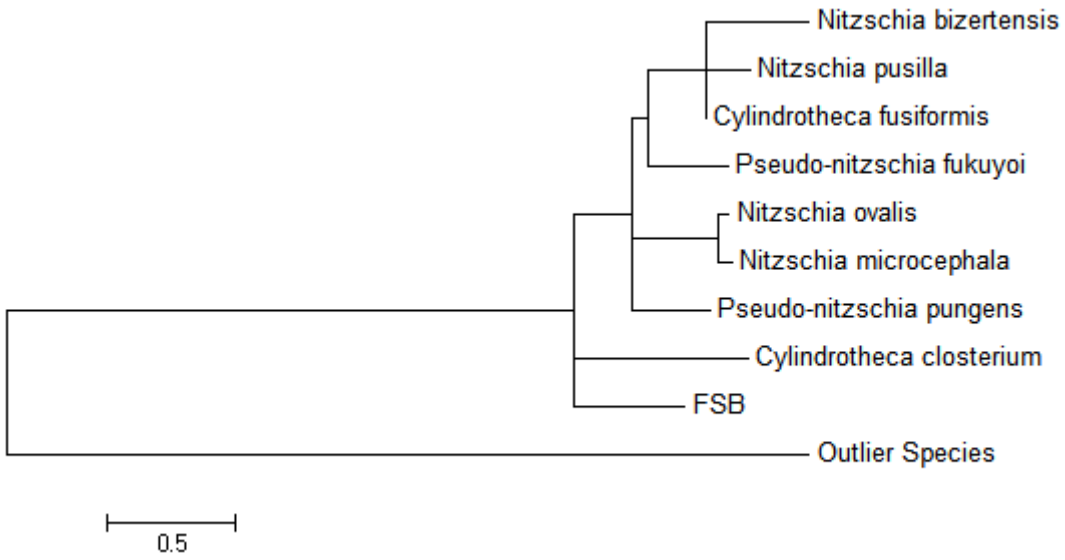

Figure 27: Phylogenetic tree detailing the genetic relationship of FSB with other microalgae species. The outlier species used was Scenedesmus costatus.

Table 11: Identity statistics of FSB.

Identity matches	Query Cover	Base pair length (bp)	E Value	Identity (%)	Gene Bank Reference
Nitzschia bizertensis	177/180	948	2.00E-82	98	KF938919.1
Nitzschia pusilla	187/193	490	1.00E-83	97	AY574381.1
Nitzschia ovalis	177/182	2587	1.00E-79	97	FR865500.1
Cylindrotheca closterium	173/177	326	1.00E-78	98	FJ864277.1
Cylindrotheca fusiformis	182/185	825	1.00E-84	98	KJ019016.1
Nitzschia microcephala	175/180	2763	1.00E-78	97	KC759159.1
Pseudo-nitzschia pungens	175/182	695	6.00E-77	96	FM207602.1
Pseudo-nitzschia fukuyoi	170/173	794	5.00E-78	98	KC147521.1

FSD

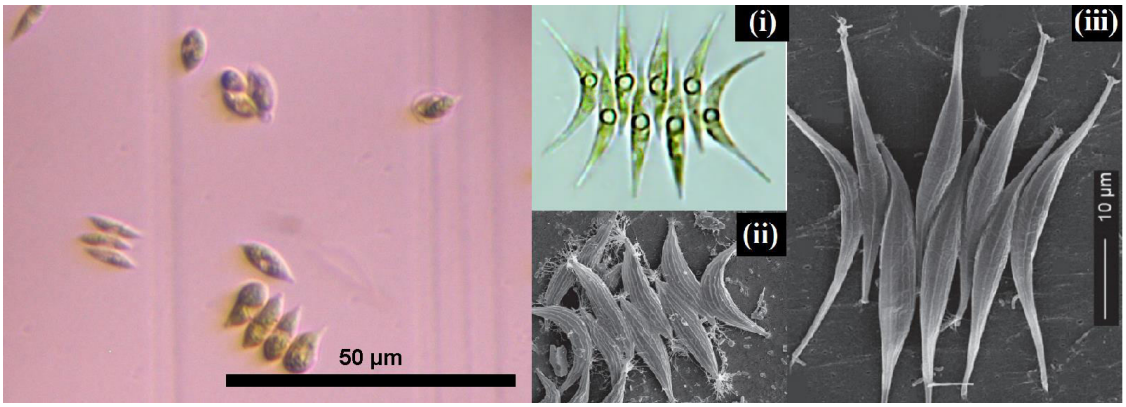

Figure 28: FSD and (i) *Scenedesmus pectinatus*, (ii) *Pectinodesdus pectinatus*, (iii) *Pectinodesmus holtmannii*; (i) Obtained from plingfactory: life in water <http://www.plingfactory.de/pling.html> ;(ii) and (iii) (Hegewald 2013) obtained from Fottea.

FSD were green spindle shaped cells that group together in chains (Figure 28). Genetic analysis of FSD's DNA showed matches with various microalgae; *Pectinodesmus pectinatus* and *Pectinodesmus hotmannii* from the *Pectinodesmus* and Scenedesmus *abundans* and *Scendesmus pectinatus* from the *Scenedesmus* genus (Figure 29). FSD was also matched with *Coelastrum sphaericum* but its morphology of spherical green cells was completely different to FSD's morphology (Tsukii 1977). *S. abundans* also had a different morphology than FSD which was green oval cells that for form cell groups with spines (Tsukii 1977). The last three microalgae shared the same morphology with FSD. Based on the BLAST, results the likely identity of FSD was *P. pectinatus* (Table 12).

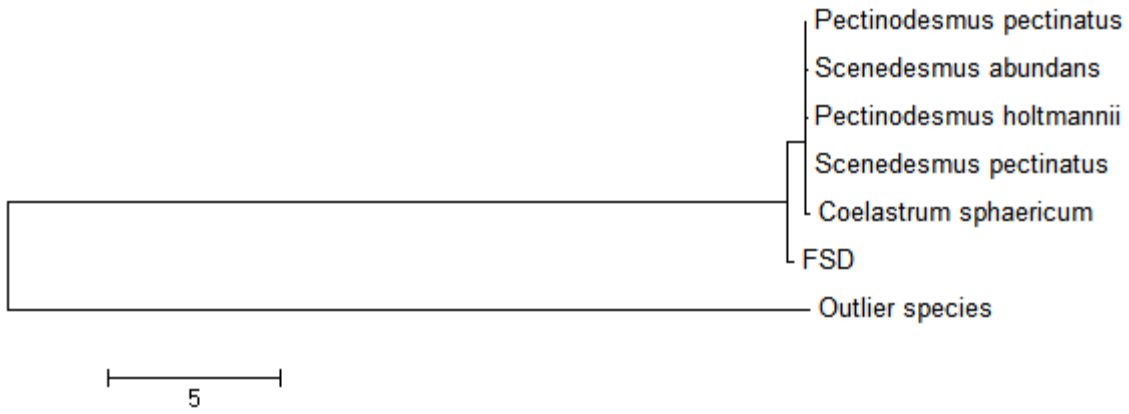

Figure 29: Phylogenetic tree detailing the genetic relationship of FSD with other microalgae species. The outlier species used was *Pseudo-nitzschia delicatissima*.

Table 12: Identity statistics of FSD.

Identity matches	Query Cover	Base pair length (bp)	E Value	Identity (%)	Gene Bank Reference
Pectinodesmus pectinatus	568/585	651	0.00E +00	97	JN703737.1
Scenedesmus pectinatus	565/583	698	0.00E +00	97	FR865735.1
Scenedesmus abundans	561/582	654	0.00E +00	96	FR865735.1
Pectinodesmus holtmannii	566/583	761	0.00E +00	97	JQ082335.1
Coelastrum sphaericum	446/480	698	0.00E +00	93	GQ375102.1

FSE

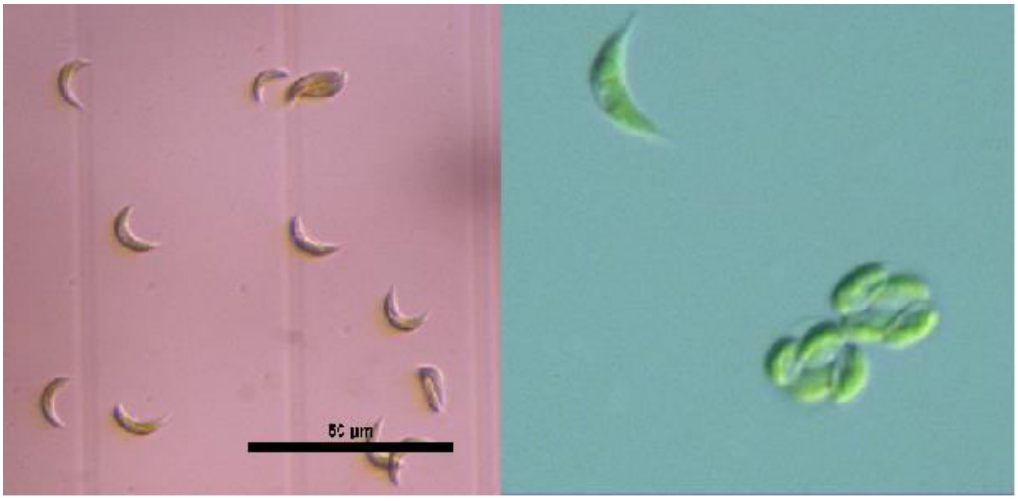

Figure 30: FSE and Nephrochlamys subsolitaria; obtained from Protist Information Server <http://protist.i.hosei.ac.jp/index.html>.

FSE's cells were a unique green, crescent shaped (Figure 30). Thus, close matches like *Ankistrodesmus gracilis* and *Ankistrodesmus falcatus* were not its identity due to the differences in morphology (Tsukii 1977) (Figure 31) (Table 13). FSE's closest identity match was *Nephrochlamys subsolitaria* which shows the same green, crescent shape (Tsukii 1977).

Figure 31: Phylogenetic tree detailing the genetic relationship of FSE with other microalgae species. The outlier species used was *Scenedesmus costatus*.

Table 13: Identity statistics of FSE

Identity matches	Query Cover	Base pair length (bp)	E Value	Identity (%)	Gene Bank Reference
Ankistrodesmus gracilis	554/584	2435	0	95	AB917098.1
Nephrochlamys subsolitaria	516/590	3900	0	87	AB917131.1
Scenedesmus regularis	518/592	674	0	88	JX138999.1
Ankistrodesmus falcatus	510/586(	868	0	87	KC145459.1

FBP1

Figure 32: FBP1 and Ankistrodesmus sp.; obtained from Protist Information Server < http://protist.i.hosei.ac.jp/index.html>.

FBP1 was a long spindle green cell microalgae (Figure 32) and was similar to *Ankistrodesmus gracilis* and *Monoraphidium* sp (Figure 33). FBP1 was more identical to *Monoraphidium* sp. (Table 14) but does not share the same morphology as *Monoraphidium* sp. covers microalgae species with swirly shaped microalgae cells (Tsukii 1977). Thus FBP1 was more closely related to *A. gracilis* (Figure 32), a

microalgae proposed as a food crop in a large scale culture research involving *A. gracilis* and *Diaphanosoma biergei* (Sipaúba-Tavares and Pereira 2008).

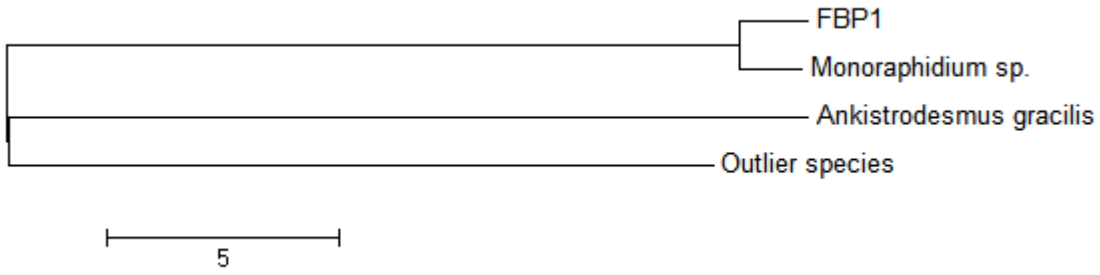

Figure 33: Phylogenetic tree detailing the genetic relationship of FBP1 with other microalgae species. The Outlier species used was Scenedesmus costatus.

Table 14: Identity Statistics of FBP1

Identity matches	Query Cover	Base pair length (bp)	E Value	Identity (%)	Gene Bank Reference
Selenastrum capricornutum	546/610	2976	0	90	JQ315794.1
Ankistrodesmus gracilis	533/607	2435	0	88	AB917098.1
Nephrochlamys subsolitaria	537/610	3900	0	88	AB917131.1
Monoraphidium sp.	548/609	979	0	90	JQ315786.1

FBP2

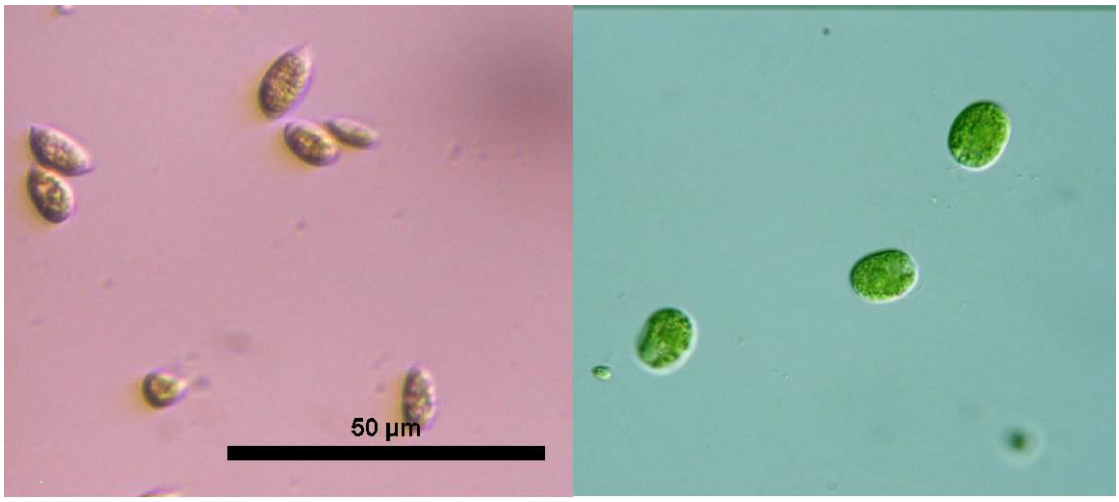

Figure 34: FBP2 and *Chlamydomonas moewusii*; obtained from Protist Information Server < http://protist.i.hosei.ac.jp/index.html>.

FBP2's cells were green and oval shaped. (Figure 34) It shared similarities with *Haematococcus pluvialis* but *Haematococcus pluvialis* sports a red color due to its production of astaxanthin (Urbani 2013) (Table 15). FBP2 also shared a similar relationship with *Scenedesmus rubescens* which also sports similar morphologies (Figure 35). The most reliable identity was *Chlamydomonas moewusii* as it had a high query cover and similar morphology as the sample strain (Figure 34). The microalgae strain has been found to produce various lipid profiles of the chloroplast lipids phosphatidylglycerol and monogalactosyldiacylglycerol from many alterations of nutrient stress (Arisz et al. 2000).

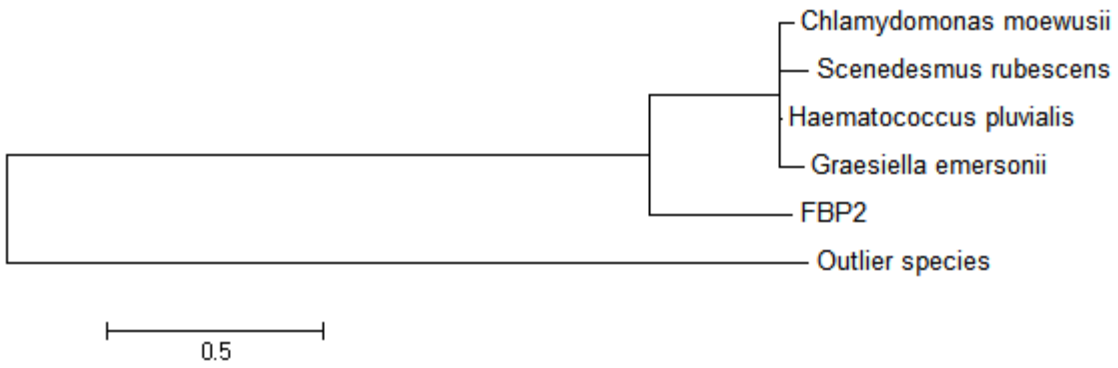

Figure 35: Phylogenetic tree detailing the genetic relationship of FBP2 with other microalgae species. The outlier species used was *Pseudo-nitzschia delicatissima*.

Table 15: Identity statistics of FBP2

Identity matches	Query Cover	Base pair length (bp)	E Value	Identity (%)	Gene Bank Reference
Chlamydomonas moewusii	563/610	720	0	92	JX290025.1
Haematococcus pluvialis	562/610	680	0	92	JX046429.1
Scenedesmus rubescens	567/611	2847	0	93	JX513884.1
Imbribryum alpinum	563/610	660	0	92	FJ593899.1
Plagiomnium medium	562/612	660	0	92	FJ796893.1
Graesiella emersonii	564/610	718	0	92	JX456465.1

FDP

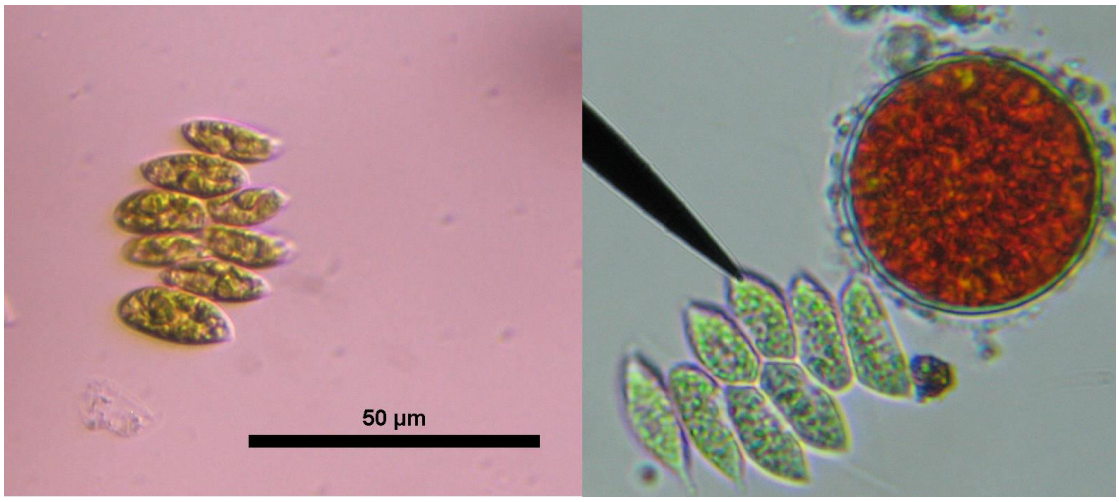

Figure 36: FDP and *Scenedesmus Obliquus*, another identity of *Acutodesmus obliquus*; obtained from Labroots.com, <http://legacy.labroots.com/default/index/index>

FDP was a microalgae strain with an oval green cell morphology (Figure 36). The microalgae strain also has an uncommon trait of forming anti-grazing groups of eight. *Scenedesmus dimorphus*, which have a high similarity with FDP (Table 16) (Figure 37), also forms anti-grazing groups of eight, but its cells were spindle shaped (Tsukii 1977). FDP's identity was most likely *Acutodesmus obliquus* (Figure 36), a freshwater microalgae (Urbani 2013) which was also classified as *Scenedesmus obliquus* (Urbani 2013). *A. obliquus* (Figure 36) has been proposed as a good bioindicator of lead in an aquatic environment (Piotrowska-Niczyporuk 2015).

Figure 37: Phylogenetic tree detailing the genetic relationship of FDP with other microalgae species. The outlier species used was *Pseudo-nitzschia delicatissima*.

Table 16: Identity Statistics of FDP.

Identity matches	Query Cover	Base pair length (bp)	E Value	Identity (%)	Gene Bank Reference
Acutodesmus Bernardii	616/634	943	0	97	JQ082329.1
Acutodesmus Obliquus	630/631	678	0	99	JX485652.1
Scenedesmus Dimorphus	616/634	688	0	97	KP645232.1

FTA1

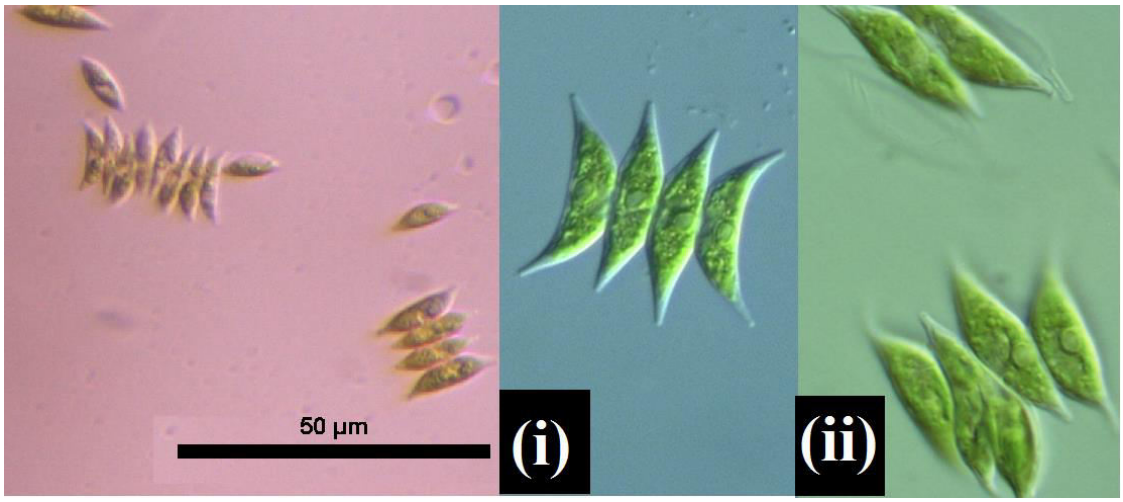

Figure 38: FTA1 and (i) *Scenedesmus acutus* and (ii) *Scenedesmus dimorphus*; (i) (Tsukii 1977) obtained from Protist Information Server <http://protist.i.hosei.ac.jp/index.html>, (ii) obtained from America Pink < http://america.pink/>.

FTA1 was composed of cells that were green, spindle shaped and arranged themselves in a row or zigzag pattern (Figure 38). FTA1 was a freshwater microalgae which was isolated from a marine water sample. When its genetic data was compared it was matched with various species of the *Scenedesmus* genus the Acutodesmus genus (Table 17, Figure 39). However, *S. obliquus* had a completely different morphology when compared to FTA1 (Urbani 2013). Scenedesmus acutus, *S. dimorphus* (Figure 38i) and *A. obliquus* (Figure 38ii) had similar morphology with FTA1 (Tsukii 1977). Thus, FTA1's identity was most likely *S. acutus* due to FTA1's higher genetic similarity to the *Scenedesmus* genus (Tsukii 1977).

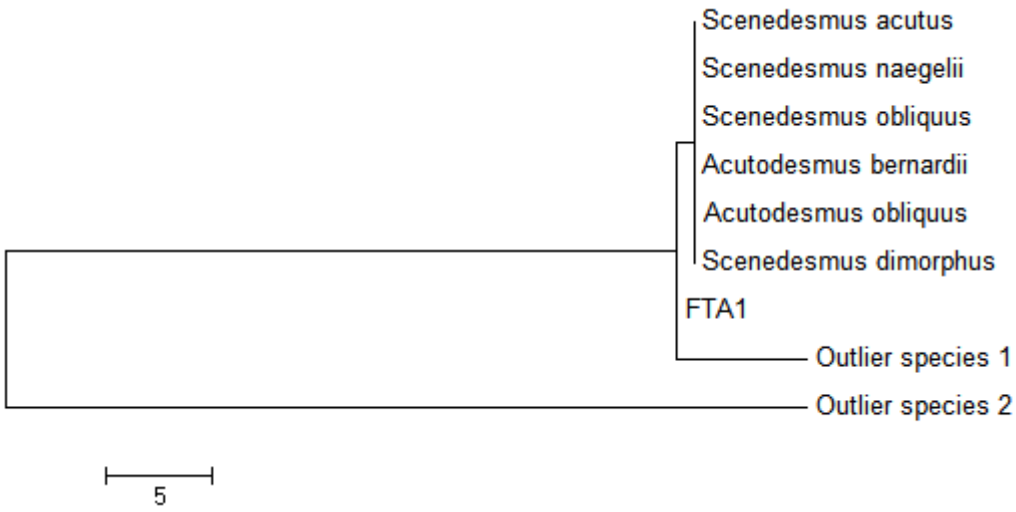

Figure 39: Phylogenetic tree detailing the genetic relationship of FTA1 with other microalgae species. The outlier species used are *Scenedesmus costatus* and *Scenedesmus ellipticus* respectively.

Table 17: Identity Statistics of FTA1

Identity matches	Query Cover	Base pair length (bp)	E Value	Identity (%)	Gene Bank Reference
Scenedesmus acutus	508/518	680	0	98	AJ249509.1
Scenedesmus naegelii	509/518	680	0	98	JX485652.1
Scenedesmus obliquus	509/518	680	0	98	AJ249506.1
Scenedesmus dimorphus	509/518	1380	0	98	KJ676127.1
Acutodesmus bernardii	509/518	943	0	98	JQ082329.1
Acutodesmus obliquus	512/514	678	0	99	AJ249510.1

FTA2

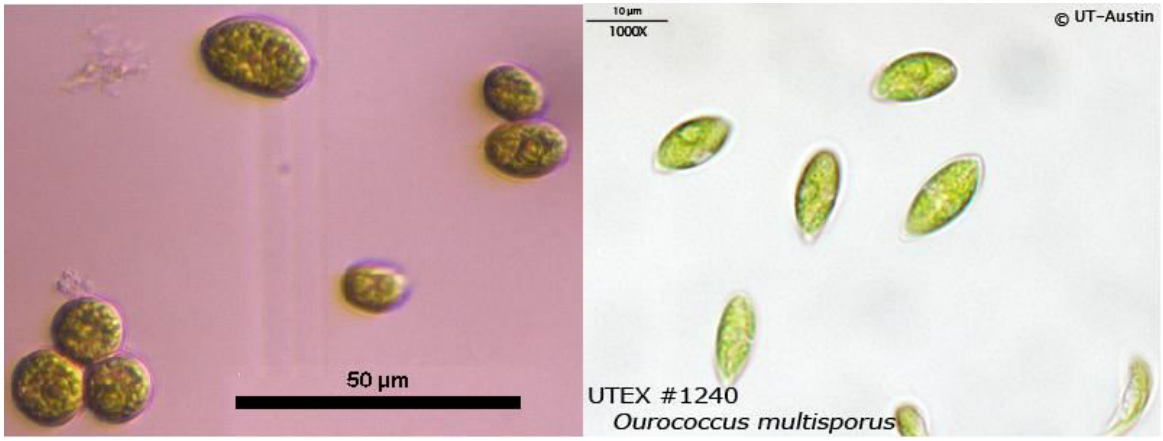

Figure 40: FTA2 and *Ourococcus multisporus*. Obtained from Center for Freshwater Biology. <http://cfb.unh.edu/>

FTA2 was composed of green cells with an oval shape (Figure 40). Genetic comparisons with the DNA database yielded various types of microalgae (Table 18). FTA2 was matched with *Ourococcus multisporus*, *Anthrospira platensis*, *Scenedesmus obliquus* and *Kirchneriella aperta*. However, *A. platensis* and *K. aperta* were shown to have completely different morphologies than FTA2 as *A. platensis* was a filamentous microalgae (Fedor 2011) and *K. aperta* had a rounded crescent shape (Tsukii 1977). FTA2 had similar morphologies to *O. multisporus* and *Scenedesmus obliquus* (*Ourococcus (Chlorophyceae)* n.d.) but a look at the phylogenetic tree (Figure 41) showed that FTA2 was genetically closer to *O. multisporus* than *S. obliquus*. Thus, FTA2's likely identity was *O. multisporus*.

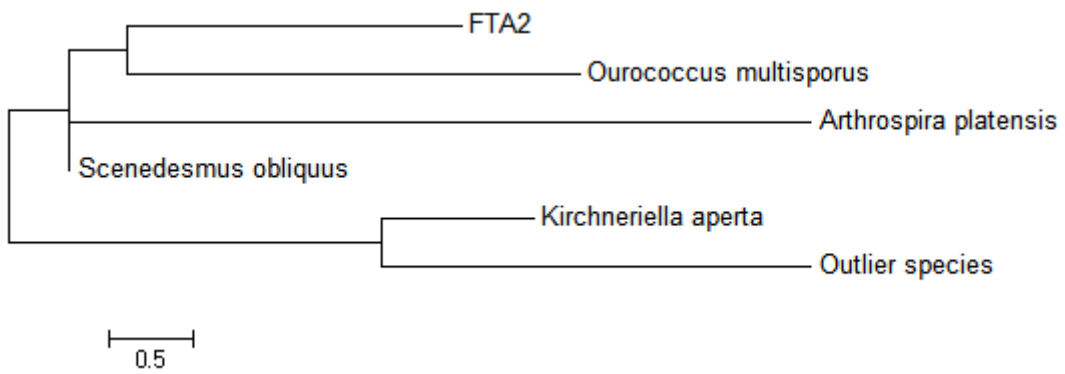

Figure 41: Phylogenetic tree detailing the genetic relationship of FTA2 with other microalgae species. The outlier species used was *Pseudo-nitzschia delicatissima*.

Table 18: Identity statistics of FTA2

Identity matches	Query Cover	Base pair length (bp)	E Value	Identity (%)	Gene Bank Reference
Ourococcus multisporus	367/392	770	1.00E-170	94	KT369474.1
Scenedesmus Obliquus	407/425	1220	0	96	AF394206.1
Kirchneriella aperta	367/392	207516	1.00E-170	94	KT199250.1
	367/392		1.00E-170	94	
Arthrospira platensis	358/370	750	1.00E-180	97	KF290490.1

FTAR

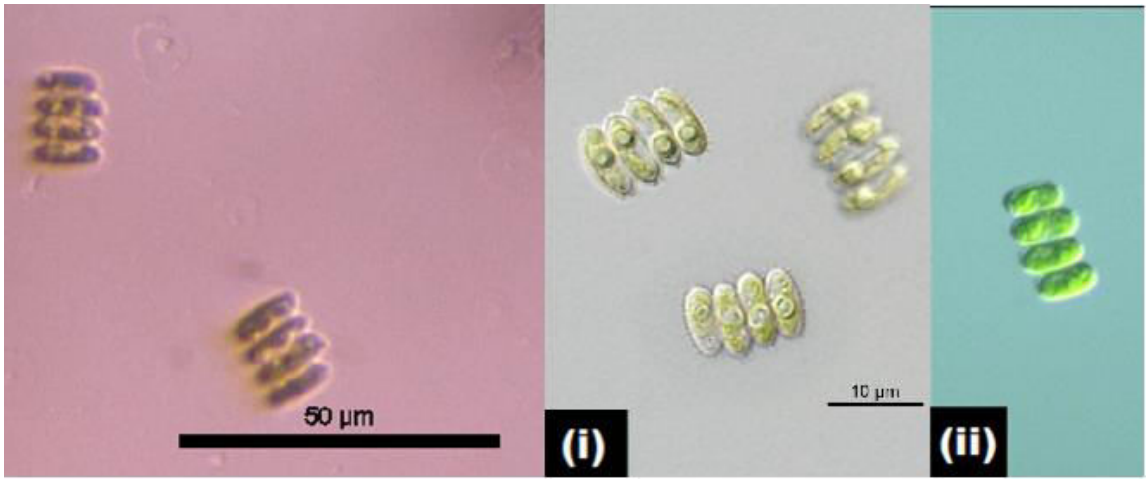

Figure 42: FTAR and (i) *Desmodesmus serratus* and (ii) *Scenedesmus incrassatulus*; (i) (Hansen n.d.) obtained from Nordic Microalgae and Aquatic protozoa <http://nordicmicroalgae.org/>, (ii) (Tsukii 1977) obtained from Protist Information Server <http://protist.i.hosei.ac.jp/index.html>.

FTAR were composed of green elliptical cells and formed rows of four (Figure 42). When its genetic data was compared to the database, it matched with various results that didn't seem to match its identity (Table 19). *Chlamydomonas* and *Coelastrealla* sp. does not have similar morphology. In terms of morphology, FTAR was found to be similar to *Scenedemus incrassatulus* (Tsukii 1977), *Desmodesmus serratus* (Hansen n.d.) and *Scenedesmus ellipticus*. Finally, when the phylogenetic tree was observed (Figure 43), *S. incrassatulus* was seen to be most likely FTAR's identity.

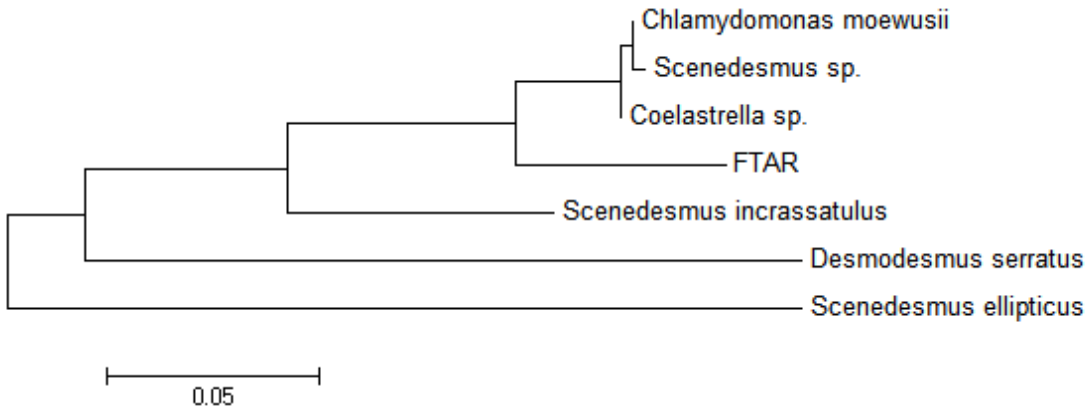

Figure 43: Phylogenetic tree detailing the genetic relationship of FTAR with other microalgae species.

Table 19: Identity statistics of FTAR.

Identity matches	Query Cover	Base pair length (bp)	E Value	Identity (%)	Gene Bank Reference
Scenedesmus sp.	543/584	681	0	93	AB762691.1
Haematococcus pluvialis	551/592	680	0	93	JX046429.1
Coelastrella	553/592	695	0	93	KP702302.1
Chlamydomonas moewusii	552/592	720	0	93	JX290025.1
Desmodesmus serratus	N/A	N/A	N/A	N/A	DQ417561.1
Scenedesmus incrassatulus	N/A	N/A	N/A	N/A	KP318982.1
Scenedesmus ellipticus	N/A	N/A	N/A	N/A	HG514420.1

FTAR2

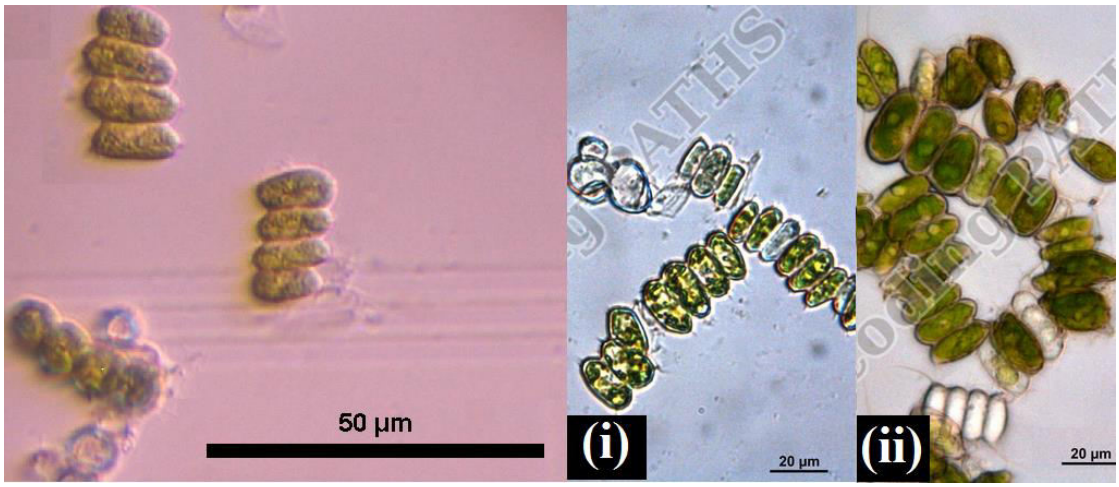

Figure 44: FTAR2 and (i) *Desmodesmus pirkollei* and (ii) *Desmodesmus communis*; (i) and (ii) (Hegewald n.d.) obtained from Barcoding P.A.T.H.S.

FTAR2 was observed to be oval green cells that form linear groups of four (Figure 44). Genetic comparison showed that FTAR2 was matched with *Desmodesmus pirkollei* (Figure 44i), *Desmodesmus communis* (Figure 44ii), *Desmodesmus anthrodesmiformis* and *Desmodesmus hystrix* which were all species originating from the *Desmodesmus* genus (Figure 45) (Table 20). Thus, it can be drawn that FTAR2 was a species from the *Desmodesmus* genus. However, when compared in terms of morphology, *D. communis*, *D. anthrodesmiformis* and *D. hystrix* all have spines protruding from their polar cells (Hegewald n.d.) while FTAR2 was observed to not have any. As a result, the final identity of FTAR2 was *D. pirkollei* which shared the same morphology (Hegewald n.d.).

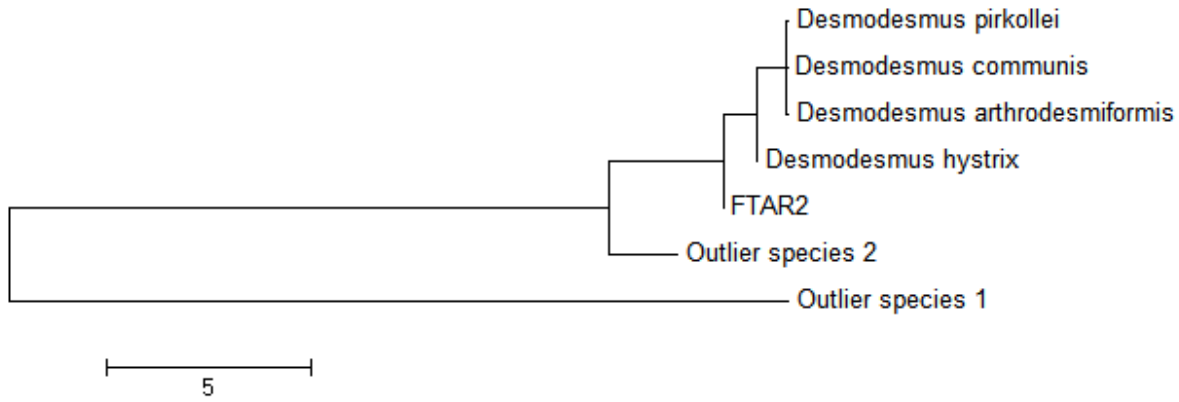

Figure 45: Phylogenetic tree detailing the genetic relationship of FTAR2 with other microalgae species. The outlier species used are *Scenedesmus costatus* and *Scenedesmus ellipticus* respectively.

Table 20: Identity statistics of FTAR2

Identity matches	Query Cover	Base pair length (bp)	E Value	Identity (%)	Gene Bank Reference
Desmodesmus hystrix	584/598	662	0	98	DQ417551.1
Desmodesmus pirkollei	574/598	649	0	96	DQ417557.1
Desmodesmus communis	532/600	653	0	89	DQ417557.1
Desmodesmus arthrodesmiformis	522/576	607	0	91	DQ417536.1

Table 21: Summary of the identities of the sequenced microalgae samples

Sample	Identity matches	Query Cover	Base pair length (bp)	E Value	Identity (%)	Gene Bank Reference
FSA	Uncultured cyanobacterium	391/391	436	0	100	KF951520.1
FSB	*Nitzschia bizertensis*	177/180	948	2.00E-82	98	KF938919.1
	Nitzschia pusilla	187/193	490	1.00E-83	97	AY574381.1
	Nitzschia ovalis	177/182	2587	1.00E-79	97	FR865500.1
	Nitzschia microcephala	175/180	2763	1.00E-78	97	KC759159.1
	Pseudo-nitzschia pungens	175/182	695	6.00E-77	96	FM207602.1
	Pseudo-nitzschia fukuyoi	170/173	794	5.00E-78	98	KC147521.1
FSD	*Pectinodesmus pectinatus*	568/585	651	0.00E+00	97	JN703737.1
FSE	*Nephrochlamys subsolitaria*	516/590	3900	0	87	AB917131.1
FBP1	*Ankistrodesmus gracilis*	533/607	2435	0	88	AB917098.1
FBP2	*Chlamydomonas moewusii*	563/610	720	0	92	JX290025.1
FDP	*Acutodesmus Obliquus*	630/631	678	0	99	JX485652.1
FTA1	*Scenedesmus acutus*	508/518	680	0	98	AJ249509.1
FTA2	*Ourococcus multisporus*	367/392	770	1.00E-170	94	KT369474.1
FTAR	*Scenedesmus incrassatulus*	N/A	N/A	N/A	N/A	KP318982.1
FTAR2	*Desmodesmus hystrix*	584/598	662	0	98	DQ417551.1

Table 21 shows the identities of the microalgae strains with a high query cover that suggests a high likelihood of the correct identity of the microalgae (Agostino 2012). The low query cover of FSB suggest an uncertain identity of the micro algae strain. This problem is due to the high frequency sequence diversification of nuclear rDNA ITS regions (Pringle et al. 2003).

Unsequenced Microalgae Strains

FBP3

Figure 46: FBP3 and Nitzschia sp. Obtained from Kaikorai tributary, Otago Regional Council and Landcare Research. <https://www.landcareresearch.co.nz>

FBP3 was a freshwater brown spindle shaped cell microalgae. The electrophoresis gel yielded no observable bands, signifying failure of the replication of the microalgae's DNA. (Figure 23) Its morphology closely resembles those of the Nitzchia and Pseudo-nitzchia genus (Figure 46). The microalgae cells have a brown spindle shaped morphology that all species from the Nitzchia and Pseudo-nitzchia genus have (Aletsee & Jahnke 1992). Thus, it can be determined that the microalgae species was another uncultured species from the Nitzchia or Pseudo-nitzchia genus.

FTAR3

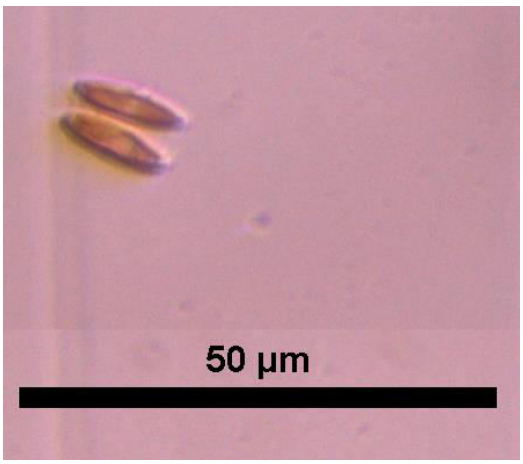

Figure 47: FTAR3 isolated from the Tunku Abdul Rahman Marine Park.

FTAR3 was a freshwater brown spindle shaped microalgae (Figure 47). It was an unidentified microalgae due to its DNA not being sequenced (Figure 23). However, the

morphology of the cell strongly suggests that the microalgae originated from the Nitzchia or Pseudo-nitzchia genus. The cells were observed to follow the brown and spindle shape cells of the Nitzchia or Pseudo-nitzchia genus (Aletsee & Jahnke 1992).

MTA1

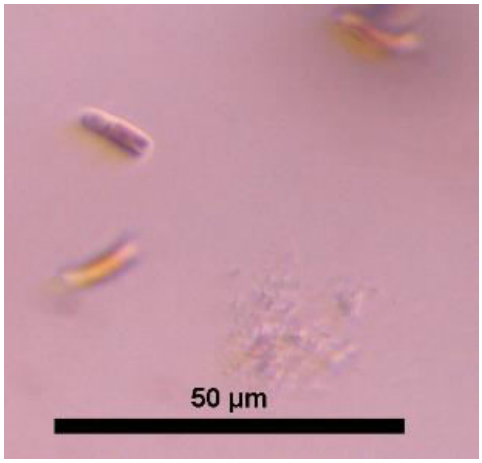

Figure 48: MAT1 isolated from the Telaga Air pier.

MTA1 was a marine microalgae which have irregular shaped cells that were brown in color (Figure 48). MTA1 showed a weak response to PCR and was not able to be sequenced, indicated by the lack of bands observed in the electrophoresis gel (Figure 23). The cause for the failed replication was likely due to the DNA's incompatibility to the primers used in the PCR.

MTA2

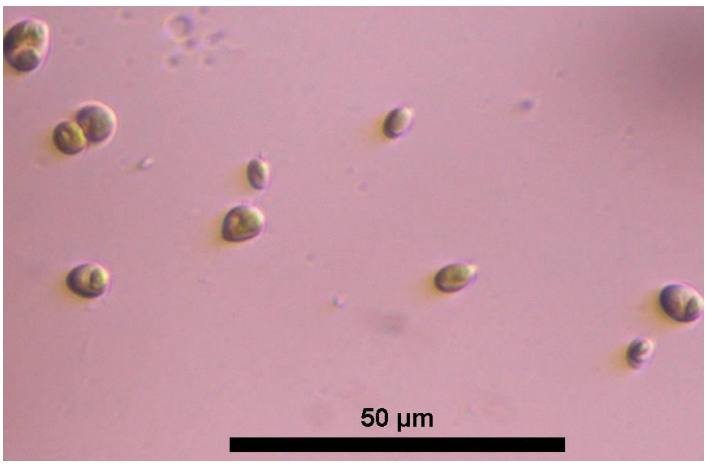

Figure 49: MTA2 microalgae isolated from the Telaga Air pier.

MTA2 was a marine microalgae that has a green oval shaped morphology (Figure 49). MTA2 showed incredible resistance during DNA extraction. Its cells were proved to be

resistant to chemical and physical attack, retaining cell structure after various methods of DNA extraction including using DNA extraction kits. The microalgae's DNA were also incompatible with the PCR primers as the PCR samples yield no bands (Figure 23). Thus, the microalgae remains unidentified.

MTAR

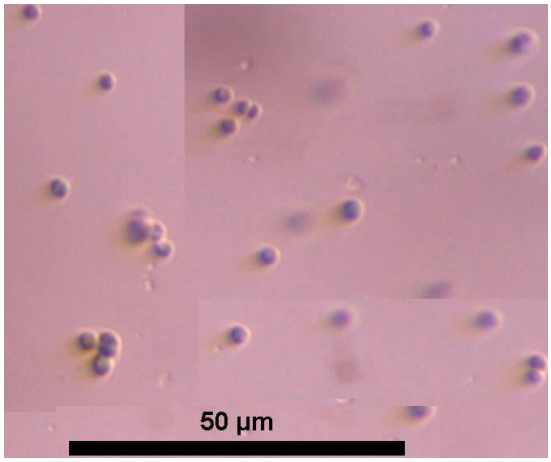

Figure 50: MTAR microalgae isolated from the Telaga Air pier.

MTAR was a microalgae with a small cell size. Its cells were green, spherical and very small (Figure 50). Its cells yielded DNA during the DNA extraction but its DNA was incompatible with the primers used in the PCR, yielding no bands in the electrophoresis gel (Figure 23). Thus, the microalgae remains unidentified.

FAME Analysis

The results of the GC were compared with the standards and the identities and amount of the FAMEs in the samples were determined. From this data, the total FAME and FAME yield percentage from the biomass could be calculated. In the following, data for each isolate is presented.

Microalgae Profiles

The microalgae strains displayed various responses to the nutrient concentration in the media. A majority of the microalgae strains showed healthy growth up to only 1x while some displayed positive growth up to the highest nutrient concentration in 10x. The microalgae showed significant growth in their cultures with the healthy cultures ranging from 10 to 50 times their initial cell count in the entire week of the experiment's duration.

FSA

Table 22: The amount of FAME produced and fats (%) of microalgae FSA under different nutrient conditions.

	FSA 0x	FSA 1x	FSA 5X	FSA 10X
C4:0	7.1E-06	4.8E-06	4.4E-06	3.4E-06
C6:0	6.1E-08	6.7E-08	6.3E-08	4.1E-08
C14:0	1.3E-08	2.2E-08	4.1E-08	1.1E-08
C16:0	4.3E-07	4.9E-07	5.9E-07	3.1E-07
C15:1	2.4E-08	0	0	0
C18:1n9t	5.8E-07	5.3E-07	6.4E-07	3.7E-07
C18:2n6c	8.4E-08	2.3E-07	4.9E-07	1.6E-07
C18:3n6	0	2.3E-08	4.3E-08	1.1E-08
C20:1n9	1E-07	3.8E-07	8.7E-07	2.6E-07
C20:5n3	0	0	0	4.9E-08
Total saturated fat (%)	0.68812	0.21401	0.18508	0.14324
Total monounsaturated fat (%)	0.05932	0.03384	0.05081	0.0223
Total polyunsaturated fat (%)	0.00688	0.00926	0.01782	0.00755
Total fats (%)	0.75432	0.25711	0.25371	0.17309

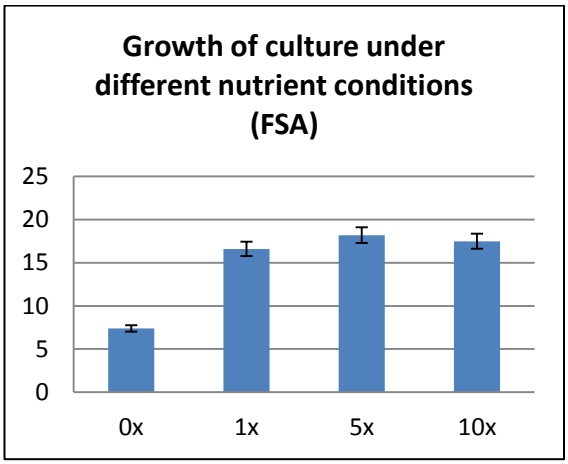

Figure 51: The growth of the culture of micro algae FSA under different nutrient conditions.

The FAME profile of FSA pointed to C4:0 FAME as its main constituent in lipid production while FAMEs of lesser presence were C16:0, C18:1n9t, C18:2n6c, and C20:1n9 (Table 22). The FAME levels showed that the FSA produced the FAMEs highest when starved of nutrients (Table 22). Under nutrient starvation, the microalgae cells couldn't reproduce and prioritized lipid accumulation instead (Vaulot et al. 1987). The growth rates of the cultures suggest that the microalgae grew optimally at 5x, shown by the increasing growth from 0x. However, in 10x the microalgae was under nutrient stress due to the high nutrient load, indicated by a slightly lower growth rate (Figure 51). The growth rate wasn't the only thing affected as the microalgae's lipid accumulation also decreased under the high nutrient load, indicated by decreasing FAME level (Table 22).

Nitzchia sp./Pseudo-nitzschia sp. (FSB)

Table 23: The amount of FAME produced and fats (%) of microalgae *Nitzchia sp./Pseudo-nitzschia sp.* (FSB) under different nutrient conditions.

	FSB 0x	FSB 1x	FSB 5x	FSB 10x
C4:0	1E-06	1E-06	1.1E-06	1.1E-06
C6:0	4E-08	1.2E-07	0	4.7E-08
C13:0	9.4E-09	9.3E-09	1E-08	1.1E-08
C14:0	3.5E-08	9.2E-08	6.3E-08	6.3E-08
C16:0	3.7E-07	6.7E-07	5.5E-07	5.7E-07
C15:1	3.8E-09	1E-08	8.2E-09	1.9E-08
C18:1n9t	2.9E-07	3.9E-07	3.7E-07	4E-07
C18:2n6t	4.7E-09	4.9E-08	2.7E-08	4.2E-08
C18:2n6c	9E-09	1.7E-08	9.5E-09	8E-09
C20:1n9	1.1E-08	1.1E-08	1.1E-08	1.9E-08
C20:3n6	7E-09	9E-09	8.7E-09	7.8E-09
C22:1n9	7.8E-09	5.9E-09	8.3E-09	5.1E-09
C20:5n3	2.8E-08	1.5E-07	9.8E-08	1.3E-07
Total saturated fat (%)	1.07856	0.6849	0.444	0.63807
Total monounsaturated fat (%)	0.21491	0.1452	0.09709	0.15334
Total polyunsaturated fat (%)	0.03326	0.07507	0.03407	0.06316
Total fats (%)	1.32673	0.90517	0.57515	0.85457

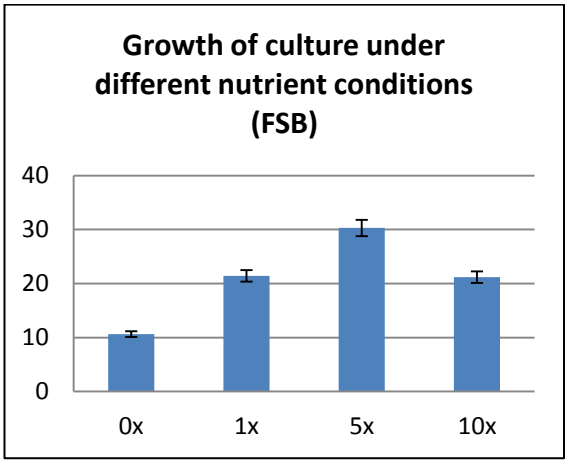

Figure 52: The growth of the culture of microalgae *Nitzchia sp./Pseudo-nitzschia sp.* (FSB) under different nutrient conditions.

The *Nitzchia sp./Pseudo-nitzschia sp.* (FSB) was shown to produce 3 main FAMEs from its lipids which are C4:0, C16:0, and C18:1n9t while lesser FAMEs were hydrocarbons C6:0, C16:0, C18:2n6t, and C20:5n3 (Table 23) The higher levels of FAMEs in 0x (Table 23) suggests that the microalgae's growth rate was impeded by the lack of nutrient leaving the microalgae to accumulate lipids from photosynthesis (Vaulot et al. 1987). The FAME levels decreased as the nutrient concentration increases up to 5x (Table 23) while the growth of the cultures increased (Figure 52), indicating that the lipids were used in cell division resulting in a lower percentage of FAME (Vitova et al. 2015). The

lowered growth rate in 10x and the increase in FAME levels also showed that the microalgae was affected by the high nutrients, inhibiting its growth rate which in turn allows more accumulation of lipids. Thus, 5x was the best concentration for optimum cell growth despite generating the lowest FAME levels while 0x gave the highest level of FAME despite generating the least biomass (Table 23).

Pectinodesmus pectinatus (FSD)

Table 24: The amount of FAME produced and fats (%) of microalgae *Pectinodesmus pectinatus* (FSD) under different nutrient conditions.

	FSD 0x	FSD 1x	FSD 5x	FSD 10x
C4:0	1.5E-06	1.4E-05	2E-06	1.8E-06
C6:0	5.7E-08	4.7E-08	5.7E-08	5.3E-08
C11:0	3.7E-09	0	0	0
C14:0	7.9E-09	1.3E-08	1.8E-08	1.4E-08
C16:0	4.4E-07	4.7E-07	5.4E-07	3.8E-07
C15:1	8.4E-09	0	4.5E-09	4E-09
C18:1n9t	3E-07	4.7E-07	6.2E-07	3.7E-07
C18:1n9c	1.6E-07	0	0	0
C18:2n6c	8.5E-08	2.4E-07	1.9E-07	1.2E-07
C20:1n9	1.4E-07	4.5E-07	3.3E-07	3E-07
C20:3n6	0	1.6E-07	2.1E-08	0
Total saturated fat (%)	0.02588	0.05808	0.01126	0.00903
Total monounsaturated fat (%)	0.00722	0.00352	0.00388	0.00255
Total polyunsaturated fat (%)	0.00099	0.0015	0.00083	0.00043
Total fats (%)	0.0341	0.0631	0.01598	0.01202

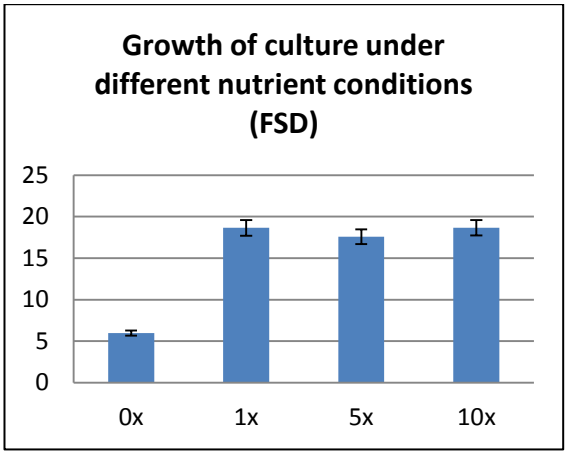

Figure 53: The growth of the culture of microalgae *Pectinodesmus pectinatus* (FSD) under different nutrient conditions.

The FAME profiles showed C4:0 FAME to be the most abundant in comparison with other FAMEs (Table 24). Other FAMEs a lesser presence were C16:0, C15:1, C18:1n9t, C18:1n9c, C18:2n6c and C20:1n9 (Table 24). *Pectinodesmus pectinatus* (FSD) produced the most FAME in 1x (Table 24) which indicates that the cells accumulate lipids under normal

conditions and their ability to accumulate the lipid was hampered by nutrient stress, either by nutrient starvation or overload of nutrients (Vitova et al. 2015) (Table 24). The culture growth showed stunted growth in nutrient starved condition while normal and high nutrient concentrations display similar levels of growth, concluding that the growth of the microalgae was already optimum at 1x (Figure 53).

Nephrochlamys subsolitaria (FSE)

Table 25: The amount of FAME produced and fats (%) of microalgae *Nephrochlamys subsolitaria* (FSE) under different nutrient conditions.

	FSE 0x	FSE 1x	FSE 5x	FSE 10x
C4:0	1.5E-06	1.1E-06	5.7E-06	5.6E-06
C6:0	7.6E-08	6.5E-08	5.7E-08	6.1E-08
C8:0	0	1.5E-08	1.3E-08	9.7E-09
C12:0	0	9.3E-09	7.5E-09	8E-09
C14:0	1.7E-08	3E-08	1.9E-08	1.6E-08
C16:0	6.5E-07	4.9E-07	3.4E-07	3.1E-07
C16:1	0	4.8E-09	0	0
C18:1n9t	3.6E-07	2.7E-07	2.8E-07	2.2E-07
C20:1n9	1.9E-07	3E-07	2.2E-07	2.3E-07
Total saturated fat (%)	0.07705	0.03119	0.10884	0.10358
Total monounsaturated fat (%)	0.01781	0.00993	0.00835	0.00713
Total polyunsaturated fat (%)	0	0	0	0
Total fats (%)	0.09487	0.04112	0.11718	0.11072

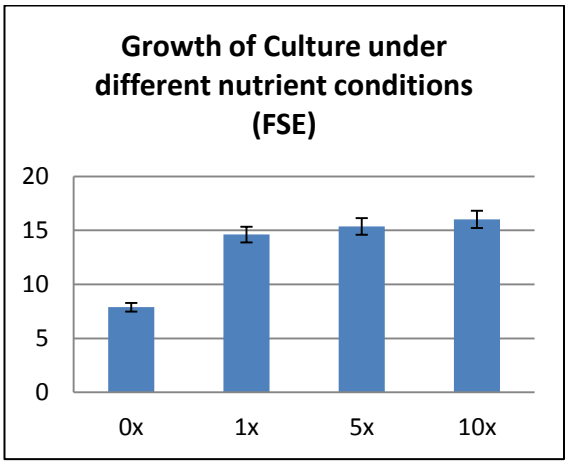

Figure 54: The growth of the culture of microalgae *Nephrochlamys subsolitaria* (FSE) under different nutrient conditions.

According to Table 25, C4:0 FAME had the highest amount in comparison with the other FAMEs. After C4:0, the FAME C16:0 was many multitudes smaller with two other FAME of similar amount, C18:1n9t FAME and C20:1n9 FAME (Table 25). *Nephrochlamys subsolitaria* (FSE) was shown to produce the least amount of lipids in normal nutrient conditions 1x and accumulate more lipids under nutrient stress from lack of nutrients in 0x and

higher nutrient concentrations in 5x and 10x, the highest being 5x (Table 25). A high percentage of lipids to biomass in 0x suggests that the microalgae's growth rate was significantly inhibited and the cells focus on photosynthesis and lipid accumulation instead (Table 25). Analysis of the FAME profile paired with the growth of the culture showed that the microalgae grew optimally in 1x (Figure 54) and started accumulating lipids in 5x (Table 25). This indicated that the microalgae reached its optimum growth rate at 1x but in 5x, the high nutrient partially inhibited its growth which allows the cells to accumulated lipids produced from photosynthesis (Vitova et al. 2015). In 10x, higher nutrient load now directly affect the accumulation of lipids resulting in a lower amount of FAME despite a slightly higher culture growth than 5x (Figure 54).

Ankistrodesmus gracilis (FBP1)

Table 26: The amount of FAME produced and fats (%) of microalgae *Ankistrodesmus gracilis* (FBP1) under different nutrient conditions.

	FBP1 0x	FBP1 1x	FBP1 5x	FBP1 10x
C4:0	3.4E-06	5.3E-06	4.3E-06	6.7E-06
C6:0	3.1E-08	7.3E-08	6.3E-08	5.4E-08
C16:0	2.4E-07	6.6E-07	4.9E-07	4.3E-07
C15:1	5.4E-09	1.6E-08	0	0
C18:1n9t	1.8E-07	4.7E-07	4.8E-07	4.7E-07
C18:1n9c	3E-08	6.8E-08	0	0
C18:2n6c	2.4E-08	2E-07	1.5E-07	1.5E-07
C20:1n9	5.9E-08	7.8E-07	5.4E-07	3.5E-07
C22:2	8.6E-09	7.8E-08	3.7E-08	0
Total saturated fat (%)	0.16157	0.09136	0.07613	0.1111
Total monounsaturated fat (%)	0.01125	0.0187	0.01464	0.01181
Total polyunsaturated fat (%)	0.00132	0.00386	0.00269	0.00212
Total fats (%)	0.17415	0.11392	0.09346	0.12503

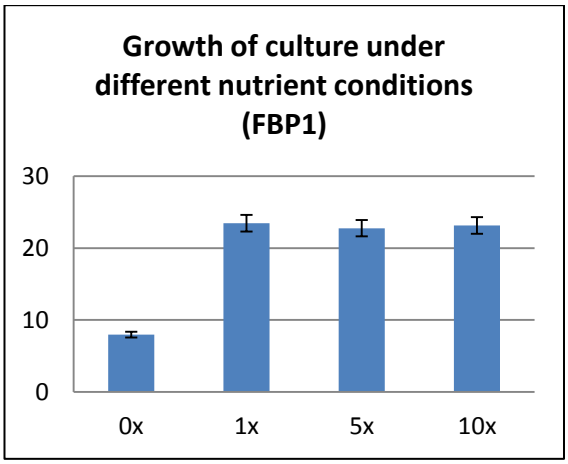

Figure 55 The growth of the culture of microalgae *Ankistrodesmus gracilis* (FBP1) under different nutrient conditions.

Ankistrodesmus gracilis (FBP1) was shown to preferentially accumulate C4:0 lipid followed by longer chained FAMEs C16:0 and C18:1n9t (Table 26). In 0x, the nutrient starved cells featured the highest FAME level (Table 26) as the microalgae accumulated lipids when it suffer from low culture growth (Figure 55) (Vaulot et al. 1987). The 1x culture displayed a healthy culture with the highest growth (Figure 55) rate at the cost of a low FAME level (Table 26). The 5x culture showed slightly lower growth (Figure 55) as the cells were likely to be healthy and tolerant to the high nutrient load. The 10x culture showed a different result, sporting similar culture growth (Table 26) but with a higher FAME level (Table 26), indicating that the cells were mildly stressed and accumulated lipids in response as the nutrient load of the 10x media was likely at near the higher end of its nutrient tolerance range (Vaulot et al. 1987).

Chlamydomonas moewusii (FBP2)

Table 27: The amount of FAME produced and fats (%) of microalgae *Chlamydomonas moewusii* (FBP2) under different nutrient conditions.

	FBP2 0x	FBP2 1x	FBP2 5x	FBP2 10x
C4:0	6.7E-06	5.3E-06	5.1E-06	4.3E-06
C6:0	6.9E-08	4.7E-08	5.6E-08	5.8E-08
C13:0	2.1E-08	1E-08	1.4E-08	1.7E-08
C14:0	1.1E-08	9.7E-09	1.6E-08	2.2E-08
C16:0	6E-07	3E-07	4.1E-07	4.7E-07
C18:1n9t	4E-07	2.7E-07	3.9E-07	5.2E-07
C18:1n9c	1.5E-07	0	0	0
C18:2n6c	7.7E-08	4.1E-08	7.5E-08	1.1E-07
C20:1n9	1.6E-07	1.1E-07	2.4E-07	3E-07
C20:3n6	0	0	0	1.5E-08
Total saturated fat (%)	1.31066	0.31793	0.33181	0.34725
Total monounsaturated fat (%)	0.07653	0.04157	0.06756	0.08797
Total polyunsaturated fat (%)	0.01245	0.00208	0.00408	0.00785
Total fats (%)	1.39965	0.36158	0.40345	0.44307

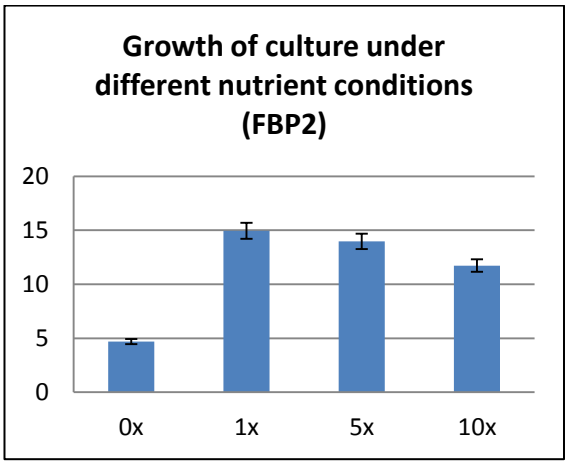

Figure 56: The growth of the culture of microalgae *Chlamydomonas moewusii* (FBP2) under different nutrient conditions.

The FAME profile of *Chlamydomonas moewusii* (FBP2) was shown to be dominated by C4:0 lipid followed by a lesser presence of longer chained FAMEs C16:0 and C18:1n9t (Table 27). *Chlamydomonas moewusii* (FBP2) was observed to have the highest total fat percentage when it was nutrient starved (Table 27). The 1x nutrient media was shown to be the optimum environment for the microalgae to grow (Vitova et al. 2015), showing the highest culture growth (Figure 56) resulting in the highest amount of FAME extracted (Table 27) despite having a low rate of lipid accumulation. Nutrient overload was observed in 5x and 10x proven by the culture growth decline. Thus, *Chlamydomonas moewusii* (FBP2) accumulate lipids only when the cells are starved of nutrients (Vaulot et al. 1987).

Nitzchia sp./Pseudo-nitzschia sp. (FBP3)

Table 28: The amount of FAME produced and fats (%) of microalgae *Nitzchia sp./Pseudo-nitzschia sp.* (FBP3) under different nutrient conditions.

	FBP3 0x	FBP3 1x	FBP3 5x	FBP3 10x
C4:0	1.9E-05	2.1E-05	2.3E-05	6.7E-06
C6:0	5.7E-08	0	6.9E-08	5.3E-08
C10:0	5E-08	6.9E-08	6.8E-08	6.1E-08
C13:0	1.4E-08	3E-08	2.3E-08	2.5E-08
C15:0	0	1.3E-08	0	0
C16:0	3.7E-07	7.9E-07	6.2E-07	5.6E-07
C16:1	5.7E-08	3.6E-07	1.7E-07	1.8E-07
C18:1n9t	3.8E-07	4.8E-07	4.9E-07	5E-07
C18:1n9c	0	1.7E-08	1.3E-08	1.1E-08
C18:2n6c	0	2E-08	0	9.4E-09
C18:3n6	0	2.7E-08	0	0
C20:5n3	0	1.4E-07	9.9E-08	9.7E-08
Total saturated fat (%)	23.9219	4.10677	3.31301	1.09624
Total monounsaturated fat (%)	0.49135	0.15124	0.08804	0.09439
Total polyunsaturated fat (%)	0	0.03245	0.01263	0.01435
Total fats (%)	24.4133	4.29046	3.41367	1.20499

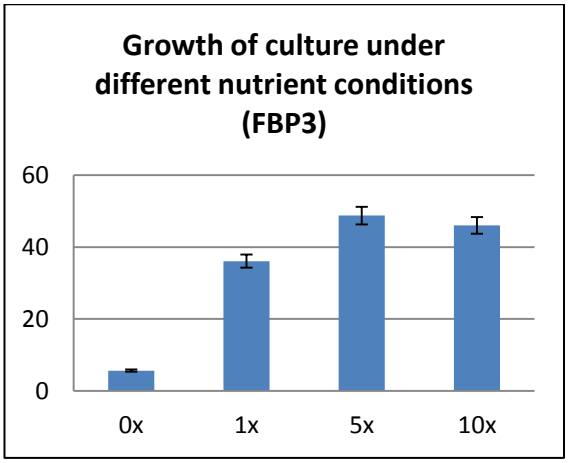

Figure 57: The growth of the culture of microalgae *Nitzchia sp./Pseudo-nitzschia sp.* (FBP3) under different nutrient conditions.

Table 28 placed C4:0 as the most significant FAME accumulated by the *Nitzchia sp./Pseudo-nitzschia sp.* (FBP3) followed by longer chained FAMEs C16:0, C16:1 and C18:1n9t. *Nitzchia sp./Pseudo-nitzschia sp.* (FBP3) had proven that it had a solid identity as an oleaginous microalgae (Tadros 1985). It sports the highest FAME levels among the microalgae, producing lipids amount multitudes above the others. Its highest FAME level was observed in 0x where the cells were starved on nutrients (Table 28). When compared with the cultures in 1x and 5x, the culture growth increased significantly (Figure 57) but the FAME levels plummet (Table 28) as the lipids produced were used up during the growth of the culture (Vitova et al.

2015). 10x on the other hand caused nutrient overload in the culture, indicated by the decrease in culture growth (Figure 57) and FAME levels affiliated with unhealthy cells (Table 28). Thus, it can be determined that the microalgae produced the most lipids only when it was starved (Vaulot et al. 1987), its optimum growth rate was observed in 5x, and stress from nutrient overload reduces the cells' lipid production.

Scenedesmus acutus (FTA1)

Table 29: The amount of FAME produced and fats (%) of microalgae *Scenedesmus acutus* (FTA1) under different nutrient conditions.

	FTA1 0x	FTA1 1x	FTA1 5x	FTA1 10x
C4:0	1.4E-06	8.7E-07	1E-06	1.2E-06
C6:0	6.2E-08	3.3E-08	4.3E-08	5.8E-08
C10:0	7.5E-08	1E-08	2.3E-08	5.1E-08
C14:0	0	0	6.6E-09	1.1E-08
C16:0	3.7E-07	1.8E-07	2.6E-07	3.2E-07
C15:1	6.1E-09	0	7.2E-09	8.5E-09
C16:1	0	0	6.2E-09	7.1E-09
C18:1n9t	2.5E-07	1.5E-07	2.4E-07	3.4E-07
C18:2n6c	2.6E-08	0	2.2E-08	2.6E-08
Total saturated fat (%)	0.269	0.10467	0.1063	0.1162
Total monounsaturated fat (%)	0.03461	0.01332	0.01856	0.02395
Total polyunsaturated fat (%)	0.00341	0	0.00156	0.00167
Total fats (%)	0.30702	0.118	0.12643	0.14182

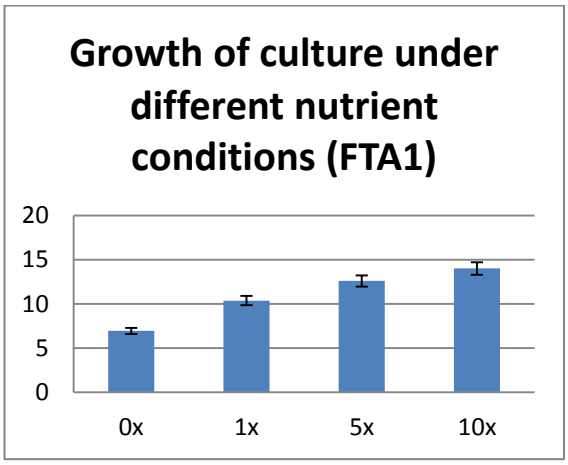

Figure 58: The growth of the culture of microalgae *Scenedesmus acutus* (FTA1) under different nutrient conditions.

Table 29 showed the FAMEs C4:0, C16:0, and C18:1n9t as *Scenedesmus acutus* (FTA1)'s primary lipid source. Based on the FAME levels, *Scenedesmus acutus* (FTA1) was considered a strong lipid producer as it produces large amounts of FAME when undergoing nutrient starvation (Vitova et al. 2015). When grown in the presence of nutrients, its growth rate increases consistently from 1x to 10x (Figure 58). This signifies that

Scenedesmus acutus (FTA1) was able to grow in high nutrient conditions and may grow better in higher levels of nutrients than 10x. This was further supported by the FAME levels in the cells which remained fairly consistent which shows a healthy culture (Table 29).

Ourococcus multisporus (FTA2)

Table 30: The amount of FAME produced and fats (%) of microalgae *Ourococcus multisporus* (FTA2) under different nutrient conditions.

	FTA2 0x	FTA2 1x	FTA2 5x	FTA2 10x
C4:0	4.6E-08	8.8E-08	1.3E-07	9.1E-08
C6:0	5.9E-10	4.9E-10	4.8E-10	6.3E-10
C10:0	4.9E-10	5.5E-10	3.8E-10	5.5E-10
C12:0	1E-10	6.8E-11	6.9E-11	1.2E-10
C13:0	1.1E-10	9.7E-11	8.1E-11	1.1E-10
C14:0	8.2E-11	8.8E-11	7E-11	1E-10
C16:0	2.3E-09	1.8E-09	2E-09	2.1E-09
C15:1	1.1E-10	9.4E-11	1.3E-10	1.1E-10
C17:0	0	0	5.6E-11	0
C18:1n9t	1.7E-09	1.8E-09	2.3E-09	2.2E-09
C18:1n9c	4.5E-10	0	0	0
C18:2n6c	2.8E-10	1.7E-10	2.5E-10	3.3E-10
C18:3n6	3.9E-11	4.8E-11	5.2E-11	5.9E-11
C20:1n9	4.7E-10	3.6E-10	4.9E-10	6.7E-10
C20:3n6	3.8E-11	5E-11	4.8E-11	3E-11
Total saturated fat (%)	0.31439	0.13974	0.21268	0.19834
Total monounsaturated fat (%)	0.04328	0.00927	0.01215	0.01636
Total polyunsaturated fat (%)	0.00552	0.00105	0.00141	0.00221
Total fats (%)	0.36319	0.15006	0.22624	0.21691

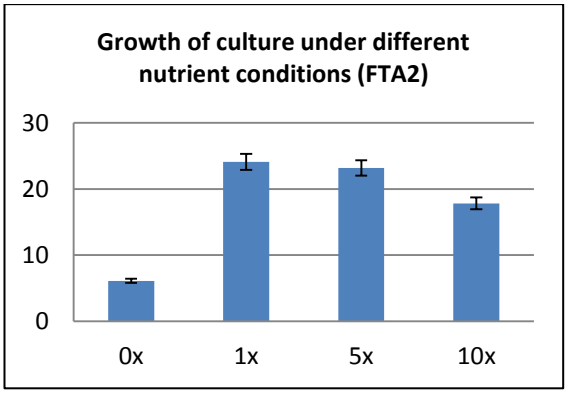

Figure 59: The growth of the culture of microalgae *Ourococcus multisporus* (FTA2) under different nutrient conditions.

Table 30 showed C4:0 lipid to be the main hydrocarbon extracted followed longer chained FAMEs C16:0 and C18:1n9t. Figure 59 demonstrated that the microalgae accumulated the most lipid per cell when starved of nutrients but also resulted in poor culture growth (Figure 59). 1x nutrient media proved to be optimum for the microalgae as the

most growth was observed (Figure 59) and a lower FAME level was observed (Table 30), showing that the microalgae still accumulate lipids when the cells were healthy (Vitova et al. 2015). The microalgae cultured in 5x were stressed at the culture growth was lower (Figure 59) and its FAME levels were higher (Table 30), indicating that the cells accumulate lipids when stressed in high nutrient albeit at a lesser degree (Vaulot et al. 1987). The 10x nutrient media further lowered the culture growth (Figure 59) and the lowered FAME level (Table 30) proved that the cells ability in accumulating lipids were also affected by the high nutrient load (Vaulot et al. 1987).

Scenedesmus incrassatulus (FTAR)

Table 31: The amount of FAME produced and fats (%) of microalgae *Scenedesmus incrassatulus* (FTAR) under different nutrient conditions.

	FTAR 0X	FTAR 1X	FTAR 5X	FTAR 10X
C4:0	1.1E-06	1.6E-06	1.5E-06	6.4E-06
C6:0	4.5E-08	7.1E-08	6.7E-08	5.6E-08
C10:0	5.6E-08	7.6E-08	7.3E-08	2.8E-08
C11:0	4.4E-09	4E-09	6.1E-09	2.6E-09
C12:0	7.2E-09	0	8.2E-09	0
C13:0	1.1E-08	1.9E-08	1.4E-08	1.6E-08
C14:0	6.1E-09	9.8E-09	9.6E-09	7E-09
C16:0	3.7E-07	4.5E-07	4E-07	3.7E-07
C17:0	1.2E-08	0	0	0
C16:1	2.6E-07	3.8E-07	3.4E-07	3.4E-07
C18:1n9t	2.3E-07	4.2E-07	3.6E-07	4.2E-07
C18:2n6c	4.7E-08	3.7E-08	2.8E-08	2E-08
C20:1n9	8.7E-08	1.1E-07	7.6E-08	3.6E-08
C20:3n6	9.9E-09	0	1.3E-08	0
Total saturated fat (%)	0.4373	0.18948	0.20153	0.64306
Total monounsaturated fat (%)	0.14567	0.07218	0.07183	0.06882
Total polyunsaturated fat (%)	0.01399	0.00288	0.00369	0.00173
Total fats (%)	0.59696	0.26454	0.27705	0.71361

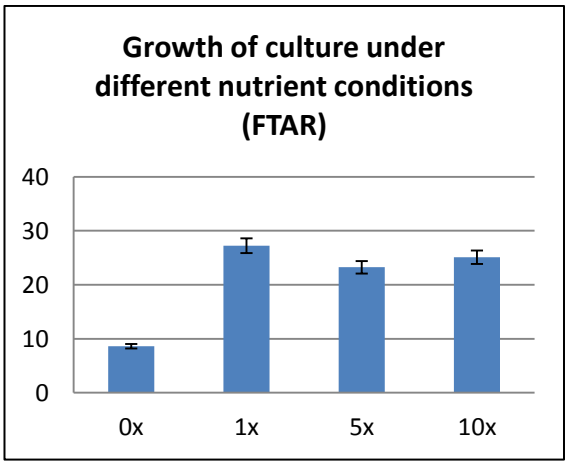

Figure 60: The growth of the culture of microalgae *Scenedesmus incrassatulus* (FTAR) under different nutrient conditions.

Scenedesmus incrassatulus (FTAR) was shown to produce C4:0 as its main lipid with secondary FAMEs C16:0, C16:1 and C18:1n9t (Table 31). Analysis of the microalgae's FAME profile showed that the microalgae produced more lipids when under stress (Table 31) (Vaulot et al. 1987). The nutrient starved culture in 0x resulted in low culture growth (Figure 60) but a high percentage of total FAME (Table 31). The culture in 1x provided the least accumulation lipids and total fat percentage (Table 31) but has the highest culture growth (Figure 60). However, stunted growth was observed in 5x (Figure 60) and the FAME levels

still remained low (Table 31). A reason for this was that *Scenedesmus incrassatulus* (FTAR) had a tolerance against high nutrient concentration and retained its optimal growth, remaining healthy despite having stunted growth (Vitova et al. 2015). FAME levels rapidly increased to its highest when the cells suffered from nutrient stress in 10x, indicating that its nutrient tolerance was overwhelmed by the high nutrient concentration of 10x (Vaulot et al. 1987). Thus, *Scenedesmus incrassatulus* (FTAR) produces FAME when it was stressed and it also had a tolerance in which 5x nutrient was within its tolerance range (Table 31).

Desmodesmus pirkollei (FTAR2)

Table 32: The amount of FAME produced and fats (%) of microalgae *Desmodesmus pirkollei* (FTAR2) under different nutrient conditions.

	FTAR2 0x	FTAR2 1x	FTAR2 5x	FTAR2 10x
C4:0	1.1E-05	1.5E-05	2.8E-06	2.7E-06
C6:0	5.8E-08	5.8E-08	4.5E-08	4E-08
C10:0	2.7E-08	3.6E-08	4.6E-08	3.9E-08
C13:0	1.8E-08	2.3E-08	1.2E-08	1.4E-08
C14:0	1.4E-08	1.5E-08	4.3E-09	1.1E-08
C16:0	6.1E-07	6.2E-07	3.5E-07	3.8E-07
C17:0	1.9E-08	1.2E-08	0	0
C18:1n9t	4.1E-07	5.5E-07	3.1E-07	3E-07
C18:1n9c	1.4E-07	0	0	0
C18:2n6c	8.9E-08	5.2E-08	1.5E-08	2.2E-08
C18:3n3	7.9E-09	0	0	0
C20:1n9	1.9E-07	1.4E-07	3.3E-08	9.1E-08
C20:3n6	1.8E-08	2.6E-08	1.2E-08	0
Total saturated fat (%)	0.9622	0.39797	0.08899	0.10163
Total monounsaturated fat (%)	0.05495	0.01635	0.00873	0.01185
Total polyunsaturated fat (%)	0.0085	0.0018	0.00069	0.00066
Total fats (%)	1.02565	0.41612	0.0984	0.11414

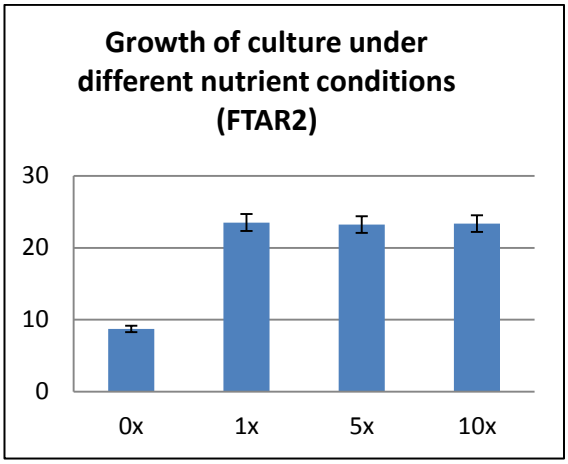

Figure 61: The growth of the culture of microalgae *Desmodesmus pirkollei* (FTAR2) under different nutrient conditions.

Desmodesmus pirkollei (FTAR2)'s FAME profile showed that C4:0 was the most dominant FAME while lesser FAMEs are C16:0 and C18:1n9t (Table 32). The increase FAME levels in 0x showed that *Desmodesmus pirkollei* (FTAR2) accumulate lipids when its growth rate was inhibited from being starved of nutrients (Table 32) (Vaulot et al. 1987). The high amount of FAME despite a lower level of FAME in 1x (Table 32) also proved that the cells did accumulate lipid when healthy (Vitova et al. 2015). Furthermore, similar culture growths in 5x and 10x (Figure 61) and a very low level of FAME (Table 32) showed that the cells were stressed from nutrient overload which affects the growth rate and lipid production (Vitova et al. 2015) and its optimal growth was observed at 1x (Figure 61).

FTAR3

Table 33: The amount of FAME produced and fats (%) of microalgae (FTAR3) under different nutrient conditions.

	FTAR3 0x	FTAR3 1x	FTAR3 5x	FTAR3 10x
C4:0	4.5E-06	5.2E-06	2.2E-05	5.6E-06
C6:0	5.3E-08	5.8E-08	6.2E-08	6.7E-08
C10:0	5.8E-08	5.6E-08	3.7E-08	7.2E-08
C13:0	1.8E-08	2.7E-08	3.6E-08	2.4E-08
C14:0	3.7E-08	8.7E-08	8.3E-08	4.6E-08
C15:0	0	1.2E-08	0	0
C16:0	6.5E-07	7.9E-07	8.2E-07	6E-07
C16:1	1.9E-07	3.7E-07	2.9E-07	1.6E-07
C18:1n9t	4.2E-07	4.5E-07	5.9E-07	4.7E-07
C18:2n6t	0	6.7E-08	1.1E-07	3.3E-08
C18:2n6c	1.6E-08	2.5E-08	0	1.2E-08
C18:3n6	1.3E-08	2.6E-08	0	0
C20:1n9	2.6E-08	0	0	2.2E-08
C24:0	0	1.6E-08	3.2E-08	1.5E-08
C20:5n3	4.5E-08	1.8E-07	2.9E-07	1.2E-07
Total saturated fat (%)	0.76784	0.31405	1.25666	0.29584
Total monounsaturated fat (%)	0.08579	0.02231	0.02108	0.00922
Total polyunsaturated fat (%)	0.00974	0.01371	0.01935	0.00718
Total fats (%)	0.86337	0.35007	1.2971	0.31224

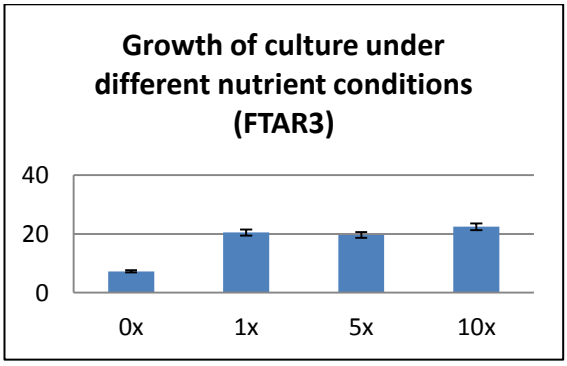

Figure 62: The growth of the culture of microalgae (FTAR3) under different nutrient conditions.

Table 33 placed C4:0 as the dominant FAME produced with secondary FAMEs C16:0, C16:1 and C18:1n9t. Figure 62 showed that the optimal nutrient concentration for the microalgae was 1x. 0x showed inhibited growth due to nutrient starvation while 5x showed stunted growth due to nutrient overload (Figure 62). It also can be determined that FTAR3 accumulate lipids when its cells were stressed as 0x and 5x showed increased FAME levels (Table 33) while 1x showed optimal growth and low FAME levels (Vaulot et al. 1987). 10x showed that nutrient saturation greatly influence FTAR3's lipid production (Vitova et al. 2015) as its FAME dropped

significantly when compared to 5x (Table 33).

Acutodesmus obliquus (FDP)

Table 34: The amount of FAME produced and fats (%) of microalgae *Acutodesmus obliquus* (FDP) under different nutrient conditions.

	FDP 0x	FDP 1x	FDP 5x	FDP 10x
C4:0	4.2E-06	8.9E-07	1.3E-06	2.3E-06
C6:0	5.1E-08	4.4E-08	6.3E-08	5.9E-08
C10:0	1.9E-08	2.8E-08	2.9E-08	2.8E-08
C12:0	1.2E-08	9.7E-09	1E-08	1.2E-08
C16:0	3.2E-07	2.4E-07	3.6E-07	3.9E-07
C18:1n9t	3.5E-07	1.6E-07	3.6E-07	4.7E-07
C18:2n6c	0	1E-07	1.9E-07	2E-07
C20:1n9	7.1E-08	4.7E-07	8.5E-07	7.8E-07
C20:3n6	0	0	0	1.5E-08
Total saturated fat (%)	0.38397	0.04542	0.05303	0.08473
Total monounsaturated fat (%)	0.03278	0.02227	0.03411	0.03499
Total polyunsaturated fat (%)	0	0.00357	0.00536	0.00604
Total fats (%)	0.41675	0.07126	0.0925	0.12576

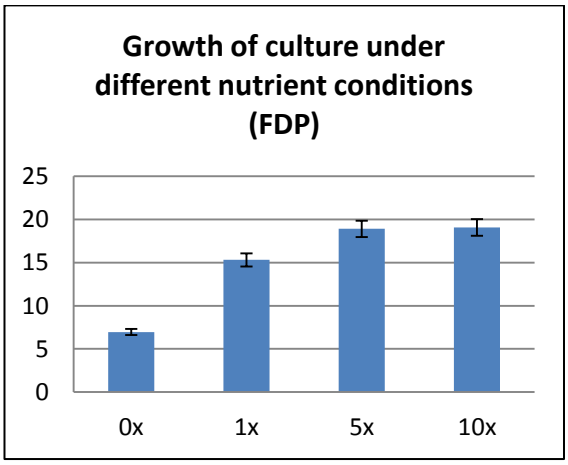

Figure 63: The growth of the culture of microalgae *Acutodesmus obliquus* (FDP) under different nutrient conditions.

Acutodesmus obliquus (FDP)'s lipid production consisted of dominantly C4:0 while lesser FAMEs C16:0, C18:1n9t C18:2n6c and C20:1n9 (Table 34). The highest amount of FAME (Table 34) and total fat percentage (Table 34) was observed in the nutrient starved culture while having the lowest culture growth (Figure 63), indicating that *Acutodesmus obliquus* (FDP) accumulated lipids when starved of nutrients (Vaulot et al. 1987). The cells in 1x and 5x had the increased growth (Figure 63) but low total fat percentage (Table 34) signifying that *Acutodesmus obliquus* (FDP) was healthy and its growth was optimum in 5x (Vitova et al. 2015). The culture in 10x showed a slightly higher growth (Figure 63), indicating that *Acutodesmus obliquus* (FDP) has ready reached its optimum growth rate.

MTA1

Table 35: The amount of FAME produced and fats (%) of microalgae MTA1 under different nutrient conditions.

	MTA1 0x	MTA1 1x	MTA1 5x	MTA1 10x
C4:0	9.6E-07	1.1E-06	1.1E-06	1E-06
C10:0	4.7E-08	5.2E-08	4.7E-08	5.4E-08
C12:0	8.5E-09	9.7E-09	1.2E-08	1.2E-08
C13:0	1.2E-08	1.3E-08	1.3E-08	1.4E-08
C14:0	8.1E-08	1.5E-07	1.5E-07	1.4E-07
C15:0	9.7E-09	1.3E-08	1.4E-08	1.4E-08
C16:0	8.5E-07	8.5E-07	8.8E-07	8.8E-07
C15:1	5.2E-09	6.5E-09	5.6E-09	7.7E-09
C17:0	0	1.6E-08	2E-08	2E-08
C16:1	4.2E-07	4.8E-07	5E-07	4.8E-07
C18:1n9t	5.3E-07	5.5E-07	5.7E-07	4.7E-07
C18:1n9c	0	2E-08	2.1E-08	2.8E-08
C18:2n6t	1.7E-08	6.5E-08	9.9E-08	6.6E-08
C18:2n6c	1.5E-08	2.6E-08	3.4E-08	2.9E-08
C18:3n6	1.1E-08	1.6E-08	2.2E-08	1.9E-08
C20:3n6	1.1E-08	1.1E-08	1.9E-08	0
C22:1n9	1.1E-08	1.2E-08	8.6E-09	0
C20:5n3	5.3E-08	1.3E-07	1.9E-07	1.8E-07
Total saturated fat (%)	0.00439	0.0047	0.00478	0.00383
Total monounsaturated fat (%)	0.00209	0.00223	0.00229	0.0017
Total polyunsaturated fat (%)	0.00023	0.00051	0.00073	0.00049
Total fats (%)	0.0067	0.00745	0.0078	0.00602

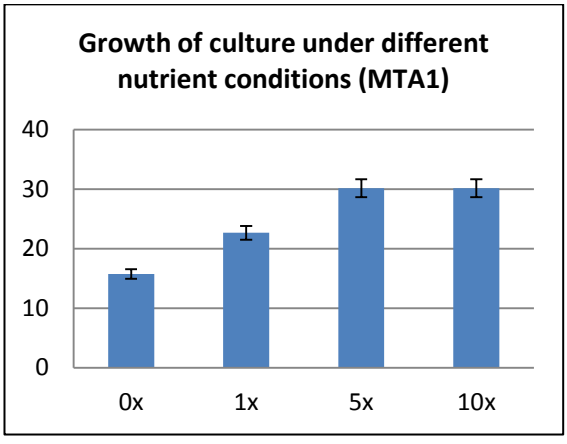

Figure 64: The growth of the culture of microalgae MTA1 under different nutrient conditions.

MTA1's FAME profile showed that C4:0, C16:0, C16:1, and C18:1n9t were significant lipid sources and C16:0 was the most significant FAME followed by C4:0 (Table 35). The growth rates (Figure 64) and FAME levels (Table 35) were similar which indicated that the FAME level correspond to the health of the culture (Vitova et al. 2015). It showed increasing growth (Figure 64) and FAME levels (Table

35) from 0x to 5x but plateaued at 10x. While the growth and FAME levels were stunted, the microalgae showed a tolerance for the high amount of nutrients in 10x as the cells were relatively healthy.

MTA2

Table 36: The amount of FAME produced and fats (%) of microalgae MTA2 under different nutrient conditions.

	MTA2 0x	MTA2 1x	MTA2 5x	MTA2 10x
C4:0	3.6E-06	3.9E-06	3.5E-06	3.3E-06
C6:0	5.9E-08	6E-08	5.1E-08	6.4E-08
C10:0	5.3E-08	7.5E-08	5.2E-08	6.3E-08
C11:0	0	3.8E-09	0	0
C13:0	1.4E-08	1.5E-08	1.4E-08	1.4E-08
C14:0	0	9.9E-09	7.9E-09	9.4E-09
C16:0	4E-07	4.6E-07	3.9E-07	4E-07
C17:0	0	1E-08	6.2E-09	0
C18:1n9t	3.9E-07	4.7E-07	3.5E-07	3.6E-07
Total saturated fat (%)	0.01338	0.01433	0.01211	0.01117
Total monounsaturated fat (%)	0.00117	0.00139	0.00099	0.00101
Total polyunsaturated fat (%)	0	0	0	0
Total fats (%)	0.01455	0.01573	0.0131	0.01218

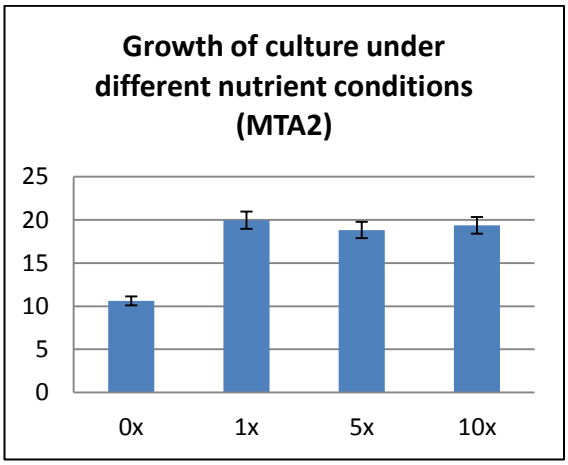

Figure 65: The growth of the culture of microalgae MTA2 under different nutrient conditions.

MTA2 provided a FAME profile which highlights C4:0 as the main lipid source with lesser sources of lipids C16:0 and C18:1n9t (Table 36). Despite extremely low levels of FAME (Table 36), the microalgae produced less FAME when nutrient starved instead of the expected result of a higher FAME level. Its highest FAME percentage was observed in 1x (Table 36) which also has the highest culture growth (Figure 65). Thus, the higher amount of FAME despite in small amount signify culture health (Vitova et al. 2015). This was further supported by stunted growth (Figure 65) and the FAME levels decreasing (Table 36) due to nutrient stress from high nutrient levels.

MTAR

Table 37: The amount of FAME produced and total fats (%) of microalgae MTAR under different nutrient conditions.

	MTAR 0x	MTAR 1x	MTAR 5x	MTAR 10x
C4:0	2.4E-06	3E-06	2.7E-06	2.4E-06
C6:0	5.3E-08	3.2E-08	3.1E-08	3.9E-08
C14:0	2.5E-08	2.8E-08	3E-08	3.4E-08
C15:0	0	3.7E-09	2.2E-09	0
C16:0	4.1E-07	3.1E-07	3.1E-07	3.5E-07
C15:1	9.5E-09	7.9E-09	7.2E-09	3E-09
C17:0	9.2E-09	3.8E-08	3.4E-08	3.8E-08
C16:1	6E-09	1E-08	9.4E-09	1.3E-08
C18:2n6c	1.5E-07	1.2E-07	1.4E-07	1.5E-07
C22:1n9	7.3E-09	3.9E-09	0	0
Total saturated fat (%)	2.6E-05	2.2E-05	1.9E-05	1.7E-05
Total monounsaturated fat (%)	1.3E-07	1E-07	9.4E-08	8.9E-08
Total polyunsaturated fat (%)	1.2E-06	6.9E-07	7.9E-07	8.1E-07
Total fats (%)	2.7E-05	2.2E-05	2E-05	1.8E-05

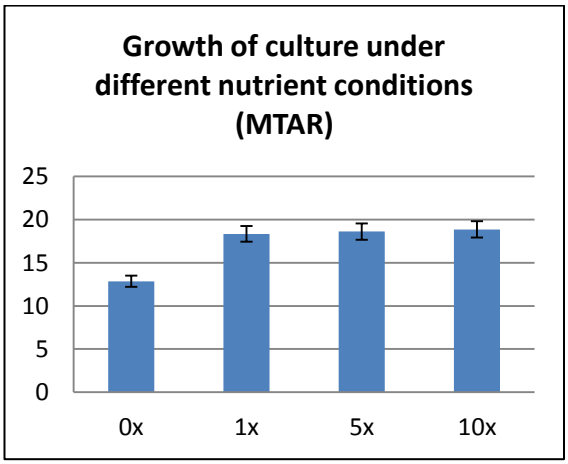

Figure 66: The growth of the culture of microalgae MTAR under different nutrient conditions.

MTAR's FAME profile showed the FAME C4:0 as the dominant lipid produced with secondary long chain FAMEs like C16:0 and C18:2n6c (Table 37). In 0x, the cells were nutrient starved resulting in a lower FAME while 1x displayed optimum growth resulting in the highest amount of total FAME (Table 37) (Vitova et al. 2015). The cells were also at their healthiest in 1x, proven by its highest FAME levels in 1x (Table 37). When in higher nutrient concentration like 5x and 10x, the growth was observed to be slightly increasing (Figure 66) but FAME levels decreased (Table 37), signifying the cells were stressed (Vitova et al. 2015).

Energy Calculation of Microalgae

Unidentified Algae (FSA)

The energy calculated for each of FSA's samples showed that the energy potential of the microalgae was the lowest among the other microalgae strains with 0x producing FAME the highest energy (Table 38). This was due to the high production of C4:0 FAME due to nutrient starvation (Vaulot et al. 1987). It was also noted that the other samples with lower energy values did not deviate much from the highest energy value (Table 38) such as the energy value increasing at 5x from 1x. The cause was the increase of longer FAMEs produced that contained a higher energy potential than C4:0 (Ramírez-Verduzco et al. 2012).

Table 38: Energy values of the FAME produced by FSA

FSA	Total Weight of FAME (g)	Total Energy of FAME (kJ)	Energy per kg (kJ/kg)
0x	8.42863E-06	-0.00026	-30653.9
1x	6.50624E-06	-0.00019	-28653.3
5x	7.11889E-06	-0.00021	-29591.6
10x	4.6149E-06	-0.00013	-28627.2

Nitzchia sp./Pseudo-nitzschia sp. (FSB)

FSB's energy value were considerably high with all of the samples having energy values that exceed -30 MJ/kg (Table 39). The highest energy value was 1x with -35 MJ/kg (Table 39) which was due to FSB producing higher levels of longer FAMEs of C16:0 and above with higher energy potential than C4:0 (Ramírez-Verduzco et al. 2012).

Table 39: Energy values of the FAME produced by *Nitzchia sp./Pseudo-nitzschia sp.* (FSB).

Nitzchia sp./Pseudo-nitzschia sp. (FSB)	Total Weight of FAME (g)	Total Energy of FAME (kJ)	Energy per kg (kJ/kg)
0x	1.83548E-06	-6.1658E-05	-33592.5053
1x	2.55595E-06	-8.9553E-05	-35036.9848
5x	2.28472E-06	-7.8663E-05	-34430.1414
10x	2.38177E-06	-8.2723E-05	-34731.6387

Pectinodesmus pectinatus (FSD)

FSD's energy value calculations showed considerably high energy potential (Table 40). The highest energy value of FSD was produced in 5x which also has the highest levels of longer FAMEs which held high energy potential (Ramírez-Verduzco et al. 2012).

Table 40: Energy values of the FAME produced by *Pectinodesmus pectinatus* (FSD).

Pectinodesmus pectinatus (FSD)	Total Weight of FAME (g)	Total Energy of FAME (kJ)	Energy per kg (kJ/kg)
0x	2.73514E-06	-9.184E-05	-33577.83334
1x	1.53765E-05	-0.00046675	-30354.7448
5x	3.78026E-06	-0.00012855	-34004.37862
10x	3.00209E-06	-0.00010016	-33362.69941

Nephrochlamys subsolitaria (FSE)

The energy calculations of FSE yielded energy potentials that exceed -30 MJ/kg (Table 41). The highest energy value was attained by 1x with its energy mostly contributed by the high energy potential of the C16:0 FAME (Table 25) (Ramírez-Verduzco et al. 2012).

Table 41: Energy values of the FAME produced by *Nephrochlamys subsolitaria* (FSE).

Nephrochlamys subsolitaria (FSE)	Total Weight of FAME (g)	Total Energy of FAME (kJ)	Energy per kg (kJ/kg)
0x	2.81315E-06	-9.5E-05	-33771.57825
1x	2.27426E-06	-7.8E-05	-34408.24799
5x	6.59381E-06	-0.0002	-30537.66375
10x	6.48962E-06	-0.0002	-30412.26443

Ankistrodesmus gracilis (FBP1)

The energy calculations of FBP1 yielded energy potentials that exceed -30 MJ/kg (Table 42). The highest energy value was attained by 1x followed closely by 5x with its energy mostly contributed by the high energy potential of the longer FAMEs like C16:0, C18:1n9t, C18:2n6c, and C20:1n9 (Table 26) (Ramírez-Verduzco et al. 2012).

Table 42: Energy values of the FAME produced by *Ankistrodesmus gracilis* (FBP1).

Ankistrodesmus gracilis (FBP1)	Total Weight of FAME (g)	Total Energy of FAME (kJ)	Energy per kg (kJ/kg)
0x	3.92E-06	-0.00012	-30573.2
1x	7.65E-06	-0.00025	-32333.1
5x	6.07E-06	-0.0002	-32130.5
10x	8.19E-06	-0.00025	-30954.7

Chlamydomonas moewusii (FBP2)

FBP2's energy value in Table 43 showed energy potentials that exceed -30 MJ/kg. The highest energy value was observed in 10x followed closely by 5x (Table 43). This was because a significant portion of the energy potential was from longer FAMEs like C16:0, C18:1n9t, C18:2n6c, and C20:1n9 (Ramírez-Verduzco et al. 2012) which were the highest in 10x (Table 27).

Table 43: Energy values of the FAME produced by *Chlamydomonas moewusii* (FBP2).

Chlamydomonas moewusii (FBP2)	Total Weight of FAME (g)	Total Energy of FAME (kJ)	Energy per kg (kJ/kg)
0x	8.19E-06	-0.00025	-30956.5
1x	6.12E-06	-0.00019	-30411.8
5x	6.27E-06	-0.00019	-31069.3
10x	5.84E-06	-0.00019	-31771.5

Nitzchia sp./Pseudo-nitzschia sp. (FBP3)

The energy calculated for each of FBP3's sample showed an increasing trend (Table 44). The increase of energy despite the decrease in the amount of FAME was due to the higher energy content of the longer FAMEs (Ramírez-Verduzco et al. 2012) which exceeds C4:0 in terms of energy. This was further supported by observing the amount of energy per kilogram of the sample which shows similar amounts of energy despite significant differences in C 4:0 amount with the highest amount of energy per kilogram seen at 10x which has the lowest levels of C 4:0 (Table 44).

Table 44: Energy values of the FAME produced by *Nitzchia sp./Pseudo-nitzschia sp.* (FBP3).

Nitzchia sp./Pseudo-nitzschia sp. (FBP3)	Total Weight of FAME (g)	Total Energy of FAME (kJ)	Energy per kg (kJ/kg)
0x	2.02E-05	-0.00059795	-29533.2
1x	2.27E-05	-0.00068091	-29965.6
5x	2.44E-05	-0.00072411	-29716.8
10x	8.2E-06	-0.00025326	-30904.1

Scenedesmus acutus (FTA1)

FTA1's energy calculation yielded energy values which exceeded -30 MJ/kg (Table 45). The highest energy potential was seen in 10x followed by 5x and 0x. This was due to the total amount of FAMEs extracted which was the highest in 10x and the lowest in 1x (Table 29).

Table 45: Energy values of the FAME produced by *Scenedesmus acutus* (FTA1).

Scenedesmus acutus (FTA1)	Total Weight of FAME (g)	Total Energy of FAME (kJ)	Energy per kg (kJ/kg)
0x	2.17E-06	-7.1E-05	-32569.4
1x	1.24E-06	-4E-05	-31986.9
5x	1.62E-06	-5.3E-05	-32741.8
10x	2.03E-06	-6.7E-05	-33055.7

Ourococcus multisporus (FTA2)

FTA2's energy values were similar except for the energy potential in 0x which was the highest (Table 46). Despite having the highest C4:0 in 5x, 0x had the highest energy potential because of the presence of the long FAME C18:1n9c which was absent in the other samples (Table 30) (Ramírez-Verduzco et al. 2012).

Table 46: Energy values of the FAME produced by *Ourococcus multisporus* (FTA2).

Ourococcus multisporus (FTA2)	Total Weight of FAME (g)	Total Energy of FAME (kJ)	Energy per kg (kJ/kg)
0x	6.46E-06	-0.00021	-31838.127
1x	1.04E-05	-0.00032	-30491.833
5x	1.51E-05	-0.00046	-30232.93
10x	1.11E-05	-0.00034	-30730.918

Scenedesmus incrassatulus (FTAR)

FTAR's energy calculation yielded energy values which exceeded -30 MJ/kg (Table 47). The highest energy potential was seen in 0x followed by 1x. Despite having the highest amount of FAME in 10x, the large amount of C4:0 yielded small amounts of energy while longer FAMEs observed in 0x yielded more energy (Ramírez-Verduzco et al. 2012). Furthermore, 5x which have higher levels of long FAMEs was still lower than 0x because of 0x having higher levels of C18:2n6c which ultimately produced enough energy to surpass the energy potential in 5x (Table 31).

Table 47: Energy values of the FAME produced by *Scenedesmus incrassatulus* (FTAR).

Scenedesmus incrassatulus (FTAR)	Total Weight of FAME (g)	Total Energy of FAME (kJ)	Energy per kg (kJ/kg)
0x	2.2866E-06	-7.8E-05	-34135.6
1x	3.19815E-06	-0.00011	-34013.5
5x	2.85806E-06	-9.7E-05	-33899.8
10x	7.74185E-06	-0.00024	-30766.1

Desmodesmus pirkollei (FTAR2)

The energy values from FTAR2's energy calculation showed that the highest energy potential was seen in 10x followed by 5x (Table 48). The disparity between the energy values was due to the low energy yield of short FAMEs and the high energy yield of long FAMEs (Ramírez-Verduzco et al. 2012). The highest amount of total FAME in 1x (Table 32) yielded the lowest energy (Table 48) because most of the total FAME was C4:0 FAME. The higher energy yields of 10x and 5x (Table 48) was due to very small amounts of long FAMEs (Table 32).

Table 48: Energy values of the FAME produced by *Desmodesmus pirkollei* (FTAR2).

Desmodesmus pirkollei (FTAR2)	Total Weight of FAME (g)	Total Energy of FAME (kJ)	Energy per kg (kJ/kg)
0x	1.27E-05	-0.00039	-30367.8
1x	1.63E-05	-0.00049	-30039.5
5x	3.64E-06	-0.00011	-31332.9
10x	3.56E-06	-0.00011	-31614.2

Unidentified Algae (FTAR3)

FTAR3's energy calculation yielded energy values which exceeded -30 MJ/kg (Table 49). The highest energy potential was seen in 1x which was due to the long FAMEs (Ramírez-Verduzco et al. 2012) like C16:1 and C20:5n3 which were the highest observed in 1x (Table 33).

Table 49: Energy values of the FAME produced by FTAR3.

FTAR 3	Total Weight of FAME (g)	Total Energy of FAME (kJ)	Energy per kg (kJ/kg)
0x	6.07E-06	-0.00019	-31611.2
1x	7.33E-06	-0.00023	-32071.5
5x	2.48E-05	-0.00075	-30047.1
10x	7.21E-06	-0.00023	-31373

Acutodesmus obliquus (FDP)

FDP's energy value were considerably high with all of the samples having energy values that exceed -30 MJ/kg (Table 50). The highest energy value was 5x with -35 MJ/kg (Table 50) which was due to *Acutodesmus obliquus* (FDP) producing higher levels of longer FAMEs of C16:0 and above with higher energy potential than C4:0 (Ramírez-Verduzco et al. 2012).

Table 50: Energy values of the FAME produced by *Acutodesmus obliquus* (FDP).

Acutodesmus obliquus (FDP)	Total Weight of FAME (g)	Total Energy of FAME (kJ)	Energy per kg (kJ/kg)
0x	4.99E-06	-0.00015	-30725.7
1x	1.95E-06	-6.8E-05	-34794
5x	3.14E-06	-0.00011	-35343.8
10x	4.25E-06	-0.00014	-33940.5

Unidentified Algae (MTA1)

MTA1's energy calculation yield the highest energy potential among the others microalgae with every sample yielding over -36 MJ/kg (Table 51). The highest energy potential was observed in 5x with -36363.3 kJ/kg (Table 51). This was due to MTA1 producing long FAMEs C16:1, C18:2n6t, C18:2n6c, C18:2n6, C20:3n6 and C20:5n3 (Ramírez-Verduzco et al. 2012), all of which were the highest in 5x (Table 35).

Table 51: Energy values of the FAME produced by MTA1.

MTA 1	Total Weight of FAME (g)	Total Energy of FAME (kJ)	Energy per kg (kJ/kg)
0x	3.03E-06	-0.00011	-36142.9
1x	3.51E-06	-0.00013	-36203.7
5x	3.7E-06	-0.00013	-36363.3
10x	3.43E-06	-0.00012	-36334.4

Unidentified Algae (MTA2)

The energy calculations of MTA2 yielded energy potentials that exceed -30 MJ/kg (Table 52). The highest energy value was observed in 1x which has the highest amount for all FAMEs in the profile (Table 36).

Table 52: Energy values of the FAME produced by MTA2.

MTA 2	Total Weight of FAME (g)	Total Energy of FAME (kJ)	Energy per kg (kJ/kg)
0x	4.53E-06	-0.00014	-31070.3
1x	5E-06	-0.00016	-31260.5
5x	4.41E-06	-0.00014	-31025.2
10x	4.18E-06	-0.00013	-31210

Unidentified Algae (MTAR)

MTAR's energy value calculations showed energy potential that were the highest in 0x (Table 53). The high energy potential of 0x was because the long FAME C22:1n9 which yielded an exceptional amount of energy (Ramírez-Verduzco et al. 2012) was highest in 0x (Table 37).

Table 53: Energy values of the FAME produced by MTAR.

MTAR	Total Weight of FAME (g)	Total Energy of FAME (kJ)	Energy per kg (kJ/kg)
0x	3.07E-06	-9.6E-05	-31219.1
1x	3.6E-06	-0.00011	-30613.6
5x	3.31E-06	-0.0001	-30783.6
10x	2.99E-06	-9.3E-05	-31143

Discussion

Culture Growth under Nutrient Stress

During the nutrient stress experiment, the culture showed growth well within predictions. All samples showed visible growth in 1x, 5x, and 10x media while minimal growth was found in the media without nutrients. Each microalgae strain displayed a unique response to the nutrient conditions but trends can be seen which groups some of the microalgae together

The microalgae's responses followed trends that closely mimic each other. However, all microalgae showed the lowest growth in media without any nutrients followed by an increase in growth in media 1x times the normal nutrient load. *O. multisporus* (FTA2) (Figure 59) and *C. moewusii* (FBP2) (Figure 56) displayed a decline in growth in 5x compared to 1x, followed by a sharper decline in 10x. *S. incrassatulus* (FTAR) (Figure 60), FTAR3 (Figure 62), MTA2 (Figure 65), *P. pectinatus* (FSD) (Figure 53), *D. pirkollei* (FTAR2) (Figure 61), MTAR (Figure 66), and *N. subsolitaria* (FSE) (Figure 54) showed a decline in growth at 5x followed by an increase in growth at 10x. *Nitzchia sp./Pseudo-nitzschia sp.* (FBP3) (Figure 57), *A. obliquus* (FDP) (Figure 63), MTA1 (Figure 64), FSA (Figure 51), and *Nitzchia sp./Pseudo-nitzschia sp.* (FSB) (Figure 52) showed slight increased growth in 5x but maintained growth or suffered lower growth in 10x. *S. acutus* (FTA1) (Figure 58) was unique in the entire microalgae set, displaying a consistent upwards trend in growth as the nutrient load increases.

Total FAME

Total Fame refers to the amount of FAME that was produced from the microalgae biomass. Every microalgae strain had its response to a unique degree but trends which group some of the strains together could still be derived.

O. multisporus (FTA2) (Table 30), *Nitzchia sp./Pseudo-nitzschia sp.* (FBP3) (Table 28), and MTA1 (Table 35) showed a consistent increase in total FAME from the lowest growth in 0x up to 5x, followed by a significant drop in total FAME at 10x. *C. moewusii* (FBP2) (Table 27) and FSA (Table 22) showed their highest total FAME in 0x which decreased in 1x, increased slight in 5x, and decline in 10x. *A. gracilis* (FBP1) (Table 26), *S. incrassatulus* (FTAR) (Table 31), and *Nitzchia sp./Pseudo-nitzschia sp*. (FSB) (Table 23) had their lowest total FAME in 0x which increased at 1x, grow similarly in 5x and increased with their highest total FAME at 10x. MTAR and MTA2 showed their highest total FAME in 1x which was an increase from 0x, followed by a steady decline up to their lowest total FAME observed in 10x. *A. obliquus* (FDP) (Table 34) and *S. acutus* (FTA1) (Table 29) both had their highest total FAME in 0x which significantly dropped in 1x and steadily increased up 10x which had a high amount of total FAME, second to 0x. FTAR3 (Table 33) and *N. subsolitari*a (FSE) (Table 25) displayed no increase in total FAME for 1x from their lowest amount seen in 0x, increased in total FAME in 5x, followed by a similar amount or decline in 10x. Finally, *D. pirkollei* (FTAR2) (Table 32) and *P. pectinatus* (FSD) (Table 24) showed a slight increase of total FAME from 0x to 1x and declined to their lowest amount in 5x and 10x.

Total FAME Percentage

Total FAME percentage refers to how much of the microalgae's biomass weight was contributed by the fatty acids produced. The microalgae showed varying percentages of FAME likely contributed directly to the nutrient conditions and in turn develop similar trends that easily placed them into groups.

O. multisporus (FTA2) (Table 30), FTAR3 (Table 33), and *N. subsolitaria* (FSE) (Table 25) displayed a higher percentage of growth in the nutrient absent 0x which plummets in 1x but rises up again in 5x before dropping in 10x. *C. moewusii* (FBP2) (Table 27), *Nitzchia sp./Pseudo-nitzschia sp.* (FBP3) (Table 28), MTAR (Table 37), *A. obliquus* (FDP) (Table 34), *D. pirkollei* (FTAR2) (Table 32), *S. acutus* (FTA1) (Table 29), and FSA (Table 22) had the similar trend of having their highest percentage of FAME when starved of nutrients in 0x, suffered a steep decline in 1x and 5x and a slight increase or decrease in 10x. *A. gracilis* (FBP1) (Table 26) and *Nitzchia sp./Pseudo-nitzschia sp*. (FSB) (Table 23) had their highest percentage of FAME in the nutrient starved culture 0x and significantly decline up to 5x before increasing at 10x. MTA2 (Table 26) and *P. pectinatus* (FSD) (Table 24) showed their highest percentage at 1x after and increased from 0x and went on a significant decline to their lowest percentage in 10x. *S. incrassatulus* (FTAR) and MTA1 have trends unique to them as *S. incrassatulus* (FTAR) had a decrease in FAME percentage from 0x to 1x but plateaued at 5x followed by an increase in 10x, while MTA1 (Table 35) had a relatively opposite trend to *S. incrassatulus* (FTAR) (Table 31), showing an increase from 0x to 1x, plateauing at 5x, and a decrease at 10x.

Further Analysis of Microalgae Culture in Different Nutrient Conditions

It could be observed that the FAME levels produced by the microalgae were exceptionally low. Most microalgae strains produce lipids equivalent to less than 1% of its biomass. This was due to the microalgae cells using the energy it collected into normal metabolism and cell division (Vitova et al. 2015). Thus, cultures with access to nutrients would sport a high growth rate (Vaulot et al. 1987), with cell performing energy intensive cell division lowering the amount of sugars that can be used to construct lipids (Vitova et al. 2015). Furthermore, when the growth of the culture was inhibited or starved of nutrients, the cells continued with its photosynthesis, accumulating sugars to be converted into lipids, resulting in a higher FAME level commonly observed in 0x (Vaulot et al. 1987). An example of lipid production via nutrient starvation is Nannochloropsis sp. which achieved 55% of ot biomass after extended periods of starvation. (Suen et. al. 1987) This was different from less energy efficient method practiced by Solazyme in the where the algae cells were fed sugar in a closed bioreactor. (Voegele 2012)

Photosynthesis was another limiting factor that contributed to the low levels of FAME in the results due to the nature of how the microalgae were cultured. The cells were cultured in small universal bottles with slightly loosened caps to prevent outside contamination to a degree while maintaining airflow. The reduced airflow would allow less carbon dioxide to be introduced to the culture, thereby limiting the rate of photosynthesis (Brune and Novak 1981). Another experiment in which the universal bottles were sealed with parafilm generated cultures with poor growth commonly observed in nutrient starved media. This was caused by the significantly restricted airflow by the parafilm which suffocated the culture resulting in compromised growth (Brune and Novak 1981). An example of an efficient culture system is an algae bioreactor which is fed flue gas from a power plant as proposed by Maeda et. al. (1995).

FAME Composition

Initial observation of the FAMEs of the microalgae had shown that FAME C4:0 was the dominant FAME in all the FAME profiles (Figure 67). Representing 90.6% of the total moles of all the FAME, C4:0 or butyric acid methyl ester was one of the shortest hydrocarbon chain, second only to C3:0 which is propanoic acid methyl ester (Brody 1999). C4:0 is a short chain FAME which means that oxidation of the FAME would yield a low amount of energy. However, C4:0 or butyric acid is an important chemical frequently used in cosmetic, pharmaceutical, chemical, and food industries (Zhu et al. 2002) and a precursor for the production of biobutanol (Tashiro et al. 2007) which is an exceptional biofuel which can be safely blended with gasoline compared to bioethanol or biodiesel (Hipolito et al. 2008). Longer chains like C16:0 are more desired in a biofuel as the FAME releases a lot of energy when oxidized (Ramírez-Verduzco et al. 2012). However, the longer FAME only takes up 7.9% of the total mole of FAME (Figure 67).

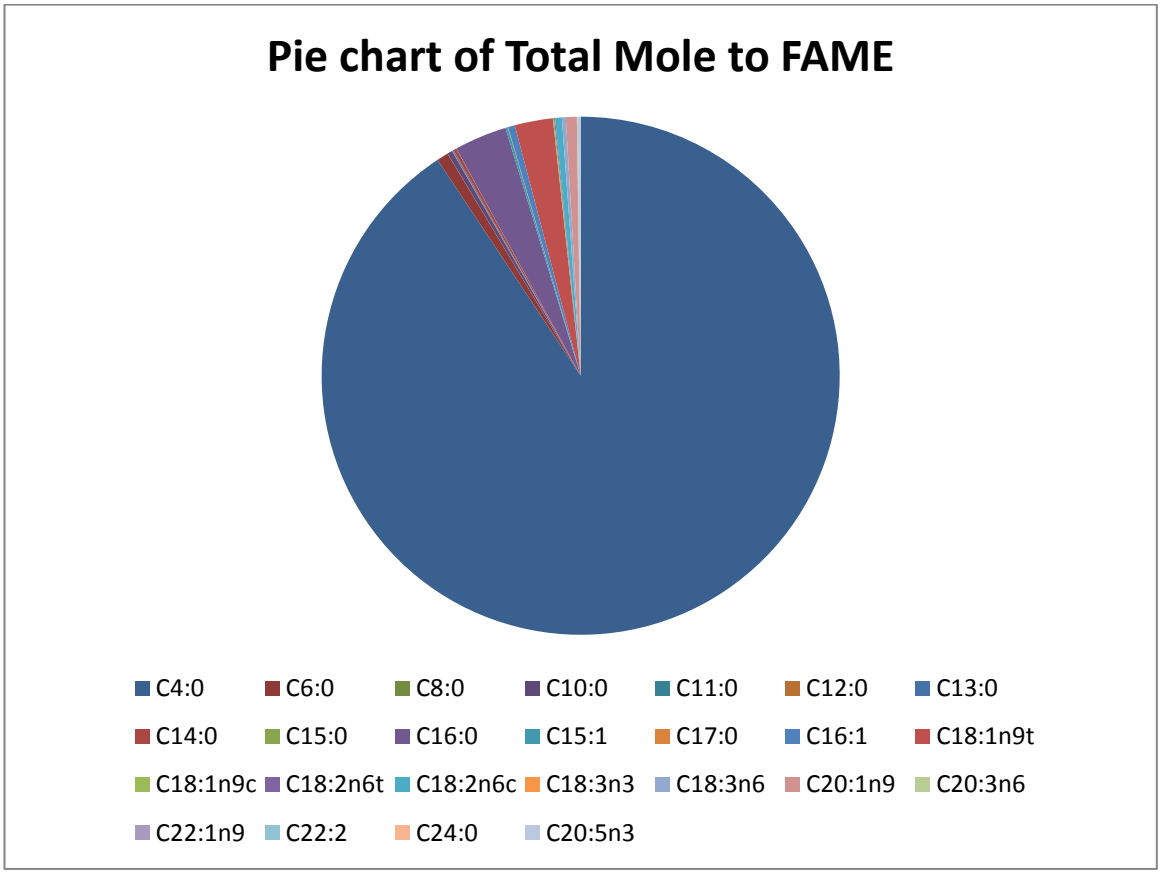

Figure 67: Pie chart of Total Mole to FAME

Microalgae as a Bioremediator

There were many microalgae strains that were viable as bioremediators candidates. For the fresh water microalgae, *N. subsolitaria* (FSE), *S. acutus* (FTA1) and *A. obliquus* (FDP) were good bioremediators as they could maintain a steady increase of growth against increasing nutrient concentration of up to 10x (Figure 54, 58, and 63). *Nitzchia sp./Pseudo-nitzschia sp*. *N. subsolitaria* has so far been cultured and identified by Krienitz et al. (1998) from the Turkwel Gorge Reservoir in Kenya. *S. acutus* (FTA1) showed interesting potential as the culture grew unfazed by the highest nutrient concentration of media 10x and could potentially grow better in more nutrient rich environments (Figure 58). *S. acutus* had been studied in a similar research in which de Alva et al. (2013) concluded that *S. acutus* grew best pretreated wastewater achieving a removal of 66% of phosphorus and 94% of organic nitrogen. *A. obliquus/S. obliquus* along with *O. multisporus* were used in a research by Ji et al. (2013) which attempted to bioremediate tertiary municipal wastewater supplemented with CO2. The microalgae achieved complete removal of 99% of nitrogen and phosphorus within 4 days Ji et al. (2013). FSA, *Nitzchia sp./Pseudo-nitzschia sp.* (FSB), and *Nitzchia sp./Pseudo-nitzschia sp.* (FBP3) on the other hand showed positive growth up to 5x (Figure 51, 52, and 57). Of all the listed microalgae strains, *Nitzchia sp./Pseudo-nitzschia sp.* (FBP3) displayed the highest culture growth which was nearly 50 times its initial cell count in a week (Figure 57) in media 5x while *Nitzchia sp./Pseudo-nitzschia sp.* (FSB) was second with 30 times its initial cell count in a week at the same nutrient concentration (Figure 52). Other microalgae in this research were also used in other research investigating bioremediation potential. *C. moewusii* was used to investigate sulphate as an essential compound to tolerance mechanisms against cadmium toxicity (Mera et al. 2014). The sulphate allowed the maximum tolerance of the microalgae in 4.46 ± 0.42 mg Cd/L at 1mM of sulphate concentration (Mera et al. 2014). *A. gracilis* was also used as a bioremediators of wastewater by Woo and Park (2012) the effect of different levels of phosphorus on the fatty acid production of the microalgae cells. For the marine microalgae, MTAR and MTA1 were good candidates as bioremediators. MTAR showed a slight but steady increase in growth up to the highest nutrient concentration of 10x and could potentially grow in nutrient loads higher than 10x (Figure 66). MTA1 displayed a higher growth rate than MTAR (Figure 64), growing approximately 30 times its initial cell count in a week up to 5x without stunted growth.

Microalgae as a Biofuel Producer

At first glance, most of the microalgae showed poor FAME levels that ranged just below 2% of its biomass weight as shown in the total fat percentage of the microalgae strains (Table 22~37). The strains of poor FAME production was likely because the energy obtained from photosynthesis has been used up on cell division which is one of the most energy taxing activities of a cell (Farabee 2001). Thus, only the nutrient starved cells showed a relatively high FAME level which unfortunately ranges below 2% of its biomass weight (Table 22~37). However, *Nitzchia sp./Pseudo-nitzschia sp.* (FBP3) showed exceptional FAME levels with its highest FAME level at approximately 25% when nutrient starved in 0x and FAME levels of 3~4% in its healthy cells growing in nutrient supplied media which were higher than the highest FAME level of the rest of the microalgae (Table 28). A research by Chen et al. 2007) also studied a species of *Nitzschia* called *N. laevis* to determine its the lipid class composition and fatty acid distribution in order to integrate the algae into the food and aquaculture industry. The main constituents of fatty acids of *N. laevis* were identified in most lipid classes were Myristic acid (C14:0), palmitic acid (C16:0), palmitoleic acid (C16:1) and Eicosapentaenoic acid (C20:5n3) (Chen et al. 2007). Furthermore, other microalgae in this research were also used in other research in lipid production. Ten et al. (2012) studied the fatty acid composition of *A. gracilis* and attained a 10% of dry weight yield of lipids which mainly consisted of various fatty acids of C16 and C18. Arias-Peñaranda et al. (2013) studied *S. incrassatulus'*s potential as a biofuel feedstock and achieved 19.5 ± 1.5% dry cell weight yield of lipid which consists of 26% methyl palmitate (C16) and 49% methyl linoleate (C18). Ji et al. (2013) also studied the lipid composition of *A. obliquus/S. obliquus* along with *O. multisporus* cultivated in wastewater, obtaining lipid yields of 21 ± 1.3% to 31.4 ± 2% dry weight which consist of palmitic acid (C16:0), stearic acid (C18:0), oleic acid (C18:1), linoleic acid (C18:2) and linolenic acid (C18:3). *S. acutus* was also studied by de Alva et al. (2013) on it potential as biofuel feedstock and achieved the highest lipid content of 28.3% with its fatty acids composed of palmitic acid (C16:0), hexadecadienoic acid (16:2), and linoleic acid (18:2).

While a majority of the microalgae used in this research yielded poor lipid content, the energy value of the lipids per kilogram was unexpectedly high. Most of the microalgae FAME profiles displayed energy potential exceeding -30 MJ/kg. MTA1 gave the highest energy potential with all of it samples exceeding -36 MJ/kg with its highest at -36.36 MJ/kg in 5x (Table 51). Following MTA1 was *A. obliquus* (FDP) with its highest energy value at -35.34 MJ/kg in 5x (Table 50) and *Nitzchia sp./Pseudo-nitzschia sp. (FSB)* with -34.73 MJ/kg in 10x (Table 39).

However, despite having high energy potential, the total energy that can be harvested was relatively small due to the low lipid yield from the biomass (Niderost 2007). Thus, the total energy of the FAMEs extract indicated the efficiency of the microalgae in lipid production. The highest energy observed was -0.00075 kJ by FTAR3 in 5x (Table 49). Following FTAR3 was *Nitzchia sp./Pseudo-nitzschia sp.* (FBP3) with -0.00072 kJ at 5x and -0.00068 kJ at 1x (Table 44).

The energy values of MTA1 (5x), *A. obliquus* (FDP) (5x), *Nitzchia sp./Pseudo-nitzschia sp.* (FSB) (10x), FTAR3 (5x), *Nitzchia sp./Pseudo-nitzschia* sp. (FBP3) (1x) and (5x) in MJ/kg were compared with the energy values of other biofuels and fossil fuels (Table 54). All of the microalgae samples were able to surpass ethanol, methanol and coal but were unable to overcome all of the biofuels and the rest of the fossil fuels (Table 54). In conclusion, the lipid production of microalgae used in this research were relatively lower than standard biofuels but nonetheless offers a good alternative for wastewater treatment in terms of the energy that it could produce during the process.

Table 54: Comparison of MTA1 (5x), Acutodesmus obliquus (FDP) (5x), Nitzchia sp./Pseudo-nitzschia sp. (FSB) (10x), FTAR3 (5x), Nitzchia sp./Pseudo-nitzschia sp. (FBP3) (1x) and (5x) with other biofuels and fossil fuels

Fuel	Energy per kg (MJ/kg)	Reference
MTA1 (5x)	-36.363	N/A
Acutodesmus obliquus (FDP) (5x)	-35.343	N/A
Nitzchia sp./Pseudo-nitzschia sp. (FSB) (10x)	-34.731	N/A
FTAR3 (5x)	-30.047	N/A
Nitzchia sp./Pseudo-nitzschia sp. (FBP3) (1x)	-29.965	N/A
Nitzchia sp./Pseudo-nitzschia sp. (FBP3) (5x)	-29.716	N/A
Ethanol (CH3-CH2-OH)	-26.80	Thomas (2000)
Methanol (CH3-OH)	-19.90	Eyidogan (2010)
Gasoline	-44.40	Thomas (2000)
Coal	-26	Fisher (2003)
Sunflower oil (C18H32O2)	-39.49	Biofuel (n.d.)
Palm Kernel Oil	-39.72	Biofuel (n.d.)
Coconut oil	37.54	Biofuel (n.d.)
Palm oil	-39.55	Biofuel (n.d.)
Physic Nut Oil	-39.00	Biofuel (n.d.)
Peanut Oil	-39.47	Biofuel (n.d.)
Soybean Oil	-39.35	Biofuel (n.d.)
Diesel	-46.80	Biofuel (n.d.)

Application

Bioremediation of nutrient waste.

In line with the main objectives of the research, the microalgae could be used as bioremediators of nutrient waste. Hasan et al. (2014) has demonstrated that various strains of microalgae can be cultured in swine wastewater and produced significant amount of lipids that can be processed into biofuel. Pittman et al. (2011) also lauded on the benefits of microalgae culture in wastewater and insisted on further development towards mass culture optimization to improve its economic viability and sustainability. *N. subsolitaria* (FSE) (Figure 54), *S. acutus* (FTA1) (Figure 58), *A. obliquus* (FDP) (Figure 63), *Nitzchia sp./Pseudo-nitzschia sp.* (FSB) (Figure 52), FSA (Figure 51) and *Nitzchia sp./Pseudo-nitzschia sp*. (FBP3) (Figure 57) which showed positive growth in high nutrient concentrations could be implemented in removing the dissolved nutrients through normal biomass reproduction in domestic wastewater and be integrated into the wastewater treatment field. This could reduce dependency on costly chemicals to treat nutrient rich wastewater and reduce operation costs by repurposing the biomass that will be generated by the microalgae (Ghosh 2004). Furthermore, the microalgae could be used to bioremediate other sources of nutrient waste, specifically the agricultural waste which includes fertilizer rich runoff from plantations and waste generated from livestock farm (*Nutrient management on your dairy farm* 2013). Marine microalgae like MTAR (Figure 66) and MTA1 (Figure 64) which also showed positive growth in high nutrient concentrations could also be developed as a bioremediator in a marine setting like marine fish farms that generate a lot of nutrient waste from fish waste and uneaten feed (Borowitzka1997). A similar implementation was mentioned by Chung et al. (2002) who recommended algae integration to improve efficiency of fish farms, create diversification and manage aquaculture waste to levels within the guidelines and regulations of several countries. Lananan et al. (2014) also utilized marine microalgae to bioremediate aquaculture wastewater in which Chlorella sp. and an effective microorganism were paired together to bioremediate aquaculture wastewater.

Biomass energy

Despite generating a relatively low amount of FAME, the microalgae could still hold potential in terms of energy. Most of the energy received by the microalgae cells from its photosynthesis was dedicated to cell reproduction (Farabee 2001). Thus, cellulose, sugars and proteins had a lot of energy stored in them and could yield some energy after combustion (Cherubini 2010). *N.subsolitaria* (FSE), *S. acutus* (FTA1), *A. obliquus* (FDP), *Nitzchia sp./Pseudo-nitzschia sp*. (FSB), FSA and *Nitzchia sp./Pseudo-nitzschia sp*. (FBP3) that function as bioremediators can be utilized in bioremediating nutrient waste and generating biomass which can be used to be burnt as fuel. The byproducts of the combustion like the ashes could be repurposed as fertilizer and the carbon dioxide produced can be captured and can be introduced to the microalgae to augment their rate of photosynthesis to boost biomass production (Ji et al. 2013).

Fertilizer

The biomass of the microalgae could also be used as a fertilizer in the agricultural field. *N. subsolitaria* (FSE), *S. acutus* (FTA1), *A. obliquus* (FDP), *Nitzchia sp./Pseudo-nitzschia sp.* (FSB), FSA and *Nitzchia sp./Pseudo-nitzschia sp.* (FBP3) could be utilized to bioremediate nutrient waste and the biomass generated by the microalgae could be used as fertilizer in agricultural installations. This method prevents the nutrients in the nutrient waste from being lost to the environment and the biomass locks the nutrients including carbon into the soil as organic matter (Mahdi et al. 2010). As a result, the nutrients would be less likely to be dissolved in water and washed away as agricultural runoff. This can alleviate the dependency of chemical fertilizers as well as eliminate problems that arise from agricultural runoff (Ghosh 2004). Furthermore, the carbon in the biomass would be sequestrated in the soil as organic soil carbon which locks the carbon away from the air (Sedjo and Sohngen 2012). The organic soil carbon would also improve the overall quality of the soil by giving agricultural crops another carbon source which will improve the crop yield (Mahdi et al. 2010).

Conclusion and Further Research

The water samples yield many freshwater and marine microalgae that have various kinds of morphology. Based on the culture experiments, the freshwater *N. subsolitaria* (FSE), *S. acutus* (FTA1) and *Acutodesmus obliquus* (FDP) displayed positive growth in all nutrient rich settings (Figure 54, 58, and 63) while *Nitzchia sp./Pseudo-nitzschia sp.* (FSB), FSA and *Nitzchia sp./Pseudo-nitzschia sp*. (FBP3) grew in nutrient rich media up to 5x (Figure 51, 52, and 57). *Nitzchia* sp./*Pseudo-nitzschia* sp. (FBP3) displayed the highest culture growth of approximately 50 times its initial cell count in a week (Figure 57) followed by *Nitzchia sp./Pseudo-nitzschia* sp. (FSB) with 30 times (Figure 52). *S. acutus* (FTA1) was observed to have a high tolerance to nutrient rich environments, showing healthy up to 10x and was believed to grow better in environments more nutrient rich than 10x (Figure 58). Marine microalgae MTAR and MTA1 were good bioremediators with MTAR showing a similar trend to *S. acutus* (FTA1) (Figure 58), showing steady increasing growth up to 10x and MTA1 showing high growth rate of 30 times its initial cell count in a week at 5x (Figure 64). However, FAME analysis deduced that the microalgae strains yielded poor amounts of lipids which was likely due to the energy being used up in reproduction and metabolism (Farabee 2001). *Nitzchia sp./Pseudo-nitzschia sp.* (FBP3) gave the highest level of FAME of approximately 25% of the biomass weight when nutrient starved in 0x (Table 28). MTA1 gave the highest energy per kilogram at -36.36 MJ/kg in 5x (Table 51) while the highest energy observed was -0.00075 kJ by FTAR3 in 5x (Table 49). All of the microalgae samples were had energy potential to surpass ethanol, methanol and coal but were lower than standard biofuels and fossil fuels. Applications of the microalgae was best in the bioremediation of nutrient waste (Pittman et al. 2011) with the biomass generated repurposed as burning fuel (Cherubini 2010) or agricultural fertilizer (Mahdi et al. 2010).

Further improvements can be done to the research in order to generate more conclusive results. More effort can be undertaken on extracting and replicating the DNA of the unsequenced microalgae. More stronger methods would be needed to break the tough cell walls of microalgae like those observed in MTA2. Despite multiple attempts at DNA extraction using strong chemicals and enzymes as well as DNA extraction kits to breach the cell wall, no DNA band could be observed in the electrophoresis gel. Bead-beating treatment and the GES method used by Fujimoto et al. (2004) could breach the

cell wall of the microalgae cell as it did on Gram positive bacteria. Furthermore, primers specific to other sites on the DNA could be used in replicating the microalgae's DNA. 28S primers which are specific to eukaryotic DNA could be used to replicate the microalgae DNA and could be cross referenced with genomic or 28S DNA in the genetic database (Lodish 1995).

Another way to improve on the research would be to improve the method of extracting the fatty acids from the cells. Instead of relying on costly chemicals, a method devised by Elliott (2013) which involves a hydrothermal liquefaction process under extreme pressure and temperature could be used to remove the lipids from the cells. In the process, an algae slurry of 20% algae by weight was cooked at 350 ˚C and 3000 psi for 30 minutes (Nguyen 2013). This would break down the algae releasing the oil into the mixture. The resulting oil would be easily removed as it forms liquid phases after settling (Figure 68). The oil collected would be chemically similar to crude oil with various hydrocarbons in the C15 to C22 range.

Figure 68 shows the algae slurry, the resulting crude oil after the hydrothermal liquefaction process and the oil after refining. Obtained from Pacific Northwest National Laboratory. <http://www.pnnl.gov/>

References

In-text References

Agostino M 2012, 'CHAPTER 3: Introduction to the BLAST Suite and BLASTN', *Practical Bioinformatics*, 1st ed., Garland Science, pp. 47-71.

Aletsee L, Jahnke J 1992, 'Growth and productivity of the psychrophilic marine diatoms Thalassiosira antarctica Comber and Nitzschia frigida Grunow in batch cultures at temperatures below the freezing point of sea water', *Polar biology*, Vol. 11, No.8, pp.643-647.

Allaby M 1992, 'Algae', *The Concise Dictionary of Botany*, Oxford University Press, Oxford, England.

Amaro HM, Guedes AC, Malcata FX 2011, 'Advances and perspectives in using microalgae to produce biodiesel', *Applied Energy*, Vol. 88, No. 10, pp. 3402-3410.

Anderson DM 1994, 'Red tides', *Scientific American*, Vol. 271, No.2, pp. 62–68.

Ang MY 2008, 'Use of marine microalgae in bioremediation of palm oil mill effluent', Masters thesis, Universiti Malaysia Sabah.

Angelakis AN, Do Monte MM, Bontoux L, Asano T 1999, 'The status of wastewater reuse practice in the Mediterranean basin: need for guidelines', *Water Research*, Vol. 33, No. 10, pp. 2201-2217.

Arias-Peñaranda MT, Cristiani-Urbina E, Montes-Horcasitas C, Esparza-García F, Torzillo G, Cañizares-Villanueva RO 2013, '*Scenedesmus incrassatulus* CLHE-Si01: A potential source of renewable lipid for high quality biodiesel production', *Bioresource technology*, Vol. 140, pp. 158-64.

Arisz SA, van Himbergen JA, Musgrave A, van den Ende H, Munnik T2000, 'Polar glycerolipids of *Chlamydomonas moewusii'*, *Phytochemistry*, Vol. 53, No. 2, pp. 265-70.

Baker KH, Herson DS 1994, *Bioremediation*, McGraw-Hill Publishing Company, New York, USA.

Bast F, Shimada S, Hiraoka M, Okuda K 2009, 'Asexual life history by biflagellate zoids in *Monostroma latissimum* (*Ulotrichales*)', *Aquatic Botany*, Vol. 91, No.3 pp. 213–218.

Beaty MH, Parker B 1992, 'Cryopreservation of eukaryotic algae', *Virginia Journal of Science*, Vol. 43, pp. 403-410.

Bianchi FJJA, Booij CJH, Tscharntke T 2006, 'Sustainable pest regulation in agricultural landscapes: a review on landscape composition, biodiversity and natural pest control', *Proceedings of The Royal Society B: Biological Science*, Vol. 273, No. 1595, pp. 1715–1727.

Biello D 2009, 'The Origin of Oxygen in Earth's Atmosphere', *Scientific American*, August 2009, viewed 10th May 2016, <http://www.scientificamerican.com/article/origin-of-oxygen-in-atmosphere/>.

Bligh EG, Dyer WJ 1959, 'A rapid method for total lipid extraction and purification', *Canadian Journal of Biochemistry and Physiology*, Vol. 37, pp. 911-917.

Biofuel n.d., PTT Public Company Limited, viewed 18th May 2016, <https://web.archive.org/web/20070927065241/http://www.pttplc.com/en/document/pdf/biofuel_en.pdf>.

Boricha H, Fulekar MH 2009, '*Pseudomonas plecoglossicida* as a novel organism for the bioremediation of cypermethrin', *Biology and Medicine*, Vol. 1, No. 4, pp. 1-10.

Borowitzka MA 1997, 'Microalgae for aquaculture: Opportunities and constraints', Journal of Applied Phycology, Vol. 9, No. 393.

Brody T 1999, *Nutritional Biochemistry*, No.2, Academic Press, pp. 320.

Brune DE, Novak JT 1981, 'Carbon and light limitation in mass algal culture', *Fuels Biomass Wastes*, pp. 99-126.

Cardozo KHM, Guaratini T, Barros MP, Falcão VR, Tonon AP, Lopes NP, Campos S, Torres MA, Souza AO, Colepicolo P, Ernani Pinto E 2007, 'Metabolites from algae with economical impact', *Comparative Biochemistry and Physiology Part C: Toxicology and Pharmacology*, Vol. 146, pp. 60–78.

Chen GQ, Jiang Y, Chen F 2007, 'Fatty acid and lipid class composition of the eicosapentaenoic acid-producing microalga, *Nitzschia laevis'*, *Food chemistry*, Vol. 104, No. 4, pp.1580-1585.

Cherubini F 2010, 'The biorefinery concept: using biomass instead of oil for producing energy and chemicals', *Energy Conversion and Management*, Vol. 51, No. 7, pp.1412-1421.

Chopin T, Buschmann AH, Halling C, Troell M, Kautsky N, Neori A, Kraemer GP, Zertuche-González JA, Yarish C, Neefus C 2001, 'Integrating seaweeds into marine aquaculture systems: aley toward sustainability', *Journal of Phycology*, Vol. 37, pp. 975–986.

Chung IK, Kang YH, Yarish C, Kraemer GP, Lee JA 2002, 'Application of seaweed cultivation to the bioremediation of nutrient-rich effluent', *Algae*, Vol. 17, No. 3, pp.187-194.

Conder JR, Young CL 1979, *Physicochemical measurement by gas chromatography*, John Wiley & Sons.

de Alva MS, Luna-Pabello VM, Cadena E, Ortíz E 2013, 'Green microalga *Scenedesmus acutus* grown on municipal wastewater to couple nutrient removal with lipid accumulation for biodiesel production', *Bioresource technology*, Vol. 146, pp. 744-748.

Demirbas A, MF Demirbas MF 2010, *Algae energy: algae as a new source of biodiesel*, Green Energy and Technology Series, Springer Science and Business Media.

Demirbas MF 2011, 'Biofuels from algae for sustainable development', *Applied Energy*, Vol. 88, No. 10, pp. 3473-3480.

Demirbas MF, Balat M, Balat H 2011, 'Biowastes-to-biofuels', *Energy Conversion and Management*, Vol. 52, No. 4, pp. 1815-1828.

Devaraja TN 2002, 'Investigation on indigenous Bacillus isolates with bioremediation properties for improving water quality and shrimp health in Malaysian aquaculture', Doctor of Philosophy Thesis, Science and Environmental Studies, Putra Malaysia University, Malaysia.

Douskova I, Doucha J, Livansky K, Machat J, Novak P Umysova D, Zachleder V, Vitova M 2009, 'Simultaneous flue gas bioremediation and reduction of microalgal biomass production costs', *Applied Microbiology and Biotechnology*, Vol. 82, pp.179–185.

Doyle A, Griffiths JB 2000, 'Haemocytometer cell counts and viability studies', *Cell and tissue culture for medical research*, pp.12-6.

Earle SA 1968, 'Phaeophyta of the Eastern Gulf of Mexico' *Phycologia*, Vol. 7, No. 2, pp. 71-254.

Eden PA, Schmidt TM, Blakemore RP, Pace NR 1991, 'Phylogenetic Analysis of *Aquaspirillum magnetotacticum* Using Polymerase Chain Reaction-Amplified 16S rRNA-Specific DNA', *International Journal of Systematic Bacteriology*, Vol. 41, No. 2, pp. 324–325.

Erwin ES, Marco GJ, Emery EM 1961, 'Volatile fatty acid analyses of blood and rumen fluid by gas chromatography', *Journal of dairy science*, Vol. 44, No. 9, pp.1768-1771.

Eyidogan M, Ozsezen AN, Canakci M, Turkcan A 2010, 'Impact of alcohol–gasoline fuel blends on the performance and combustion characteristics of an SI engine', Fuel, Vol. 89, No. 10, pp. 2713-2720.

Fawley MW, Fawley KP 2004, 'A simple and rapid technique for the isolation of DNA from Microalgae', *Journal of Phycology*, Vol. 40, No. 1, pp. 223–225.

Ferrell J, Sarisky-Reed V 2010, *National Algal Biofuels Technology Roadmap: A technology roadmap resulting from the National Algal Biofuels Workshop*, Energy efficiency and renewable energy, U.S. Department of Energy.

Fisher J 2003, 'Energy density of coal', *The Physics Factbook*.

Fujimoto S, Nakagami Y, Kojima F 2004, 'Optimal bacterial DNA isolation method using bead-beating technique', *Memoirs Kyushu Univ Dep Of Health Scis Of Medical Sch*, Vol. 3, pp. 33-38.

Ghosh N 2004, Reducing dependence on chemical fertilizers and its financial implications for farmers in India, *Ecological Economics*, Vol. 49, pp. 149 – 162.

Greenwell HC, Laurens LML, Shields RJ, Lovitt RW, Flynn KJ 2009, 'Placing microalgae on the biofuels priority list: A review of the technological challenges', *Journal of the Royal Society Interface*, Vol. 7, No. 46, pg. 703.

Guiry MD 2012, 'How Many Species of Algae Are There?', *Journal of Phycology*, Vol. 48, No. 5, pp. 1057–1063.

Gully AR, Kennedy CA 1987, 'Comparison of phytoplankton, periphyton, and benthic algae in two different beach pools off of Douglas Lake', *Phycology*, Biological Station, University of Michigan, USA.

Guschina IA, Harwood JL 2006, 'Lipids and lipid metabolism in eukaryotic algae', *Progress in Lipid Research*, Vol. 45, pp 160–186.

Hamzah A, Phan CW, Abu Bakar NF, Wong KW 2013, 'Biodegradation of Crude Oil by Constructed Bacterial Consortia and the Constituent Single Bacteria Isolated From Malaysia', *Bioremediation Journal*, Vol. 17, No.1, pp. 1-10.

Harris DC 1999, '24. Gas Chromatography', *Quantitative chemical analysis*, 5th ed., WH Freeman and Company, pp. 675–712.

Hasan R, Zhang B, Wang L, Shahbazi A 2014, 'Bioremediation of Swine Wastewater and Biofuel Potential by using *Chlorella vulgaris*, *Chlamydomonas reinhardtii*, and *Chlamydomonas debaryana'*, *Journal of Petroleum and Environmental Biotechnology*, Vol. 5, No. 175.

Herndon A 2013, 'Tesoro is first customer for Sapphire's algae-derived crude oil', *Bloomberg Business*, Bloomberg, March 2013, viewed 14th April 2016, <http://www.bloomberg.com/news/articles/2013-03-20/tesoro-is-first-customer-for-sapphire-s-algae-derived-crude-oil>.

Heyrman J, Mergaert J, Denys R, Swings J 1999, 'The use of fatty acid methyl ester analysis (FAME) for the identification of heterotrophic bacteria present on three mural paintings showing severe damage by microorganisms', *FEMS Microbiology Letters*, Vol. 181, No.1, pp. 55-62.

Higson S 2004, *Analytical Chemistry*, OXFORD University Press.

Hilz H, Wiegers U, Adamietz P 1975, 'Stimulation of Proteinase K action by denaturing agents: application to the isolation of nucleic acids and the degradation of 'masked' proteins', *European Journal of Biochemistry*, Vol. 56, No. 1, pp. 103–108.

Hipolito CN, Crabbe E, Badillo CM, Zarrabal OC, Mora MA, Flores GP, Cortazar MD, Ishizaki A 2008, 'Bioconversion of industrial wastewater from palm oil processing to butanol by *Clostridium saccharoperbutylacetonicum* N1-4 (ATCC 13564)', *Journal of Cleaner Production*, Vol. 16, No. 5, pp. 632-638.

Hoek C, Mann DG, Jahns HM 1995, 'Algae', *An Introduction to Phycology*, Cambridge University Press, Cambridge, England.

Ichihara K, Fukubayashi Y 2010, 'Preparation of fatty acid methyl esters for gas-liquid chromatography', *Journal of Lipid Research*, Vol. 51, No. 3, pp. 635–640, National Center for Biotechnology Information.

Idris A, Hashim R, Abdul Rahman R, Ahmad WA, Ibrahim Z, Abdul Razak PR, Mohd Zin H, Bakar I 2007, 'Application of bioremediation process for textile wastewater treatment using pilot plant', *International Journal of Engineering and Technology*, Vol. 4, No. 2, pp. 228-234.

Jarvinen KT, Melin ES, Puhakka JA 1994, 'High-rate bioremediation of chlorophenol contaminated groundwater at low temperatures', *Environmental Science and Technology*, Vol. 28, No. 13, pp. 2387-2392.

Ji MK, Abou-Shanab RA, Kim SH, Salama ES, Lee SH, Kabra AN, Lee YS, Hong S, Jeon BH 2013, 'Cultivation of microalgae species in tertiary municipal wastewater supplemented with CO 2 for nutrient removal and biomass production', *Ecological Engineering*, Vol. 58, pp.142-148.

Johnson MB, Wen 2009, 'Production of Biodiesel Fuel from the Microalga *Schizochytrium limacinum* by Direct Transesterification of Algal Biomass', *Energy Fuels*, Vol. 23, pp. 5179–5183.

Kanekar PP, Sarnaik SS, Kelkar AS 1998, 'Bioremediation of phenol by alkaliphilic bacteria isolated from alkaline lake of Lonar, India', *Journal of Applied Microbiology*, Vol. 85, No. 51, pp. 128–133.

Karthikeyan S, Balasubramanian R, Iyer CSP 2007, 'Evaluation of the marine algae *Ulva fasciata* and *Sargassum sp*. for the biosorption of Cu(II) from aqueous solutions', *Bioresource Technology*, Vol. 98, No. 2, pp. 452-455.

Keeling PJ 2008, 'Chromalveolates and the Evolution of Plastids by Secondary Endosymbiosis', *Journal of Eukaryotic Microbiology*, Vol. 56, Iss. 1, pp. 1–8.

Kerswell AP 2006, 'Global biodiversity patterns of benthic marine algae', *Ecology*, Vol. 87, Ecological Society of America, pp. 2479–2488.

Khataee AR, Zarei M, Pourhassan M, 2010, 'Bioremediation of Malachite Green from Contaminated Water by Three Microalgae: Neural Network Modeling', *Clean Soil Air Water*, Vol. 38, pp. 96–103.

Koh LP, Wilcove DS 2008, 'Is oil palm agriculture really destroying tropical biodiversity?', *Conservation Letters*, Vol. 1, pp.60–64.

Kokinos JP, Anderson DM 1995, 'Morphological development of resting cyst in cultures of the marine dinoflagellate *Lingulodinium polyedrum* (= *L. machaerophorum*)', *Palynology*, Vol. 19, pp. 143–66.

Krienitz L, Kotut K, Hegewald E 1998, 'Some interesting coccal green algae (Chlorellales) from Turkwel Gorge Reservoir, Kenya', *Algological Studies*, Vol. 91, pp.57-69.

Lananan F, Abdul Hamid SH, Sakinah Din WN, Ali N, Khatoon H, Jusoh A, Endut A 2014, 'Symbiotic bioremediation of aquaculture wastewater in reducing ammonia and phosphorus utilizing Effective Microorganism (EM-1) and microalgae (*Chlorella* sp.)', *International Biodeterioration and Biodegradation*, Vol. 95, Part A, pp. 127-134

Lane DJ, Pace B, Olsen GJ, Stahl DA, Sogin, ML, Pace NR 1985, 'Rapid determination of 16S ribosomal RNA sequences for phylogenetic analyses', *Proceedings of the National Academy of Sciences*, Vol. 82, No. 20, pp. 6955–6959.

Lawton LA, Codd GA 1991, 'Cyanobacterial (blue-green algae) toxins and their significance in UK and European waters', *Journal of Soil and Water Conservation*, Vol. 40, pp. 87–97.

Lee RE 2008, *Phycology*, No. 4. Cambridge University Press, Cambridge, England.

Lei J, Sansregret JL, Cyr B 1994, 'Biopiles and biofilters combined for soil cleanup', *Pollution Engineering*, Vol. 26, Iss 24, pp. 56-58.

Li XN, Song HL, Li W, Xi W, Nishimura O 2010, 'An integrated ecological floating-bed employing plant freshwater clam and biofilm carrier for purification of eutrophic water', Ecological Engineering, Vol. 36, pp. 382–390.

Lim SL, Chu WL, Phang SM 2014, 'Use of *Chlorella vulgaris* for bioremediation of textile wastewater', *Bioresource Technology*,Vol. 101, No. 19, pp. 7314–7322.

Liu J, Daily GC, Ehrlich PR, LuckGW 2003, 'Effects of household dynamics on resource consumption and biodiversity', *Nature*, Vol. 421, pp. 530-533.

Lodish H 1995, *Molecular Cell Biology*, 3rd edn.

Ma L, Velthof GL, Wang FH, Qin W, Zhang WF, Liu Z, Zhang Y, Wei J, Lesschen JP, Ma WQ, Oenema O, Zhang FS 2012, 'Nitrogen and phosphorus use efficiencies and losses in the food chain in China at regional scales in 1980 and 2005', *Science of the Total Environment*, Vol. 434, pp. 51-61.

Maeda K, Owada M, Kimura N, Omata K, Karube I 1995, 'CO 2 fixation from the flue gas on coal-fired thermal power plant by microalgae', *Energy Conversion and Management*, Vol. 36, No. 6, pp.717-720.

Mahdi SS, Hassan GI, Samoon SA, Rather HA, Dar SA, Zehra B 2010, 'Bio-fertilizers in organic agriculture', *Journal of Phytology*, Vol. 2, No. 10, pp.42-54.

Mann P, Gahagan L, Gordon MB 2003, 'Tectonic setting of the world's giant oil and gas fields', *Giant Oil and Gas Fields of the Decade 1990–1999*, Vol. 78, pp.15-105.

Margulis L, Corliss JO, Melkonian M, Chapman DJ 1990, *Handbook of Protoctista*, Jones and Bartlett Publishers, Boston.

Martinez T, Bertron A, Gilles Escadeillas G, Ringot 2014, “Algal growth inhibition on cement mortar: Efficiency of water repellent and photocatalytic treatments under UV/VIS illumination”, International Biodeterioration and Biodegradation, Vol. 89, pp. 115–125.

Mata TM, Martins AA, Caetano NS 2010, ‘Microalgae for biodiesel production and other applications: A Review”, *Renewable and Sustainable Energy Reviews*, Vol.14, no. 1, pp217–232.

Meffe GK, Snelson FF 1989, ‘An ecological overview of poeciliid fishes’, *Ecology and evolution of livebearing fishes (Poeciliidae)*, pp. 13-31.

Mekhilef S, Siga S, Saidur R 2011, ‘A review on palm oil biodiesel as a source of renewable fuel’, Renewable and Sustainable Energy Review, Vol. 15, no. 4, pp. 1937–1949.

Mera R, Torres E, Abalde J 2014, ‘Sulphate, more than a nutrient, protects the microalga *Chlamydomonas moewusii* from cadmium toxicity’, *Aquatic Toxicology*, Vol. 148, pp.92-103.

Moheimani NR 2005, ‘The culture of coccolithophorid algae for carbon dioxide bioremediation’, Doctor of Philosophy thesis, Murdoch University, Australia.

Nelson DL, Cox MM 2000, *Lehninger, Principles of Biochemistry*, 3rd Ed., Worth Publishing, New York, USA.

Neori A, Shpigel M, Ben-Ezra D 2000, ‘A sustainable integrated system for culture of fish, seaweed and abalone’, *Aquaculture*, Vol. 186, No. 3–4, pp. 279-291.

Nguyen TC 2013, ‘Scientists Turn Algae Into Crude Oil In Less Than An Hour’, *Smithsonian Magazine*, December 2013, viewed 3rd May 2016, <http://www.smithsonianmag.com/innovation/scientists-turn-algae-into-crude-oil-in-less-than-an-hour-180948282/?no-ist>.

Niderost R 2007, *«Biofuel» does not necessarily mean ecologically friendly: Empa-study scrutinizes the ecological balance of various biofuels*, Swiss Federal Laboratories for Materials Science and Technology, May 2007, viewed 17th May 2016, <https://www.empa.ch/web/s604/biotreibstoffe>.

Nixon SW 1995, 'Coastal marine eutrophication: A definition, social causes, and future concerns', *Ophelia*, Vol. 41, No. 1, pp. 199-219.

NOAA's National Ocean Service: Nonpoint Source Pollution 2007, National Oceanic and Atmospheric Association (NOAA), Washington DC, USA.

Nozaki H, Maruyama S, Matsuzaki M, Nakada T, Kato S, Misawa K 2009, 'Phylogenetic positions of *Glaucophyta*, green plants (*Archaeplastida*) and *Haptophyta* (*Chromalveolata*) as deduced from slowly evolving nuclear genes', *Molecular Phylogenetics and Evolution*, Vol. 53, No. 3, pp.872-880.

Nutrient management on your dairy farm 2013, DairyNZ, viewed 24th April 2016, <http://www.dairynz.co.nz/media/757901/nutrient_management_on_your_dairy_farm.pdf>.

O'Leary MH 1988, 'Carbon Isotopes in Photosynthesis', *Bioscience*, Vol. 38, No. 5, pp. 328–336.

Olguin EJ 2003, 'Phycoremediation: key issues for cost-effective nutrient removal processes', *Biotechnology Advances*, Vol. 22, No. 1–2, pp. 81-91.

Pavia DL, Lampman GM, Kritz GS, Engel RG 2006, *Introduction to Organic Laboratory Techniques*, 4th Ed., Thomson Brooks/Cole, pp. 797–817.

Philp R 2015, 'Bioremediation: The pollution solution?', *Microbe Post*, December 2015, viewed 10th May 2016, <https://microbepost.org/2015/12/08/bioremediation-the-pollution-solution/>.

Pienkos PT, Darzins A 2009, 'The promise and challenges of microalgal-derived biofuels', *Biofuels, Bioproducts and Biorefining*, Vol. 3, No. 4, 431–440. Piotrowska-

Niczyporuk A, Bajguz A, Talarek M, Bralska M, Zambrzycka E 2015, 'The effect of lead on the growth, content of primary metabolites, and antioxidant response of green alga *Acutodesmus obliquus* (*Chlorophyceae*)', *Environmental Science and Pollution Research*, Vol. 22, Iss. 23, pp. 19112-19123.

Pittman JK, Dean AP, Osundeko O 2011, 'The potential of sustainable algal biofuel production using wastewater resources', *Bioresource Technology*, Vol. 102, No. 1, pp. 17-25.

PowerWater® DNA Isolation Kit Instruction Manual 2015, MO BIO Laboratories, viewed 24th September 2015, <https://mobio.com/media/wysiwyg/pdfs/protocols/14900.pdf>.

Pringle A, Moncalvo JM, Vilgalys R 2003, 'Revisiting the rDNA sequence diversity of a natural population of the arbuscular mycorrhizal fungus Acaulospora colossica', *Mycorrhiza*, Vol. 13, No. 4, pp. 227-231.

Qian Y, Wen XH, Huang X 2007, 'Development and application of some renovated technologies for municipal wastewater bioremediation in China', *Frontiers of Environmental Science and Engineering in China*, Vol. 1, pp. 1–12.

Rakmi AR 1993, 'Characterisation and prospects for biological treatment of textile finishing wastewater', *Waste management in Malaysia: current status and prospects for bioremediation*, pp. 99-108.

Ralph A. Lewin RA 2002, Prochlorophyta – a matter of class distinctions, *Photosynthesis Research*, Vol. 73, Iss. 1-3, pp. 59-61.

Ramírez-Verduzco LF, Rodríguez-Rodríguez JE, del Rayo Jaramillo-Jacob A 2012, 'Predicting cetane number, kinematic viscosity, density and higher heating value of biodiesel from its fatty acid methyl ester composition', *Fuel*, Vol. 91, No.1, pp.102-111.

Rao CS 2007, *Environmental pollution control engineering*, New Age International.

Refaat AA 2009, 'Correlation between the chemical structure of biodiesel and its physical properties', *International Journal of Environmental Science and Technology*, Vol. 6, No. 4, pp 677-694.

Rosemond AD, Mulholland PJ, Elwood JW 1993, 'Top-Down and Bottom-Up Control of Stream Periphyton: Effects of Nutrients and Herbivores', *Ecology*, Vol. 74, No. 4, pp. 1264-1280.

Schell LM, Denham M 2003, 'Environmental pollution in urban environments and human biology', *Annual Review of Anthropology*, Vol. 32, No. 1, pp.111-134.

Sedjo R, Sohngen B 2012. 'Carbon Sequestration in Forests and Soils', *Annual Review of Resource Economics*, Vol. 4, pp. 127–144.

Sharma GK, Khan SA 2013, Bioremediation of Sewage Wastewater Using Selective Algae for Manure Production, *International Journal of Environmental Engineering and Management*, Vol. 4, No. 6, pp. 573-580.

Sharma KK, Schuhmann H, Schenk PM 2012, 'High Lipid Induction in Microalgae for Biodiesel Production', *Energies*, Vol. 5, No. 5, pp. 1532-1553.

Sheehan J, Dunahay T, Benemann J, Roessler P 1998, *A look back at the U.S. Department of Energy's aquatic species program-Biodiesel from algae*, National Renewable Energy Laboratory US Department of Energy, No. DE-AC36-83CH10093.

Sipaúba-Tavares LH, Pereira AML 2008, "Large scale laboratory cultures of *Ankistrodesmus gracilis* (Reisch) *Korsikov* (Chlorophyta) and *Diaphanosoma biergei Korinek (Cladocera)*", 1981, Brazilian Journal of Biology, Vol.68, No.4.

Subramaniam S, Fahy E, Gupta S, Sud M, Byrnes R., Cotter D, Dinasarapu AR, Maurya MR 2011, 'Bioinformatics and Systems Biology of the Lipidome', *Chemical Reviews*, Vol. 111, No. 10, pp. 6452–6490.

Suen Y, Hubbard JS, Holzer G, Tornabene TG 1987, 'Total lipid production of the green alga Nannochloropsis sp. QII under different nitrogen regimes', *Journal of Phycology*, Vol. 23, No. 2, pp.289-296.

Stoecker DK 1999, 'Mixotrophy among Dinoflagellates', *The Journal of Eukaryotic Microbiology*, Vol. 46, Iss. 4, pp. 397–401.

Tadros MG 1985, *Screening and characterizing oleaginous microalgal species from the southeastern United States*', Alabama A&M University, Solar Energy Research Institute, US Department of Energy, No. DE-AC02-83CH10093.

Tang H, Abunasser N, Garcia MED, Chen M, Ng SKY, Salley SO 2011, 'Potential of microalgae oil from *Dunaliella tertiolecta* as a feedstock for biodiesel', *Applied Energy*, Vol. 88, No. 10, pp. 3324-3330.

Tamura K, Stecher G, Peterson D, Filipski A, Kumar S 2013, 'MEGA6: Molecular Evolutionary Genetics Analysis Version 6.0', *Molecular Biology and Evolution*, Vol. 30, No. 12, pp. 2725–2729.

Tashiro Y, Shinto H, Hayashi M, Baba SI, Kobayashi G, Sonomoto K 2007, 'Novel high-efficient butanol production from butyrate by non-growing *Clostridium saccharoperbutylacetonicum* N1-4 (ATCC 13564) with methyl viologen', *Journal of bioscience and bioengineering*, Vol. 104, No. 3, pp. 238-40.

Ten LN, Oh YK, Chue KT, Woo SG, Lee M, Cho CY, Yoo SA 2012, 'Fatty acid compositions of three microalga species', *Chemistry of Natural Compounds*, pp.1-2.

'The Food Web' 2004, Water on the Web, March 2004, viewed April 2016, <http://waterontheweb.org/under/lakeecology/11_foodweb.htm>

Thurman HV 1997, *Introductory Oceanography*, Prentice Hall College, New Jersey, USA.

Thomas D 2002, 'Seaweeds', *Life Series*, Natural History Museum, London, England.

Thomas G 2000, *Overview of Storage Development DOE Hydrogen Program*, Sandia National Laboratories, San Ramon, California, USA.

Thrush SF, Hewitt JE, Gibbs M, Lundquist C, Norkko A 2006, 'Functional Role of Large Organisms in Intertidal Communities: Community Effects and Ecosystem Function', *Ecosystems*, Vol. 9, No. 6, pp. 1029-1040.

Tsai YL, Olson BH 1991, 'Rapid method for direct extraction of DNA from soil and sediments' *Applied and Environmental Microbiology*, Vol. 57, No. 4, pp. 1070-1074.

Vaulot D, Olson R, Merkel S, Chisholm S 1987, 'Cell-cycle response to nutrient starvation in two phytoplankton species, *Thalassiosira weissflogii* and *Hymenomonas carterae'*, *Marine Biology*, Vol. 95, No. 4, pp 625-630.

Vitova M, Bisova K, Kawano S, Zachleder V 2015, 'Accumulation of energy reserves in algae: From cell cycles to biotechnological applications', *Biotechnology advances*, Vol. 33, No.6, pp.1204-1218.

Voegele E 2012, 'Propel, Solazyme make algae biofuel available to the public', *Biomass Magazine*, November 2012, viewed 14th April 2016 <http://biomassmagazine.com/articles/8307/propel-solazyme-make-algae-biofuel-available-to-the-public>.

Waggoner B n.d., *Introduction to Bacillariophyta (The Diatoms)*, University of California Museum of Paleontology, Berkeley, California, United States.

Wang PF, Martin J MorrisonG 1999, 'Water Quality and Eutrophication in Tampa Bay, Florida', *Estuarine, Coastal and Shelf Science*, Vol. 49, No. 1, pp. 1–20.

Wenping C, Houhu Z, Yinmei W, JiZheng P 2012, 'Bioremediation of polluted surface water by using biofilms on filamentous bamboo', *Ecological Engineering*, Vol.42, pp. 146–149.

Woo SG, Park JH 2012, 'Effects of Phosphorus Starvation on Fatty Acid Production by Microalgae Cultivated from Wastewater Environment', *Journal of The Korean Society of Civil Engineers*, Vol. 32, No.4B, pp.253-259.

Wu RSS 1995, 'The environmental impact of marine fish culture: Towards a sustainable future', *Marine Pollution Bulletin*, Vol. 31, No. 4–12, pp. 159-166.

White TJ, Bruns T, Lee S, Taylor J 1990, 'Amplification and direct sequencing of fungal ribosomal RNA genes for phylogenetics' *PCR Protocols: a Guide to Methods and Applications*, Vol. 18, pp. 315–322.

Xin L, Hong-ying H, Ke G, Ying-xue S 2010, 'Effects of different nitrogen and phosphorus concentrations on the growth, nutrient uptake, and lipid accumulation of a freshwater microalga *Scenedesmus sp.*', *Bioresource Technology*, Vol. 101, No. 14, pp. 5494-5500.

Zinoviev S, Arumugam S, Miertus S, Müller-Langer F, Kaltschmitt M, Vogel A, Thraen D, Fornasiero P 2007, 'Background paper on biofuel production technologies', *Area of Chemistry*, ICS-UNIDO, International Centre for Science and High Technology United Nations Industrial Development Organization.

Zhou Y, Yang H, Hu H, Liu Y, Mao Y, Zhou H, Xu X, Zhang F 2006, 'Bioremediation potential of the macroalga *Gracilaria lemaneiformis* (Rhodophyta) integrated into fed fish culture in coastal waters of north China', *Aquaculture*, Vol. 252, No. 2–4, pp. 264-276.

Zhu Y, Wu Z, Yang ST 2002, 'Butyric acid production from acid hydrolysate of corn fibre by *Clostridium tyrobutyricum* in a fibrous-bed bioreactor', *Process Biochemistry*, Vol. 38, pp. 657-666.

Figure and Table References

50 bp DNA Ladder n.d. [image], New England Biolabs, viewed 16th May 2016, <https://www.neb.com/~/media/Catalog/All-Products/28C3CA6BCEF449CC8744E5A36A6221FE/Gel%20Photos/N3236-new-photo.gif>.

'*Acutodesmus pectinatus* (*Scenedesmus pectinatus*)' [image] 2006, *Acutodesmus pectinatus (Scenedesmus pectinatus)*, *Plingfactory: life in water*, viewed 23rd September 2015, <http://www.plingfactory.de/Science/Atlas/Kennkarten%20Algen/Chlorophyta/image/Scenedesmus-dimorphus.jpg>.

Astrium 2016, *Map of Sarawak river near Jaln Batu Kawa* [image], Google Maps, viewed 3rd March 2016, <https://www.google.com/maps/@1.5133996,110.2739118,1191m/data=!3m1!1e3>.

Astrium 2016, *Tunku Abdul Rahman National Park* [image], Google Maps, viewed 5rd March 2016, <https://www.google.com/maps/place/Tunku+Abdul+Rahman+Park/@5.9741922,116.0076884,834m/data=!3m1!1e3!4m2!3m1!1s0x0:0x89b82df32fd890cb>.

'Diagram of agarose gel setup, for agarose gel electrophoresis' [image] 2016, *Module 1.2: Agarose Gel Electrophoresis*, MIT Open Course Ware, viewed 24th September 2016, <https://mobio.com/media/catalog/product/cache/1/image/9df78eab33525d08d6e5fb8d27136e95/1/4/14900-50.jpg>.

Eutrophication [image] 2014, BBC, viewed 24th April 2016, <http://www.bbc.co.uk/staticarchive/05e29b2e4fb11a0954c97cbe5273999767ea9fff.jpg>.

Fedor K 2011, '*Arthrospira platensis'* [image], *Arthrospira platensis*, Microbe Wiki, viewed 24th September 2015, <https://microbewiki.kenyon.edu/index.php/Arthrospira_platensis>.

Gerloff 1940, '*Chlamydomonas moewusii'* [image], *Chlamydomonas moewusii,* Protist Information Server, viewed 9 May 2015, <http://protist.i.hosei.ac.jp/PDB5/PCD0066/htmls/85.html>.

Hansen G n.d., 'SCCAP K-1726 *Desmodesmus Serratus'* [image], *Desmodesmus serratus (Corda) An, Friedl and Hegewald, 1999*, Nordic Microalgae and Aquatic protozoa, viewed 26th June 2015, <http://media.nordicmicroalgae.org/original/Desmodesmus%20serratus_1.jpg>.

Hegewald EH n.d., "*Desmodesmus communis*" [image], 'Plant and Algal Type and Historical Specimens', *Taxonomy*, Barcoding P.A.T.H.S. database, viewed 23rd April 2016, <http://barcoding-paths.it/public/media/cache/45/17/4517429f6ef11ed3080f4e6c2b18df2f.jpg>.

Hegewald EH n.d., "*Desmodesmus pirkollei*" [image], 'Plant and Algal Type and Historical Specimens', *Taxonomy*, Barcoding P.A.T.H.S. database, viewed 23rd April 2016, <http://barcoding-paths.it/public/media/cache/cb/f1/cbf19bd9734dcffd7096935629fd68e7.jpg>.

Hegewald E, Bock C, Krienitz L 2013, "*Pectinodesdus pectinatus*" and "*Pectinodesmus holtmannii*" [image], 'A phylogenetic study on *Scenedesmaceae* with the description of a new species of *Pectinodesmus* and the new genera *Verrucodesmus* and *Chodatodesmus* (*Chlorophyta*, *Chlorophyceae*)', *Fottea*, Vol. 13, No.2, pp. 149–164, viewed 23rd September 2015, <http://www.fottea.czechphycology.cz/pdfs/fot/2013/02/05.pdf>.

Koshigaya S 2001, '*N. subsolitaria'* [image], *N. subsolitaria,* Protist Information Server, viewed 7 May 2015, <http://protist.i.hosei.ac.jp/pdb/images/Chlorophyta/Nephrochlamys/index.html>.

‘*Nitzschia*, Kaikorai tributary, X400’ [image] n.d., *Algal factsheet: Nitzschia (Bacillariaceae)*, Kaikorai tributary, Otago Regional Council and Landcare Research, viewed 21st July 2015, <https://www.landcareresearch.co.nz/resources/identification/algae/identification-guide/interpretation/indicator-taxa/poor-streams/nitzschia>.

‘Nitzschia Navicula MC’ [image], n.d., *Nitzschia Navicula MC,* University of Wisconsin Plant teaching Collection, viewed 16th May 2016, <http://botit.botany.wisc.edu/Resources/Botany/Heterokonts/Diatoms/Various%20diatoms/Nitzschia%20Navicula%20MC.jpg>.

‘*Ourococcus multisporus’* [image] n.d., *Ourococcus (Chlorophyceae)*, Center for Freshwater Biology, viewed 15th June 2016, <http://cfb.unh.edu/phycokey/Choices/Chlorophyceae/unicells/flagellated/OUROCOCCUS/Ourococcus_01_400x300_multisporus.jpg>.

‘PowerWater® DNA Isolation Protocol’ [image] 2015, *PowerWater® DNA Isolation Kit,* MO BIO Laboratories, viewed 23rd September 2015, <https://mobio.com/media/catalog/product/cache/1/image/9df78eab33525d08d6e5fb8d27136e95/1/4/14900-50.jpg>.

Rickey T 2013, ‘Algae to crude oil’ [image], *Algae to crude oil: Million-year natural process takes minutes in the lab*, Pacific Northwest National Laboratory, viewed 3rd May 2016, <http://www.pnnl.gov/news/release.aspx?id=1029>.

‘Scendesmus dimorphus’ [image] n.d., *Scendesmus dimorphus,* America Pink, viewed 23rd September 2015, <http://america.pink/images/3/9/3/9/5/8/1/en/2-scenedesmus-dimorphus.jpg>.

Schmid E, ‘Division Chlorophycophyta: Filamentous Algae’ [image], *Algae*, Professor Schmid’s Biology Website, viewed 10th May 2016, <http://classroom.sdmesa.edu/eschmid/Lectur83.jpg>.

‘Standard MyTaq Red Mix Protocol’ [image], *mytaq red mix product manual*, Bioline, viewed April 5th 2016, <http://www.bioline.com/de/downloads/dl/file/id/2697/mytaq_red_mix_product_manual.pdf>.

‘The Transesterification Reaction’ [image] n.d., *Generating Biodiesel*, Global CCS Institute, viewed 21 June 2015, <http://hub.globalccsinstitute.com/sites/default/files/publications/books/138128/images/fig08.jpg>.

Tsukii Y 1977, ‘*Ankistrodesmus sp.*’ [image], *Illustrations of The Japanese Fresh-water Algae*, Protist Information Server, viewed 24 September 2015, <http://protist.i.hosei.ac.jp/pdb/images/chlorophyta/Ankistrodesmus/sp_4b.html>.

Tsukii Y 1977, ‘*Coelastrum sphaericum*’ [image], *Illustrations of The Japanese Fresh-water Algae*, Protist Information Server, viewed 24 September 2015, <http://protist.i.hosei.ac.jp/PDB/Images/chlorophyta/coelastrum/sphaericum/sp_01.html>.

Tsukii Y 1977, ‘*Kirchneriella acuminata’* [image], *Illustrations of The Japanese Fresh-water Algae*, Protist Information Server, viewed 24 September 2015, <http://protist.i.hosei.ac.jp/pdb/images/chlorophyta/Kirchneriella/sp_03.html>.

Tsukii Y 1977, ‘*Monoraphidium sp.*’ [image], *Illustrations of The Japanese Fresh-water Algae*, Protist Information Server, viewed 24 September 2015, <http://protist.i.hosei.ac.jp/pdb/images/chlorophyta/Monoraphidium/contortum/sp_02.html>.

Tsukii Y 1977, '*Scendesmus abundans'* [image], *Illustrations of The Japanese Fresh-water Algae*, Protist Information Server, viewed 24 September 2015, <http://protist.i.hosei.ac.jp/pdb/images/chlorophyta/scenedesmus/abundans/index.html>
.
Tsukii Y 1977, '*Scendesmus acutus'* [image], *Illustrations of The Japanese Fresh-water Algae*, Protist Information Server, viewed 24 September 2015, <http://protist.i.hosei.ac.jp/PDB4/PCD3221/D/52.jpg>.

Tsukii Y 1977, '*Scenedesmus acuminatus'* [image], *Illustrations of The Japanese Fresh-water Algae*, Protist Information Server, viewed 24 September 2015, <http://protist.i.hosei.ac.jp/pdb/images/chlorophyta/scenedesmus/acuminatus/sp_09.html>.

Tsukii Y 1977, '*Scenedesmus incrassatulus'* [image], *Illustrations of The Japanese Fresh-water Algae*, Protist Information Server, viewed 24 September 2015, <http://protist.i.hosei.ac.jp/pdb/images/Chlorophyta/Scenedesmus/incrassatulus/incrassatulus4.html>.

Urbani NC 2013, '*Scenedesmus obliquus'* [image], *Haematococcus pluvialis Astaxanthin Rich Resting Spores and Scenedesmus obliquus in an Algal Biodiversity Pond*, Labroots.com, viewed 15 May 2015, <http://legacy.labroots.com/public/files/entry/Haematococcus_pluvialisAstaxanthinRichRestingSporesScenedesmus_obliquusAlgalBiodiversityInPondSSQ2013IV13_IMG_3025.JPG>.

Yamagishi T 1998, *'Ankistrodesmus gracilis'* [image], *Guide book to Photomicrographs of the freshwater algae*, Protist Information Server, viewed 7 May 2015,
<http://protist.i.hosei.ac.jp/pdb/images/chlorophyta/Ankistrodesmus/densus/sp_04.jpg>.

Appendix

Table 55: Dry mass of FSA

	0x	1x	5x	10x
1	0.0012	0.0023	0.0030	0.0025
2	0.0014	0.0027	0.0029	0.0029
3	0.0012	0.0035	0.0035	0.0037
Average	0.0013	0.0029	0.0031	0.0030

Table 56: Dry mass of FSB

	0x	1x	5x	10x
1	0.0002	0.0002	0.0003	0.0003
2	0.0002	0.0003	0.0005	0.0003
3	0.0001	0.0004	0.0005	0.0003
Average	0.0002	0.0003	0.0004	0.0003

Table 57: Dry mass of FSD

	0x	1x	5x	10x
1	0.0084	0.0182	0.0188	0.0247
2	0.0089	0.0296	0.0292	0.0259
3	0.0096	0.0360	0.0311	0.0332
Average	0.0090	0.0280	0.0264	0.0280

Table 58: Dry mass of FSE

	0x	1x	5x	10x
1	0.0029	0.0035	0.0038	0.0039
2	0.0031	0.0049	0.0049	0.0061
3	0.0039	0.01	0.0107	0.0102
Average	0.0033	0.00613	0.00647	0.00673

Table 59: Dry mass of FBP1

	0x	1x	5x	10x
1	0.0021	0.0077	0.0078	0.0081
2	0.0027	0.0079	0.0078	0.0073
3	0.0030	0.0071	0.0064	0.0070
Average	0.0026	0.0076	0.0073	0.0075

Table 60: Dry mass of FBP2

	0x	1x	5x	10x
1	0.0006	0.0013	0.0015	0.0009
2	0.0007	0.0027	0.0014	0.0024
3	0.0007	0.0022	0.0030	0.0016
Average	0.0006	0.0021	0.0019	0.0016

Table 61: Dry mass of FBP3

	0x	1x	5x	10x
1	0.0001	0.0008	0.0003	0.0013
2	0.0001	0.0006	0.0011	0.0004
3	0.0001	0.0005	0.0010	0.0006
Average	0.0001	0.0006	0.0008	0.0008

Table 62: Dry mass of FTA1

	0x	1x	5x	10x
1	0.0008	0.0010	0.0011	0.0012
2	0.0007	0.0012	0.0012	0.0016
3	0.0009	0.0014	0.0020	0.0020
Average	0.0008	0.0012	0.0014	0.0016

Table 63: Dry mass of FTA2

	0x	1x	5x	10x
1	0.001816	0.006227	0.006602	0.006621
2	0.002068	0.008397	0.007923	0.004535
3	0.002169	0.009225	0.008431	0.006484
Average	0.002018	0.00795	0.007652	0.00588

Table 64: Dry mass of MTA1

	0x	1x	5x	10x
1	0.0429	0.0453	0.0457	0.0548
2	0.0454	0.0465	0.0446	0.0554
3	0.0436	0.0462	0.0476	0.0552
Average	0.04397	0.046	0.04597	0.05513

Table 65: Dry mass of MTA2

	0x	1x	5x	10x
1	0.0343	0.0354	0.0378	0.0391
2	0.0366	0.0367	0.0385	0.0379
3	0.0344	0.0352	0.0374	0.0387
Average	0.0351	0.03577	0.0379	0.03857

Table 66: Dry mass of FTAR

	0x	1x	5x	10x
1	0.0004	0.0012	0.0008	0.0010
2	0.0004	0.0012	0.0012	0.0013
3	0.0004	0.0017	0.0014	0.0014
Average	0.00043	0.00135	0.00115	0.00124

Table 67: Dry mass of FTAR2

	0x	1x	5x	10x
1	0.0013	0.0028	0.0032	0.0020
2	0.0015	0.0059	0.0030	0.0052
3	0.0014	0.0048	0.0065	0.0034
Average	0.0014	0.0045	0.0042	0.0035

Table 68: Dry mass of FTAR3

	0x	1x	5x	10x
1	0.0008	0.0034	0.0032	0.0014
2	0.0008	0.0023	0.0018	0.0019
3	0.0008	0.0011	0.0015	0.0041
Average	0.0008	0.0023	0.0022	0.0025

Table 69: Dry mass of MTAR

	0x	1x	5x	10x
1	0.1337	0.1512	0.1355	0.2031
2	0.1342	0.1488	0.1344	0.1872
3	0.1318	0.1503	0.1365	0.1943
Average	0.13323	0.1501	0.13547	0.19487

Table 70: Dry mass of FDP

	0x	1x	5x	10x
1	0.0013	0.0029	0.0035	0.0038
2	0.0014	0.0032	0.0039	0.0037
3	0.0014	0.0029	0.0038	0.0038
Average	0.0014	0.0030	0.0037	0.0038

FSA

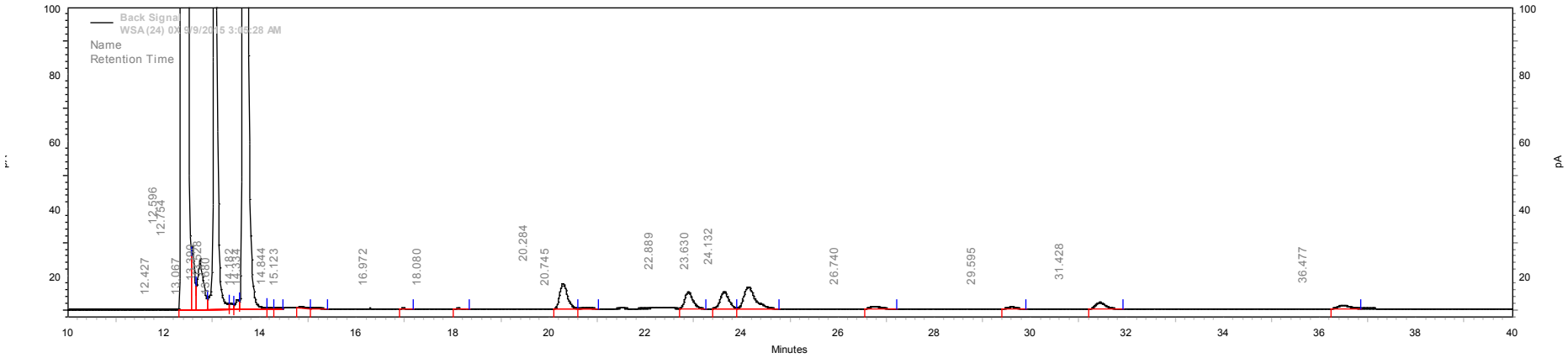

Figure 69: FSA FAME sample (0x) chromatograph

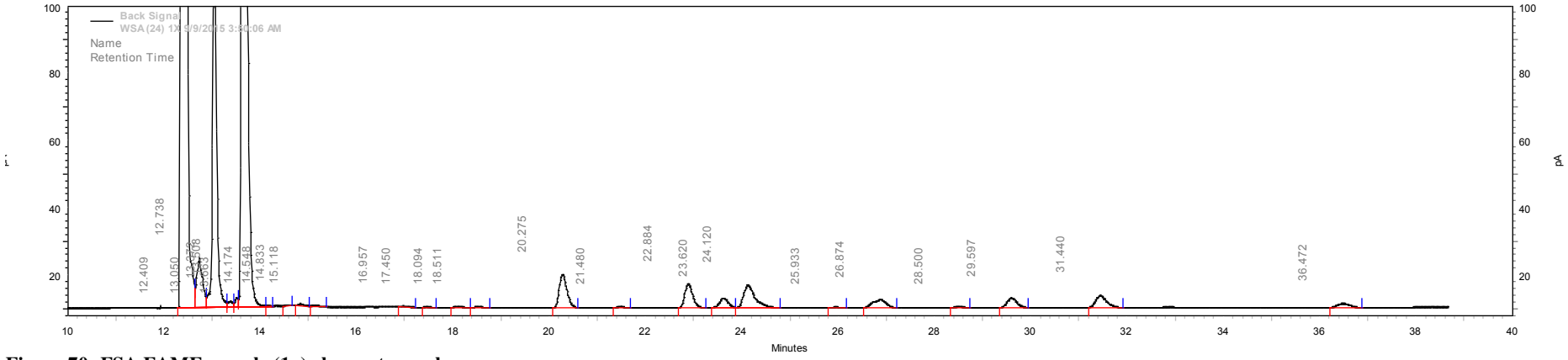

Figure 70: FSA FAME sample (1x) chromatograph

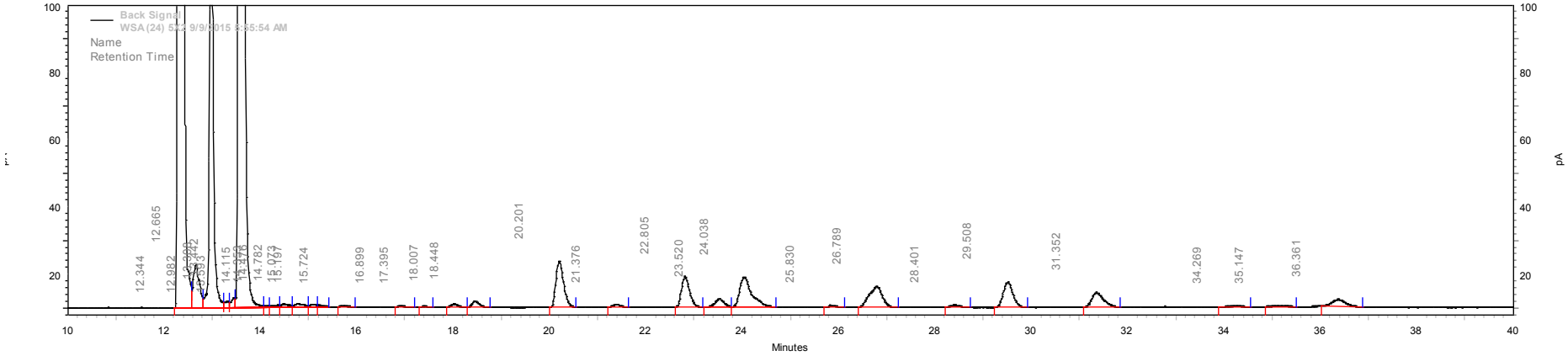

Figure 71: FSA FAME sample (5x) chromatograph

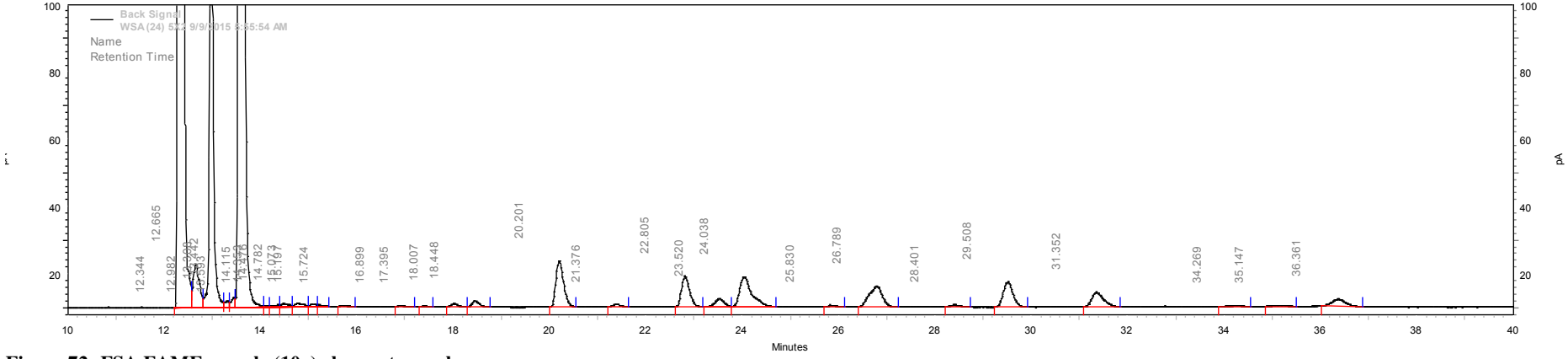

Figure 72: FSA FAME sample (10x) chromatograph

FSB

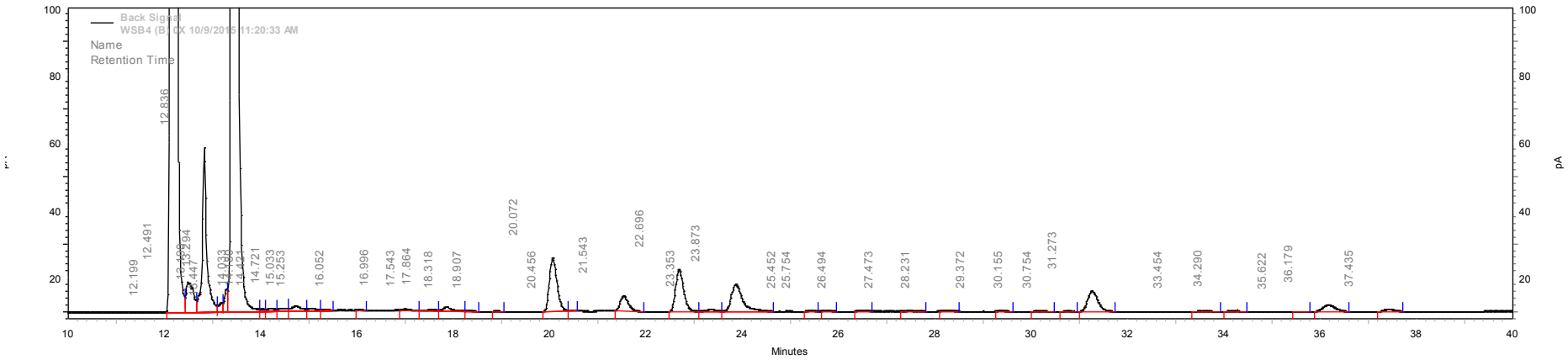

Figure 73: FSB FAME sample (0x) chromatograph

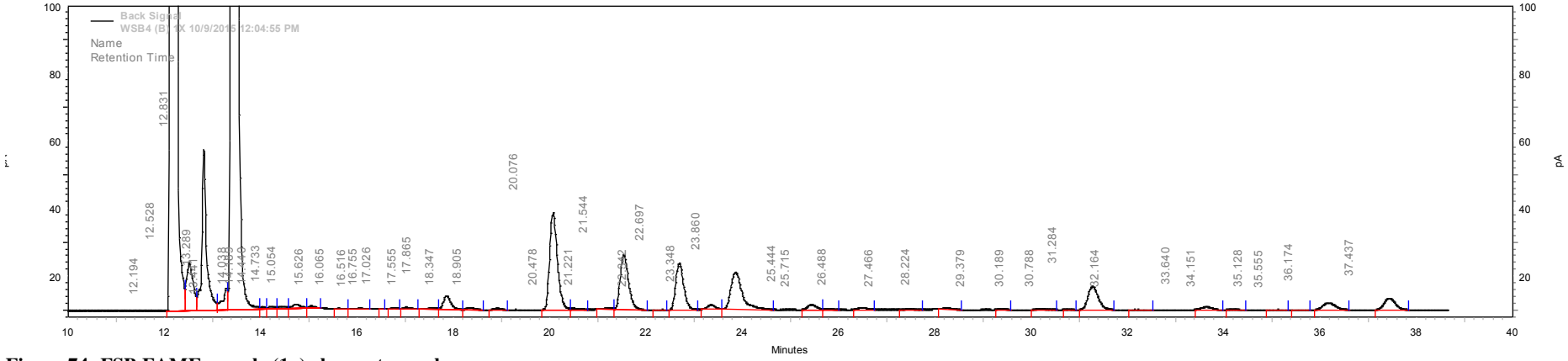

Figure 74: FSB FAME sample (1x) chromatograph

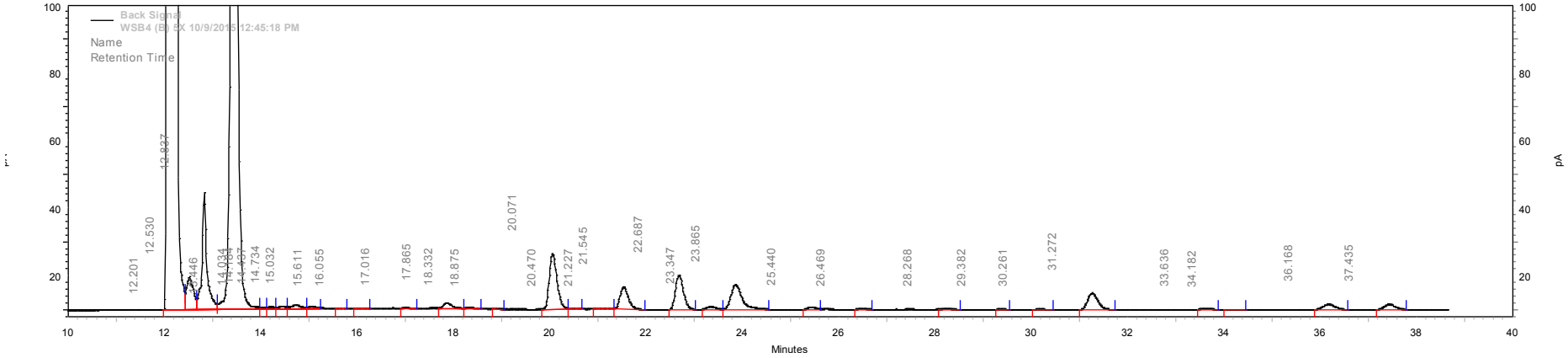

Figure 75: FSB FAME sample (5x) chromatograph

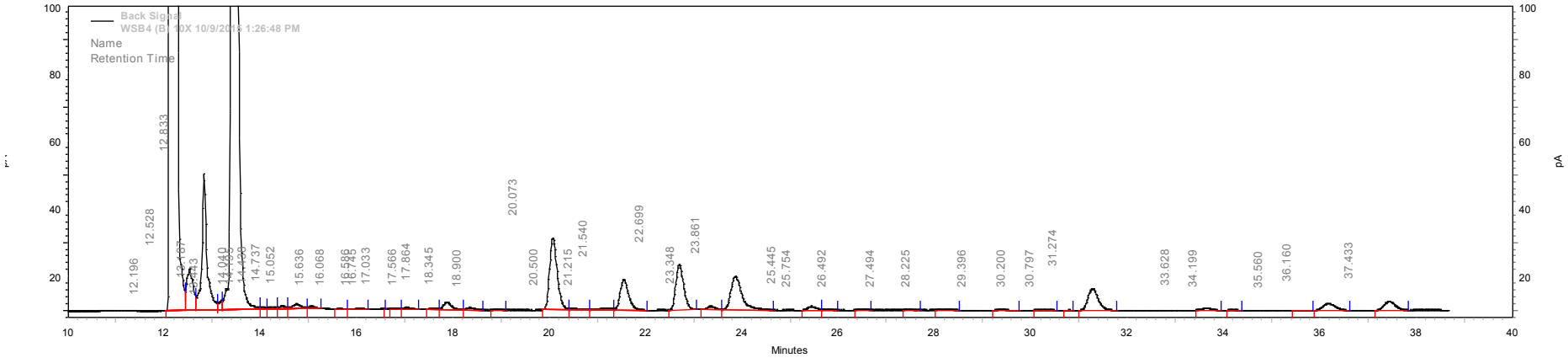

Figure 76: FSB FAME sample (10x) chromatograph

FSD

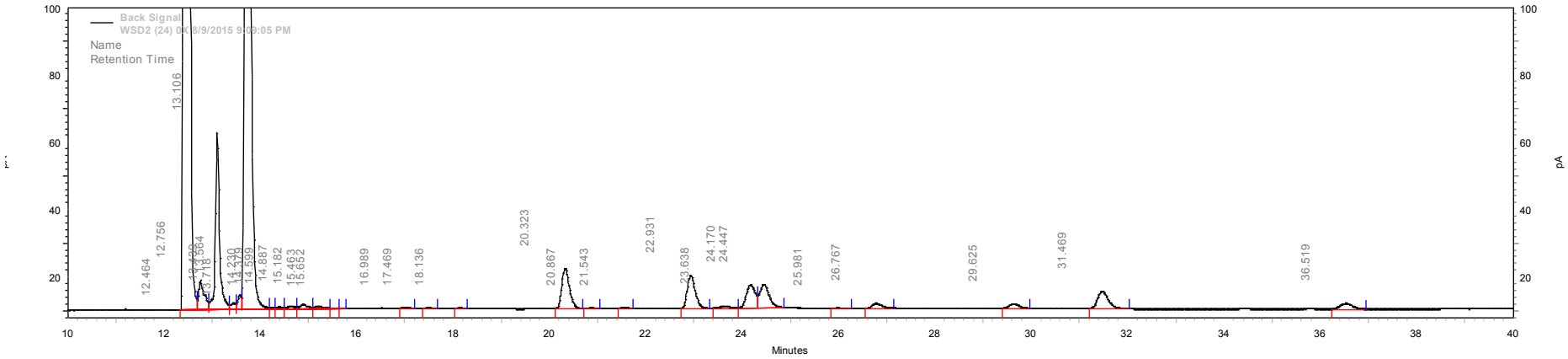

Figure 77: FSD FAME sample (0x) chromatograph

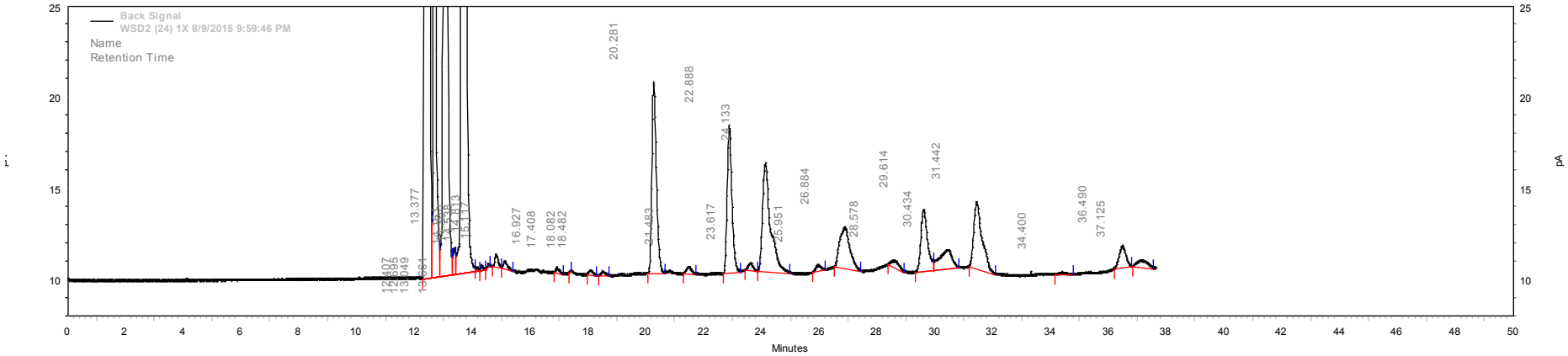

Figure 78: FSD FAME sample (1x) chromatograph

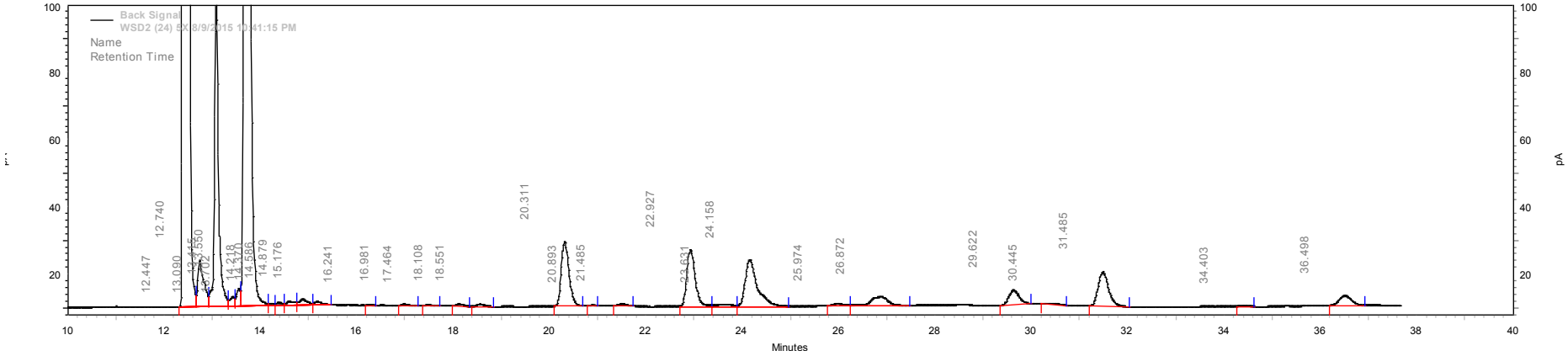

Figure 79: FSD FAME sample (5x) chromatograph

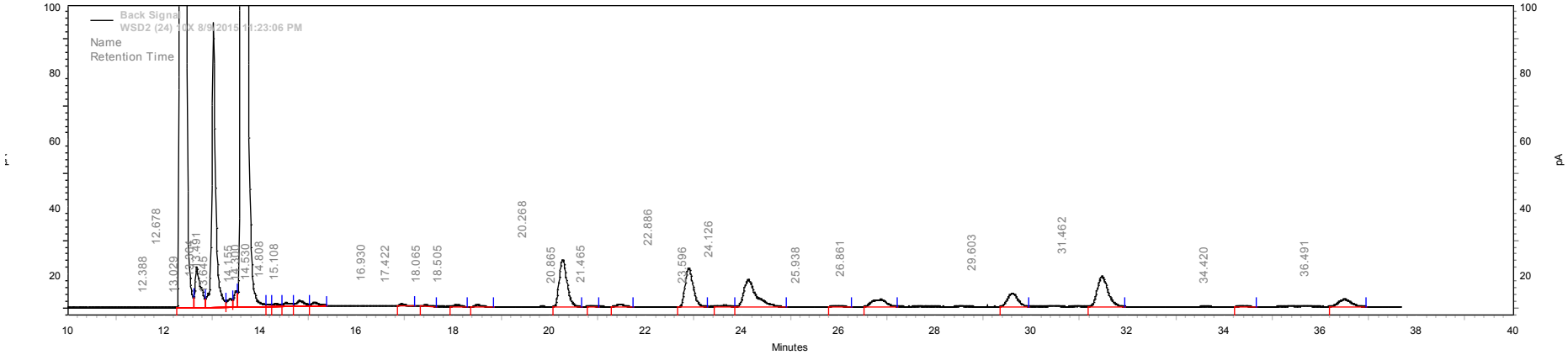

Figure 80: FSD FAME sample (10x) chromatograph

FSE

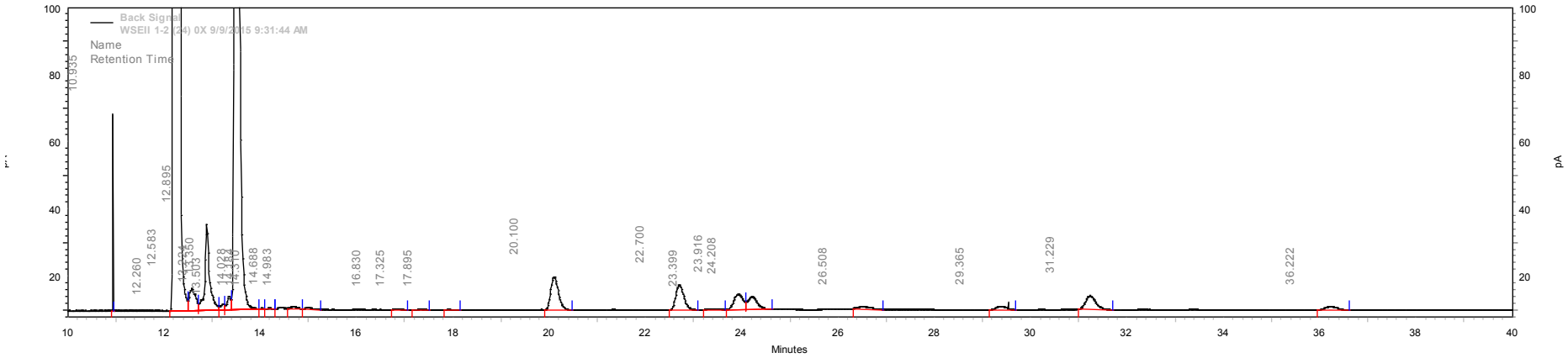

Figure 81: FSE FAME sample (0x) chromatograph

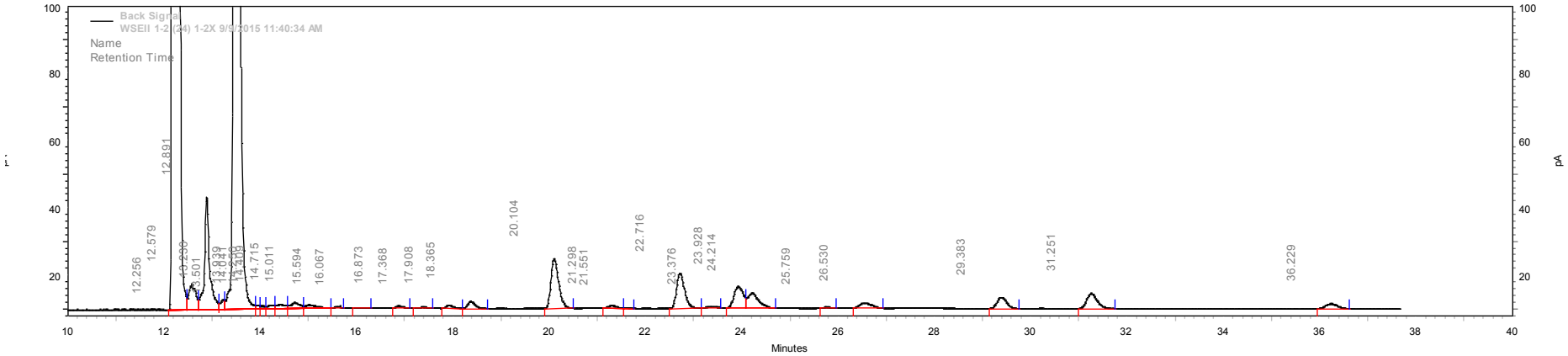

Figure 82: FSE FAME sample (1x) chromatograph

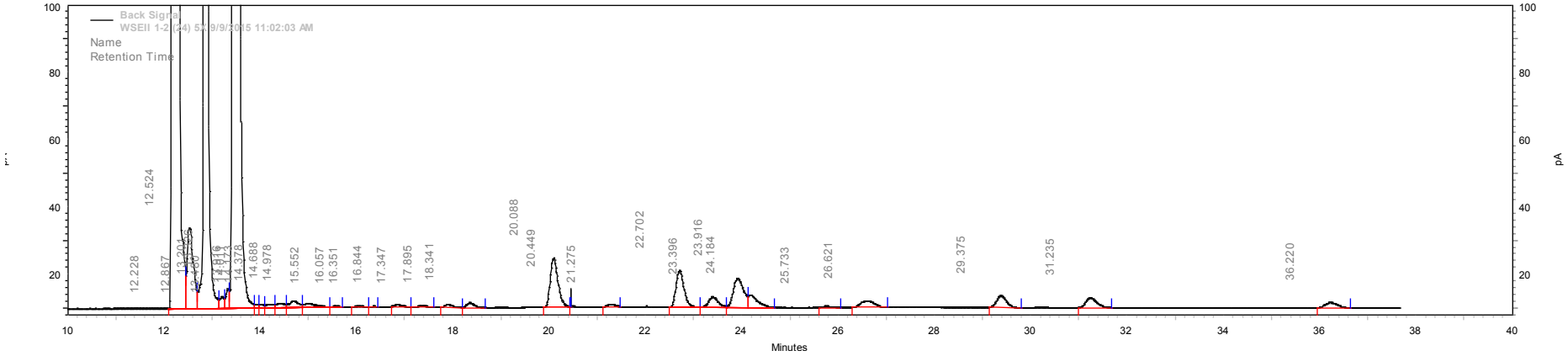

Figure 83: FSE FAME sample (5x) chromatograph

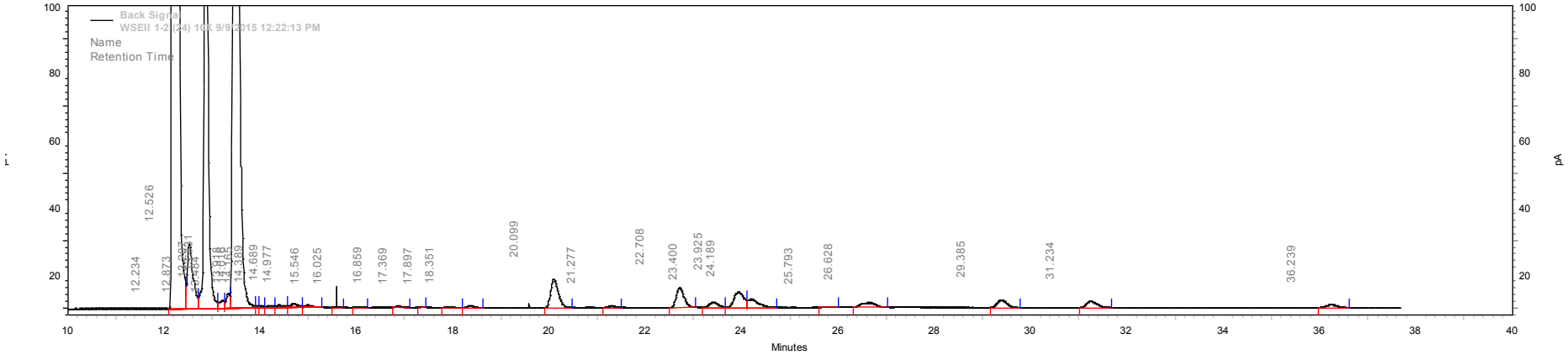

Figure 84: FSE FAME sample (10x) chromatograph

FBP1

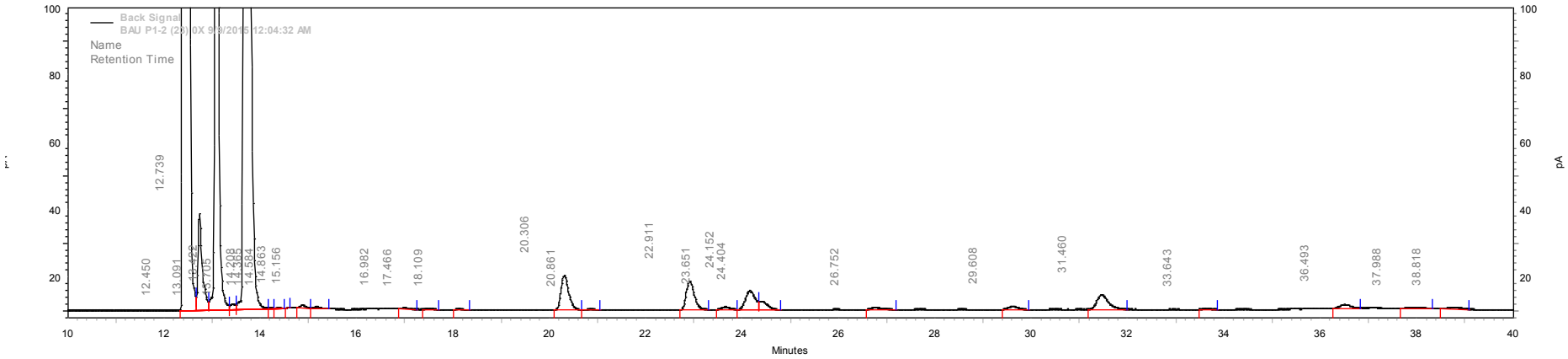

Figure 85: FBP1 FAME sample (0x) chromatograph

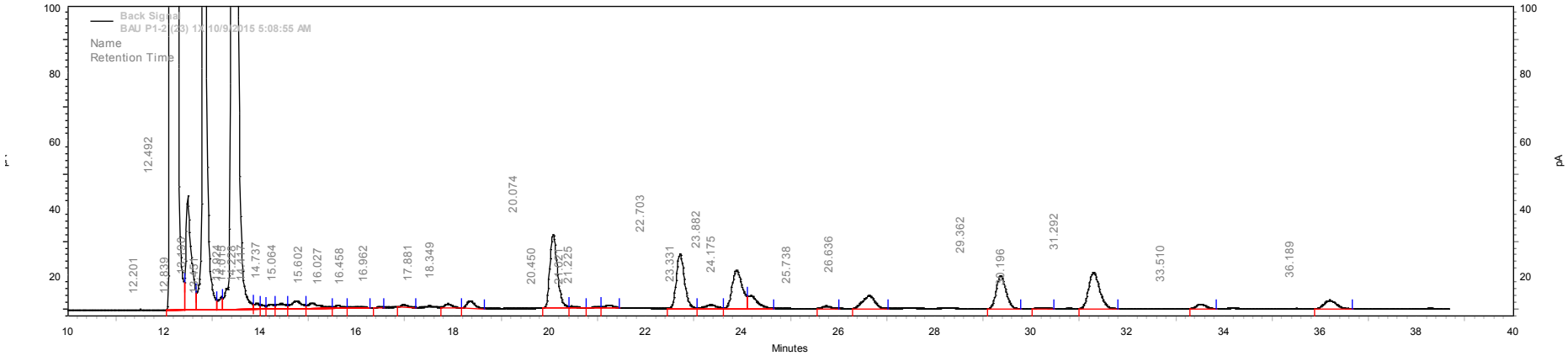

Figure 86: FBP1 FAME sample (1x) chromatograph

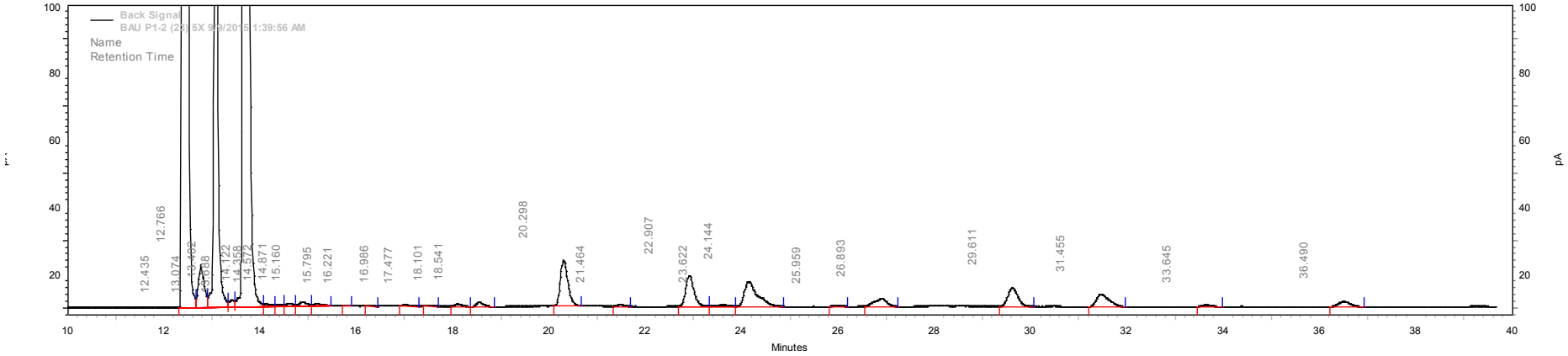

Figure 87: FBP1 FAME sample (5x) chromatograph

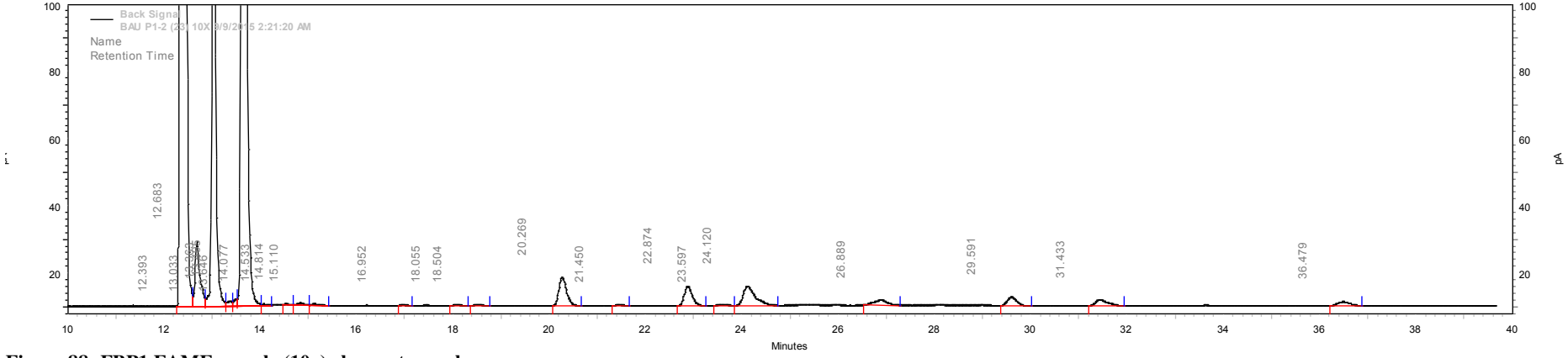

Figure 88: FBP1 FAME sample (10x) chromatograph

FBP2

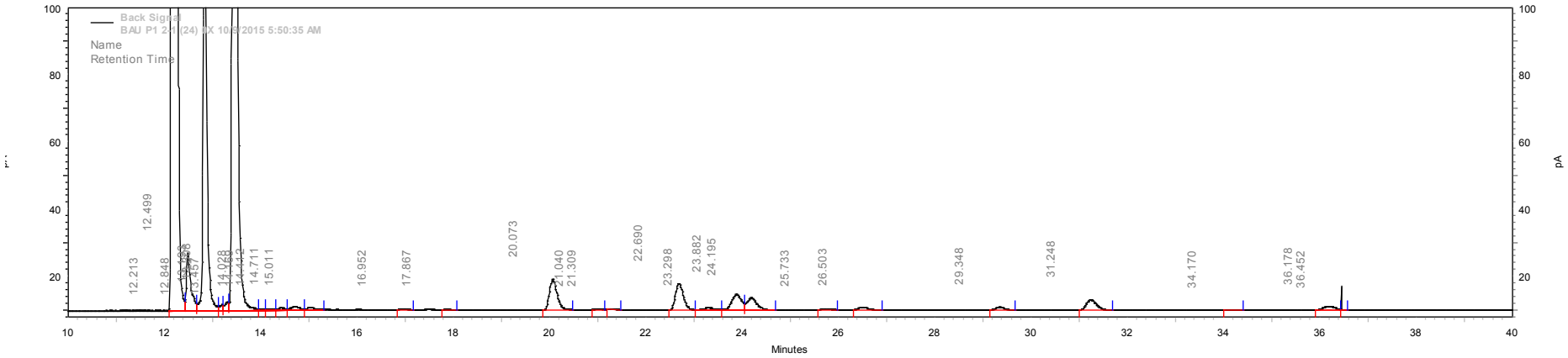

Figure 89: FBP2 FAME sample (0x) chromatograph

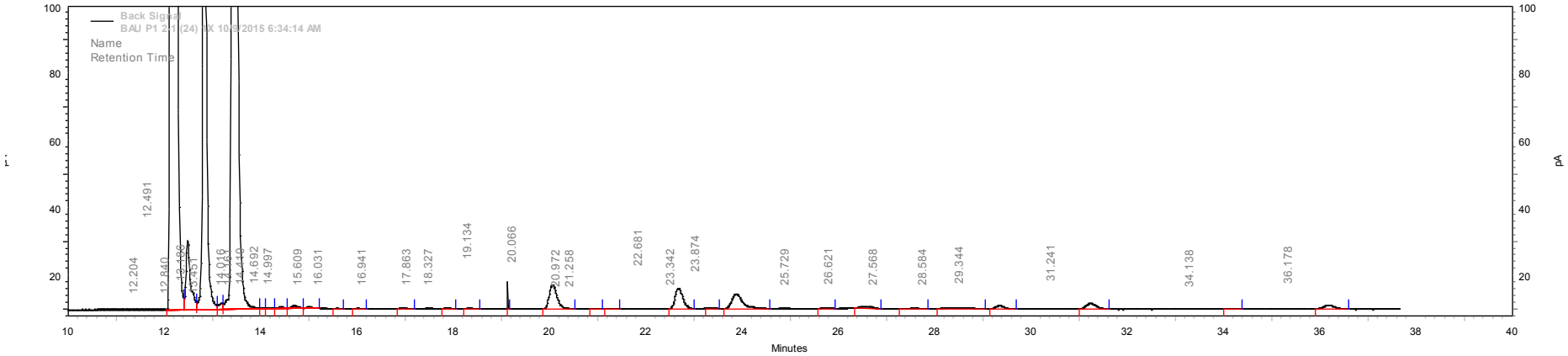

Figure 90: FBP2 FAME sample (1x) chromatograph

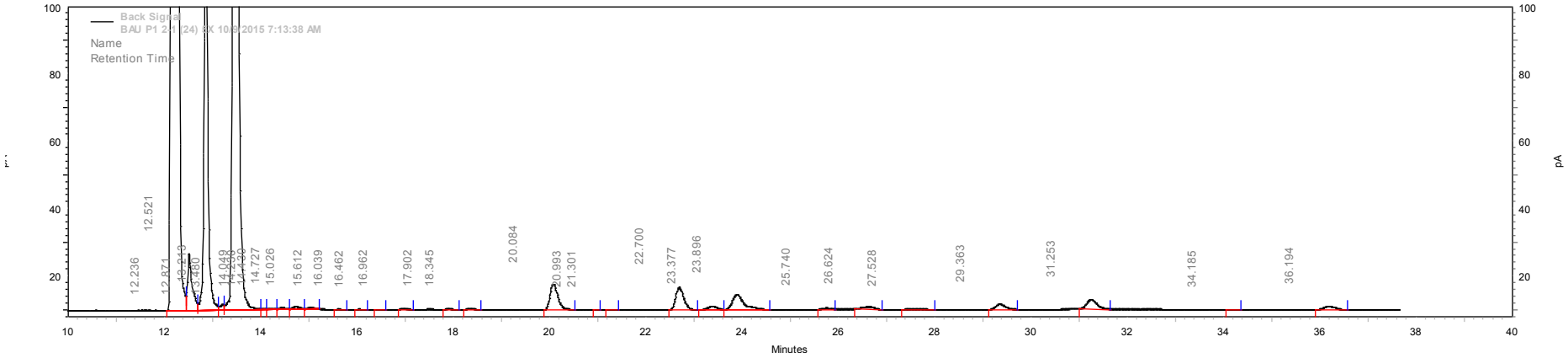

Figure 91: FBP2 FAME sample (5x) chromatograph

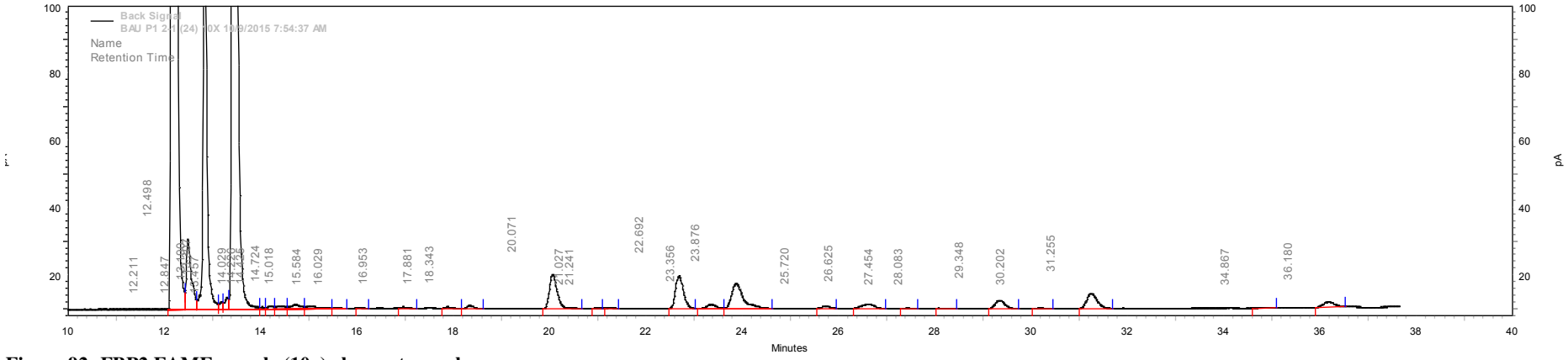

Figure 92: FBP2 FAME sample (10x) chromatograph

FBP3

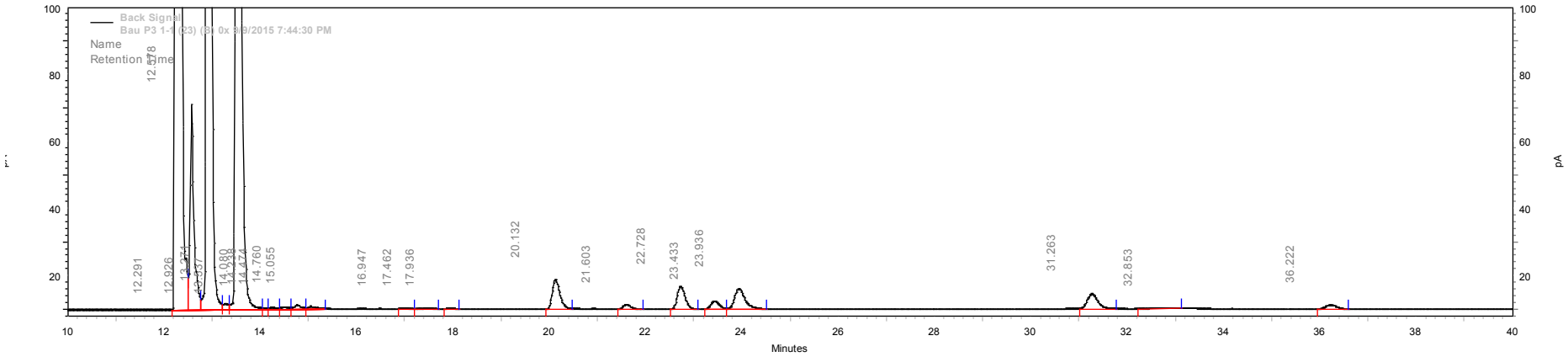

Figure 93: FBP3 FAME sample (0x) chromatograph

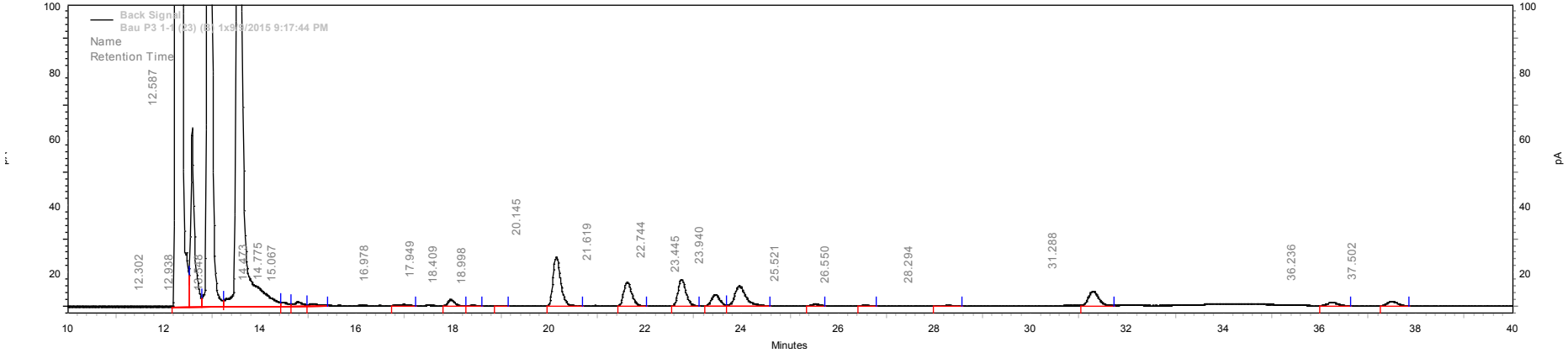

Figure 94: FBP3 FAME sample (1x) chromatograph

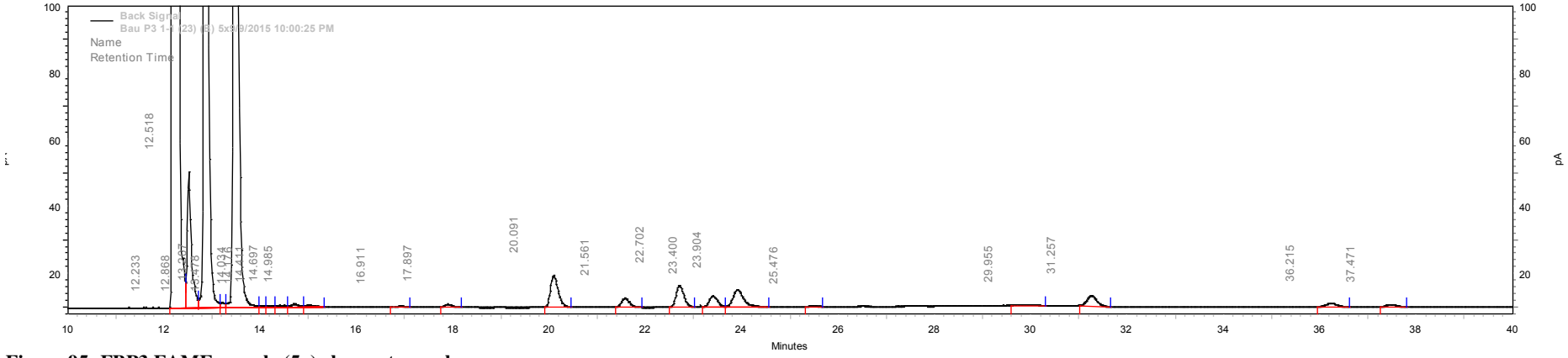

Figure 95: FBP3 FAME sample (5x) chromatograph

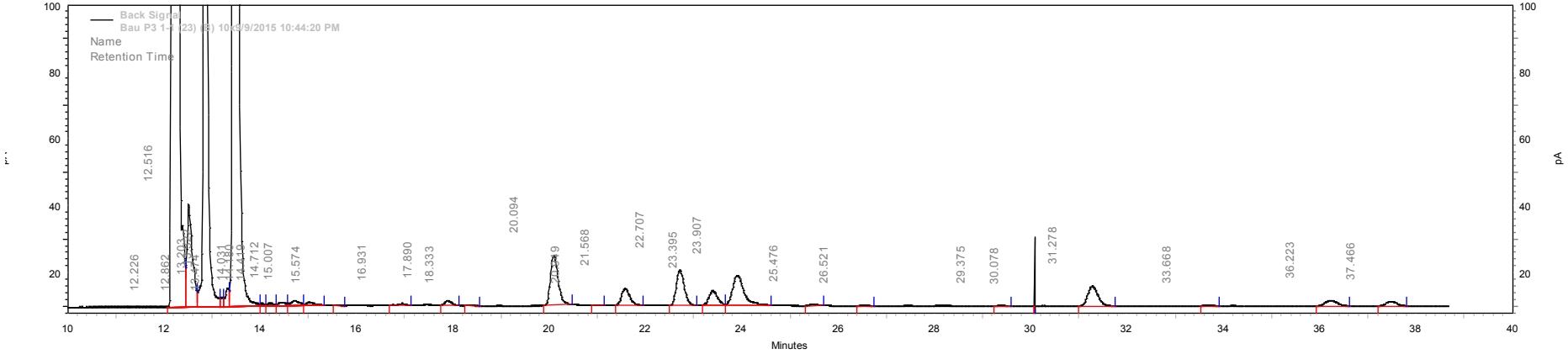

Figure 96: FBP3 FAME sample (10x) chromatograph

FTA1

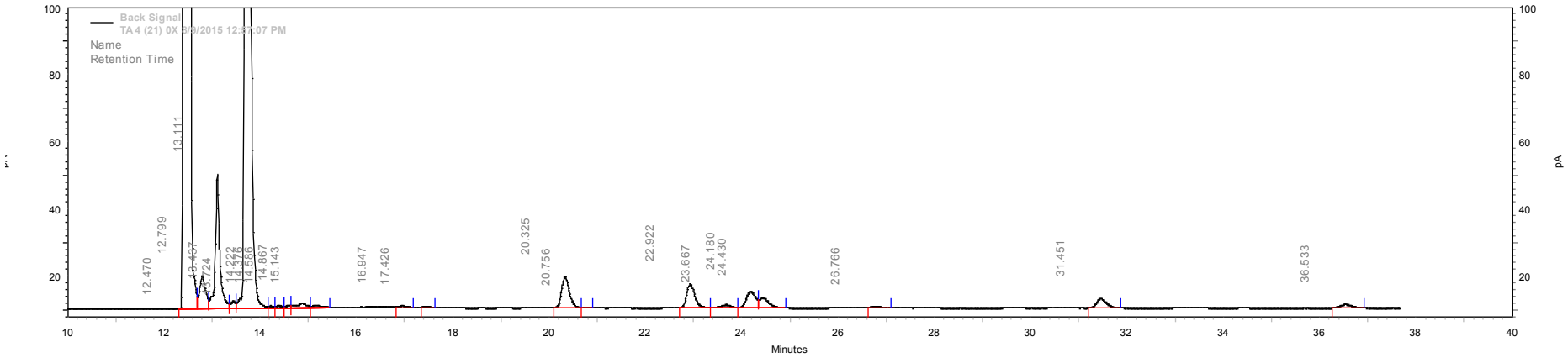

Figure 97: FTA1 FAME sample (0x) chromatograph

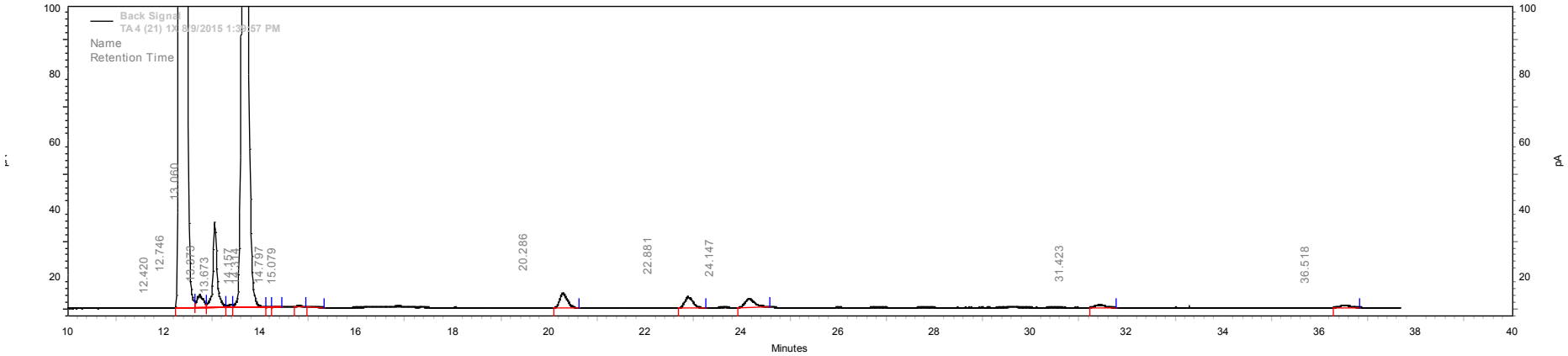

Figure 98: FTA1 FAME sample (1x) chromatograph

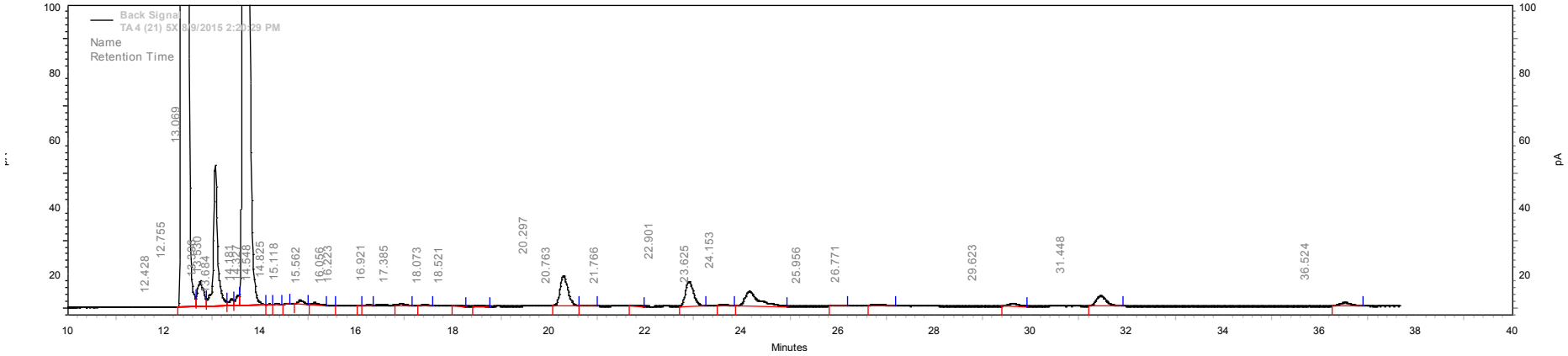

Figure 99: FTA1 FAME sample (5x) chromatograph

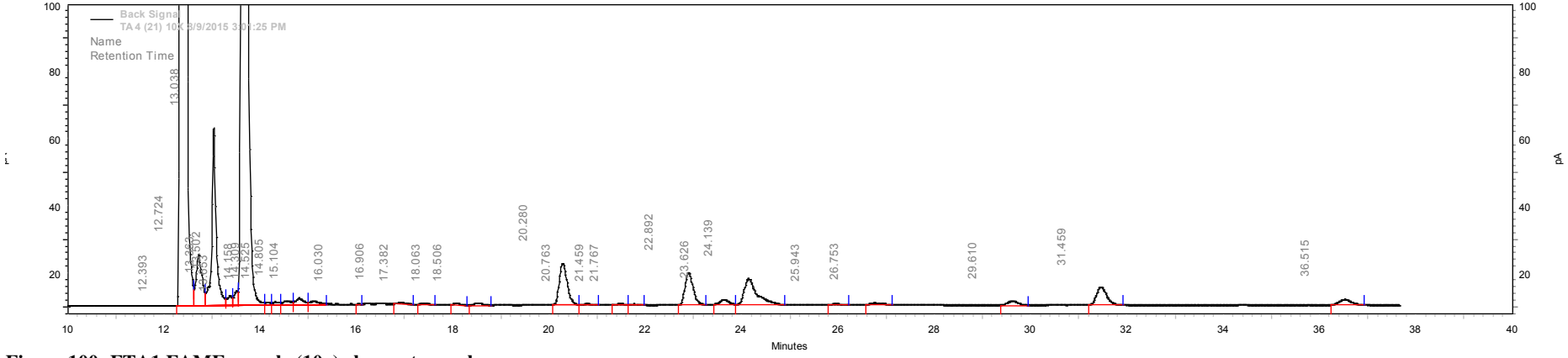

Figure 100: FTA1 FAME sample (10x) chromatograph

FTA2

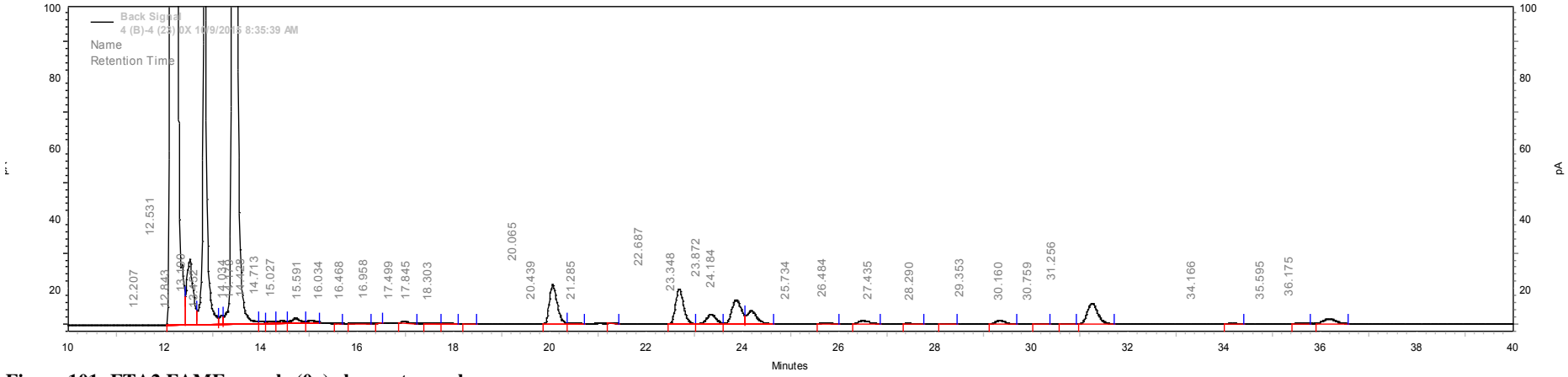

Figure 101: FTA2 FAME sample (0x) chromatograph

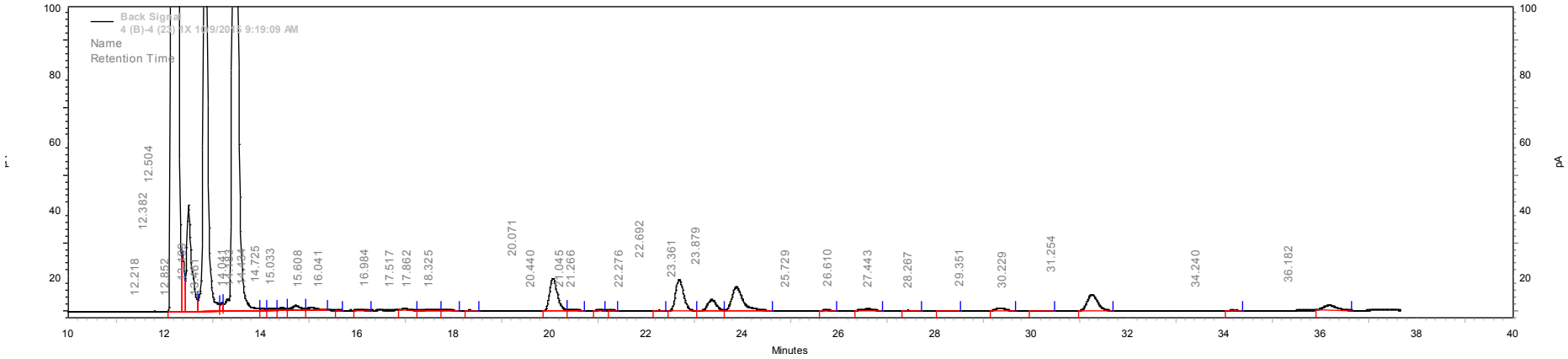

Figure 102: FTA2 FAME sample (1x) chromatograph

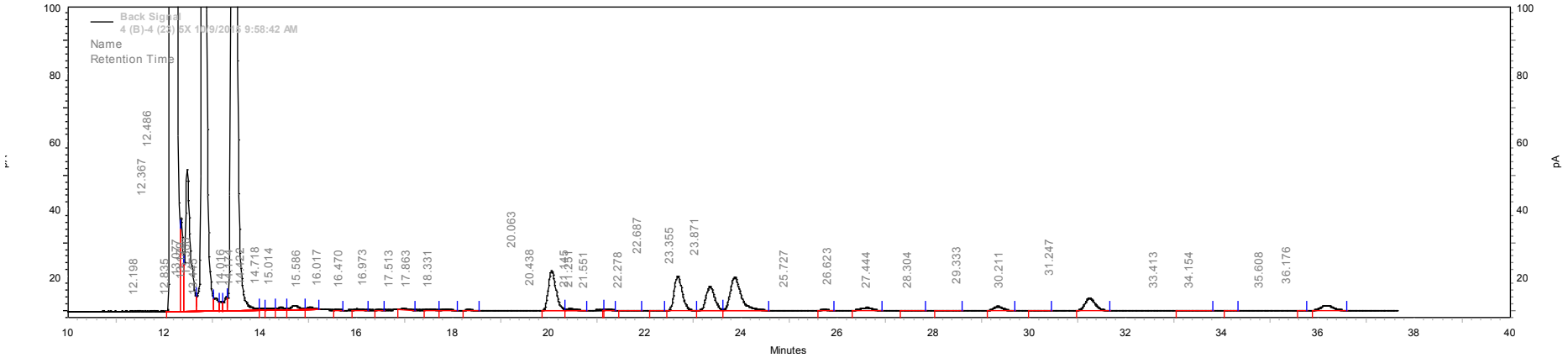

Figure 103: FTA2 FAME sample (5x) chromatograph

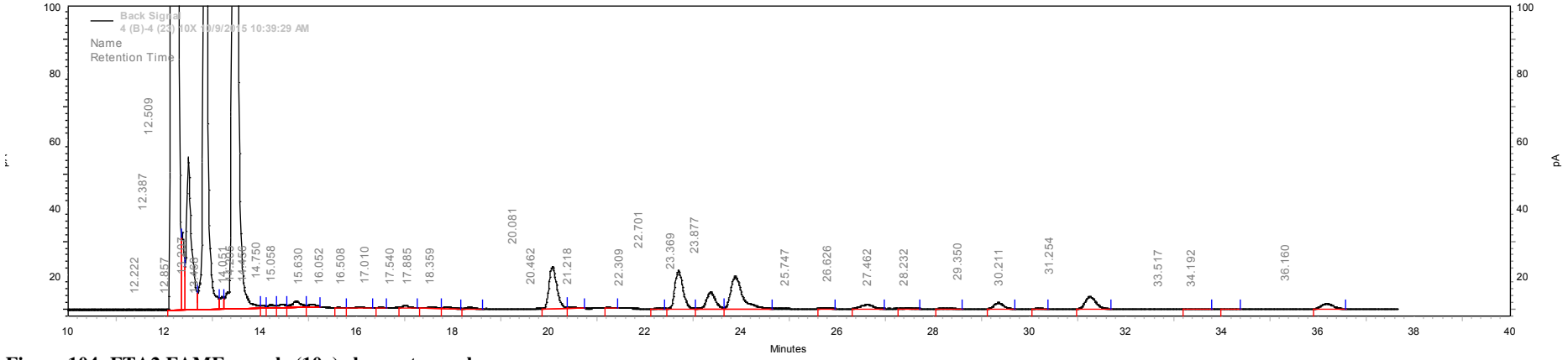

Figure 104: FTA2 FAME sample (10x) chromatograph

MTA1

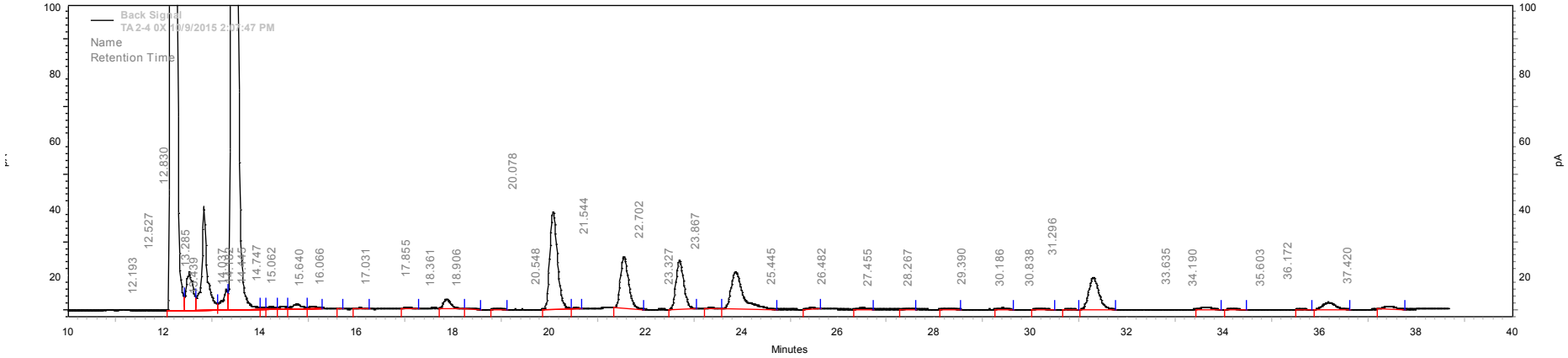

Figure 105: MTA1 FAME sample (0x) chromatograph

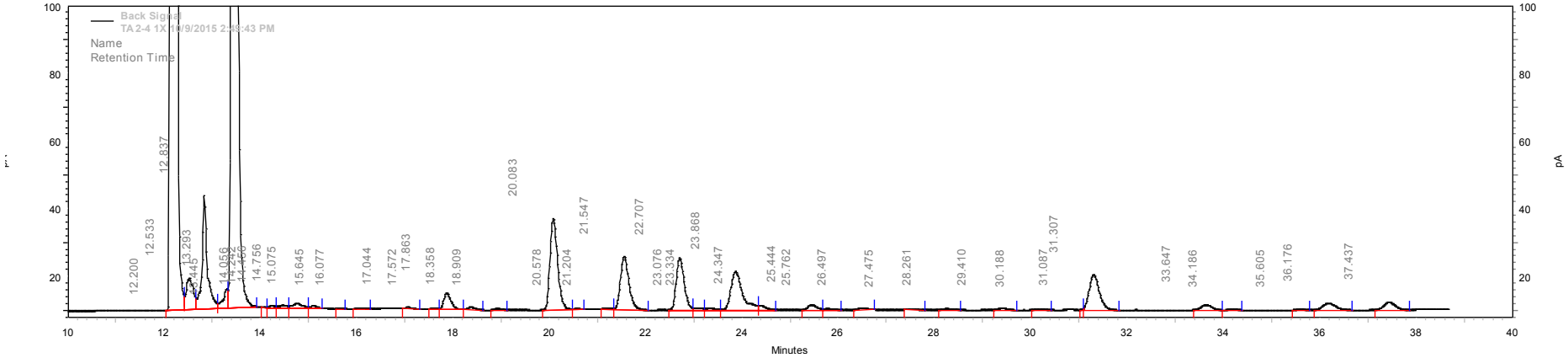

Figure 106: MTA1 FAME sample (1x) chromatograph

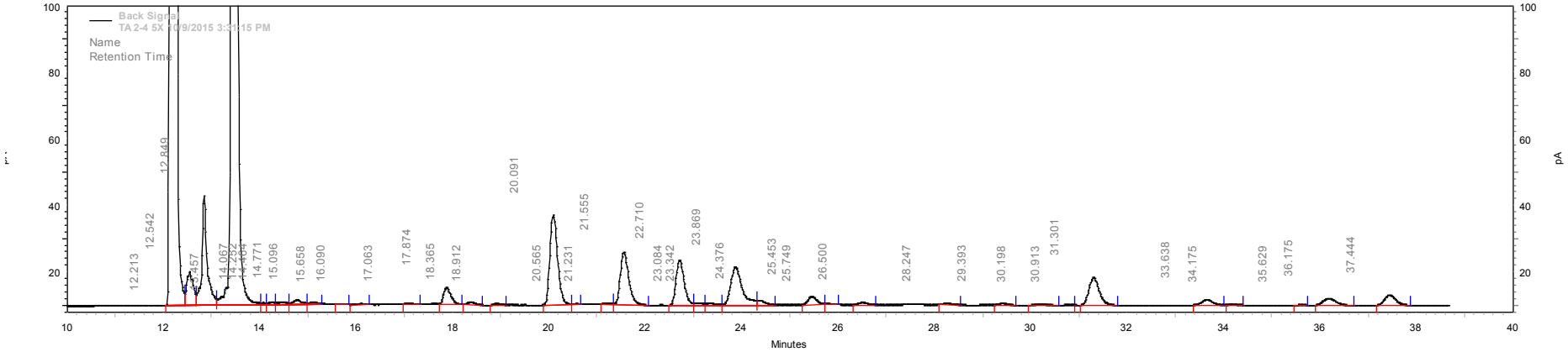

Figure 107: MTA1 FAME sample (5x) chromatograph

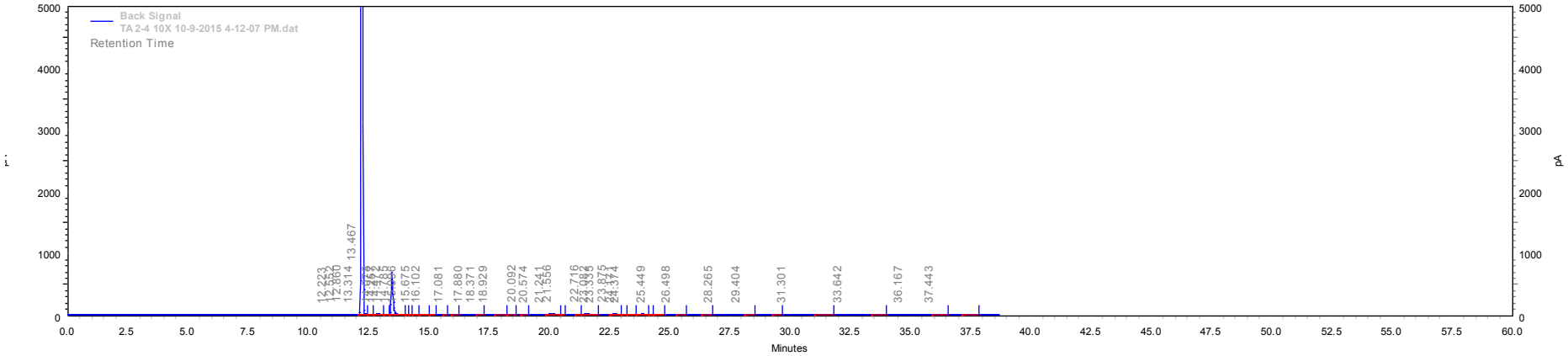

Figure 108: MTA1 FAME sample (10x) chromatograph

MTA2

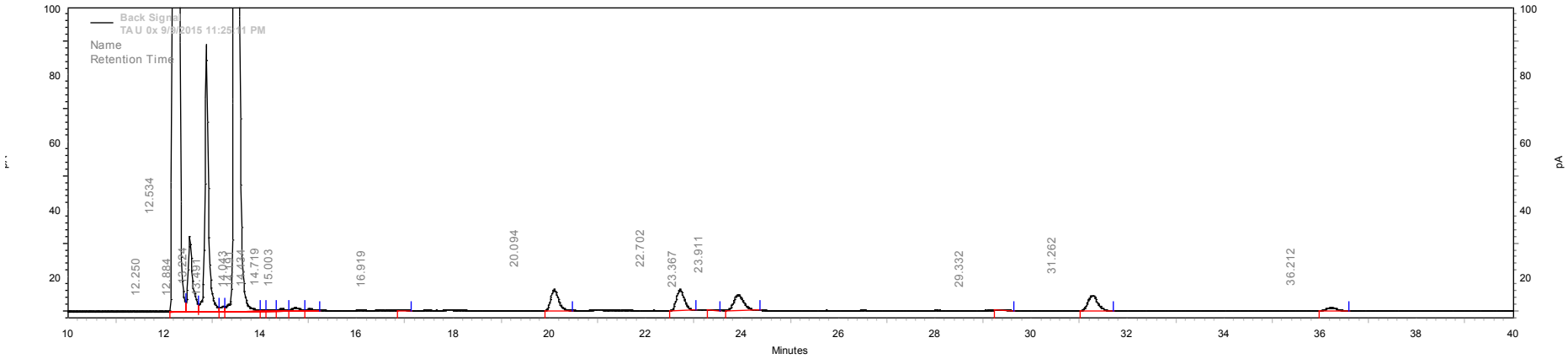

Figure 109: MTA2 FAME sample (0x) chromatograph

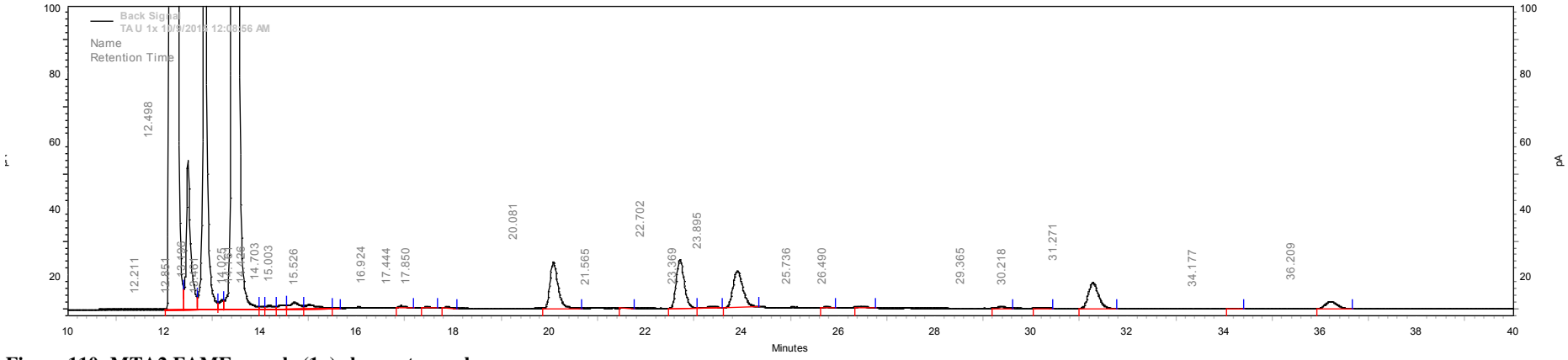

Figure 110: MTA2 FAME sample (1x) chromatograph

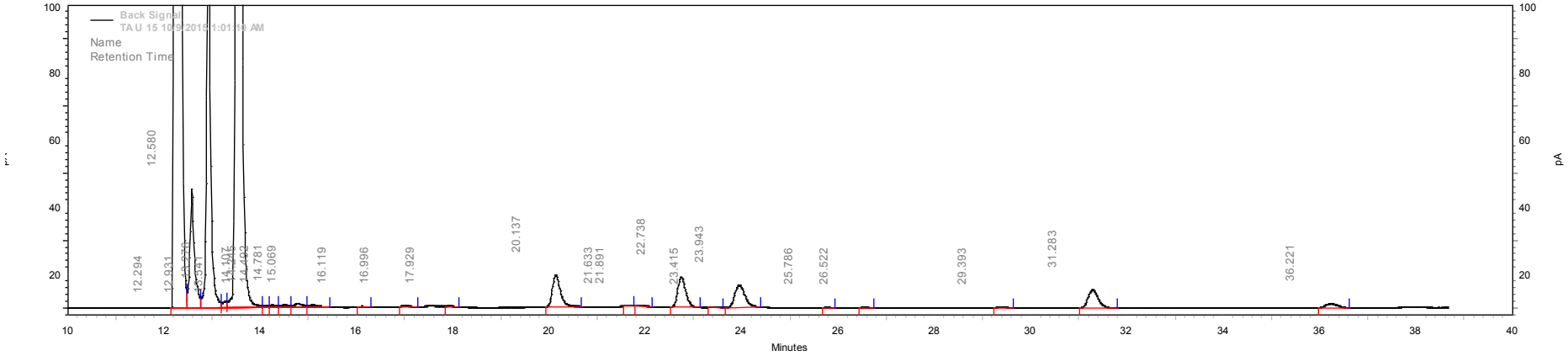

Figure 111: MTA2 FAME sample (5x) chromatograph

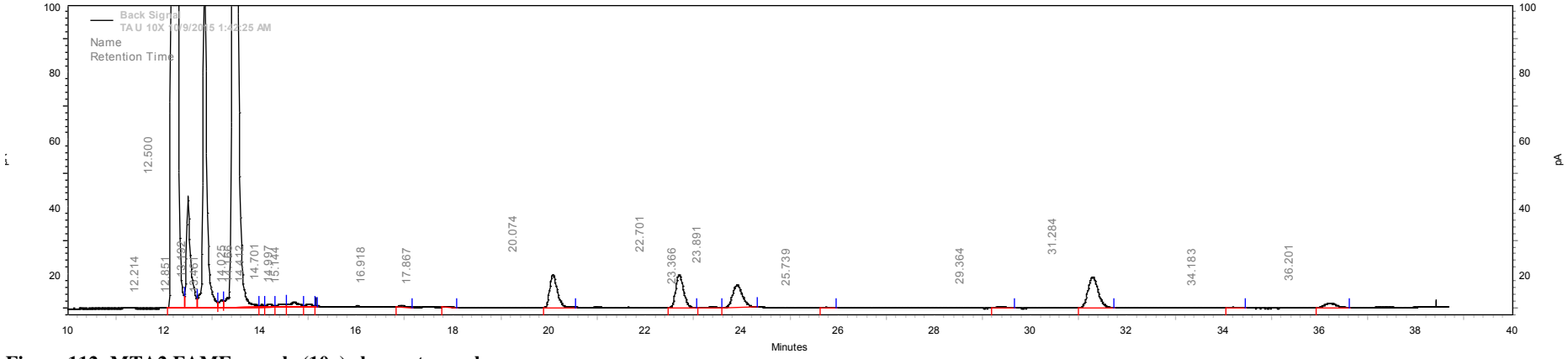

Figure 112: MTA2 FAME sample (10x) chromatograph

FTAR

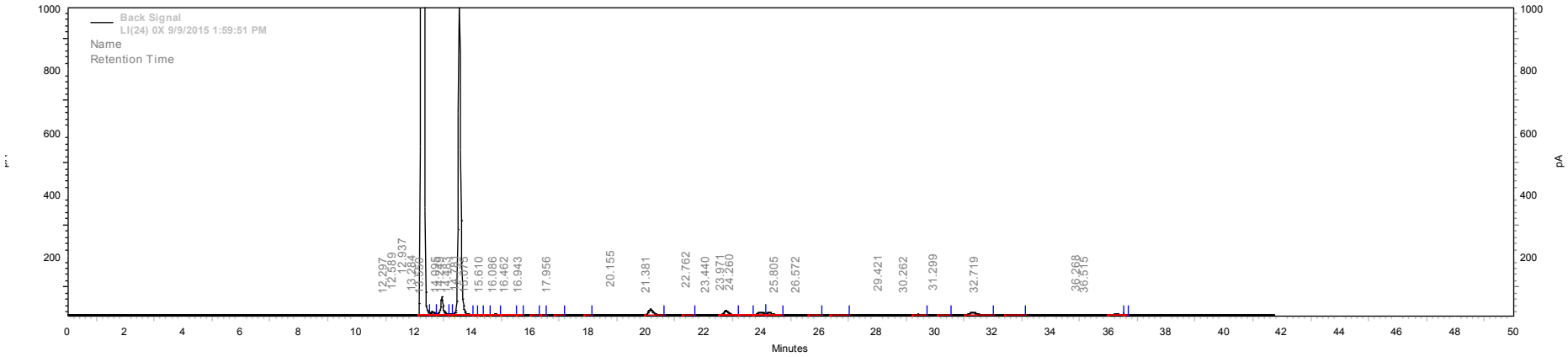

Figure 113: FTAR FAME sample (0x) chromatograph

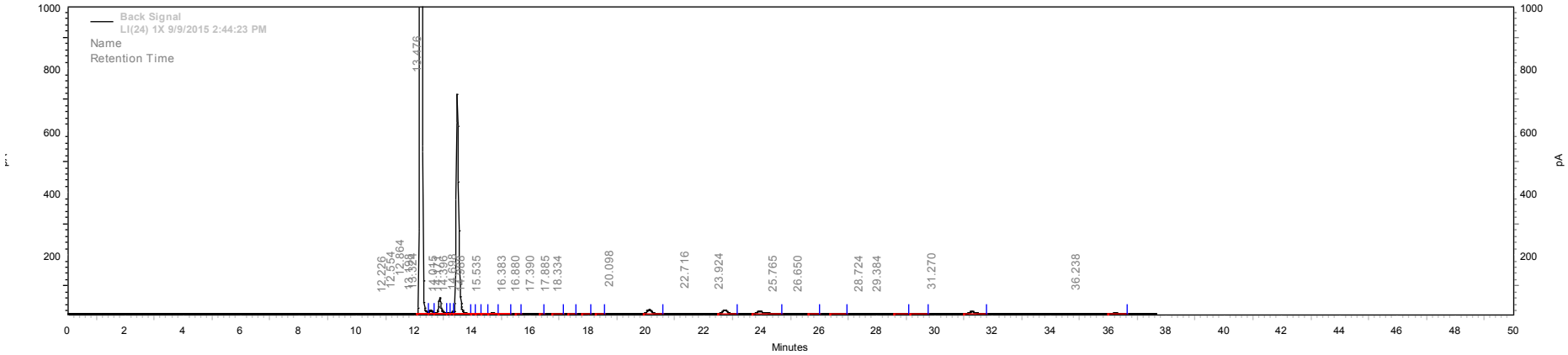

Figure 114: FTAR FAME sample (1x) chromatograph

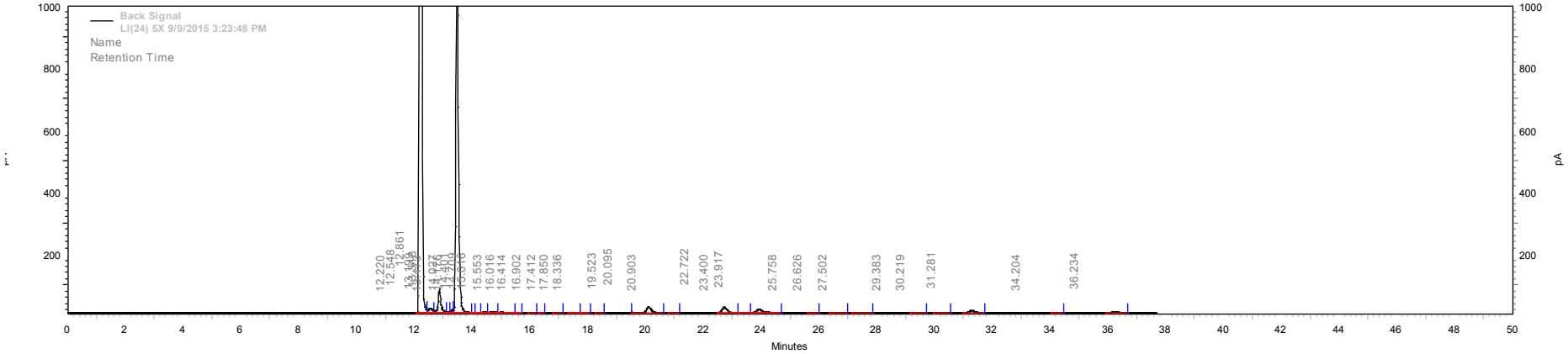

Figure 115: FTAR FAME sample (5x) chromatograph

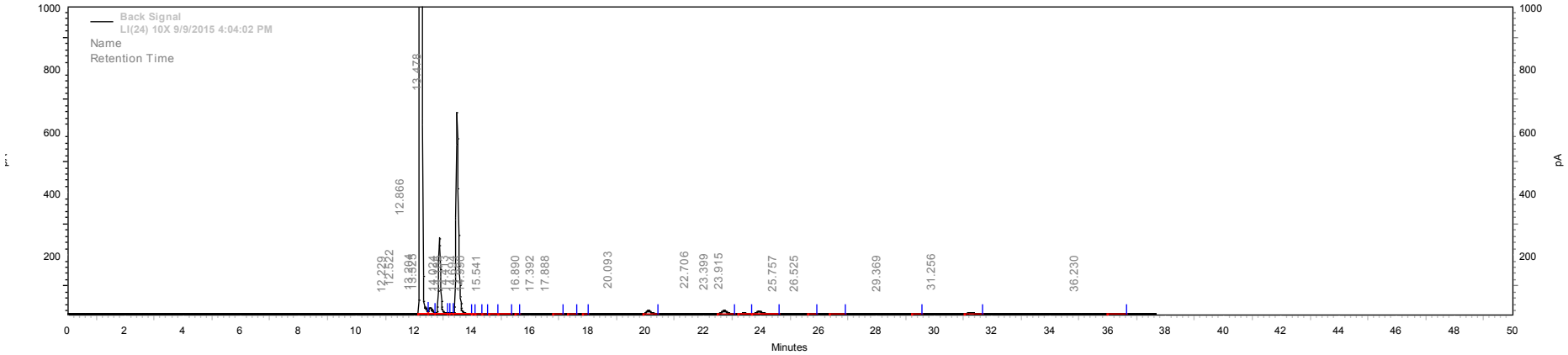

Figure 116: FTAR FAME sample (10x) chromatograph

FTAR2

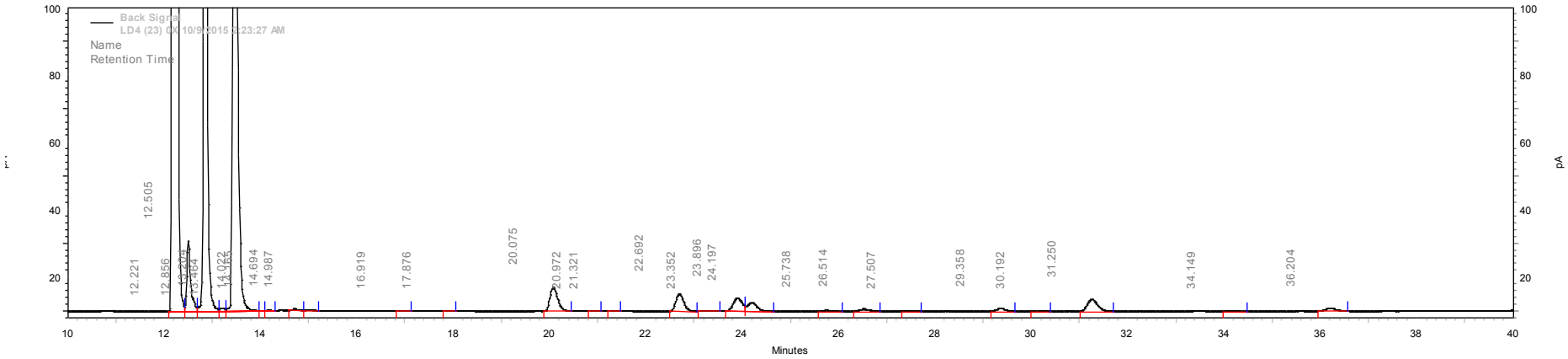

Figure 117: FTAR2 FAME sample (0x) chromatograph

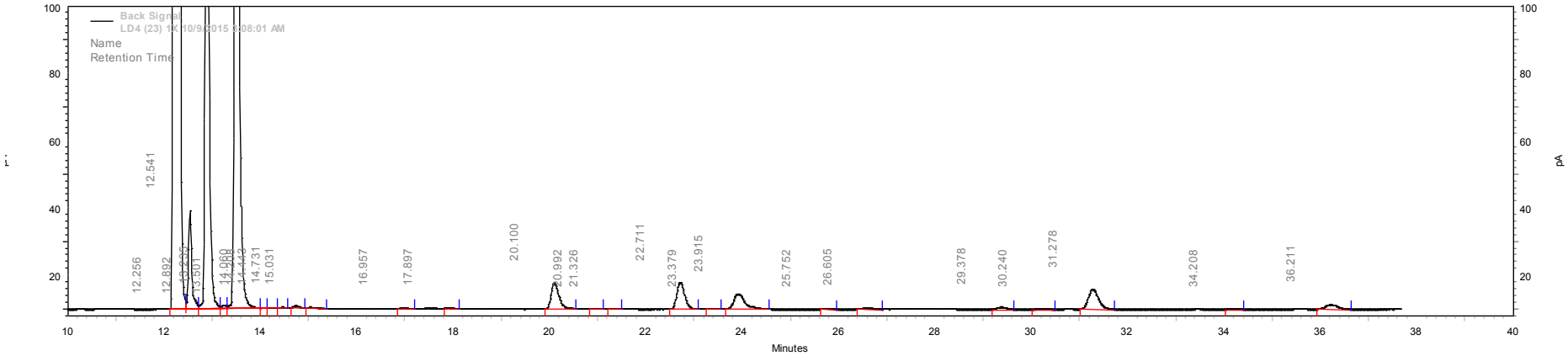

Figure 118: FTAR2 FAME sample (1x) chromatograph

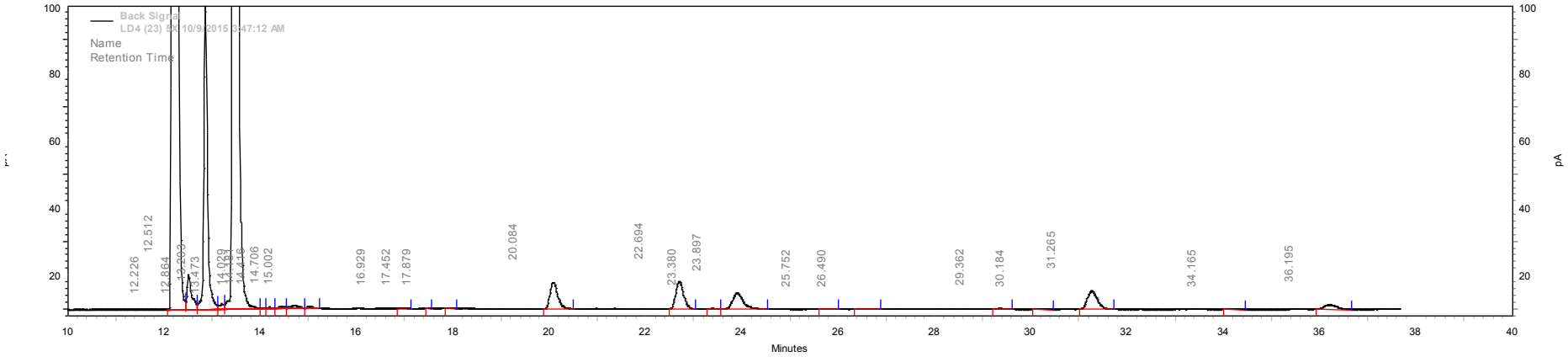

Figure 119: FTAR2 FAME sample (5x) chromatograph

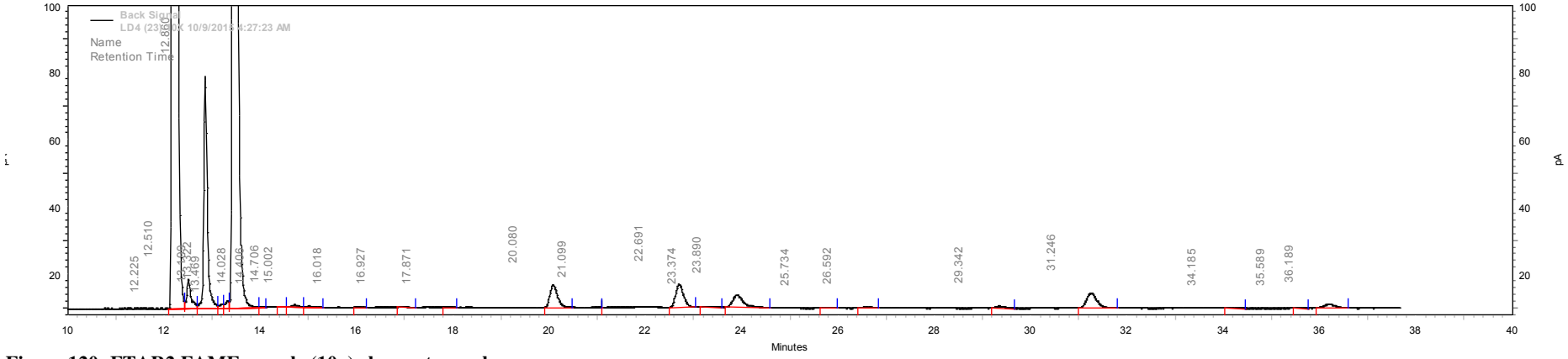

Figure 120: FTAR2 FAME sample (10x) chromatograph

FTAR3

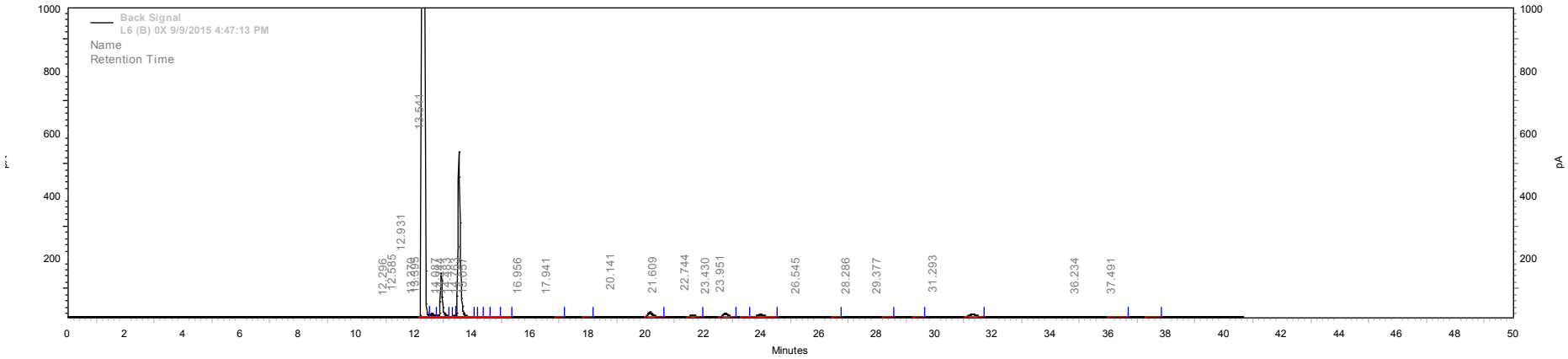

Figure 121: FTAR3 FAME sample (0x) chromatograph

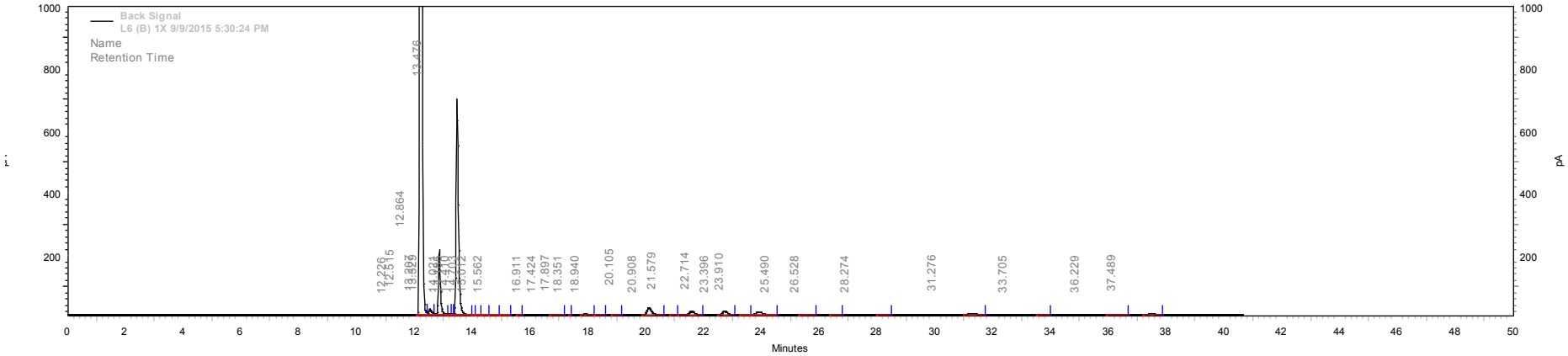

Figure 122: FTAR3 FAME sample (1x) chromatograph

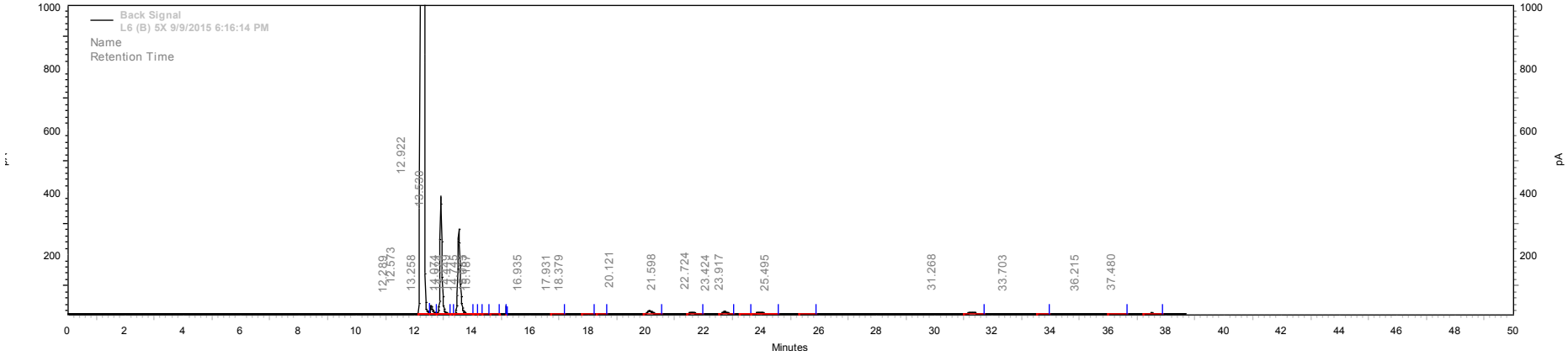

Figure 123: FTAR3 FAME sample (5x) chromatograph

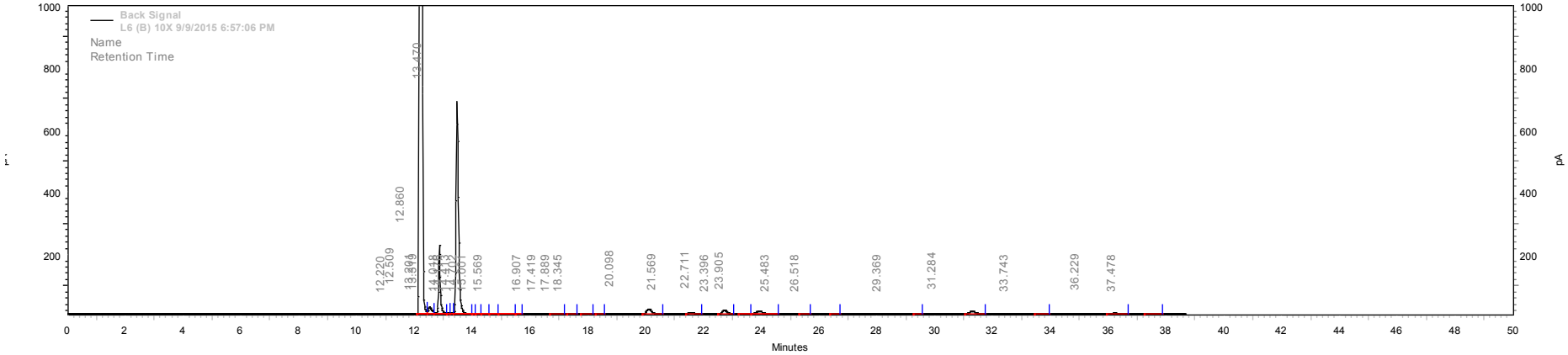

Figure 124: FTAR3 FAME sample (10x) chromatograph

MTAR

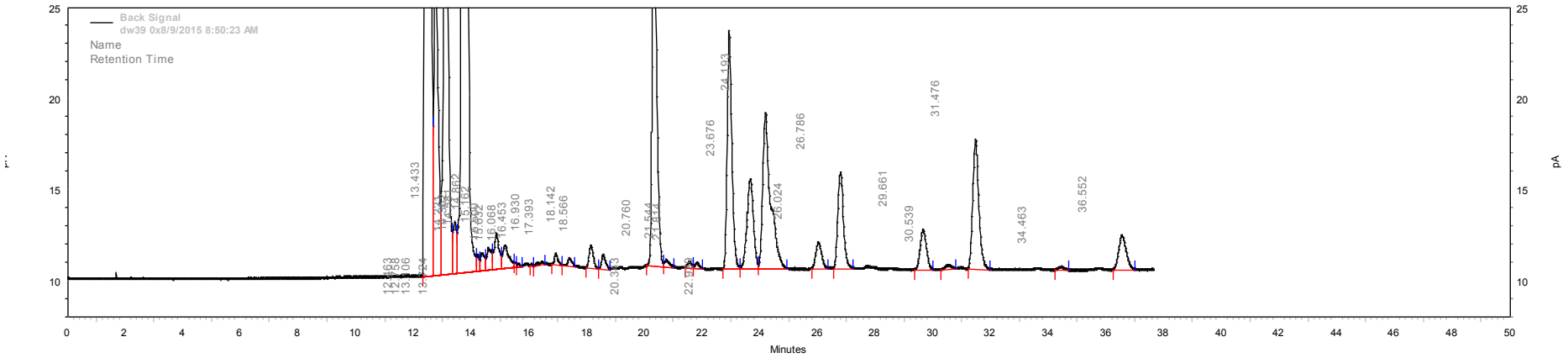

Figure 125: MTAR FAME sample (0x) chromatograph

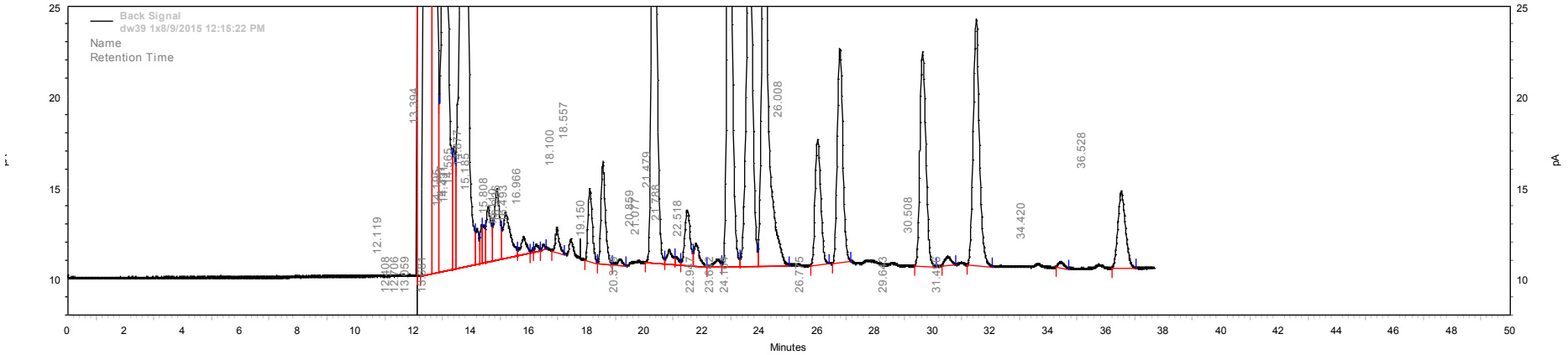

Figure 126: MTAR FAME sample (1x) chromatograph

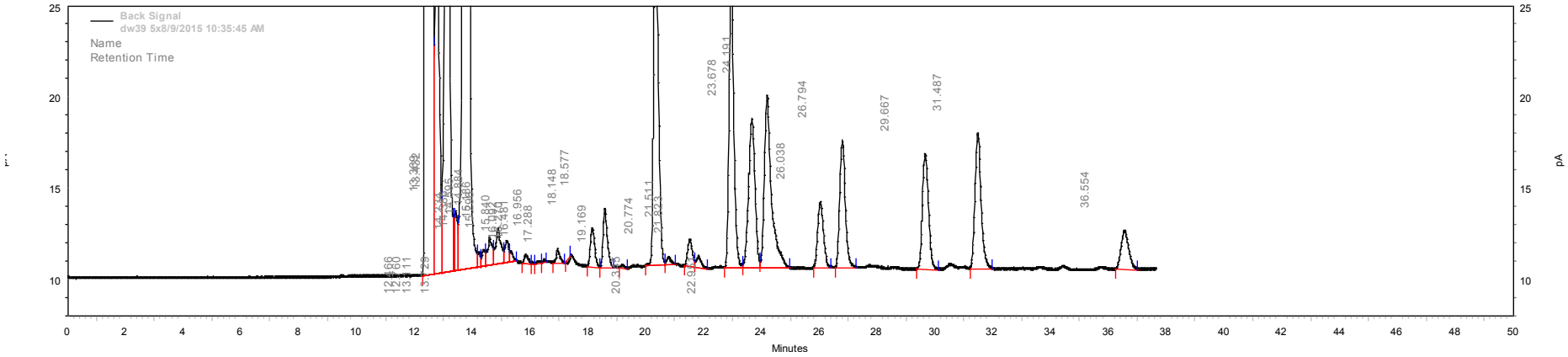

Figure 127: MTAR FAME sample (5x) chromatograph

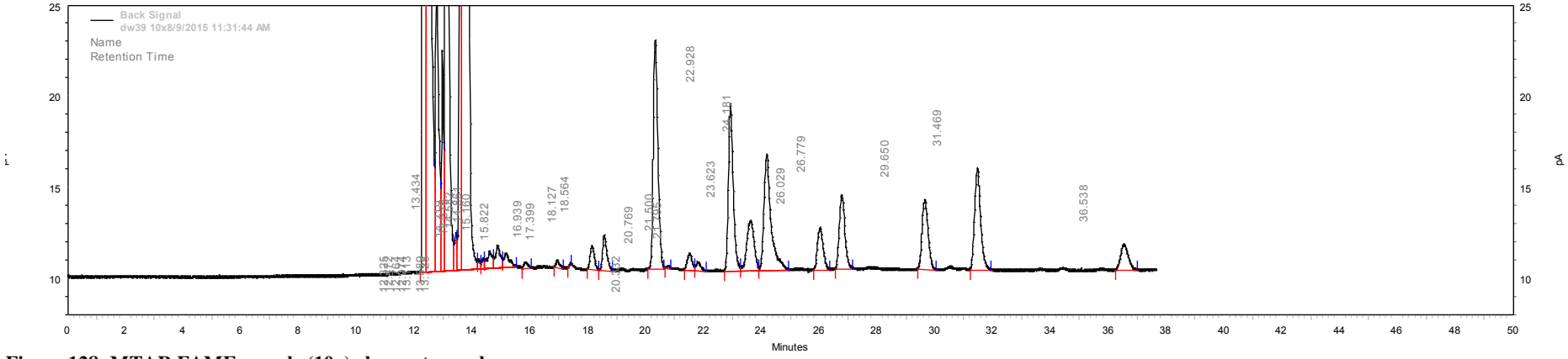

Figure 128: MTAR FAME sample (10x) chromatograph

FDP

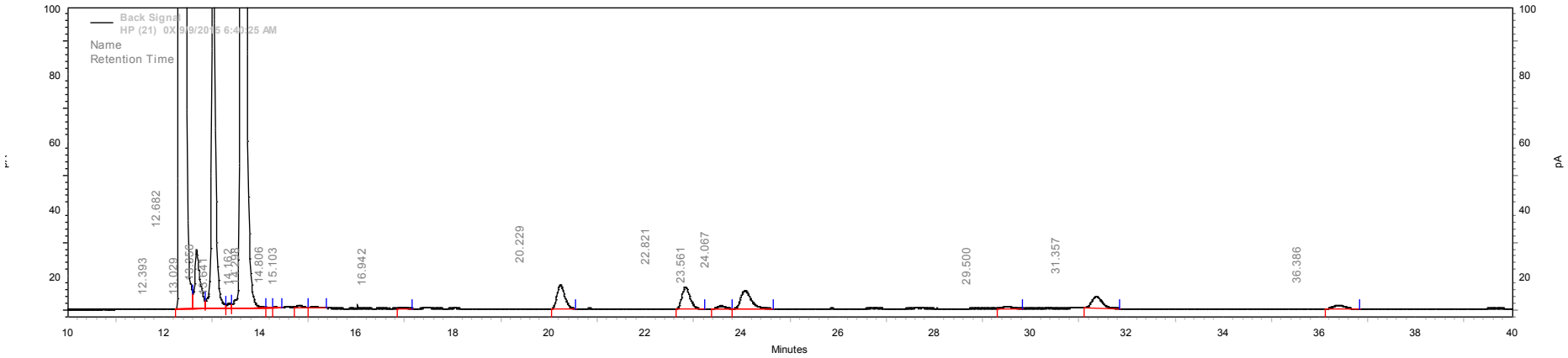

Figure 129: FDP FAME sample (0x) chromatograph

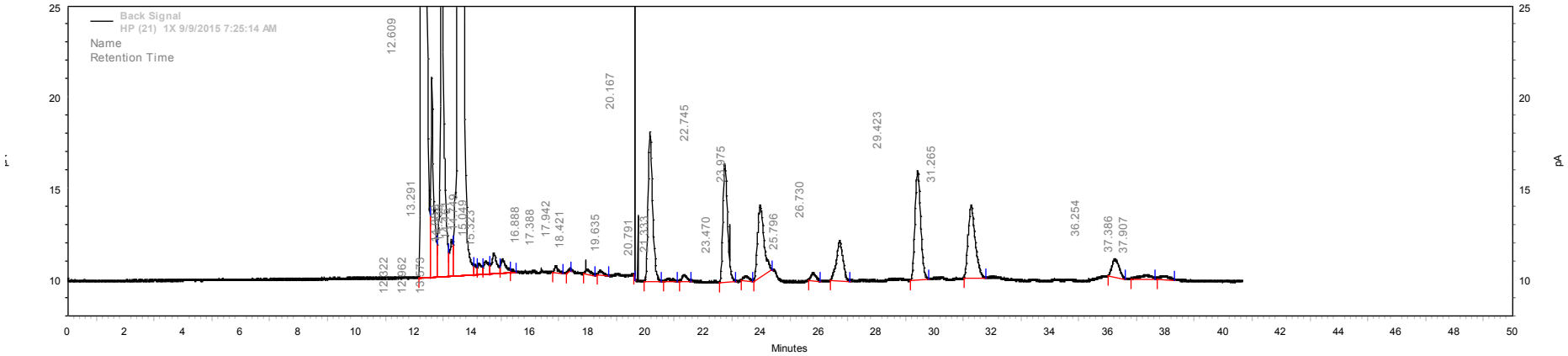

Figure 130: FDP FAME sample (1x) chromatograph

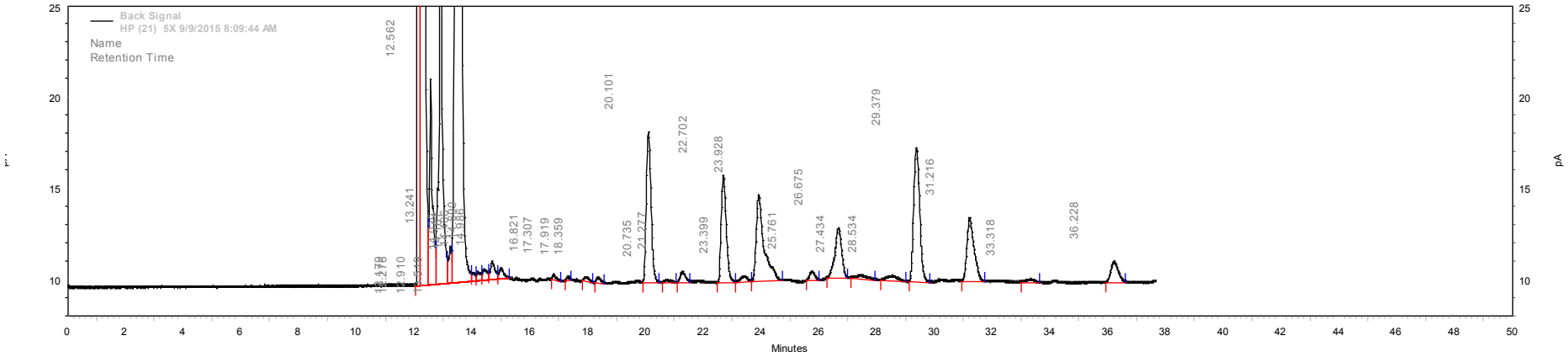

Figure 131: FDP FAME sample (5x) chromatograph

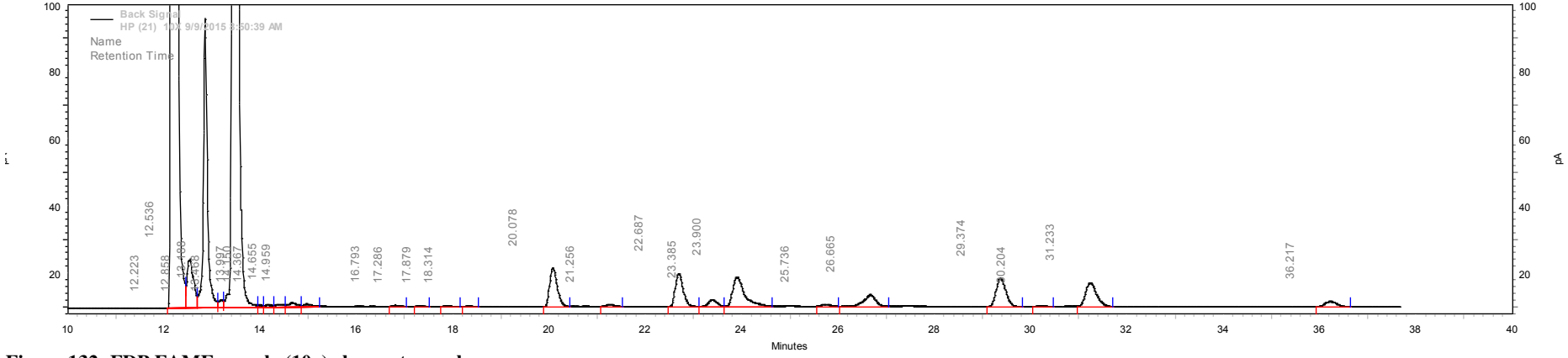

Figure 132: FDP FAME sample (10x) chromatograph